REPUBLIQUE ALGERIENNE DEMOCRATIQUE ET POPULAIRE
MINISTRY OF HIGHER EDUCATION AND SCIENTIFIC RESARCEH
المـــدرســـة الوطنيـــة العليـــا للأشغـال العمومية
فرانسيس جانسون
Ecole Nationale Supérieure des Travaux Publics
Francis Jeanson

Postgraduate Studies & Scientific Research Directorate

Registration No: ……/……/……..

Reference: ……..……

THESIS

Submitted in fulfillment of the requirements for the degree of

DOCTORATE

In : Civil Engineering

Specialty : Roads and Structures

Presented by:

Rania ALLALOU

THEME :

Diagnostic and Mapping of Road Infrastructure Vulnerability in the Mitidja Plain against Flood Risk A BIM-GIS Integrated Approach

Defended on 06/05/2026, before the examination board composed of:

Mr. Ferhat FEDGHOUCHE	Professor, ENSTP	President
Mr. Rafik HEBIB	Associate Professor, ENSTP	Thesis Supervisor
Mr. Mohand BERSI	Associate Professor, USTHB	Co-Supervisor
Mr. Abdelouahab LEFKIR	Professor, ENSTP	Invited Member
Mr. Ghani CHEIKHLOUNIS	Professor, USTHB	Examiner
Mr. Abdelmalek BERMAD	Professor, ENP	Examiner
Mr. Abdelmalek BERMAD	Associate Professor, ENSTP	Examiner

© ENSTP-FJ / 2026

الإهداء

أهدي هذا العمل إلى شعب غزة المقاوم،
إلى ذلك الشعب الذي تعرّض للظلم على مرأى العالم،
وهو ثابتٌ يدافع عن مقدسات الأمة الإسلامية،
عن قدسِها، ثالثِ الحرمين الشريفين،
عن مسجدٍ دُنِّس أمام أعين البشرية.
أهديه إلى شهداء غزة وفلسطين،
إلى أرواحٍ ارتقت ظلمًا وعدوانًا،
وإلى الأسرى في سجون الاحتلال،
المسجونين ظلمًا وبهتانًا.
أهديه إلى كلِّ حرٍّ شريفٍ يأبى الظلم،
ويتنفّس الحرية كحقٍّ لا يُنتزع،
إلى أحرار العالم بمختلف دياناتهم وأعراقهم،
كلّ من رفض الظلم وعشق الحرية.
أما بعد،
أهدي هذا العمل إلى حبيبي والدي،
ألطفَ من عرفت، وأصدقَ من أحببت،
ذلك الطيب الذي لم أرَ لطيبته مثيلًا،
العاشق للحرية، المؤمن بالكرامة.
سلامٌ على روحك، وسلامٌ عليك أينما كنت.
يا من لأجلك، ولأجل إحياء ذكراك،
كان لا بدّ لي أن أنال هذه الشهادة.
يا قدوتي... هذا الإنجاز بعضُ وفاءٍ لك.
وأهديه إلى عنادي الجميل، وحبيبتي، وقدوتي،
ومربيتي ومعلمتي... والدتي الغالية،
يا من حفظتِ الأمانة وصنتِ العهد،
وقمتِ بدور الأب والأم معًا،
ولم أرَ في الوفاء نظيرًا لوفائك.
لكِ من هذا الجهد نصيبُ القلب قبل الحروف.
وأهديه إلى سندي وأحبّتي،
إخوتي وأخواتي الذين أتكئ عليهم،
وكانوا لي خير سندٍ في كل المراحل.
وأهديه إلى أصدقائي؛
فإن سُئلتُ يومًا: ما هو أجمل نجاحٍ في حياتك؟
كان جوابي: اختياري لكم،
يا أفضل الأصدقاء.
وأهديه إلى من استحقّ من عائلتي هذا الإهداء.
وفي الختام،
إلى كلِّ من علّمني حرفًا،
وإلى كلِّ من مرّ في حياتي فتعلّمتُ منه درسًا،
قريبًا كان أو بعيدًا...
هذا العمل ثمرةُ رحلةٍ لم أكن وحدي فيها.

Acknowledgments

First and foremost, I thank **Allah**, the Almighty.

If I have been able to accomplish this work, it is by His will, His mercy, and His guidance. He granted me the strength, patience, and perseverance necessary to overcome the challenges encountered throughout this doctoral journey.

I would like to express my sincere gratitude to my supervisor, **Dr. HEBIB**, for his constant guidance, insightful advice, open-mindedness, and continuous availability. His rigorous and supportive supervision played a decisive role in the successful completion of this thesis.

My sincere thanks also go to my co-supervisor, **Dr. BERSI**, for his valuable remarks, precious assistance, and the opportunities he offered me, particularly the opportunity to undertake an enriching research internship that broadened my scientific perspectives.

I warmly thank the Director of the Laboratory, **Prof. LEFKIR**, for his moral and material support, for providing the necessary resources for this research, and for his continuous encouragement.

I express my deep gratitude to **Prof. CHIKH** for giving me the opportunity to pursue a PhD, for his encouragement, and for his constant availability.

I would like to extend my appreciation to **Prof. DERRICHE** for his valuable advice, availability, and relevant remarks. My thanks also go to **Prof. HADID** for his scientific rigor and positive spirit.

I would like to express my deep appreciation to the Director of Studies, **Prof. FEDROUCHE**, my former master's research supervisor and President of the Jury, for his academic guidance and trust.

I also thank all the members of the Jury **Prof. BERMAD**, **Prof CHEIKH LOUNIS** and **Dr. BAKHTI** who kindly accepted to examine and evaluate this work.

My sincere thanks also go to **Dr. BEINAISSA** for her assistance and for the opportunities she offered me to undertake research internships.

I would also like to thank **Dr. BOUSSAADI and Dr. ANNAD** for his valuable remarks.

My thanks are extended to the Postgraduate Program Directeur **Mr. ADEM**, and to **Ms. Souad** for facilitating administrative procedures.

I would also like to thank all members of the research laboratory for the scientific and human environment they fostered. Special thanks go to my neighbour **Ania** for her moral support; to **Ayemen** and **Abdellatif** for their technical assistance; and to **Fatima**, **Manel**, **Safia**, **Selma**, **Said**, **Hiba**, **Molay**, **Rafik**, and **Abderahmane** for their support and camaraderie.

I also extend my appreciation to **Athmane**.

My very special, warm, and sincere thanks go to my friends in the Pedagogical Laboratory, **Nada** and **Asma**, for their unwavering moral support during these three years and for all that I have learned from them.

I also thank the members of the Pedagogical Laboratory, particularly **Fatima**, **Fatiha**, and **Amina**, as well as the directors, including **Souad**, for their availability and support.

I would like to thank the DIB Department, its members, and administrative staff, especially **Imen** and **Mahdia**, for their assistance and support.

My deepest and warmest gratitude goes to **Dr. MAHIOUI**, Head of the Department, for her constant support, kindness, and unwavering encouragement, as well as to **Prof. BADAOUI** for his encouragement.

I also extend my thanks to the DMS Department, particularly to its Head, **Dr. ZOURGUI**, for his availability and support, as well as to all department members, especially **Amina**.

I sincerely thank all professors of ENSTP, the research laboratory, and the library for their indirect contribution to my academic training and to the completion of this thesis.

My gratitude goes to the Director of ENSTP, **Prof. MEKIDECHE-CHAFA**, for her availability and support, as well as to the Secretary General **Mr. MAOUCHI** and the entire ENSTP administrative team.

Finally,
I thank myself for persevering, for staying strong despite the challenges, and for reaching this milestone with determination and faith.

ملخص

في ظل تزايد حدة الظواهر الهيدرولوجية، لا سيما في حوض البحر الأبيض المتوسط، أصبحت مرونة البنى التحتية للنقل قضية محورية .نظرًا لطبيعتها الخطية وتعرضها المباشر، تقف شبكات الطرق في الخط الأمامي أمام أخطار فيضانات السهول والتدفقات الطينية .ومع ذلك، تواجه المناهج التحليلية التقليدية صعوبة في تقديم تشخيص شامل، إذ غالبًا ما تكون مجزأة بين مقاربات مجالية تعتمد على نظم المعلومات الجغرافية (GIS) وتفتقر إلى الدقة على مستوى المنشأة .كما أنها تعتمد على تحليلات هندسية تفصيلية لكنها منفصلة عن السياق الهيدرولوجي العام. تهدف هذه الأطروحة إلى سد هذه الفجوة المنهجية من خلال تطوير والتحقق من إطار تحليلي مبتكر، قائم على التكامل بين نمذجة معلومات البناء BIM ونظم المعلومات الجغرافية (GIS).وتتمثل الفرضية الأساسية في أن الجمع بين الرؤية الشمولية لنظم المعلومات الجغرافية والدقة التفصيلية لنمذجة معلومات البناء يتيح تشخيصًا أكثر شمولًا ودقة وقابلية للتطبيق لتحديد قابلية تأثر البنى التحتية الطرقية .وقد تم تطبيق هذا الإطار على الحالة الدراسية المعقدة والاستراتيجية لسهل المتيجة في الجزائر. وينتظم البحث في ثلاثة محاور رئيسية :المحور الأول :تشخيص قابلية التأثر المجالية على المقياس الكلي، ويهدف إلى تحديد المناطق الأكثر عرضة للأخطار من خلال مقارنة الطرق متعددة المعايير (AHP) مع مقاربات التعلم الآلي(Machine Learning). المحور الثاني :تحليل هشاشة البنية التحتية على المقياس الجزئي، ويقوم بقياس الأثر الفيزيائي للفيضانات على مقطع طرقي بدقة عالية باستخدام إطار(BIM-HDM) . المحور الثالث : تقييم استراتيجيات المرونة، ويعتمد على النمذجة لقياس فعالية الحلول المبتكرة مثل مفهوم المدينة الإسفنجية (Sponge City). يبرهن هذا العمل أن تكامل (BIM-GIS Integration) لا يمثل مجرد تقدم تقني، بل يعد تحولًا مفاهيميًا يسمح بالانتقال من مجرد تحديد مواقع الخطر إلى القياس الدقيق لتأثيراته، مما يفتح المجال أمام إدارة استباقية للمخاطر، وتصميم إجراءات تخفيف موجهة، وتخطيط مجالي أكثر مرونة واستدامة.

الكلمات المفتاحية: البنى التحتية الطرقية، أخطار الفيضانات، التكامل بين نظم المعلومات الجغرافية ونمذجة معلومات البناء، النمذجة الهيد وديناميكية، هشاشة البنية التحتية، سهل المتيجة.

ABSTRACT

In the face of the intensification of extreme hydrological events, particularly in the Mediterranean basin, the resilience of transport infrastructure has become a critical issue. Due to their linear nature and direct exposure, road networks are on the front line of floodplain flooding and debris flow hazards. However, traditional analytical methods struggle to provide a comprehensive diagnosis, as they are often compartmentalized between territorial approaches (GIS) that lack precision at the infrastructure scale, and detailed engineering analyses that remain disconnected from the broader hydrological context. This thesis aims to bridge this methodological gap by developing and validating an innovative analytical framework based on the synergistic integration of Building Information Modelling (BIM) and Geographic Information Systems (GIS). The central hypothesis is that combining the macroscopic perspective of GIS with the microscopic precision of BIM enables a more comprehensive, accurate, and operational assessment of road infrastructure vulnerability. Applied to the complex and strategic case study of the Mitidja Plain in Algeria, this research is structured into three main parts1.Territorial susceptibility assessment (macroscopic scale), which identifies the most hazard-prone areas by comparing multicriteria methods (AHP) with Machine Learning approaches.2.Infrastructure vulnerability analysis (microscopic scale), which quantitatively evaluates, with high fidelity, the physical impact of flooding on a road section using the BIM-HDM (BIM – Hazard and Damage Modeler) framework.3.Evaluation of resilience strategies, which relies on modelling to quantify the effectiveness of innovative solutions such as the “Sponge City” concept. This work demonstrates that BIM–GIS integration is not merely a technical advancement, but a paradigm shift that moves from simple risk localization toward precise impact quantification, thereby paving the way for proactive risk management, the design of targeted mitigation measures, and more resilient territorial planning.

Keywords: Road infrastructure, Flood risk, BIM-GIS integration, Hydrodynamic modeling, Infrastructure vulnerability, Mitidja Plain.

RÉSUMÉ

Face à l'intensification des événements hydrologiques extrêmes, particulièrement dans le bassin méditerranéen, la résilience des infrastructures de transport est devenue un enjeu capital. Les réseaux routiers, par leur nature linéaire et leur exposition directe, sont en première ligne face aux risques d'inondation de plaine et de laves torrentielles (debris flows). Les méthodes d'analyse traditionnelles peinent cependant à fournir un diagnostic complet, étant souvent cloisonnées entre des approches territoriales (SIG) manquant de précision au niveau de l'ouvrage, et des analyses d'ingénierie détaillées mais déconnectées du contexte hydrologique global. Cette thèse propose de combler ce vide méthodologique en développant et validant un cadre d'analyse innovant fonder sur l'alliance synergique du Building Information Modeling (BIM) et des Systèmes d'Information Géographique (SIG). L'hypothèse centrale est que la combinaison de la vision macroscopique du SIG avec la précision microscopique du BIM permet un diagnostic de la vulnérabilité des infrastructures routières à la fois plus complet, plus précis et plus opérationnel. Appliquée au cas d'étude complexe et stratégique de la plaine de la Mitidja en Algérie, cette recherche se déploie en trois grandes parties : 1. Le diagnostic de la susceptibilité du territoire (échelle macroscopique), qui identifie les zones les plus exposées aux aléas en confrontant des méthodes multicritères (AHP) et de Machine Learning. 2. L'analyse de la vulnérabilité de l'infrastructure (échelle microscopique), qui quantifie avec une haute-fidélité l'impact physique d'une inondation sur un tronçon routier grâce au Framework BIM-HDM (BIM - Hazard and Damage Modeler). 3. L'évaluation de stratégies de résilience, qui utilise la modélisation pour quantifier l'efficacité de solutions innovantes comme le concept de « Ville Éponge » (Sponge City). Ce travail démontre que l'intégration BIM-SIG n'est pas seulement un progrès technique, mais un changement de paradigme permettant de passer d'une simple localisation du risque à une quantification précise de l'impact, ouvrant ainsi la voie à une gestion des risques proactive, à la conception de mesures de mitigation ciblées et à une planification du territoire plus résiliente.

Mots-clés : Infrastructure routière, Risque d’inondation, Intégration BIM-GIS, Modélisation hydrodynamique, Vulnérabilité des routes, Plaine de la Mitidja.

Table of Content

1 GENERAL INTRODUCTION 1

1.1 Research Background 1
1.2 Problem Statement 1
1.3 Research Questions 2
1.4 Research Scope and Methodology 2
1.5 Thesis Structure 3

2 Flood Risk and Infrastructure Vulnerability: Concepts and Challenges 4

2.1 Introduction 4
2.2 From Hazard to Risk: Definitions and Fundamental Concepts 6
2.2.1 Risk: From Fatality to the Measurement of Uncertainty 6
2.2.2 Hazard (H): The Physics of Chaos 8
2.2.3 Exposure (E): From Static Presence to Systemic Assets 9
2.2.4 Vulnerability: The Factor Transforming Hazard into Damage 10
2.2.4.1 Physical Vulnerability ($\boldsymbol{VPhysical}$): Structural Resistance 11
2.2.4.2 Socio-Economic Vulnerability ($\boldsymbol{VSocio - Econ}$): Inequality in the Face of Shock .. 11
2.2.4.3 Functional Vulnerability ($\boldsymbol{VFunctional}$): Service Paralysis 11
2.2.5 Resilience (A): From Resistance to Adaptive Recovery 11
2.2.6 A Critical Analysis of International Models: Toward a Necessary Synthesis 12
2.2.6.1 The French Model (“Inondabilité” Method): Spatial Management (E) 13
2.2.6.2 The American Model (USACE/FEMA): Structural Control (H) 13
2.2.6.3 The Japanese Model (DRR): Managing Time and Response (A) 13
2.2.6.4 The Case of Algeria: Between Legacy and the Urge for Adaptation 13
2.3 Specificities of Flood Hazards and Associated Phenomena 15
2.3.1 Genesis and Legacy: Flooding from Archetype to Physical Phenomenon 15
2.3.2 Mechanisms and Typology: The Physical Classification of Floods 16
2.3.2.1 The Primary Distinction: Marine versus Inland Origins 16
2.3.3 Physics of Inland Flooding: A Scientific Causal Chain 17
2.3.3.1 Hydrological Genesis: The Complexity of the Rainfall-Runoff Transformation 18
2.3.3.2 Hydraulic Transformation: From Fluid Chaos to Numerical Modelling 19
2.3.3.3 Rheological Distinction: The Physics of Matter 21
2.3.4 Continentals Operational Classification of Inland Flooding 22
2.3.4.1 Pluvial Flooding (Urban Runoff): "Upstream Drainage Saturation" 23
2.3.4.2 Riverine Flooding (Plain Flood): "Systemic Overflow" 23
2.3.4.3 Flash Floods: "Kinetic Violence" 23
2.3.4.4 Debris Flows: "The Geotechnical Projectile" 23
2.3.4.5 Methodological Synthesis: The Imperative for Physical Discrimination 24
2.3.5 The Methodological Evolution of Hazard Assessment: From Hydrological Theory to Operational Decision-Making 24
2.3.5.1 Qualitative and Semi-Quantitative Methods: Predicting the "Spatial" Dimension (Where?) 24
2.3.5.2 Statistical Hydrological Methods: Predicting the "Temporal" Dimension (When?) 25

2.3.5.3 Hydrodynamic Methods: Predicting Physical Impact (What Force Intensity?) 26
2.3.5.4 The Cross-Cutting Data-Driven Approach: Artificial Intelligence in Flood Research 26
2.3.5.5 Strategic Synthesis: Aligning Methodologies with Decision-Making Scales 27
2.4 The Critical Stake: The Vulnerability of Road Infrastructure 28
2.4.1 Road Infrastructure: Origins, Functions, and the Hydrological Conflict..... 28
2.4.2 Failure Mechanisms: From Hydraulic Loading to Systemic Collapse 29
2.4.2.1 Physical Vulnerability: The Conversion of Floodwaters into Structural Loadings 30
2.4.2.2 Functional Vulnerability: Service Loss and the Urban Trap 31
2.4.2.3 Socio-Economic Vulnerability: The True Cost of Infrastructure Failure 32
2.4.3 Methodological State of the Art: Aligning Vulnerability Assessment with Objectives 32
2.4.3.1 Risk Prevention and Management (Existing Networks)..... 32
2.4.3.2 Design and Advanced Diagnosis (New or Critical Structures) 33
2.4.3.3 Methodological Synthesis: The Common Impasse..... 33
2.4.4 Scientific Diagnosis: The "Scale Gap" Impasse 33
2.4.4.1 Epistemological Confusion: General vs. Asset-Specific Vulnerability 33
2.4.4.2 The Mechanics of Compartmentalization: Two Disconnected Worlds 34
2.4.4.3 Thesis Response: An Integrated Multi-Scale Approach 34
2.5 Conclusion 36

3 Digital Tools for Risk Assessment: From Hydraulic Modelling to BIM-GIS Integration 37

3.1 Introduction..... 37
3.2 The Technological Foundation: From Computational Power to Digital Architecture 38
3.2.1 The Computer and the Internet: Genesis and the Revolution of Computing..... 38
3.2.2 The Fundamental Distinction: From Specialized Tools to Integrative Environments . 39
3.3 Hydro-Hydraulic Modelling: The Simulation Engines 40
3.3.1 Hydrological Modelling: From Watershed Geometry to Discharge Generation..... 40
3.3.2 Hydrodynamic Modelling: Spatializing Propagation 41
3.3.3 Coupling: Toward Seamless Interaction..... 42
3.4 Geographic Information Systems (GIS): The Platform for Territorial Intelligence (Macro) 43
3.4.1 Conceptual Foundations: Snow’s Cholera Map (1854)..... 43
3.4.2 Technological and Functional Evolution..... 43
3.4.3 Systemic Role and Applications: GIS as the Analytical Backbone..... 44
3.4.3.1 Domain-Specific Applications..... 44
3.4.3.2 The Central Role of GIS: The Backbone of Risk Analysis 44
3.4.3.3 The Structural Limitation: The "Scale Barrier" 44
3.5 BIM: The High-Fidelity Platform (Micro-Scale) 46
3.5.1 Definition and Paradigm Shift: From Geometry to Shared Semantics..... 46
3.5.2 Genesis and Evolution: From the Drawing Board to the Database 46
3.5.3 Strategic Applications: BIM as a Tool for Diagnostics and Resilience..... 47
3.5.4 Strengths and Limitations 48
3.6 Technological Convergence: Toward BIM-GIS and AI Integration 49
3.6.1 Definition and Genesis of Integration: From Juxtaposition to Synergy 49

3.6.2 Systemic Synergy: The Benefits of an Integrated Approach 49
3.6.3 Operational Applications for Flood Management 50
3.6.4 Integration Methodology: The Three Levels of Fusion 50
3.6.5 Persistent Technical Challenges: The Interoperability Bottlenecks 51
3.6.6 The Artificial Intelligence Frontier: An Accelerator, not a Replacement 51
3.7 Conclusion 53
Toward a Strategic Multi-Scale Methodology 53
4 The Mitidja Plain: A Strategic Territory Facing Multiple Risks 54
4.1 Introduction 54
4.2 Presentation of the Study Area: Between Geographical Heritage and Strategic Stakes 55
4.2.1 Historical and Geometric Foundations: From Swamplands to Vital Basin 55
4.2.2 Geomorphology and Topography: The Trap of Gentle Gradients 55
4.2.3 Geology and Hydrogeology: A Vulnerable Reservoir 56
4.2.4 Climatology: Mediterranean Intensity and the Breakdown of Stationarity 56
4.3 Hydrological and Anthropogenic Issues: The Production of Risk 58
4.3.1 The Hydrological System: Torrentiality and Overexploitation 58
4.3.2 Urban Sprawl: Soil Sealing as an Aggravating Factor 58
4.3.3 Historical Disasters: A Proven and Recurring Threat 59
4.4 Rationale for the Strategic Selection: From Territorial Complexity to Structural Precision. 60
4.4.1 A Territory of National Strategic Importance: The Gordian Knot 60
4.4.2 Hydrological Complexity Mandating Macro-Scale Zoning 60
4.4.3 The Failure of Conventional Models and the High-Fidelity Imperative (Micro-Scale) 61
4.5 Conclusion: 62
5 Regional Susceptibility Mapping and Zoning 63
5.1 Introduction 63
5.2 Strategic Rationale: Justifying the Multi-Criteria Approach (AHP-GIS) 64
5.2.1 Addressing Data Scarcity 64
5.2.2 Economic and Spatial Efficiency: The Principle of Parsimony 64
5.2.3 The Multidimensional and Systemic Nature of Risk 64
5.3 The Standard Approach: Multi-Criteria Decision Analysis (AHP-GIS) Mapping 66
5.3.1 Methodological Protocol: The Geospatial Processing Workflow 66
5.3.2 Characterization and Analysis of Influencing Factors 67
5.3.2.1 Morphometric Factors (Source: SRTM 30 m DEM) 68
5.3.2.2 Hydrological Factors (Derived from DEM and Network Analysis) 68
5.3.2.3 Geo-Environmental Factors (Heterogeneous Datasets) 69
5.3.2.4 Critical Assessment of Data Quality 70
5.3.3 Identification and Weighting of Influencing Factors 70
5.3.4 Preliminary Results and Methodological Critique 72
5.4 The Robust Approach: Uncertainty Management through Fuzzy-AHP and Sensitivity Analysis 73
5.4.1 Methodological Protocol: Objectifying Uncertainty 73
5.4.1.1 Literature-Based Benchmarking 73

5.4.1.2 The Contribution of Fuzzy Logic (Fuzzy AHP) 74
5.4.1.3 Contrasting Scenario Strategy (Sensitivity Analysis) 74
5.4.2 Characterization of Influencing Factors (Robust Approach) 81
5.4.2.1 Topographic and Geomorphological Factors 81
5.4.2.2 Hydrographic and Climatic Factors 82
5.4.2.3 Soil, Vegetation, and Land Use Factors 84
5.4.3 Detailed Analysis of Susceptibility Maps and Historical Confrontation 85
5.4.3.1 The Qualitative Benchmark Map (Scenario 00 – Literature-Based) 85
5.4.3.2 The Physical Scenarios (Scenarios 01 to 05) 86
5.4.3.3 The Anthropogenic Scenario (Scenario 06 – LULC) 88
5.4.3.4 Confrontation with Historical Reality (Remote Sensing) 89
5.4.4 Results Analysis and Historical Validation 90
5.5 The Data-Driven Approach: Statistical Validation via Machine Learning 92
5.5.1 Methodology: Logistic Regression (LR) via Orange Data Mining 92
5.5.2 Results: Statistical Convergence and "Hard Core" Validation 93
5.6 Conclusion 95
Convergence of Evidence and the Shift in Scale 95

6 Susceptibility Mapping of Debris Flow Hazards 96

6.1 General Introduction 96
6.2 Presentation of the Study Area: The Strategic Choke Point of the Chiffa 97
6.2.1 A Constrained Geographical Corridor 97
6.2.2 The Infrastructure Stake: RN1 in the Eye of the Storm 97
6.2.3 An Aggravating Hydro-Geological Context 98
6.3 Sediment Dynamics: From Erosion Potential to Functional Connectivity (IC-RUSLE) 101
6.3.1 Problem Statement: Structural versus Functional Connectivity 101
6.3.2 Methodology: The IC-RUSLE Coupling Approach 101
6.3.2.1 Modelling Potential Soil Erosion (RUSLE) 101
6.3.2.2 Calculation of the Functional Index (***ICRUSLE***) 102
6.3.3 Characterization of Input Factors: Topography and Erosion Potential 102
6.3.3.1 Topography and Surface Roughness (Structural Impedance) 103
6.3.3.2 RUSLE Erosion Potential (Functional Impedance) 104
6.3.4 Results and Discussion: Pinpointing Agricultural "Hotspots" 105
6.4 Debris Flow Hazard: The Ballistic Threat to Infrastructure 108
6.4.1 Morphometric Methodology and Simulation 108
6.4.1.1 Identification of Initiation Zones 108
6.4.1.2 Runout Simulation 108
6.4.2 Results: From Morphometric Characterization to the Threat on RN1 110
6.4.2.1 Initial Morphometric Characterization 110
6.4.2.2 Hazard Zonation 111
6.4.2.3 Composite Susceptibility and Connectivity Map 113
6.4.2.4 Estimation of Impact Simulation on the RN1 115
6.4.3 Synthesis: The Critical Exposure Profile of the RN1 116

6.5 Conclusion 117
From Physical Understanding to the High-Fidelity Imperative 117
7 Analysis of Flood-Infrastructure Interaction through BIM-HDM Integration 118
7.1 Introduction 118
7.2 Problem Statement: Limitations of the Conventional Approach (C-HDM) 119
7.2.1 The Topographic Blindness of DEMs 119
7.2.2 Application to the Chiffa Case Study: Proof through Failure 119
7.2.2.1 Simulation Protocol and Mesh 120
7.2.2.2 Hydraulic Results Analysis 120
7.2.2.3 Error Quantification 121
7.2.2.4 Assessment of the C-HDM Approach: A Strategic Screening Tool 121
7.3 High-Fidelity Methodology: The BIM-HDM Framework 122
7.3.1 The Tripartite Architecture of the Integrated Framework 122
7.3.2 Experimental Validation: The Chiffa Wadi Case Study 122
7.3.2.1 Implementation of the Simulation Workflow 123
7.3.2.2 In-Depth Analysis of Simulation Results 123
7.3.2.3 Quantitative Validation and Error Analysis 127
7.3.2.4 Visual Confrontation and Functional Validation 129
7.4 Discussion and Perspectives: Toward High-Fidelity Engineering 130
7.4.1 Generalizing the Model across the Vulnerability Triad 130
7.4.2 Toward the Resilience Digital Twin 130
7.5 Conclusion 131
From Diagnostic Precision to Strategic Action 131
8 Risk Treatment Strategies: Mitigation, Resilience, and Crisis Management 132
8.1 Introduction 132
The Imperative for a Hybrid Response 132
8.2 Civil Engineering Interventions: Balancing Resistance and Hydraulic Transparency 134
8.2.1 Structural Mitigation: Strategies for Avoidance and Control 134
8.2.2 Structural Adaptation: Coexisting with the Hazard (Robustness) 134
8.2.3 BIM-HDM Interoperability as a Decision-Support Engine 135
8.3 Organizational Resilience: Early Warning Systems (EWS) Optimized by FRH 137
8.3.1 From Model to Operational Digital Twin: The BIM-HDM Advantage 137
8.3.2 Zoning Protocol and Crisis Management for the RN1 138
8.3.3 Synthesis: Efficiency through Physical Precision 139
8.4 Sustainable Strategy: A Proof-of-Concept Study of the "Sponge City" (Rouiba Case Study) 140
8.4.1 Methodology: Urban Hydrological Modelling (SWMM) 140
8.4.2 Geospatial Characterization: Urban Vulnerability Diagnosis 141
8.4.2.1 Morphology and Flow Dynamics 141
8.4.2.2 Flow Accumulation and Urban Thalwegs 143
8.4.2.3 Imperviousness and Infiltration 144

8.4.2.4 Selection of Target Sub-catchments 144
8.4.3 Results: A Radical Transformation of Hydrological Response 145
8.4.4 Discussion: Proof of Concept for the Mitidja 148
8.5 Synthesis of Strategic Levers: Navigating between Minimization and Coexistence 150
8.5.1 Mitigation Logic (Attenuation and Minimization) 150
8.5.2 Adaptation Logic (Coexistence and Resilience) 150
8.6 Conclusion 151
9 Perspectives and Future Outlook 152
9.1 Introduction 152
9.2 From Clear Water to Complex Media Physics: The Rheological Evolution 154
9.2.1 Rationale for the Approach Inherited from Chapter 6 154
9.2.2 The Research Gap: From Form (GIS) to Force (Numerical Simulation) 154
9.2.3 Future Perspective: Impact Engineering for Infrastructure 154
9.3 From Static Diagnostics to Cognitive Digital Twins: The Temporal Evolution 156
9.3.1 From BIM to the Digital Twin 156
9.3.2 From Proactive Response to "Cognitive" Infrastructure 156
9.3.3 Radical Reduction of Recovery Time 157
9.4 AI as a "Surrogate Model" for Real-Time Analysis: Computational Evolution 158
9.4.1 AI as an Accelerator: Shifting from Offline Simulation to Real-Time Inference 158
9.4.2 The Nature of AI: A Predictive "Black Box" 158
9.4.3 Toward "Physics-Informed Machine Learning" (PINN) 158
9.5 Toward Multi-Hazard and Structural Resilience: The Systemic Evolution 160
9.5.1 From Unavailability to Failure: Structural Vulnerability 160
9.5.2 The Road as a Multi-Hazard System 160
9.5.3 The Final Horizon: Resilient Asset Management 161
9.6 Conclusion 162
10 Recommendations for Integrated Risk Management on the Mitidja Road Network 163
10.1 Introduction 163
Bridging the Gap between Scientific Knowledge and Public Action 163
10.2 Methodological Synthesis: The Integrated Risk Equation (Conceptual Model) 165
10.2.1 Formalizing the Resilience Framework 165
10.2.2 Resilience ($\boldsymbol{A}$) as a Divisor: A Paradigm Shift 165
10.2.3 An Optimal Methodology for Data-Scarce Contexts 165
10.2.4 Operational Application across the Infrastructure Lifecycle 166
10.3 Decision-Making Synthesis: The Multi-Scale Diagnosis as a Strategic Compass 167
10.3.1 Resolving the Scale Gap: An Operational Breakthrough 167
10.3.2 The FRH Indicator: The New Benchmark for Assessment 167
10.3.3 Toward Predictive and Proactive Asset Management 167
10.4 Prioritized Action Plan: From Emergency Management to Long-term Sustainability 169
10.4.1 Short-Term Horizon: Crisis Control and User Safety 169
10.4.2 Medium-Term Horizon: Structural Retrofitting and Managed Coexistence 169
10.4.3 Long-Term Horizon: Systemic Prevention and Green Resilience 169

10.5Future Vision: The Geospatial Digital Twin and Resilience Engineering 4.0 171
10.5.1 Cyber-Physical Fusion: BIM, GIS, and IoT 171
10.5.2 A National Platform for the Country's Vital Arteries 171
10.5.3 Lifecycle Optimization and Sustainability..... 171
10.6Conclusion 173
11 GENERAL CONCLUSION 174
11.1Synthesis of Major Contributions..... 174
11.2Theoretical Synthesis: The Integrated Risk Model..... 175
11.3Limitations and Perspectives 175

List Of Figures

Figure 4.1. Location of Mitidja plain. 57
Figure 4.2. Geology Map of Mitidja plain. 57
Figure 4.3. Hydrology map of Mitidja plain. 59
Figure 5.1. Methodology steps 67
Figure 5.2. Topographical Factors: a-Elevation, b-Slope, c-Curvature 68
Figure 5.3. Hydrological Factors: a-TWI, b-Drainage density, c-Flow accumulation. 68
Figure 5.4. a-Pluviometry carte, b-delimitation of pluviometry carte in the Mitidja plain. 69
Figure 5.5. a-Geological carte, b-delimitation of geological carte in the Mitidja plain. 69
Figure 5.6. a-Land cover carte, b-delimitation of Land cover carte in the Mitidja plain. 70
Figure 5.7. Flood Susceptibility Mapping. 72
Figure 5.8. Methodology steps. 75
Figure 5.9. Frequency of Factor Usage Across Studies. 76
Figure 5.10. Elevation map of Mitidja Plain. 81
Figure 5.11. Slope map of Mitidja Plain. 81
Figure5.12. Curvature map of Mitidja Plain. 82
Figure 5.13. River distance map of Mitidja Plain. 82
Figure 5.14. Drainage density map of Mitidja Plain. 83
Figure 5.15. TWI map of Mitidja Plain. 83
Figure 5.16. Precipitation map of Mitidja Plain. 84
Figure 5.17. Sol texture map of Mitidja Plain. 84
Figure 5.18. NDVI map of Mitidja Plain. 85
Figure 5.19. LCLU map of Mitidja Plain. 85
Figure 5.20. Flood qualitative susceptibility map of Mitidja Plain. 86
Figure 5.21. Scenario 01 map of Mitidja Plain. 86
Figure 5.22. Scenario 02 map of Mitidja Plain. 87
Figure 5.23. Scenario 03 map of Mitidja Plain. 87
Figure 5.24. Scenario 04 map of Mitidja Plain. 88
Figure 5.25. Scenario 5 map of Mitidja Plain. 88
Figure 5.26. Scenario 06 map of Mitidja Plain. 89
Figure 5.27. Historical zone flood [180] map of Mitidja Plain. 89
Figure 5.28. Historical flood map of Mitidja Plain. 90
Figure 5.29. Methodology steps. 93
Figure 5.30. Flood susceptibility ML map of Mitidja Plain. 94
Figure 6.1. A. Extent of the Chiffa watershed. B. Three-dimensional model of the watershed. C. Photograph upstream of the watershed. D. Photograph at the watershed outlet. 98
Figure 6.2. Descriptive maps of the study area [91] . A. Hydrological context. B. Climatic context. C. Geological context. 100
Figure 6.3. Consequence of climate change (from[185]). A. Evolution of the position of the 300 mm isohyets between the periods 1942-1989 and 1965-2004. B. Evolution of average annual temperature. 100
Figure 6.4. Methodology steps. 102

Figure 6.5. DEM map of Chiffa watershed. 103
Figure 6.6. Roughness map of Chiffa watershed. 103
Figure 6.7. Rusle map of Chiffa watershed. 104
Figure 6.8. Rusle inverse map of Chiffa watershed. 105
Figure 6.9. Ic structure of Chiffa watershed. 106
Figure 6.10. Ic RUSLE of Chiffa watershed. 107
Figure 6.11. Methodology steps 109
Figure 6.12. DEM map of Chiffa watershed. 110
Figure 6.13. Surface roughness index map of Chiffa watershed. 111
Figure 6.14. Channel network of the Oued Chiffa watershed. 112
Figure 6.15. Classification of the channel network reaches based on potential debris flow processes (initiation, propagation, deceleration, and stopping). 112
Figure 6.16. Density map of potential debris flow initiation points. 113
Figure 6.17. Sediment Connectivity Index (IC) map. 114
Figure 6.18. Final debris flow susceptibility map, obtained by combining the initiation density and connectivity indices. 114
Figure 6.19. Final debris flow susceptibility map, obtained by combining the initiation density and connectivity indices. 115
Figure 7.1. Methodology steps. 119
Figure 7.2. Identification of areas with high flood hazard. 120
Figure 7.3. Identifying Road flood levels of the river station n° 6239. 120
Figure 7.4. Framework BIM-HDM. 122
Figure 7.5. Methodological Workflow for the Comparative Study. 123
Figure 7.6. Flood Depth in the study area. A. InfraWorks results. B. HEC-RAS result in RasMapper. C. HEC-RAS results in ArcGIS PRO. 124
Figure 7.7. Flood velocity in the study area. A. InfraWorks results. B. HEC-RAS result in RasMapper. C. HEC-RAS results in ArcGIS PRO. 125
Figure 7.8. Process for identifying road-flood interaction using C-HDM. A. First step. B. Second step. C. third step. 126
Figure 7.9. Process for identifying road-flood interaction using BIM-HDM.A. Reading the elevation from contour lines.B.3D visualization. C. Profile view of the road. D. Measurement of a partially flooded element. 126
Figure 7.10. Methodology for estimating observed water depth for model validation. (A) On-site measurement of the safety guardrail height (80 cm) used as a reference object. (B, C, D) Archival imagery from historical flood events (Feb 2017, Apr 2018, Dec 2018) used 128
Figure 7.11. Comparison of Flooded Road Height (FRH) – Bar Chart Representation. 128
Figure 7.12. Flooded area. A. Flood simulation by GIS-BIM-HDM approach (InfraWorks software). B. Picture of a flood that occurred on 05/02/2017. 129
Figure 8.1. Specific characteristics of the PK 65,862 km area. A.Low road elevation. B.Low permeability schist substratum. 135
Figure 8.2. Examples of BIM interoperability: A. Pictures illustrate the sinuosity of the terrain. B. Infraworks to Civil 3D. C. Civil 3D to geotechnical software. 136
Figure 8.3. Alert system flowchart. 137

Figure 8.4. Zone description. A. High flood risk Zone. B. Safety Zone. C. The first diversion. 138
Figure 8.5. Methodology steps..... 141
Figure 8.6. Dem of Rouiba city 142
Figure 8.7. Slope of Rouiba city. 142
Figure 8.8. Curvature of Rouiba city. 143
Figure 8.9. Flow accumulation of Rouiba city. 143
Figure 8.10. Infiltration of Rouiba city. 144
Figure 8.11. Selected sub-catchments. 145
Figure 8.12. Runoff graph - Grey vs Green 147
Figure 8.13. Peak Flow- Grey vs Green. 147
Figure 8.14. Synthetic Hydrographs - Grey vs Green 148

List Of Tables

Table 5.1. Flood Susceptibility Assessment Table by Hierarchical Analysis (AHP)..... 71
Table 5.2. Comparison of the Weightings of Flood Causative Factors in the Literature (1994–2025). 77
Table 5.3. Standard Factor Weights (%) for the Six AHP and Fuzzy AHP Scenarios, and Consistency Ratios (CR) of the Standard AHP 91
Table 6.1. Main Physical and Environmental Characteristics of the Chiffa Catchment. 99
Table 7.1. Comparison of Flood Levels and Road Elevations. 121
Table 7.2. Comparison of Flood Levels and Road Elevations. 127
Table 7.3. Validation of Simulated Flood Depths against Photo-Estimated Observations at PK 65.862..... 127
Table 8.1. Comparative analysis of hydrological indicators (Conventional "Grey" Scenario vs. "Green" Strategy). 146

List of Symbols

- H: Hazard
- E : Exposure
- V : Vulnerability
- A: Resilience
- R : Risk
- T : Return period
- Q : Discharge
- Q_{max} / Q_{peak} : Peak discharge
- H_s : Inundation Depth
- V_s : Flow Velocity
- P : Precipitation
- I : Infiltration
- t_c : Time of Concentration
- μ: Viscosity
- ρ: Density
- g : Gravity
- n : Manning-Strickler roughness coefficient
- q : Dynamic Pressure ($q = \frac{1}{2}\rho V_s^2$)
- C_v :Volumetric Sediment Concentration
- Fr : Froude number
- W_i : Weight of criterion
- R_i : Rating of the class

List of Abbreviations

- **AHP** : Analytic Hierarchy Process
- **BIM** : Building Information Modelling
- **CDE** : Common Data Environment
- **C-HDM** : Conventional Hydrodynamic Modelling
- **DEM** : Digital Elevation Model
- **EWS** : Early Warning Systems
- **FEMA** : Federal Emergency Management Agency
- **FRH** : Flooded Road Height
- **FSI** : Flood Susceptibility Index
- **GIS / SIG** : Geographic Information Systems
- **HDM** : Hydrodynamic Modelling
- **HEC-RAS / HEC-HMS** : Logiciels du Hydrologic Engineering Center
- **IC** : Index of Connectivity
- **IoT** : Internet of Things
- **LID** : Low Impact Development
- **LULC** : Land Use / Land Cover
- **ML** : Machine Learning
- **MSF** : Modified Single Flow
- **NBS** : Nature-Based Solutions
- **NDVI** : Normalized Difference Vegetation Index
- **PINN** : Physics-Informed Neural Networks
- **RUSLE** : Revised Universal Soil Loss Equation
- **SPI** : Stream Power Index
- **SWE** : Shallow Water Equations
- **SWMM** : Storm Water Management Model
- **TWI** : Topographic Wetness Index

1 GENERAL INTRODUCTION

1.1 Research Background

Flood risk has emerged as one of the most frequent and destructive natural hazards worldwide [1]. This threat is exacerbated by dual forcing dynamics: on one hand, the intensification of extreme rainfall events attributed to climate change [2], and on the other, increasing anthropogenic pressure on land use. According to international databases, floods account for nearly **40%** of recorded natural disasters over the last two decades, affecting more than **2 billion** people and causing economic losses estimated at over **$100** billion annually[3].

The Systemic Vulnerability of Transport Networks

At the heart of this crisis, transport infrastructure represents the "**Achilles' heel**" of modern societies. Due to their linear nature and near-systemic exposure, these networks are on the front lines of hydrological hazards. A major study by [4] reveals that nearly **27%** of global road assets are exposed to at least one major hazard. These "**vital arteries**" suffer a threefold impact:

a) **Physical Damage:** Destruction of bridges due to scouring and the collapse of embankments [5]**.**

b) **Functional Paralysis:** Even simple submersion can disrupt entire supply chains, generating indirect costs that often exceed direct repair costs [6].

c) **Socio-Economic Impact:** The breach of vital links isolates populations, compromising access to essential services (healthcare, emergency services) and exacerbating territorial inequalities, particularly in regions with low network density [7]**.**

The Mediterranean "Hotspot" and the Algerian Case

This vulnerability is particularly critical in **the Mediterranean basin**, identified by the **IPCC** (Intergovernmental Panel on Climate Change) as a climate change "**hotspot**," warming **20%** faster than the global average. This region frequently experiences flash floods of extraordinary violence, capable of devastating infrastructure within hours [8], [9].

Algeria, through its geographical position and climatic characteristics, tragically illustrates this reality. Floods(whether fluvial or pluvial) represent a major and recurring risk [10]. Catastrophic events in the country's recent history [11] highlight the growing vulnerability of urbanized areas and the critical infrastructure serving them. In this context, securing the national road network, the backbone of development, has become an absolute priority for civil security and economic sovereignty. Managing this risk is now a central pillar of public policy to ensure citizen safety and the sustainability of socio-economic development.

1.2 Problem Statement

Evaluating the vulnerability of road infrastructure is a multidimensional challenge that faces physical, methodological, and operational **bottlenecks**.

a) The Challenge of the Linear Asset (Field): Roads are complex structures traversing heterogeneous environments over hundreds of kilometres. This linear nature exposes the infrastructure to extreme spatial variability in flood hazards, making a homogeneous analysis difficult [12]. Capturing this diversity of impacts(from plain submersion to embankment erosion and debris flows in mountainous areas [13]) requires moving beyond point-based analysis [14].

b) The Methodological Challenge (Tools): There is a fundamental disconnect between analysis scales. Territorial tools (GIS) are often too coarse to accurately represent the geometry of the structure, while civil engineering tools (BIM) often ignore the broader hydrological context. This "**scale gap**" prevents the precise quantification of Fluid-Structure Interaction and its complex consequences, such as bridge pier scouring [15]. How can investments be prioritized if the diagnosis remains blurred? [16]**.**

c) The Decisional Challenge (Management): Faced with this diagnostic uncertainty, choosing mitigation and adaptation solutions (structural or non-structural) becomes hazardous. The difficulty in assessing their actual effectiveness in specific contexts complicates decision-making for managers [17]. **How can investments be prioritized when the diagnosis is unclear?** [18]**.**

Central Question:

The core problem of this thesis is: **How can an integrated methodological framework be constructed to link territorial analysis (Macro) to structural diagnosis (Micro) to guarantee the resilience of road infrastructure against flood hazards?**

1.3 Research Questions

To address this problem, our work is structured around three fundamental questions:

- **RQ1 (Macro Scale / Identification):** How can flood susceptibility zones be effectively identified and prioritized across a vast, heterogeneous territory despite data uncertainty?
- **RQ2 (Micro Scale / Diagnostics):** To what extent does the integration of BIM technologies and hydrodynamic modelling allow for the precise quantification of the physical and functional vulnerability of critical road infrastructure?
- **RQ3 (Solutions / Resilience):** What risk treatment strategies (structural, organizational, or nature-based) can be derived from this diagnosis to strengthen the long-term resilience of the network?

1.4 Research Scope and Methodology

To overcome the identified scientific barriers, this thesis proposes the development and validation of an innovative methodological framework based on the **BIM-GIS integration**. Our core hypothesis is that combining the macroscopic vision of GIS with the microscopic precision of BIM bridges the "**scale gap**," offering a diagnostic that is both more comprehensive and more accurate [19].

This scientific strategy is divided into two complementary phases:

a) **High-Fidelity Diagnostics:** Through BIM-GIS-Hydrodynamic coupling, we integrate the micro-topography of the structure into territorial simulations. This fusion allows for the precise quantification of physical interaction (depth, velocity) and the functional vulnerability of infrastructure, where traditional methods fall short [6].
b) **Resilience Strategy:** Based on this diagnosis, we explore sustainable mitigation solutions. In particular, we evaluate the potential of the **Sponge City** concept to reduce runoff at the source, acting as a passive resilience lever to relieve the network [20].

Geographical Focus:

This approach is applied to **the Mitidja Plain**. This territory was selected for its critical representativeness: it combines a flat topography prone to water stagnation, rapid urbanization causing soil sealing [21], and an exceptional concentration of vital infrastructure exposed to torrential floods, providing an ideal laboratory to test our multi-scale approach.

This doctoral research is conducted within the framework of the **PRFU National Research Project (Code: A12N01ES161320230001)**, entitled **'Diagnostic and mapping of road infrastructure vulnerability in the Algiers region to flood and landslide hazards - Using the BIM-GIS alliance'**. Key methodological developments and preliminary results of this work were notably presented and discussed during the **CCRTI 2025 seminar**.

1.5 Thesis Structure

This manuscript is organized into five progressive parts:

Part I: Conceptual Framework and Tools. This section defines key concepts and presents the state-of-the-art in the digital technologies that underpin our approach.
Part II: Multi-Scale Hazard Analysis. This part employs a "funnel approach": starting with regional susceptibility zoning in the **Mitidja**, followed by a detailed characterization of complex morpho-dynamic hazards in the critical **Oued Chiffa** basin.
Part III: High-Fidelity Diagnostics (Micro). This is the methodological core. It details the **BIM-HDM Framework**, validated on the **RN1** (national road) case, demonstrating how geometric precision transforms functional vulnerability diagnostics regarding submersion.
Part IV: Resilience Strategies. This section explores risk treatment solutions, ranging from structural and non-structural protection measures to sustainable "Sponge City" approaches for flood management.
Part V: Synthesis and Recommendations. The work concludes by proposing an operational roadmap for infrastructure managers.

PART I:

CONCEPTUAL FRAMEWORK AND RISK CONTEXTUALIZATION IN THE MITIDJA PLAIN

2 Flood Risk and Infrastructure Vulnerability: Concepts and Challenges

2.1 Introduction

The Necessity of a New Analytical Paradigm

The concept of risk embodies humanity's systemic and permanent confrontation with the forces of nature. Among these threats, flooding holds a predominant position on a global scale, both due to its recurring frequency and its increasing destructive capacity. As **Smith and Ward** emphasize in their seminal work, water is no longer merely a resource; it has become the primary vector for natural disasters [22].

Today, the study of this phenomenon is no longer just an academic choice, but an imperative necessity dictated by an alarming reality: **the global intensification of hydrological disasters.**

The Breakdown of Stationarity and Dual Pressures

We are thus witnessing an epistemological shift: the global scientific community now acknowledges that "**stationarity is dead**" [23]. Historical hydrological data are no longer sufficient to predict the future [24]. Recent reality serves as a cruel reminder: the Derna catastrophe in Libya (2023), occurring in a semi-arid context previously considered at moderate risk, and the extreme Mediterranean episodes in Spain, demonstrate that rainfall intensities now exceed the historical records upon which our protection models were based. These events corroborate historical analyses suggesting that we have entered a new era of hydrological uncertainty [25].

From Hazard to Risk: Integrating Consequences

Faced with this growing uncertainty, it is imperative to revisit our understanding of flood risk. The answer lies in the operational distinction between two notions that have long been conflated:

a) **Hazard:** The flood as a raw physical phenomenon (the danger itself).

b) **Risk:** The probability that this danger will result in damage to exposed assets [26].

The modern scientific approach lies in this integration of consequences: water is not feared for itself, but for the destruction it inflicts upon the human sphere.

Towards a Systemic Approach: Vulnerability and Resilience

The history of risk management reflects the evolution of societies: we have moved from **resigned submission** (*fatum*) to a commitment to **proactive management**. Consequently, research has shifted from an exclusive focus on Hazard control (dikes, dams) toward a systemic vision centred on **Vulnerability and Resilience** [27]. To manage risk effectively, it is no longer enough to understand the threat; one must understand how the human-built environment will react and recover [28].

The Critical Stake: Road Infrastructure

This is where the strategic importance of road infrastructure crystallizes. A road is not merely a construction; it is Critical Infrastructure (CI). In times of crisis, it becomes the vehicle for survival(the fundamental pillar for evacuation plans and emergency response [29]. Studying the vulnerability of roads is, therefore, a quest to guarantee citizen safety and economic continuity [30]**.**

However, a major scientific gap persists, current methods remain siloed. They separate territorial analysis (macro-scale/GIS) from the structural diagnosis of the asset (micro-scale/Engineering), creating an assessment deficit that hinders effective crisis management [6], [12]**.**

Chapter Objectives and Structure

This chapter aims to deconstruct the logical chain of risk to bridge this gap and accurately diagnose the threats facing our infrastructure. To achieve this, we adopt a progressive approach:

Section 2.2: General Theoretical Framework. We trace the evolution of fundamental concepts (Risk, Hazard, Exposure, Vulnerability, Resilience) based on international risk reduction frameworks [31].

Section 2.3: Specific Hazards. We characterize the hydrological and rheological specificities of flood hazards (floods, runoff, debris flows) and synthesize the history of study methods, highlighting their current limitations [32].

Section 2.4: The Critical Asset – The Road. Finally, we analyse the core of our problem: the vulnerability of road infrastructure. This section presents the state-of-the-art regarding physical and functional degradation mechanisms [15] and highlights the need to overcome current silos through the multi-scale, high-fidelity approach that is the subject of this thesis.

2.2 From Hazard to Risk: Definitions and Fundamental Concepts

This section establishes the epistemological foundations of our research by adopting a **genealogical approach**. As suggested by the analysis of the evolution of disaster knowledge [33]**,** scientific concepts are not static; they are products of their time. To build a relevant management model in the face of current climate uncertainties, it is essential to trace the historical evolution of the concepts that structure our thinking [25].

We will analyse how humanity transitioned from a fatalistic vision of danger toward a drive for rational quantification [34], transforming the "**game of dice**" (*alea*) into scientific **Hazard**, and the **maritime reef** (*risicum*) into calculated **Risk**. This conceptual archaeology is not a mere academic exercise; it is necessary to understand why yesterday's linear and stationary models are no longer sufficient to predict tomorrow's crises, as asserted by the famous manifesto "Stationarity is Dead" [23].

By deconstructing the progressive sedimentation of the notions of **Exposure**, **Vulnerability**, and finally **Resilience**, we will demonstrate that the emergence of the latter concept responds to the proven limitations of the absolute control paradigm [27]. This intellectual trajectory leads today to the compelling need for an integrated strategy, capable of capturing the systemic complexity of our road infrastructure [6].

2.2.1 Risk: From Fatality to the Measurement of Uncertainty

To fully comprehend the current complexity of flood management, it is essential to return to the genesis of the concept of "Risk" [35]. This notion, far from being a static constant, has evolved significantly over the centuries, reflecting the shifting relationship between humanity and nature.

History reveals a transition from a perspective of mystical fatalism(where flooding was endured as an inescapable fate or divine wrath [25] (to a rational and scientific construct aimed at taming the future through the quantification of uncertainty [34]. This epistemological shift marks the birth of modern management: ***risk is no longer something that simply "happens" to us, but something we measure to act.***

Etymological Roots: "Risicum" as a Calculated Bet

The etymology of the term provides a fundamental interpretive lens for this study. The word "risk" derives from the medieval Latin *risicum* or *resecum* ("that which cuts"), initially referring to a maritime reef or a submerged rock that threatened merchant vessels [36]**.**

At its inception, the term did not signify the catastrophe itself, but rather the physical proximity to danger. However, a crucial nuance emerged with the historical rise of maritime trade: risk was no longer merely **the presence of the reef**, but **the navigator's voluntary decision** to **approach it** to shorten the journey and maximize profit [25].

Key Insight: From its very origin, risk has been embedded with the notion of strategic choice. It does not arise solely from the violence of nature, but from a **stakeholder's** decision to

expose an asset (the ship of yesterday, the infrastructure of today) to uncertainty in pursuit of economic benefit. This same mechanism of a "calculated bet" governs modern urbanization in flood-prone areas: the risk is accepted to capitalize on the socio-economic attractiveness of the territory [37].

Historical Evolution: From "Fatum" to Management

The history of humanity's relationship with flooding illustrates a progressive shift from submission to quantification.

Absolute Peril (Antiquity to the Middle Ages): Floods were perceived as manifestations of divine wrath or destiny (*fatum*). The societal response was limited to resignation or liturgical interventions. Within this paradigm, "risk" did not exist as an object of scientific study, as these events were deemed unmanageable by human means [25].

Calculated Bets and Insurance (The Renaissance to the Enlightenment): With the rationalization of thought, society sought to "tame the future." Risk became the raw material of insurance, centred on the pooling of potential losses. This period marks a major conceptual breakthrough: while the hazard remains a natural occurrence, its consequences become financial and remediable [36].

Modern Quantification and its Limits: From Engineering to Complexity

In the 20th century, driven by scientific positivism and statistical hydrology, risk was formalized as a measurable quantity. The objective was no longer to ward off fate, but to "formulate the future." This quest for rationality manifested through the application of Probability and Extreme Value Theory (EVT) to define normative return periods, effectively converting natural uncertainty into engineering data [38].

However, this technocratic approach long fostered a dangerous illusion: the belief in the total mastery of nature through "**Hard Engineering**" (dikes, dams). As Smith and Ward analyse, this "**Flood Control**" paradigm often led to a false sense of security, encouraging the occupancy of risk-prone areas behind protective structures a phenomenon often exacerbated by the "levee effect" [22].

Yet it is precisely this static vision that has become obsolete today. In the face of global changes, the modern definition of risk can no longer be reduced to a simple mathematical probability; it must integrate the dynamic complexity and interdependencies of exposed systems, marking a necessary shift from control to resilience [27].

In concluding this conceptual genesis, we recognize that risk is a **hybrid** construct, both social and technical. It is formally defined as the convergence of a stochastic threat (the legacy of the "reef") and a planning decision (the legacy of the "navigator"). This fundamental duality mandates, for the remainder of this thesis, a methodological dissociation between the physical event (**Hazard**, which will be discussed next) and its systemic consequences (**Risk** itself).

2.2.2 Hazard (H): The Physics of Chaos

While Risk is a human construct tied to societal choice [36], **Hazard (H)** remains nature's raw and indifferent manifestation.

To grasp this fundamental component, we must examine how science has sought to domesticate an inherently chaotic and turbulent phenomenon, converting it into measurable and predictable data [22]. The history of this quantification reveals a compelling scientific trajectory: the gradual shift from the empirical observation of historical floods to the complex numerical modelling of physical processes [39].

Conceptual Origins: The Contingency of the "Game of Dice"

The term *Aléa* (Hazard) finds its roots in the Latin *aleatorius*, derived from *alea*, literally meaning a "**game of dice**." This etymology is rich in epistemological significance: it embeds the notions of contingency, unpredictability, and pure randomness at the very core of the concept.

Scientific ambition has sought to frame this natural "**roll of the dice**," **moving from a state of submission to one of forecasting** [35]. It was no longer a matter of merely accepting chaos, but of quantifying it through two fundamental vectors:

a) **Time (Frequency):** The probabilistic definition of an event's occurrence [38].
b) **Force (Intensity):** The characterization of the physical magnitude of the phenomenon. In the case of flooding, these characteristics are measured using hydrodynamic parameters such as **water depth** and **flow velocity** [22], [34].

Mastering Time: The Stationarity Hypothesis and its Limits

Hydrology's primary quest has been to predict the "**when**." In the 20th century, this drive for temporal control was formalized through the rigorous application of Extreme Value Theory (EVT) and probabilistic modelling [38].

The central objective was to calculate standardized **return periods (T)** (such as the 100-year flood (Q_{100})) based on the fundamental **stationarity hypothesis**. This paradigm operated under the assumption that climatic "rules of the game" remained constant and that historical statistics provided a reliable mirror of the future [23]. While this approach facilitated the design of the major protection works that structure our modern landscapes [40], it is now being fundamentally challenged by the accelerating intensity and variability of hydrological cycles.

Characterizing Intensity: From Hydrology to Physical Impact

However, knowing *when* the water will arrive is insufficient for estimating damage to infrastructure. It is imperative to characterize the physical interaction between the water and the structure at the moment of impact [6].

We have witnessed a major evolution in intensity indicators, shifting from a macroscopic hydrological perspective to a localized hydraulic focus [34]:

Discharge (Q): Historically, this was the "primary variable" for hydrologists, measuring the total volume of water passing through a specific point in the catchment area [35].

Damage Criteria (H_s, V_s): For vulnerability analysis, discharge remains an abstract value. Consequently, research has shifted toward direct impact variables at the point of contact: **Inundation Depth (H_s)** and **Flow Velocity (V_s)** [15]. These local physical parameters exert the actual hydrodynamic pressure capable of destroying infrastructure or flooding a vehicle engine [41].

Epistemological Shift: The End of Stationarity

Today, the classical definition of Hazard is undergoing a profound crisis. The intensification of climate extremes [2], coupled with anthropogenic pressures such as rapid urbanization [42], has shattered the stationarity hypothesis [43]. As famously proclaimed by [23] in their seminal manifesto: "**Stationarity is dead**." The climate "dice" are now loaded: historical statistical series no longer provide a reliable guide for the future [40]. Consequently, Hazard can no longer be modelled as a cyclic constant but must instead be understood as a non-stationary and evolving variable.

In summary, the study of Hazard has undergone a radical transformation: it has evolved from the passive observation of randomness toward a high-resolution physical characterization of local intensity (H_s, V_s) [32]. However, in the face of accelerating climate change, mere reliance on historical frequency analysis has become obsolete, necessitating the use of dynamic and adaptive predictive models [44].

2.2.3 Exposure (E): From Static Presence to Systemic Assets

While Hazard represents the raw force of nature, **Exposure (E)** reflects the consequences of societal choices. It is the pivotal factor that transforms a neutral natural phenomenon into a risk; as emphasized in the literature, risk remains non-existent in the absence of exposed assets, regardless of the hazard's intensity [27]. This causal relationship is fundamental to the assessment of urban networks, where the mere presence of road infrastructure "activates" the risk potential [45].

Etymology and Primary Meaning: "Exponere"

The concept draws its roots from the Latin verb *exponere*, literally meaning "to put forth" or "to present." Within the "grammar of risk," Exposure refers to the deliberate or involuntary act by which humanity places its assets, activities, and life itself in the trajectory of danger.

Historically, this exposure was often dictated by geographical and economic necessity: communities settled in alluvial zones (**floodplains**) to exploit their fertility and ensure access to water resources, thereby tacitly accepting proximity to hydrological threats [22].

Anthropogenic Acceleration: Urbanization as a Driver of Exposure

The Industrial Revolution and the demographic explosion of the 20th and 21st centuries have radically reshaped the scale of Exposure.

Massive and frequently unplanned urbanization(as exemplified by the critical case of **Greater Algiers**)has led to an unprecedented concentration of capital and populations within high-risk areas [46]. This shift represents more than just a diffuse human "presence"; it is an extreme densification of **high-value assets**. Such a dynamic explains why, even if climatic hazards were to remain constant, disaster-related losses would **increase mechanically** due to the sheer growth of the exposed value (E) [3]**.**

The Critical Infrastructure Turn: The Linear Challenge

The most recent evolution of the concept of Exposure concerns the typology of the assets under consideration. Modern research no longer limits itself to inventorying flooded buildings; instead, the focus has shifted toward **Critical Infrastructure (CI)** [30]**.**

This paradigm shift is central to our study. Unlike a building, which is a **point-based asset**, a road or a railway constitutes a **linear and networked asset** [14]**.**

Linear Specificity: Due to their geometry, these networks inevitably intersect hazard zones over extensive distances, resulting in near-systemic exposure.

Functional Threat: The exposure of a single critical segment (such as a bridge or a strategic interchange) can paralyze the entire network. This was dramatically demonstrated by the 2016 closure of the A10 motorway in France, where localized flooding disrupted a major national corridor [47], [48]**.**

In conclusion, the analysis of Exposure has migrated from a simple cadastral inventory toward a **functional network analysis**. Today, quantifying Exposure (E) is no longer merely about "locating assets"; it involves identifying the **critical nodes** whose failure could trigger a systemic crisis through **cascading effects** [49].

2.2.4 Vulnerability: The Factor Transforming Hazard into Damage

While Exposure determines *what* is affected, **Vulnerability (V)** dictates *how* and *to what extent* the asset will suffer. It represents the intrinsic propensity of an element to sustain damage when confronted with a given hazard [50]. It is the "weakest link" in the risk equation, yet also the most powerful operational lever for modern risk management; indeed, it is technically and economically more feasible to reinforce a bridge than to stop the rainfall [28].

Conceptual Foundations: The Potential for Harm

The term originates from the Latin *vulnerare* ("to wound") or *vulnus* ("a wound"). Etymologically, vulnerability thus denotes the intrinsic capacity to be wounded or harmed. For a long period, through the lens of classical engineering, this "wound" was perceived exclusively from a physical perspective: a failing wall or a breaching dike. During this era, vulnerability was synonymous with raw structural fragility a reductionist view that modern frameworks have since transcended to integrate functional and human dimensions [22].

Conceptual Expansion: Toward Systemic Vulnerability

Beginning in the 1970s, spurred by the **Behavioural Geography** school and in response to catastrophic lessons learned from past disasters, the scientific community realized that mere material resistance was insufficient to explain the full magnitude of disasters.

Consequently, the concept evolved into a more complex, systemic framework. Today, specialized literature [51] agrees on a **tripartite framework** of vulnerability, which is essential for understanding road risk in its entirety:

2.2.4.1 Physical Vulnerability ($V_{Physical}$): Structural Resistance

This is the direct legacy of civil engineering. It measures the mechanical susceptibility of infrastructure to the physical forces of a hazard (hydrodynamic pressure, scouring).

Measurement Tools: It is now quantified using **fragility curves** [52], which correlate hazard intensity (Depth H_s, Velocity V_s) with a probability of physical damage or failure**.**

Aggravating Context: In developing countries, this vulnerability is often exacerbated by a lack of stringent building codes and informal urbanization, as observed in the case of Algiers [46].

2.2.4.2 Socio-Economic Vulnerability ($V_{Socio-Econ}$): Inequality in the Face of Shock

This dimension serves as a reminder that **risk is not democratic**. It measures the capacity of populations and managers to absorb financial and human losses. It depends on resources, preparedness, and governance [53]. A single flood event will not produce the same impact on a wealthy, insured territory as it will on a precarious, marginalized area.

2.2.4.3 Functional Vulnerability ($V_{Functional}$): Service Paralysis

This is the most critical dimension for transport networks [54]. It does not measure the destruction of the asphalt itself, but rather the **loss of service** (accessibility and connectivity). A road may remain physically intact yet be rendered unusable by as little as 30 cm of water; in such a case, it is functionally vulnerable. This failure generates massive indirect damages (detour costs, supply chain disruptions) that often far exceed the direct costs of physical repair [49].

In summary, shifting from **risk analysis** to **vulnerability analysis** represents a transition from identifying the threat to analysing our own internal weaknesses. For road infrastructure, the challenge is no longer just preventing structural collapse ($V_{Physical}$) but ensuring that **serviceability** is maintained ($V_{Functional}$) precisely when society needs it most.

2.2.5 Resilience (A): From Resistance to Adaptive Recovery

The final milestone in this conceptual evolution is the emergence of **Resilience (A)**. Faced with the technical and economic infeasibility of eliminating Hazard or Exposure, risk management underwent a fundamental paradigm shift at the turn of the 21st century: transitioning from the illusory pursuit of absolute control toward a pragmatic capacity for adaptation [27].

Etymology and Metaphor: The Art of the Rebound

The term finds its etymological roots in the Latin verb *resilire*, literally meaning "to leap back," "to rebound," or "to recoil." Initially formalized in **materials science** by [55] to describe the capacity of a physical body to absorb an elastic shock without permanent failure, the concept was subsequently transposed to **ecology** [56] and eventually to **disaster management**. It embodies the philosophy that a system should not merely be "rigid like stone" (static resistance) but "flexible like a reed"(capable of bending under impact **to facilitate a more effective recovery** [57]**.**

Beyond Robustness: A Dynamic Capability

It is scientifically crucial to distinguish between **Robustness** and **Resilience**:

Robustness (frequently correlated with low physical vulnerability) is a static and material-based property: it refers to an asset's capacity to withstand shock without sustaining irreversible structural damage.

Resilience (A) is a dynamic and temporal property. While it encompasses robustness, it also incorporates the systemic capacity to absorb disturbances, adapt during the event (graceful degradation), and(most importantly)**recover** functionality rapidly in the post-crisis phase [27].

Consequently, for road infrastructure, resilience is not measured solely by the thickness of concrete or pavement, but by the speed of traffic restoration and the availability of alternative routes **(network redundancy)** [58].

Holistic Action: Resilience as a Comprehensive Strategy

Resilience is defined as a "**Collective Adaptive Capacity**" [28]. It introduces a **holistic vision** where a wide array of interventions is considered viable, provided they serve the ultimate objective of maintaining system functionality.

Consequently, mitigating hazards through **nature-based solutions (NBS)**(such as wadi restoration or implementing the **"Sponge City"** concept) is no longer perceived as an outdated defensive method. Instead, it is viewed as an environmental adaptation strategy designed to reduce hydrological stress at its source [59]**.**

Ultimately, resilience synthesizes a broad spectrum of societal responses (including **Knowledge, Anticipation, and Reaction**) to minimize net impact. It does so by pragmatically acknowledging the existence of an inevitable yet manageable **Residual Risk** [60].

2.2.6 A Critical Analysis of International Models: Toward a Necessary Synthesis

While risk theory has evolved toward systemic complexity, its operational implementation often remains fragmented across different national doctrines. Each historical model has prioritized a specific strategic lever (**E, H, or A**), giving rise to distinct "schools of thought" whose critical analysis reveals significant limitations when confronted with contemporary challenges.

2.2.6.1 The French Model ("Inondabilité" Method): Spatial Management (E)

The French doctrine (embodied by the "**Inondabilité**" method and Flood Risk Prevention Plans (**PPRi**)) is rooted in a strategy of **spatial avoidance**.

Methodology: It involves overlaying the Hazard (calculated for a 100-year reference flood) with the Assets to produce **Regulatory Zoning**. The response is binary: Red Zones (construction prohibited) or Blue Zones (construction permitted under specific conditions).

Objective: To control **Exposure (E)** by freezing further urbanization [61].

Structural Limitation: This approach is static and essentially defensive. While effective at preventing future urbanization, it is inadequate for managing existing urban fabrics and established infrastructure. It struggles to integrate functional resilience, hindered by a rigid "all-or-nothing" regulatory framework that offers few solutions for living with **residual risk** [62].

2.2.6.2 The American Model (USACE/FEMA): Structural Control (H)

Historically, the United States has epitomized the **Flood Control** paradigm, characterized by technical and insurance-based responses.

Methodology: It relies on the massive construction of hydraulic works (dikes, levees, channels) by the **U.S. Army Corps of Engineers** to contain hazards, coupled with a federal insurance system (**NFIP**) based on Flood Insurance Rate Maps (**FIRM**).

Objective: Physically reduce the hazard (H) to protect assets [18].

Structural Limitation: Catastrophes such as Hurricane Katrina (2005) demonstrated the failure of purely structural mitigation. This model generates a "**levee effect**": a false sense of security that encourages investment behind protective structures. When an event exceeds the design return period (non-stationarity), the system collapses without a "Plan B," revealing a dramatic underestimation of social and functional vulnerability [3].

2.2.6.3 The Japanese Model (DRR): Managing Time and Response (A)

Japan offers a unique counter-perspective. Faced with extreme hazards that are impossible to fully contain, Japan has shifted toward **Disaster Risk Reduction (DRR)**.

Methodology: It combines robust infrastructure with extreme community preparedness (the "**Bosai**" culture of risk, evacuation drills) and adaptive reconstruction (**Build Back Better**).

Objective: To maximize **Resilience (A)** and rapid recovery capacity [25].

Transposability Limits: While this model confirms the crucial importance of resilience, it is technically difficult to generalize. It relies on a specific social contract and collective discipline unique to Japanese culture. This model cannot simply be "imported" to Algeria without first establishing a widespread civic culture of risk.

2.2.6.4 The Case of Algeria: Between Legacy and the Urge for Adaptation

In Algeria, flood management is currently marked by a difficult transition.

Methodology: The approach remains largely focused on classical hydraulic engineering (protection via dams, wadi dredging), a legacy of the **Hazard control (H)** vision. Although regulatory frameworks exist (notably **Law 04-20**), the actual integration of **Vulnerability (V)** into urban planning instruments remains incomplete.

Limitation: There is often a significant disconnect between technical hazard mapping and the reality of land-use planning. Management remains predominantly **reactive** (post-event crisis management) rather than proactive. This leaves critical infrastructure exposed to **cascading failures** due to the lack of prior systemic diagnostics [46].

2.3 Specificities of Flood Hazards and Associated Phenomena

While the concept of "risk" is an intellectual construct aimed at rationalizing uncertainty, flooding remains a stark and tangible physical reality. Long before it became a subject of technical management, the flood was a foundational traumatic experience for humanity, driving a transition from fatalistic resignation to a rigorous scientific pursuit of understanding [25].

This section explores the intrinsic nature of flood hazards. Moving beyond standard hydrological definitions, we will trace the evolution of human perception (from primordial myths of the Great Deluge to **contemporary** hydrodynamic modelling. We will examine the complex physical mechanisms involved) ranging from urban runoff to devastating debris flows which endow this hazard with a highly heterogeneous impact signature. Finally, we will highlight how, in the face of established climate change, flooding has transformed into a systemic, non-stationary threat that defies traditional prediction methods and necessitates a fundamental overhaul of our analytical tools [23].

2.3.1 Genesis and Legacy: Flooding from Archetype to Physical Phenomenon

Flooding holds a unique position in human history. It is arguably the first natural disaster to be universally recorded within the collective consciousness, profoundly shaping our long-term relationship with risk [25]. Long before it became a quantifiable scientific subject, it existed for millennia as a source of myth, dread, and reverence, catalysing the development of early social structures centred on the mastery of water [22].

The Archetype of the Great Deluge: The Foundational Catastrophe

Water, the source of life, carries within it the threat of annihilation. This duality is deeply embedded in the foundational texts of most civilizations. The myth of the **Great Deluge** (*Diluvium* in Latin) transcends eras and cultures, from the Mesopotamian *Epic of Gilgamesh* to the narratives of Genesis in both the Quran and the Bible [22].

In these primordial narratives, flooding is not a random meteorological event but a **cosmic weapon**. It is depicted as a total and purifying rise of waters, submerging the entire world to purge a humanity deemed flawed.

Epistemological Impact: This cultural legacy long fossilized the social perception of flooding. It was viewed as an inevitable punishment (*fatum*) or divine wrath, against which technical intervention was neither conceivable nor permitted. The primordial flood was perceived as a return to **original chaos**(a brutal rupture of the fragile alliance between habitable land and the liquid element [25].

From Etymology to Scientific Definition: The Rationalization of the Phenomenon

The shift from myth to rationality is first reflected in the evolution of language. The term "inundation" (flood) derives from the Latin *inundatio*, which itself stems from *unda* (wave) literally, "the movement of water encroaching upon the land." This movement describes both overflow and submersion [22]. It was only with the advent of modern hydrology and contemporary

legislative frameworks that the definition detached itself from its mythological emotional weight to become objective and operational.

The Standard Definition: According to the European Union Floods Directive (2007/60/EC) and current scientific consensus, a flood is defined as the **"temporary covering by water of land not normally covered by water"** [63]. This definition marks a major intellectual breakthrough in three key aspects:

a) **Temporality:** The event is characterized as "temporary," rendering it finite in duration.
b) **Spatiality:** It precisely delineates the phenomenon as the overflow from the **river channel** (low-water bed) into the **floodplain** (high-water bed), thereby distinguishing the river's natural domain from human territory [22].
c) **Physical Causality:** Flooding is no longer viewed as divine fate, but as the mechanical result of a localized hydrological imbalance.

This **desacralization** of the phenomenon facilitated the transition **from the priest to the engineer**: if flooding is an observable physical phenomenon, it can be studied, measured, and, to a certain extent, anticipated [24].

2.3.2 Mechanisms and Typology: The Physical Classification of Floods

Fundamentally, a flood is defined as the temporary intrusion and accumulation of an uncontrolled volume of water onto land surfaces [22]. From a physical perspective, it represents a **breach of confinement**: water escapes its natural boundaries (such as the **main channel** (*lit mineur*) or the shoreline) or its artificial constraints to occupy **anthropogenic space**.

However, treating "water" as a uniform and abstract variable would constitute a major methodological error in risk engineering. The landmark work by [22] establishes the fundamental **taxonomic distinction** that structures modern hydrology. Floods are not a homogeneous entity; instead, they are divided into two primary families defined by their **geographic origin** and the **governing geophysical forces**:

a) **Marine-Sourced Floods (Coastal Flooding):** Where the threat is an external intrusion, driven by atmospheric forcing (storm surges) or tectonic events (tsunamis).
b) **Inland Floods (Fluvial/Pluvial Flooding):** Where the threat is generated from within the territory itself, through the **hydrological response** of a catchment area (watershed).

This dichotomy is not merely academic; it dictates the nature of the physical equations to be employed(**wave mechanics** versus **open-channel hydraulics**(as well as the corresponding protection strategies [32].

2.3.2.1 The Primary Distinction: Marine versus Inland Origins

This binary classification constitutes the first level of risk analysis. It is fundamental because it defines the **boundary conditions** of the system; it dictates not only the physicochemical nature of the fluid but also the forcing mechanisms that initiate the hazard [22].

The Marine Family (Coastal Flooding): External Aggression

In this scenario, the flood is characterized by marine intrusion.

Forcing Mechanisms: The hazard results from a **storm surge** driven by atmosphere-ocean interaction. This combines the "inverse barometer effect" (where low pressure sucks the water level upward) and **wind stress**, which pushes water masses toward the shoreline [64].

Impact Specificities: For infrastructure, this family presents a unique level of aggressiveness. Beyond the kinetic energy of the waves, saltwater introduces major **chemical aggression** (steel corrosion and **chloride-induced attacks**), often rendering structural damage irreversible [65].

The Inland Family (Inland Flooding): The Endogenous Catchment Response

This family encompasses freshwater phenomena, which are the focus of our study in the Mitidja Plain. Unlike marine flooding, which attacks from the boundary, inland flooding is an **endogenous product** of the territory.

Fundamental Mechanism: It is the physical manifestation of a disruption in the **hydrological balance** (water balance) at the watershed scale. Flooding occurs when the atmospheric input (Precipitation, P) exceeds the combined storage capacity (Infiltration, I) and transfer capacity (Discharge, Q) of the system[66].

Saturation: The saturated watershed loses its function as a **regulating buffer**. The excess water, unable to infiltrate or drain rapidly enough, is forced to **spread laterally**, transforming the landscape into a temporary storage zone [67].

2.3.3 Physics of Inland Flooding: A Scientific Causal Chain

Within the inland family, flooding must not be perceived as a mere **stochastic** event, but rather as the deterministic culmination of a complex, sequential physical process [22]. To accurately model the threat to infrastructure, engineers must deconstruct this phenomenon into three distinct scientific domains, each governed by its own conservation laws and epistemological boundaries [32].

This disciplinary segmentation is operational for diagnostic purposes:

a) **Hydrology (Statistical Genesis):** Quantifies the available water volume (m^3) based on climatic probabilities and precipitation time series [68].
b) **Hydraulics (Mechanical Propagation):** Governs the spatial distribution of energy (**depth** and **velocity**) according to the laws of gravity and fluid mechanics [69].
c) **Rheology (Material Behavior):** Defines the intrinsic nature of the fluid and its destructive capacity based on its **sediment load**, distinguishing clear water from **debris flows** [70].

It is only through the coupling of these three disciplines that one can transition from rainfall forecasting to the reliable estimation of structural damage.

2.3.3.1 Hydrological Genesis: The Complexity of the Rainfall-Runoff Transformation

The first link in the causal chain is the transformation of a meteorological signal (precipitation) into a flood hydrograph (discharge). While the underlying principle rests on the simple conservation of mass, its modelling remains one of the most daunting challenges in modern engineering. Indeed, a catchment area is not a linear system; it is a complex entity governed by thresholds, hysteresis, and cumulative uncertainties that make prediction particularly delicate [71].

Mass Balance and the "Error Term" (ϵ)

Theoretically, a watershed acts as an open system where the runoff volume (R) is the mathematical residual of a classical hydrological balance ($P\,(\boldsymbol{Precipitation}) - I(\boldsymbol{Infiltration}) - E(\boldsymbol{Evapotranspiration})$)[22]. In practice, however, every term in this equation is an estimate fraught with uncertainty. The actual equation must therefore include an **error term (ϵ)** to account for the structural uncertainty stemming from limited knowledge of subsurface processes and the spatial variability of rainfall(given that a point-based weather station can never perfectly represent the heterogeneity of an entire basin [72].

Temporal Dynamics: Response Time (t_c)

Hydrology extends beyond mere volume; it examines the speed of reaction through **the Transfer Function**. The central question is kinetic: how does a raindrop falling upstream reach the outlet?

Time of Concentration (t_c): This is the pivotal variable. It theoretically represents the time required for a drop of water from the hydraulically most distant point to reach the outlet [73].

The Acceleration Problem: In natural basins, vegetation slows the flow (long t_c, leading to attenuated floods). Conversely, in urbanized basins or on saturated soils, surface roughness decreases drastically. The $t_c$collapses, transforming average rainfall into a flash flood with an instantaneous **peak discharge (Q_{max})**. It is this violent response rate that surprises and destroys infrastructure [74].

Transformation Models and Their Limitations

To mathematically transform Rainfall (P) into Discharge (Q), engineers utilize four main families of approaches, each with its own **intrinsic biases**:

a) **Empirical Approach (Rational Method $Q = CIA$):** Widely used for small road structures, it assumes a perfect linearity between rainfall and discharge. This hypothesis is flawed for large, complex basins and completely neglects storage effects [75].
b) **Conceptual Approach (Unit Hydrograph):** Based on **convolution theory**, it assumes the basin always reacts identically to a unit impulse. It fails to reproduce non-linear behaviours during extreme events, such as threshold [32].
c) **Physical Approach (Infiltration Laws):** This uses explicit equations (e.g., Horton, Green-Ampt) to model infiltration loss $I(t)$ as a function of soil saturation. The primary challenge is that these equations require soil parameters (such as **hydraulic conductivity**) that are often unknown at the scale of a heterogeneous basin, introducing **equifinality uncertainty** [76].

d) **Data-Driven Approach (Artificial Intelligence):** More recent methods employ Recurrent Neural Networks (such as **LSTM**) to learn the rainfall-runoff relationship without explicit physical modelling. Its limit lies in its dependence on training data: it cannot reliably predict events never seen in historical records [77].

Spatial Representation: From Lumped to Distributed Architectures

As classified in the review by [78] , technological evolution has allowed for a transition across three distinct architectures:

- **Lumped Models:** The historical "black box" approach. The entire basin is treated as a single entity with averaged parameters.
- **Semi-Distributed Models:** The basin is divided into connected sub-basins, allowing for a first level of spatialization.
- **Distributed Models:** Enabled by the digital revolution (**DEM/GIS**), these models solve physical equations at the scale of each elementary grid cell, finally capturing the spatial heterogeneity of the phenomenon.

Conclusion on Complexity: The Probabilistic Imperative

The quantification of hydrological input cannot be reduced to an exact deterministic value; it intrinsically represents a range of probabilities. The error in estimating **peak flow (Q_{peak})** is not trivial: it propagates and amplifies during the next stage (**Hydraulics**), potentially distorting the calculation of **inundation depth (H_s)** on the roadway. This is why pure deterministic approaches are reaching their epistemological limits when faced with the stochastic complexity of the water cycle, necessitating the explicit inclusion of uncertainties in impact models [6].

2.3.3.2 Hydraulic Transformation: From Fluid Chaos to Numerical Modelling

Once the water volume is generated by the watershed, the nature of the problem shifts fundamentally. We move from the realm of hydrological statistics into the field of **Fluid Mechanics**. The challenge is no longer to predict a probability, but to simulate the physical movement of a deformable water mass over complex topography [22]. This transition necessitates solving the fundamental equations of **conservation of mass** and **momentum** to spatialize the flow energy [32].

The Physical Reality: The Navier-Stokes Challenge

In absolute reality, the movement of any flood is governed by the **Navier-Stokes equations**. These are the universal laws describing the motion of real (viscous) fluids [71]. They express the conservation of momentum (Newton's second law) applied to a fluid particle. The vector equation represents a balance of four competing forces:

$$\underbrace{\rho \frac{D\vec{v}}{Dt}}_{\text{Inertia}} = \underbrace{-\nabla p}_{\text{Pressure}} + \underbrace{\mu \nabla^2 \vec{v}}_{\text{Viscosity}} + \underbrace{\rho \vec{g}}_{\text{Gravity}}$$

The Core Problem: The Viscosity Term ($\mu\nabla^2\vec{v}$)

This term describes the internal friction between water molecules. It is the source of **Turbulence**, a chaotic phenomenon where energy dissipates into vortices of varying scales, rendering motion unpredictable at the microscopic level [79].

Mathematically, the exact resolution of these turbulences (**DNS - Direct Numerical Simulation**) for a flood at a city scale is impossible, as it would require near-infinite computational power. This physical constraint forces engineering to rely on averaged models (**RANS - Reynolds-Averaged Navier-Stokes** or Saint-Venant equations) [71].

Engineering Simplification: The Saint-Venant Equations (SWE)

To make the problem solvable and operational for risk management, fluvial hydraulics employs a radical simplification. The complex 3D model is reduced to a 2D averaged model governed by the **Shallow Water Equations (SWE)**. These equations, a two-dimensional generalization of the Saint-Venant model, constitute the core of standard software such as HEC-RAS or TELEMAC [80].

This transition rests on two major physical hypotheses:

a) **The Hydrostatic Hypothesis (Shallow Flow):** It is assumed that the water depth is negligible compared to its horizontal width. This allows for vertical accelerations to be ignored, reducing the problem from 3D to 2D.

b) **Rheological Simplification (Friction):** Instead of calculating the actual internal viscosity (μ) responsible for turbulence, it is replaced by an empirical law for bed friction (**Manning-Strickler roughness coefficient** n).

Physical Significance: Energy dissipation is no longer considered to result from the water rubbing against itself, but solely from its friction against the bed (channel roughness) [81].

Hazard Vectors: Energy and Impact

The numerical resolution of these equations on a **Digital Elevation Model (DEM)** transforms the global discharge into two local vectors that define the hydraulic hazard [82].

- **Inundation Depth (H_s):** This reflects the **Potential Energy** of the water column. It exerts **Hydrostatic Pressure** ($P = \rho g H_s$). This is the static constraint that floods low-lying areas and saturates porous materials [15].
- **Flow Velocity (V_s):** This reflects the **Kinetic Energy** of the fluid. It exerts **Dynamic Pressure** ($q = \frac{1}{2}\rho V_s^2$). This is the dynamic constraint that generates direct thrust forces.
    - If the velocity is moderate (**Subcritical Flow**, $Fr < 1$), the flow is fluvial: the water manoeuvres around obstacles smoothly.

- If the velocity is high (**Supercritical Flow**, $Fr > 1$), the flow is torrential: inertia dominates gravity. The water no longer bypasses the obstacle but strikes it with a shockwave (**hydraulic jump**), maximizing destructive potential [16].

Critical Conclusion: The Triad of Uncertainty

This mechanics demonstrates that the reliability of a flood model depends not only on the physics of the equations but on the quality of its three fundamental input parameters. Since the chaos of the Navier-Stokes equations makes the system hypersensitive to **initial conditions**, any error in these factors is amplified in the result:

a) Hydrological Uncertainty ($Q(t)$): If the peak flow estimate is biased (ϵ), the model simulates an incorrect volume from the outset [72].

b) Parametric Uncertainty (n): The Manning coefficient is a subjective empirical value. An incorrect estimate distorts the propagation velocity [32].

c) Geometric Uncertainty (z): This is the **decisive factor**. The equations calculate motion based on the **hydraulic gradient** (energy slope). If the DEM is imprecise (low resolution), the local slope is incorrect, and the water is misdirected [76].

While hydrological error (Q) affects the overall volume, **geometric error (z) is critical for infrastructure vulnerability analysis**. A coarse DEM can "erase" a road embankment. Consequently, even with a perfect discharge estimate, a poor terrain model will inevitably lead to an erroneous diagnosis of the structure **(Chanjin Jeong et al., 2023)**.

2.3.3.3 Rheological Distinction: The Physics of Matter

Any hydraulic modelling rests upon a fundamental assumption regarding the nature of the matter itself: the fluid's rheological properties. In a continental context, a flood is never purely water; it is a **biphasic mixture** (water and solids). As it flows, the water erodes the soil and transports sediments, the proportion of which radically alters the viscosity and the physical laws governing the flow [70].

The operational validity of fluid mechanics equations depends strictly on the **rheology of the mixture**. The landmark classification by [83] identifies three critical regimes based on the **Volumetric Sediment Concentration (C_v)**:

a) Water Flood [$C_v < 20\%$]: The Newtonian Domain

Physical Nature: The fluid is **Newtonian**. Shear stress remains linearly proportional to the strain rate (constant viscosity).

Modelling Validity: This is the strict domain of validity for the **Saint-Venant equations**. Standard software packages (HEC-RAS, TELEMAC) are perfectly applicable here and provide reliable results [80].

b) **Hyper concentrated Flow [$20\% < C_v < 47\%$]: The Transition Zone**

Physical Nature: A transitional fluid. Apparent viscosity increases, turbulence is dampened, and the mixture becomes "muddy."

Consequences for Infrastructure: Although the fluid remains mobile, its erosive capacity is magnified by the **abrasive load**. This significantly increases the risk of **scouring** around engineering structures, where clear water would have simply flowed by without causing damage [16].

c) Debris Flow [$C_v > 47\%$]: The Non-Newtonian Breakthrough

Physical Nature: The fluid becomes **non-Newtonian** (often a **Bingham-type Visco-plastic**). The solid phase dominates the liquid phase.

Mechanical Specificity: The mixture acquires a **yield strength**. It possesses internal cohesion, allowing it to transport large boulders in "suspension." This is no longer a mere flood; it is a **fluidized landslide** [70].

Major Scientific Consequence: The Saint-Venant equations are no longer valid. Applying a standard flood model to a debris flow constitutes a fundamental physical error. It neglects the density of the material, drastically underestimating the **ballistic impact forces** on structures and the bed's potential for **obstruction** [32].

The Physical Limits of Models

The study of rheology is not an abstraction. It reveals a fundamental limitation of conventional hydraulic models, which implicitly rely on the Newtonian fluid assumption (water).

- **The Fallacious Postulate:** The assumption that water consistently behaves as a constant-viscosity fluid is invalidated when faced with hyper concentrated flows and, critically, debris flows ($C_v > 47\%$).
- **The Consequence:** The Saint-Venant equations (the cornerstone of engineering software (are not valid for these phenomena. Applying a standard flood model to a debris flow, such as those threatening mountainous regions (e.g., the **Blidean Atlas**), is a fundamental physical oversight. It leads to a dramatic underestimation of the hazard's actual intensity (impact force, clogging capacity) on structures [70].

This gap highlights the imperative, for a reliable diagnosis, of precisely identifying the physical nature of the fluid. It underscores that "**high-fidelity**" pertains not only to the geometry of the structure but also to the physics of the attacking fluid, necessitating an adaptation of simulation models.

2.3.4 Continentals Operational Classification of Inland Flooding

For the road engineer, a granular understanding of **kinematics** (rise rate, response time) and **rheology** (Newtonian vs. viscoplastic nature of the fluid) is essential for categorizing hazards. By intersecting these physical variables, we establish a typological reference that defines the precise nature of the aggression against the road network [6]. This classification is not merely

descriptive but operational: it dictates the selection of protection measures tailored to each hydraulic regime [22].

2.3.4.1 Pluvial Flooding (Urban Runoff): "Upstream Drainage Saturation"

- **Origin:** Occurs through direct precipitation on impervious or saturated surfaces, before the water even reaches the natural hydrographic network [84].
- **Rheology:** Newtonian fluid (often carrying urban pollutants).
- **Kinematics:** Near-instantaneous response to rainfall intensity.
- **Impact Signature:** The risk is primarily **functional**. Although inundation depths are often moderate, they cause immediate paralysis of urban mobility (aquaplaning, waterlogged engines, sewer system surcharging). The infrastructure is not physically destroyed, but it instantly loses its serviceability [85].

2.3.4.2 Riverine Flooding (Plain Flood): "Systemic Overflow"

- **Origin:** Gradual overflow of a watercourse from its main channel into the floodplain, generally following prolonged precipitation over a large catchment area [12].
- **Rheology:** Newtonian fluid.
- **Physical Signature:** Slow kinematics (rise and recession over several days), low flow velocity (V_s), but significant inundation depth (H_s) and prolonged stagnation.
- **Impact on Roads:** The danger here is **delayed and structural**. Prolonged immersion leads to the soaking of the **pavement structure** and the saturation of foundation soils. The resulting **loss of bearing capacity** (drop in CBR - California Bearing Ratio) causes major distresses(such as **fatigue cracking**, **potholes**, and **rutting**(which often appear several weeks after the floodwaters have receded [86].

2.3.4.3 Flash Floods: "Kinetic Violence"

- **Origin:** A sudden response of small or steep watersheds (dry wadis) to intense convective storms [87].
- **Rheology:** Newtonian to hyper concentrated fluid (significant sediment transport).
- **Physical Signature:** Violent kinematics (response time < 6h), **steep wave fronts**, and very high velocities (V_s).
- **Impact on Roads:** The risk is both **lethal and structural**. The kinetic energy of the fluid generates hydrodynamic pressure capable of sweeping away vehicles [3] and **scouring bridge piers** [15]. This is the deadliest hazard for road users due to the "surprise effect."

2.3.4.4 Debris Flows: "The Geotechnical Projectile"

- **Origin:** Massive mobilization of sediment, woody debris, and boulders in high-gradient areas (e.g., the Blidean Atlas).
- **Rheology:** Non-Newtonian fluid (Visco-plastic behaviour).
- **Physical Signature:** High bulk density (up to 2.2 t/m^3), colossal impact force.

- **Impact on Roads:** Here, we move beyond hydraulics into the realm of **dynamic geotechnics**. The flow acts as a **battering ram**: it does not bypass the obstacle; it strikes and buries it. The consequences are often irreversible: destruction of bridge piers by ballistic impact, total clogging of drainage structures, and the complete disappearance of the **road platform** under meters of debris [70].

2.3.4.5 Methodological Synthesis: The Imperative for Physical Discrimination

This classification demonstrates that flood hazards cannot be reduced to a uniform phenomenon; they constitute a **complex physical matrix** whose properties vary radically across contexts. A major methodological error in current engineering often involves applying a standard hydraulic model (designed for Newtonian water in plains) indiscriminately across a territory, including mountainous areas threatened by non-Newtonian debris flows. Effective risk management thus requires prior **physical discrimination**: it is imperative to identify the rheological and kinematic nature of the process (P) for each road segment to select the appropriate simulation tool (Hydraulics vs. Geotechnics). This level of physical diagnostic precision is what fundamentally determines the validity of all subsequent vulnerability assessments.

2.3.5 The Methodological Evolution of Hazard Assessment: From Hydrological Theory to Operational Decision-Making

Flood hazard assessment should not be conflated with mere hydrological or statistical analysis. A fundamental distinction exists between the **Theoretical Objective**, which aims to intrinsically characterize the phenomenon (its frequency and raw intensity), and the **Practical Objective**, which focuses on quantifying its consequences to inform **Decision-Making** regarding land-use planning and protection strategies [39].

To be operational, engineering must return to the foundational definition of a flood: a phenomenon that is **spatially delineated**, **temporally finite**, and **physically aggressive**. Consequently, the evolution of hazard assessment methodologies can be interpreted as a progressive effort to address three decisive questions for engineers:

a) **Where will it occur?** (Spatiality of the threat)

b) **When will it happen?** (Temporality and probability)

c) **What force will it exert?** (Physical intensity and impact)

Accordingly, we structure this state of the art into three functional categories corresponding to these key questions, each drawing upon distinct scientific disciplines [24].

2.3.5.1 Qualitative and Semi-Quantitative Methods: Predicting the "Spatial" Dimension (Where?)

The primary objective of these methods is **Spatial Delineation**. They seek to identify exposed zones (zoning) and prioritize their intrinsic susceptibility without necessarily quantifying the physical power of the phenomenon.

Historical and Naturalist Approaches (Qualitative Assessment)

These constitute the original empirical methods, which remain essential for calibrating any model.

- **The Historical Approach (Memory):** This relies on recording flood marks (*laisses de crues*), analysing archives, and determining the **Highest Known Water Levels (HKWL)**. While it provides an irrefutable reality ("the water has reached this point before"), it remains fragmentary and lacks predictive power in the face of climatic non-stationarity [88].
- **The Hydro-Geomorphological Approach (Landscape Interpretation):** Before the advent of numerical modelling, geographers defined the river's **freedom space** (floodplain, alluvial terraces) through stereoscopic analysis. This is a highly robust method that defines the maximum possible flood extent, independent of rainfall statistics [89].

Spatial Index-based Approaches (Semi-Quantitative Prioritization)

Faced with the need to cover vast territories that are often **data-scarce regions**, engineering has developed methods based on relative indices, drawing on satellite imagery and multi-criteria analysis.

- **Remote Sensing (Space-based Observation):** The use of satellite sensors (optical such as Sentinel or Radar SAR) allows, via spectral indices (e.g., **NDWI**), the extraction of flooded areas following an event. Although effective for post-flood assessment, it only measures the 2D surface area and remains dependent on weather conditions [90].
- **GIS Morphometric Analysis:** This method utilizes Geographic Information Systems to calculate purely topographical indices (such as the **Topographic Wetness Index (TWI)** from Digital Elevation Models (DEMs). It identifies potential accumulation zones based solely on terrain geometry [66].
- **AHP-GIS Coupling (Weighted Expert Opinion):** This is the most advanced method for preventive mapping. It enhances morphometric analysis by integrating expert judgment via the **Analytic Hierarchy Process (AHP, Saaty 1980)**, a robust and long-standing decision-making weighting method (*An Exposition on the AHP*). By weighting the relative influence of each factor (Slope vs. Soil vs. Rainfall), this coupling produces a spatialized **Susceptibility Index** that allows for a granular prioritization of risk [91].

Decision-making Application: These methods support **Avoidance Strategies (Planning)**. They help define non-buildable zones; however, as their output is a relative index without physical units, they are unsuitable for the technical design and dimensioning of **civil engineering structures** (bridges and culverts).

2.3.5.2 Statistical Hydrological Methods: Predicting the "Temporal" Dimension (When?)

These methods represent a paradigm shift: they move away from spatial considerations to focus on **Frequency**. The core objective is to link an event to a **probabilistic timescale** to manage uncertainty.

- **Frequency Analysis:** This involves fitting probability distributions such as Gumbel, Generalized Extreme Value (GEV), or Pearson Type III(to measured **discharge time series** [92].
- **Decision-making Application:** This is the primary tool for the **regulatory and insurance** sectors. It enables the definition of a legal reference flow (Q_{100}), serving as the "acceptable risk" threshold for the design and dimensioning of structures [38].
- **Critical Limitation:** This is essentially a **0D or point-based approach**. While it provides the discharge at the **watershed outlet**, it remains silent on the spatial propagation of the flood (i.e., where exactly the banks overflow) and localized water depths. Consequently, it is insufficient for a comprehensive infrastructure vulnerability diagnosis [40].

2.3.5.3 Hydrodynamic Methods: Predicting Physical Impact (What Force Intensity?)

This represents the ultimate stage of assessment, essential for infrastructure vulnerability diagnosis. It aims to solve the governing laws of fluid mechanics to quantify the energy involved in the phenomenon. According to the review by [78], two levels of increasing complexity can be distinguished:

- **Hydrodynamic Modelling (Propagation):** This approach solves the **Saint-Venant equations** (1D/2D) to propagate a known discharge over a **Digital Elevation Model (DEM)**. It transforms hydrological information into localized **force vectors**: depth (H_s) and velocity (V_s) [80].

- **Integrated Coupled Models (DBCM):** This is the most sophisticated approach for capturing the dynamics of complex flood events. Models such as the **Rainfall-Runoff-Inundation (RRI)** simultaneously solve hydrological (rainfall-runoff) and hydraulic (channel flow) equations, allowing for **dynamic bidirectional interaction**. In these models, water can overflow its banks but also return to the main channel, providing the most realistic representation of the **flood-recession cycle** [93].

Decision-making Utility: This is the primary tool for **Structural Design and Resilience**. It is the only approach capable of calculating whether a bridge will withstand **hydrodynamic thrust** or if a road section is at risk of being **washed out**.

2.3.5.4 The Cross-Cutting Data-Driven Approach: Artificial Intelligence in Flood Research

The current research frontier lies in the integration of **Machine Learning (ML)** and **Deep Learning (DL)**. Its unique strength is its cross-cutting capability to enhance or accelerate the three approaches:

- **For Spatial Susceptibility:** Ensemble learning algorithms, such as **Random Forests (RF)** or **Support Vector Machines (SVM)**, now frequently outperform traditional AHP methods in mapping high-risk zones by learning complex correlations from historical events [94].

- **For Temporal Discharge Forecasting:** Recurrent Neural Networks, specifically **Long Short-Term Memory (LSTM)** architectures, predict peak flows with accuracy comparable to physical models but at near-instantaneous computational speeds[77].
- **For Physical Impact Estimation:** AI facilitates the real-time estimation of localized inundation depths (H_s) using **IoT sensor data**, bypassing the high computational overhead of hydrodynamic modelling for **early warning systems** [95].

Key Limitation: These remain "**Black Box**" models, highly dependent on the quality and volume of the training data. If an extreme event is not represented within the historical training set, the model's predictive capability fails a phenomenon known as **extrapolation error** or the **generalization gap**.

2.3.5.5 Strategic Synthesis: Aligning Methodologies with Decision-Making Scales

The review of the state of the art demonstrates that no single hazard assessment method is inherently superior in absolute terms; rather, each address specific decision-making questions based on a logic of **scale, cost, and purpose**. The choice of tool ultimately dictates the scope of the management strategy:

- **Spatial Methods →Avoidance Strategy:** Ideal for large-scale urban planning ("Where should we not build?"), yet insufficient for structural engineering and dimensioning.
- **Statistical Methods → Regulatory Strategy:** Essential for establishing legal reference standards (Q_{100}) and defining "acceptable risk" thresholds, but "blind" to the localized physical reality of submersion.
- **Hydrodynamic (Physical) Methods →Resilience Strategy:** Indispensable for the technical diagnosis of vulnerability ("Will the structure withstand the impact?").

Conclusion for this Thesis: This study prioritizes the **Hydrodynamic approach** for the vulnerability assessment of critical infrastructure. However, to be fully effective, this method must imperatively bridge the **"scale gap"** by integrating the micro-topography of the structure.

2.4 The Critical Stake: The Vulnerability of Road Infrastructure

Having deconstructed the complex mechanics of flood hazards, it is now imperative to focus on the primary target of our research: **Road Infrastructure**.

Far from being merely passive stretches of asphalt, roads constitute the "vital arteries" (**lifelines**) that sustain the flow of modern territories [29]. They serve as the essential physical foundation for economic activity, social cohesion, and the delivery of essential public services, ensuring the continuity of operations during emergency situations [22].

However, in the face of the increasing frequency of extreme hydrological events and the breakdown of climatic stationarity, these networks(originally designed for stability(are revealing an alarming **systemic fragility** [6].

This section analyses the core of our scientific inquiry: by what mechanisms do these structures, specifically engineered to guarantee mobility, paradoxically become the primary casualties of water? Furthermore, we examine how their failure transforms a localized natural hazard into a **systemic societal catastrophe**.

2.4.1 Road Infrastructure: Origins, Functions, and the Hydrological Conflict

To diagnose the root causes of vulnerability, it is essential to examine the intrinsic nature of infrastructure and the historical conflict it maintains with the aquatic environment [37]. This conflict is not a random occurrence; it is **structural** and inherent to the very design of modern transport networks [6].

The Foundation of Connectivity and the Development Paradox

Understanding the intrinsic vulnerability of a road requires questioning its *raison d'être*. The term "Infrastructure," derived from the Latin *infra* ("below") and *structura* ("construction"), literally refers to the invisible foundation that supports the visible organization of society. Historically (from the *Via Appia* to the modern motorway) the road has been designed to meet an absolute civilizational imperative: **connectivity**. It is the preeminent tool for land-use planning, enabling society to overcome the **friction of distance** for trade, defence, and social cohesion [37]. In times of crisis, this role becomes vital, ensuring the mobility of emergency services and the evacuation of threatened populations [29].

However, road infrastructure embodies a fundamental paradox. While it acts as the primary driver of urbanization, the very development it induces leads to massive **soil sealing** (impermeabilization) [46]. This artificial land cover radically alters the water cycle, drastically increasing runoff volumes that ultimately threaten the infrastructure itself.

Thus, road infrastructure becomes a victim of its own territorial success. By catalysing urban sprawl and the impermeabilization of watersheds, it generates the hydrological conditions for heightened runoff hazards to which it is directly exposed [14]. This **negative feedback loop** creates an anthropogenic vicious circle that places network resilience at the heart of sustainable development challenges.

The "Original Sin" of Design: Between Impermeability and Obsolescence

The current vulnerability of road infrastructure is not a matter of chance, but the direct consequence of a 20th-century design paradigm based on the absolute control of flows. This model, now challenged by climate change, rests on two pillars that have transformed into structural weaknesses

- **The Drainage Philosophy: Infrastructure as an Obstacle**

Traditional road engineering was conceived as a struggle against water. The primary objective is to protect the **bearing capacity** of foundation soils by waterproofing the pavement and evacuating water as quickly as possible through networks of ditches and culverts [96].

The Hydrological Consequence: In doing so, the road (often elevated on an **embankment**) acts as an impermeable linear barrier that fragments watersheds and disrupts both ecological and **hydraulic continuity**. Rather than integrating water, the road rejects or constrains it, creating devastating flow concentration points downstream [14].

- **Static Dimensioning: The Obsolescence of Norms**

The second pillar is the dimensioning of **hydraulic transparency structures** (culverts, box culverts, bridges). These structures are calculated based on historical statistics assumed to be stationary (e.g., Q_{10} or Q_{100} return periods).

The Result (Systemic Failure): When faced with a non-stationary climatic event (such as a record-intensity flash flood), the system's hydraulic capacity is instantaneously overwhelmed. The road embankment, designed to remain clear of water, transforms into an **unintentional dam** that stores water upstream until catastrophic failure occurs, or into a diversion channel that accelerates flows toward inhabited areas [75]. This failure of static design mandates a paradigm shift: the road must no longer be viewed as an obstacle, but as a resilient component of the water cycle.

2.4.2 Failure Mechanisms: From Hydraulic Loading to Systemic Collapse

For the road engineer, vulnerability analysis cannot be limited to a simple spatial overlay of flood zones and road networks. It requires a deep understanding of **physical load transfer**: specifically, how the kinetic and potential energy of the fluid is converted into **mechanical stress** (thrust, shear, and uplift pressure) capable of exceeding the **permissible capacity** of the structure [97].

This analysis must establish a fundamental distinction between two categories of assets with diverging mechanical behaviours:

a) **Point-Based Structures (Bridges, Culverts):** These act as **hydraulic singularities** within the flow. They are subject to intense stress concentrations, including physical impacts from debris and **localized scouring**.

b) **Linear Assets (Pavements, Embankments):** These are subjected to diffuse and internal stressors, such as saturation and **longitudinal erosion**, which often remain invisible until the point of failure [98].

2.4.2.1 Physical Vulnerability: The Conversion of Floodwaters into Structural Loadings

In the context of inland flooding, the hazard manifests as a suite of static and dynamic loads that assault the structural integrity of the asset.

Critical Case of Point-Based Assets (Bridges): Thrust, Uplift, and Scouring

A bridge acts as a **hydraulic singularity**. By constraining the flow section, it forces the fluid to accelerate, triggering three primary failure modes:

- **Hydrodynamic Loading (Lateral Thrust):** Moving water exerts **dynamic pressure** ($q = \frac{1}{2}\rho V^2$) on the piers. If the water level reaches the superstructure (deck), the exposed surface area increases abruptly, generating a massive lateral thrust capable of shearing the bearings or causing failure through an **overturning moment** [5].
- **Buoyancy-Induced Uplift:** Often overlooked, this mechanism is devastating. When a bridge deck becomes submerged, **Archimedes' Principle** applies. If the buoyancy force exceeds the combined self-weight of the deck and the resistance of the anchorages ($F_{uplift} > W_{dead}$), the deck is literally lifted off its bearings and swept away by the current [99].
- **Local Scour:** This is the predominant failure mechanism. The contraction of the **flow vein** around the piers creates **horseshoe vortices** that erode the riverbed. This is essentially a **geotechnical failure**: the bridge does not collapse due to structural breakage, but because its foundations lose their **lateral confining pressure** and stability [15].
- **Debris Accumulation (Logjams):** The buildup of floating debris (trees, vehicles) against the piers acts as a "mobile dam," artificially increasing the thrust surface and exacerbating scouring through flow obstruction [100].

The Case of Linear Assets (Roadways): Saturation, Erosion, and Piping

Unlike bridges, a roadway absorbs energy along its entire length. In this case, failure is often internal and remains invisible during the event itself.

- **Hydrostatic Loading (Saturation):** Prolonged immersion (H_s) alters material properties. The increase in **pore water pressure** (u) within the pavement structure reduces **effective stress** ($\sigma' = \sigma - u$). Consequently, granular materials lose their cohesion. The roadway becomes "soft" and undergoes irreversible deformation(such as **rutting** and **fatigue cracking**(under the weight of heavy emergency vehicles [86].
- **Embankment Erosion and Peeling:** If the tangential velocity of the water exceeds the **critical shear velocity**, the **embankment toe** begins to erode. At the surface, rapid currents can cause the "peeling" (stripping) of the **bituminous wearing course**, exposing the underlying base layers [16].
- **Internal Erosion (Piping / "Effet Renard"):** In road embankments, a **hydraulic head differential** between the upstream and downstream sides can initiate internal water circulation,

known as **piping**. These micro-currents wash away fine particles, creating underground cavities that lead to the collapse of the pavement (**sinkholes**), which often occurs well after the floodwaters have receded [84].

2.4.2.2 Functional Vulnerability: Service Loss and the Urban Trap

Even if a structure maintains its mechanical integrity, the infrastructure may still fail to fulfil its primary mission. This constitutes **functional vulnerability**, which measures the unavailability of service and its subsequent behavioural impacts.

The Serviceability Limit State (SLS)

From an operational perspective, a road is considered "lost" well before its physical destruction.

- **Inundation Threshold:** Scientific literature generally establishes a critical threshold of **30 cm**. Beyond this depth, the buoyancy of light vehicles (**Archimedes' Principle**) negates tire traction, rendering the vehicle uncontrollable [101].
- **Loss of Visibility:** Even shallow submersion conceals road markings and hazards, such as **dislodged manhole covers**, transforming the roadway into a lethal trap for users [102].

The Phenomenon of Self-Locking Gridlock

In dense urban environments, functional vulnerability takes on a critical behavioural dimension known as **self-locking gridlock**.

- **Mechanism:** When specific road segments are flooded, drivers simultaneously attempt to perform U-turns or converge onto the few remaining **dry corridors** [103].
- **Consequence:** Vehicles accumulate, blocking intersections upstream of the flooded zone and effectively trapping themselves. The network reaches a **zero-velocity state** (paralyzed not necessarily by water depth, but by collective panic. This gridlock physically prevents emergency services from reaching the disaster area, thereby increasing the potential for human casualties [104].

The Domino Effect: Systemic Network Failure

The closure of a bridge (**node**) or the paralysis of a route (**link**) severs an **edge** of the transport graph.

- **Systemic Isolation:** If the severed link is critical (e.g., a single-access bridge in a valley with **low redundancy**), entire regions become isolated. Localized vulnerability thus escalates into a major territorial crisis, cutting off access to hospitals and vital services [49]. This **cascading phenomenon** has been extensively documented during major urban flood events [105].

2.4.2.3 Socio-Economic Vulnerability: The True Cost of Infrastructure Failure

Ultimately, the failure of transport infrastructure translates into a heavy societal impact, highlighting the critical importance of this research.

- **Damage Statistics and Economic Weight:** Transport infrastructure consistently accounts for a major portion of public asset losses during natural disasters. According to global studies, these networks often represent over 30% of total damage costs [4].
- **The Dominance of Indirect Costs:** It is essential to distinguish between **Direct Costs** (e.g., physical reconstruction and debris removal) and **Indirect Costs** (e.g., travel time delays, increased fuel consumption, and supply chain disruptions). On strategic corridors, the indirect economic losses resulting from traffic interruptions can often surpass the actual reconstruction costs within just a few days [106].
- **Social Inequity and the Burden of Isolation:** Road vulnerability exacerbates the vulnerability of the population. Isolation disproportionately affects precarious areas, severing access to emergency medical care and humanitarian aid during a crisis. This creates a **"double burden"** (or double penalty) for disadvantaged communities, where physical isolation compounds existing socio-economic fragility [7].

2.4.3 Methodological State of the Art: Aligning Vulnerability Assessment with Objectives

The methodology for vulnerability assessment is not a "one-size-fits-all" solution; it must be selected in direct response to the failure mechanisms previously identified (physical, functional, or socio-economic). The choice of tool fundamentally depends on the engineer's objective: managing an existing risk (**Prevention and Management**) or dimensioning a future structure (**Design and Engineering**).

2.4.3.1 Risk Prevention and Management (Existing Networks)

In this context, the goal is to prioritize interventions across an extensive **infrastructure asset portfolio**. Approaches that capture **functional** and **socio-economic** vulnerability are preferred.

Qualitative Approach (Visual Inspection)

- **Method:** Relies on field expertise and structural condition databases (e.g., the **IQOA** method). It records visible signs of structural weakness or deterioration.
- **Application:** Routine maintenance and operational monitoring.

Semi-Quantitative Approach (Multi-Criteria Indices)

- **Method:** Development of a **Vulnerability Index (VI)** using methods such as the **Analytic Hierarchy Process (AHP)**. This involves aggregating heterogeneous factors: the physical condition of the structure, **Average Daily Traffic (ADT)**, strategic importance, and the size of the population served [107].

- **Application:** Serves as a decision-making lever for infrastructure managers, allowing them to identify **critical network nodes** to prioritize budget allocation [108].
- **Relationship to Failure:** Effectively captures the risk of functional paralysis and social isolation but remains imprecise regarding the specific mechanics of structural rupture.

2.4.3.2 Design and Advanced Diagnosis (New or Critical Structures)

Here, the objective is to guarantee **structural integrity** and mechanical stability. The focus shifts toward **physical and structural** vulnerability.

Quantitative Approach (Fragility Curves)

- **Method:** Establishment of probabilistic functions relating hazard intensity (Depth, Velocity) to the probability of physical damage or failure (e.g., **scouring** or **overturning**).
- **Application:** A core tool for **Structural Design**. It allows the structure to be dimensioned to withstand a specific hydraulic load [15].
- **Relationship to Failure:** Directly addresses the physics of hydrodynamic loading and erosion mechanisms.

2.4.3.3 Methodological Synthesis: The Common Impasse

Regardless of the chosen method (whether using indices for management or curves for design) they all share a common intrinsic vulnerability: an absolute dependence on **input data quality**. To calculate a reliable index or an accurate fragility curve, it is imperative to know the actual water depth at the specific structure. This requirement represents the current **scientific bottleneck** (or research gap).

2.4.4 Scientific Diagnosis: The "Scale Gap" Impasse

While the physical mechanisms of structural failure are scientifically mastered (we know exactly *how* a bridge collapses) and despite the existence of sophisticated assessment tools (Indices, Fragility Curves), a fundamental question remains: why does operational engineering still struggle to reliably predict the failure of a specific structure during a flood event?

The answer lies in a major methodological bottleneck: the incompatibility of the analysis scales used by different disciplines, creating what we define as the **"Scale Gap"** [6]. This disciplinary siloing prevents the reliable transfer of information from the watershed scale (**Macro**) to the asset scale (**Micro**) [39].

2.4.4.1 Epistemological Confusion: General vs. Asset-Specific Vulnerability

This scale gap is rooted in a fundamental dichotomy within risk assessment, which is often conflated in regulatory practice:

- **General Vulnerability (Territorial/Macro Approach):** This is the scale of Flood Risk Prevention Plans and FEMA maps. It follows a binary urban planning logic: "Is this zone flood-

prone?" Its purpose is to define land-use regulations (buildable vs. non-buildable). While essential for planning, it is technically insufficient for engineers because it fails to quantify the precise mechanical aggression (depth H_s and velocity V_s) sustained by the asset [39] .

- **Asset-Specific Vulnerability (Structure/Micro Approach):** This is the scale of maintenance and safety diagnostics. It addresses critical questions: "What is the probability of failure for *this* specific bridge? Will *this* roadway be submerged by 10 cm or 50 cm?" This diagnostic precision is critically lacking today, as it requires high-resolution data that macroscopic models are inherently unable to provide [15].

2.4.4.2 The Mechanics of Compartmentalization: Two Disconnected Worlds

The current state of the art reveals a critical disciplinary siloing (working in silos) that induces a major loss of information between the watershed and the infrastructure [6].

The Hydrologist's Bias (Topographic Blindness): Current hydraulic models (**C-HDM**) are designed for territorial scales. They rely on spatial **Digital Elevation Models (DEMs)** with resolutions typically ranging from 10m to 30m [109].

- **The Physical Problem:** At this coarse resolution, the model "smooths" reality. It sees the valley but "misses" the road. It ignores drainage ditches, erases pavement cross-slopes, and fails to perceive the river's contraction caused by bridge piers.
- **The Consequence:** The model calculates flow on a physically inaccurate virtual topography. It often overestimates water spread (**"ghost flooding"**) or underestimates local velocity through roughness smoothing. Consequently, the calculated intensity (H_s, V_s) at the road's location is physically erroneous.

The Structural Engineer's Bias (The "Garbage In, Garbage Out" Principle): Conversely, structural engineers possess advanced tools(such as fragility curves and **Finite Element Analysis (FEA)**(capable of predicting material resistance with extreme precision [15].

- **The Impasse:** These structural models are "data-hungry" for precise inputs. However, in current practice, they are fed with the coarse and inaccurate hydraulic data derived from territorial models.
- **The Result:** We calculate, with great precision, the reaction of a bridge to a force that does not exist. The vulnerability diagnosis becomes methodologically invalid because the input (the localized hazard) is disconnected from the geometric reality of the structure. This is the perfect illustration of the **GIGO (Garbage In, Garbage Out)** principle applied to risk engineering [84].

2.4.4.3 Thesis Response: An Integrated Multi-Scale Approach

To resolve this scale conflict, this thesis proposes a disruptive methodology that seeks to hybridize rather than oppose these disciplines.

It is fundamental to reiterate that **Hydrodynamic simulation** is "blind" without the territorial context provided by **GIS (Macro scale)**. GIS enables the modelling of the watershed and flow over vast areas(an indispensable step for understanding flood genesis [82].

However, for a specific engineering structure, this macroscopic vision is no longer sufficient. Our approach is based on an unprecedented digital coupling (**Interoperability**) between:

a) **Territorial Context (GIS - Macro):** Providing boundary conditions and basin-wide topography.

b) **Geometric Precision (BIM - Micro):** Capturing the exact **"As-built"** geometry and correcting DEM errors [19].

c) **Fluid Physics (Distributed Hydrodynamics):** Solving equations on this hybrid model.

Research Hypothesis: Only this fusion can reconstruct the physical reality of the **Water-Infrastructure interaction**. It transforms hazard uncertainty into a **High-Fidelity diagnosis**, capable of predicting not only the inundated area but the exact mechanical load sustained by the structure.

2.5 Conclusion

The Necessity of Digital Tools

This introductory chapter has demonstrated that road infrastructure vulnerability is a multifaceted phenomenon situated at the intersection of fluid mechanics, civil engineering, and land-use planning. We have shown that conventional methodologies, constrained by disciplinary silos, are reaching their operational limits (characterized by the "Scale Gap") when confronted with contemporary climate challenges.

The proposed solution (an integrated multi-scale approach) rests on a core hypothesis: the necessity of fostering a technical dialogue between disparate engineering and modelling domains. This convergence is made possible exclusively by the emergence of a new generation of advanced technologies.

The following chapter is dedicated to this objective: exploring the potential of **Digital Tools** (specifically **Hydraulic Modelling, GIS, BIM, and AI**) which serve as the operational engine of our research methodology.

3 Digital Tools for Risk Assessment: From Hydraulic Modelling to BIM-GIS Integration

3.1 Introduction

The Digital Revolution as a Driver of Resilience

The characterization and management of natural risks have been radically transformed by a major driving force: the digital revolution. While the fundamental laws of physics(such as the Navier-Stokes equations(remain immutable, our capacity to solve them to understand the world has been amplified tenfold by the exponential increase in computational power [32].

The history of this technological evolution can be interpreted as a progressive mastery of complexity. It began with the advent of computing, evolving from early rudimentary calculators to modern **High-Performance Computing (HPC)** systems capable of processing terabytes of hydrological data in real time [79]. This evolution accelerated with the rise of the Internet, which broke the isolation of individual workstations to weave a global network for geospatial data exchange, giving birth to the **Big Geo-Data** paradigm [110].

Today, we stand at the threshold of a new epistemological shift driven by **Artificial Intelligence (AI)** and **Digital Twins**, which promise a transition from mere simulation toward intelligent prediction [111].

However, to master these tools, it is crucial to distinguish their functional nature. In this regard, we differentiate between **Software** (specialized computational engines) and **Platforms** (integrative management environments).

This chapter explores this technological trajectory by detailing the three pillars at the heart of our methodology:

a) **Hydraulic Modelling: The software for the physical simulation of the hazard.**

b) **GIS (Geographic Information System):** The platform for macroscopic territorial management.

c) **BIM (Building Information Modelling):** The platform for microscopic asset description.

We will conclude by **demonstrating** that true innovation lies not in the isolated use of these technologies, but in their convergence through **interoperability** [19](the only path to achieving the high-fidelity assessment required for the resilience of critical infrastructure.

3.2 The Technological Foundation: From Computational Power to Digital Architecture

Before discussing the domain-specific tools for hydraulics or civil engineering, it is essential to understand the underlying digital infrastructure that supports and enables them. Risk modelling is not an abstract discipline; it is contingent upon the technological materiality of its era [112]. From Moore's Law, which governs the exponential growth of processing power, to the networked architecture of the Web, which facilitates the fluid circulation of data, each technological leap has opened new simulation horizons that were previously unattainable.

This section explores the foundations of our digital era: the computer as a computational engine, the Internet as the "nervous system" of information, and the fundamental distinction between **Software** (the specialized tool) and **Platforms** (the integrative environment)(the keystone of modern interoperability[113].

3.2.1 The Computer and the Internet: Genesis and the Revolution of Computing

To grasp the scope of today's tools, it is necessary to return to the original intent behind their creation.

The computer: Extending the Calculative Brain

The French term *"Ordinateur"* (adopted by IBM in 1955 at the suggestion of philologist Jacques Perret) is derived from the Latin *ordinare* (to set in order, to regulate), signifying one who brings order to chaos. Humanity invented the machine to transcend the cognitive limits of manual calculation. From the Turing machine to modern **High-Performance Computing (HPC)**, the objective has remained immutable: to process massive amounts of information at extraordinary speeds.

Impact on Hydraulics: This raw processing power served as the catalyst for modelling. It enabled the transition from simplified analytical solutions to the **iterative numerical resolution** of complex differential equations (Navier-Stokes), making it possible to simulate real physical phenomena that were previously **computationally intractable** [79].

The Internet: Weaving the Web of Information

If the computer is an isolated brain, the Internet is its nervous system. The term is a contraction of "Inter-connected Networks." Born from the ARPANET project to ensure communication resilience, it embodies the ambition to abolish distance in information exchange.

Impact on Data: For risk management, the Internet has transformed localized data into a global resource. It provides instantaneous access to satellite observations, global topographic databases (SRTM), and **real-time data streams** [114]. Without this interconnection, hydraulic modelling would have remained a laboratory science, detached from field reality.

The Convergence: The fusion of these two revolutions(processing capacity (the Computer) and data access (the Internet)(gave birth to **modern Geomatics** [112], the indispensable foundation of any contemporary risk analysis.

3.2.2 The Fundamental Distinction: From Specialized Tools to Integrative Environments

To navigate the complex digital ecosystem, it is essential to clarify the conceptual ambiguity between two structural notions: **Software** and **Platforms**.

Software: The Domain-Specific Expert Tool

The term "Software," which appeared in the 1950s, designates the "soft" or malleable component of a machine, as opposed to the hardware. Historically, software was developed to meet a need for specialization. It is an algorithmic tool designed to execute a precise task beyond human cognitive capacity (such as solving an integral or simulating a flow). In hydraulics, computational codes like HEC-RAS or TELEMAC are pure software: they represent the mathematical **"engine"** that transforms an equation into a result [32].

Platforms: The Convergence and Integration Space

Etymologically, "Platform" refers to a flat, elevated surface serving as a support. In the digital world, the platform emerged from the need for integration. Its primary function is not to calculate, but to link. GIS and BIM are not merely software packages; they are **Information Management Environments**. They act as a **"chassis"** or a territorial operating system, capable of hosting, structuring, and fostering a dialogue between heterogeneous datasets derived from multiple specialized software applications [115].

Synthesis: The success of modern modelling does not rely on one or the other, but on their **seamless integration**: the software (the engine) must be fitted into the platform (the chassis) to produce a comprehensive systemic analysis [116].

3.3 Hydro-Hydraulic Modelling: The Simulation Engines

Flood risk simulation does not rely on a monolithic tool; rather, it is based on a complex, **sequential processing chain**. This process leverages two distinct yet complementary software families, the **coupling** of which is critical to the quality of the final output:

a) **Hydrological Models** for flow generation (**Production**).

b) **Hydraulic Models** for spatial propagation (**Transfer**).

The modern engineer's challenge lies in transforming **stochastic climatic inputs** (rainfall) into **deterministic physical outputs** (flooding), while managing the **propagation of uncertainty** at each stage of the computational workflow [32].

3.3.1 Hydrological Modelling: From Watershed Geometry to Discharge Generation

Before flood simulation can occur, the volume of water produced by the catchment must be quantified. Hydrological modelling is the critical step that transforms the climatic signal (rainfall) into a hydrological response (**discharge at the outlet**). This process is divided into two distinct technical phases: territorial spatialization and transfer simulation.

Spatial Watershed Modelling: The Role of GIS

The initial stage is geomatic rather than hydraulic; it involves constructing the model’s "skeleton." The use of **Geographic Information Systems (GIS)** tools, such as ArcGIS or QGIS, is essential for processing **Digital Elevation Models (DEMs)** and extracting the watershed's physiographic characteristics:

Automatic delineation of drainage divides (watershed boundaries) and stream networks.

Calculation of morphometric parameters (slope, thalweg length, time of concentration) that govern the catchment's response time [66].

Rainfall-Runoff Simulation: Computational Engines (HEC-HMS, SWMM)

Once the geometric basin is defined, specialized software takes over to simulate the water cycle.

The Industry Standard: HEC-HMS (Hydrologic Modelling System). Developed by the USACE, it is the global standard for natural and semi-urban basins. It facilitates the modelling of losses (infiltration via Green-Ampt or SCS-CN), transformation (**Unit Hydrograph**), and **river routing** [117].

The Urban Alternative: SWMM (Storm Water Management Model). More suited to dense urban environments, it excels in managing drainage networks and runoff on impervious surfaces.

Critical Analysis: Model Typologies and Limitations

Technological evolution has diversified modelling approaches, each carrying its own intrinsic biases [32] :

a) **Lumped Models:** These treat the watershed as a homogeneous **"black box."**

Advantages: Simplicity, computational speed, and low data requirements.
Disadvantages: Incapable of pinpointing the specific spatial source of runoff.

b) **Distributed Models:** These divide the watershed into elementary grid cells (pixels).

Advantages: High spatial precision, ideal for heterogeneous basins.
Disadvantages: **Computationally intensive** and highly dependent on soil data, which are often unavailable (**data scarcity**).

3.3.2 Hydrodynamic Modelling: Spatializing Propagation

Hydrodynamic modelling serves as the **core engine** of flood risk analysis. It is the discipline that enables the transition from statistical abstraction (probabilistic discharge) to physical materiality (destructive force).

More than a mere computational tool, hydraulic software (such as HEC-RAS or TELEMAC) acts as a **virtual laboratory**. It numerically solves the fundamental laws of fluid mechanics(specifically the conservation of mass and momentum(to simulate water behaviour across a given geometry [79].

This computational power allows engineers to transform an input discharge (Q) into localized **intensity vectors** (Depth (H_s) and Velocity (V_s)). These are the only parameters capable of quantifying the actual mechanical aggression against infrastructure, whether along a river **reach** or across a complex floodplain [32].

Input and Integration

This model requires the output of hydrological modelling (the flood hydrograph) as its primary **Input**. This data transfer can be achieved in two ways: either through external file importation (Hydrological Output) or directly within an **integrated software suite**.

Dimensional Evolution: From Streamlines to Full Physics

The history of hydraulic software mirrors the exponential growth of computing power. With each technological leap (governed by Moore's Law), engineers have gained an additional spatial dimension and increased physical granularity.

a) **1D Models (One-Dimensional): Cross-Sectional Abstraction**

Pioneering the field of hydraulic computing (such as the legacy HEC-2 code from the 1970s), these models simplify 3D reality into a single line.

Physical Principle: They solve the **Saint-Venant equations** along a single x-axis. They do not calculate spatial water distribution but rather **cross-sectional averages**. The water is constrained to follow a predefined path.

Application: Due to their high computational speed, they remain the industry standard for simple fluvial studies where the flow remains confined within a narrow valley.

b) 2D Models (Two-Dimensional): The Spatial Revolution

Now the benchmark for modern engineering, 2D models represent an epistemological breakthrough. They no longer model lines but rather **meshed surfaces** (x, y).

Physical Principle: They solve the full **Shallow Water Equations (SWE)**. The velocity vector is calculated at every point (node) of the mesh. The water acquires lateral freedom of movement: it can bypass a building, spread across a street, or stagnate in a topographical depression.

Critical Contribution: These models are indispensable for simulating complex phenomena where the flow direction is not known *a priori*, such as levee breaches or urban flooding [32], [78].

c) **3D Models (Three-Dimensional): The Physics of Turbulence**

This represents the current research frontier. Beyond merely adding the vertical dimension (z), these models capture the internal complexity of the fluid.

Physical Principle: They solve the **Navier-Stokes equations** (often via the **RANS** (Reynolds-Averaged Navier-Stokes) method for turbulence). Unlike 2D models, which average velocity over the water column, 3D models calculate the **vertical velocity profile** and helical flow patterns.

Application: Due to their **prohibitive computational cost**, they are reserved for highly detailed local analyses (**micro-scale**), such as studying complex scouring around bridge piers. They are currently inapplicable for city-scale simulations.

3.3.3 Coupling: Toward Seamless Interaction

Innovation in this field lies in the methodology used to link these two modelling domains. According to the review by [78] , two main approaches are distinguished:

Loose (External) Coupling: This involves the exchange of data files between two distinct software packages (e.g., HEC-HMS → HEC-RAS). This remains the most common engineering practice.

Tight (Internal / DBCM) Coupling: This approach utilizes a single integrated code that simultaneously solves both hydrological and hydraulic equations. The **Dynamic Bidirectional Coupled Model (DBCM)**, exemplified by the **Rainfall-Runoff-Inundation (RRI)** software, enables a highly realistic interaction. In this setup, water can overflow from the river channel onto the floodplain and(crucially(flow back into the channel as levels recede, thus capturing the **full flood dynamics** [93].

3.4 Geographic Information Systems (GIS): The Platform for Territorial Intelligence (Macro)

While hydraulic modelling provides the "physics" of the hazard, the **Geographic Information System (GIS)** is the indispensable tool that contextualizes it within the territory, providing its geographical "meaning."

Historically defined as an integrated platform for capturing, storing, analysing, and displaying spatially referenced data [118], GIS represents a major epistemological shift: the transition from the **static map** (a frozen image of the world) to the **georeferenced relational database** (a dynamic model of the world) [119].It serves as the privileged interface where the laws of nature (the calculated hazard) and societal stakes (actual exposure) intersect to inform public policy [26].

3.4.1 Conceptual Foundations: Snow's Cholera Map (1854)

Long before the digital era, Dr. John Snow established the conceptual foundations of spatial analysis. By manually overlaying the locations of water pumps with cholera deaths in London, he demonstrated that geography could save lives, thereby inaugurating the era of **spatial epidemiology** [118]**.**

The Birth of "GIS" (1963): The Management Mandate

The term "Geographic Information System" was coined by Roger Tomlinson in Canada to manage the country's vast national land inventory. The primary objective was not merely to draw maps, but to calculate and manage resources across thousands of square kilometres. This marked the birth of **Geomatics** [118]**.**

3.4.2 Technological and Functional Evolution

GIS has evolved significantly, progressing from early adoption to a state of critical maturity for disaster management [120].

- **1980s–1990s (The Digitalization Era):** This period saw the introduction of data transfer standards and the digitization of paper maps. During this phase, GIS acted primarily as a **"digital blueprint cabinet"** [119].
- **2000s (The Analysis Era):** GIS expanded into civil engineering and urban planning, becoming a tool for complex spatial analysis, including slope calculations, network analysis, and interpolation [119].
- **Today (Web-GIS and Big Data):** GIS has transformed into a cloud-connected platform capable of ingesting massive **real-time data streams** (from IoT sensors and satellites) for continuous monitoring and crisis management [110].

3.4.3 Systemic Role and Applications: GIS as the Analytical Backbone

Today, GIS serves as a dedicated platform for data production and management [116]. It excels at processing large-scale geographic features (**macro-level**), such as topography, infrastructure networks, and natural hazards [121], [122].

3.4.3.1 Domain-Specific Applications

Its functionalities cover the entire spectrum of risk management [123] :

a) **Susceptibility Mapping:** Identifying risk-prone areas through multi-criteria analysis and the overlay of thematic layers [34].
b) **Resilient Planning:** Supporting the development of adaptive infrastructure and evaluating vulnerability levels and potential damage [120].
c) **Resilient Planning:** Supporting the development of adaptive infrastructure and evaluating vulnerability levels and potential damage [124].
d) **Hydrological Data Management:** Preparing **Digital Elevation Models (DEMs)** and morphometric parameters to feed into hydraulic models [19].

3.4.3.2 The Central Role of GIS: The Backbone of Risk Analysis

Within the methodological framework of this thesis, GIS should not be perceived as a mere visualization tool, but as the **"Backbone"** of territorial analysis. It acts as a universal integrator, connecting raw data to decision-making intelligence.

Upstream (Pre-processing): GIS functions as a data processing factory. It ingests, cleans, and structures raw geometric data (DEM, LiDAR) and thematic data (land use, soil types). It is responsible for generating calculation meshes and defining the **boundary conditions** (roughness, slopes) essential for powering hydraulic models [19].

Downstream (Vulnerability Assessment): Once the hydraulic simulation is complete, the results (H_s, V_s) are exported as **raster maps**. GIS imports these maps and performs the crucial **spatial intersection** between this distributed hazard and the vector layers of the assets (roads, buildings). This overlay allows for the extraction of intensity values for each exposed object and the quantification of potential damage [125], [126], [127].

3.4.3.3 The Structural Limitation: The "Scale Barrier"

Despite its power in territorial analysis, GIS encounters a structural "glass ceiling." Inherently designed for the **"Macro" scale**, it operates in **2.5D** (a surface draped over relief) and models infrastructure as simplified **geometric primitives** (points, polylines). In a standard GIS environment, a road is often reduced to a simple 1D axis or a flat 2D strip(lacking thickness, **cross-slopes**, and vertical details for engineering structures [128].

This topographic simplification renders GIS "blind" to the internal and volumetric complexity required for structural diagnostics [129]. This fundamental physical limitation necessitates a **scale shift** and justifies the imperative move toward **BIM** [123].

3.5 BIM: The High-Fidelity Platform (Micro-Scale)

While GIS provides a broader understanding of the territory, **Building Information Modelling (BIM)** represents the technological revolution that enables the mastery of the asset itself. It embodies the most profound paradigm shift in the construction industry since the invention of linear perspective: the transition from **isolated drafting** to **collective knowledge**.

More than a mere 3D modelling tool, BIM is a collaborative methodology that addresses a dual historical imperative: the ability to anticipate reality (simulating before building) and the creation of a universal language for the asset. From the wooden scale models used by cathedral builders to the paper blueprints of the industrial age, engineers have always sought a medium for a "single source of truth."

BIM fulfils this promise by creating an intelligent **Digital Twin**: a centralized spatial database where every component (beams, walls, culverts) is not only geometrically precise (**"High-Fidelity"**) but also **semantically documented** and interoperable across all stakeholders [116]. This transparency of information makes BIM an indispensable tool today for diagnosing the **inherent vulnerability** of infrastructure when confronted with hazards [115].

3.5.1 Definition and Paradigm Shift: From Geometry to Shared Semantics

BIM is defined not by 3D visualization but by **Information management** (the "I"). It is a shared digital representation of the physical and functional characteristics of an infrastructure, serving as a reliable knowledge resource throughout its entire lifecycle [130].

a) **The Semantic Shift (The Intelligent Object):** Unlike traditional CAD, which produces unstructured vector drawings (often described as an "empty shell"), BIM is an **object-oriented database**. Within a BIM environment, a bridge is not an inert volume; it is a **systemic assembly of intelligent objects** (piers, decks) embedded with intrinsic data, such as material properties, structural resistance, and cost [131].
b) **The Micro-Scale (High-Resolution Granularity):** BIM operates at a level of detail inaccessible to other modelling tools, extending down to the resolution of individual bolts or reinforcement bars. This **microscopic granularity** is crucial for vulnerability analysis: it enables the simulation of water impact on the **actual geometry** of the structure(such as specific pier shapes or guardrail profiles(rather than on a simplified abstraction [132].
c) **Collaborative Vocation (Breaking Information Silos):** Beyond geometry, BIM is designed to bridge disciplinary gaps. It provides a **common language** that allows all stakeholders(designers, hydrologists, and infrastructure managers(to understand and query the asset's status through a **single, centralized model** [123].

3.5.2 Genesis and Evolution: From the Drawing Board to the Database

The acronym BIM (Building Information Modelling) emerged relatively recently, yet the concept addresses a long-standing need: unifying fragmented project information to master its inherent complexity. Its evolution mirrors the quest for computational intelligence, transitioning from simple graphical representation to comprehensive knowledge management [131].

- **The 1970s: The Conceptual Era (Eastman's "BDS"):** As early as 1975, Professor Charles Eastman theorized the **Building Description System (BDS)**. His visionary intuition critiqued 2D drafting for losing 3D information, proposing instead a single database where view changes were automated. This was the philosophical ancestor of BIM: "describing" a building rather than merely drawing it [131].
- **The 1980s–1990s: The Computer-Aided Design (CAD) Era:** With the arrival of AutoCAD, the industry digitalized but remained tethered to the **"paper metaphor."** Engineers were essentially drawing digital lines. While this was a revolution in productivity, it was not one of intelligence: the computer still did not "understand" the objects it was drawing [130].
- **The 2000s: The Parametric Turning Point:** The advent of **parametric modelling** marked a true breakthrough. Objects became interdependent: for instance, moving a wall caused the associated door to follow automatically. The model became "intelligent" and responsive to change, integrating built-in behavioural rules.
- **Today: The Era of InfraBIM and Collaboration (CDE):** BIM has now reached a stage of critical maturity, expanding from "vertical" building construction to "horizontal" infrastructure projects (**InfraBIM**)[133]. It has evolved from simple file exchanges toward true model-based collaboration through a **Common Data Environment (CDE)** [134]. The current challenge is **interoperability**: breaking down proprietary silos through open standards such as **IFC (Industry Foundation Classes)**. This standardization is precisely what enables the technical dialogue with **GIS** [135].

Consequently, BIM is now formally defined not merely as software, but as a shared management process of the physical and functional characteristics of a built asset [136].

3.5.3 Strategic Applications: BIM as a Tool for Diagnostics and Resilience

Beyond its initial function in design and construction, BIM has emerged as a systemic lever for risk management and infrastructure resilience. It transforms passive structures into **intelligent assets** capable of communicating their structural health status [122].

a) **Predictive Simulation and Risk Mitigation (Prevention):** This is the focal point of modern research. BIM goes beyond mere geometric representation; it enables the simulation of **failure physics**. By integrating rich semantic data(such as material properties, constitutive laws, and loading history(it becomes possible to assess the **intrinsic vulnerability** of each critical component [137]**.**
b) **Crisis Management and Virtual Reality (Response):** During an emergency, the BIM model serves as the **single source of truth** (referential) for the situation. Coupled with **Virtual Reality (VR)** or **Augmented Reality (AR)**, it allows managers to visualize 3D scenarios to streamline evacuation plans or train emergency response teams within a safe, virtual environment [138].
c) **Asset Management and Sustainability (Recovery):** In the aftermath of an event, BIM facilitates **Rapid Assessment**. By comparing the **"As-built"** state archived in the model with post-crisis surveys (**Scan-to-BIM**), engineers can precisely quantify the volume of materials

required for replacement and optimize reconstruction costs, thereby integrating both economic and ecological sustainability [139].

3.5.4 Strengths and Limitations

The Major Asset (LoD)

The strength of BIM lies in its **Level of Detail (LoD)**. It captures the critical micro-topography necessary for hydraulic accuracy (such as curb heights, embankment slopes, and culvert diameters) which satellite-based DEMs typically ignore. Furthermore, its **Semantic Richness** provides the essential physical parameters required for structural analysis, such as **Young's Modulus** and yield strength.

Intrinsic Limitation (Geographical Myopia)

However, BIM suffers from "geographical myopia." While it excels at the object scale (**Micro**), it is inherently incapable of managing the extensive territorial context(such as the watershed or the complete hydrographic network(required for hydrological simulation [115]. This insurmountable scale boundary makes its standalone use impossible for flood studies and necessitates its mandatory coupling with **GIS**.

3.6 Technological Convergence: Toward BIM-GIS and AI Integration

While GIS analyses the territorial "context" (**Macro scale**) and BIM describes the "built asset" (**Micro scale**), their historical separation into watertight silos now represents a significant bottleneck for systemic risk analysis. Disruptive innovation today lies in their **integration**. This fusion is the *sine qua non* for the emergence of **Geospatial Digital Twins**.

Indeed, without the semantic richness of BIM, a digital twin remains merely a geometric "empty shell." It is the contribution of BIM that provides the model with its structural **"intelligence,"** enabling the simulation of dynamic interactions between the structure and its natural environment with unprecedented fidelity [19].

3.6.1 Definition and Genesis of Integration: From Juxtaposition to Synergy

BIM-GIS integration is more than a mere visual overlay of layers. It involves the organic fusion of detailed semantic and geometric data from asset modelling (BIM) with large-scale contextual and geospatial data provided by Geographic Information Systems (GIS). The fundamental objective is to bridge the epistemological and technical divide between the component scale and the territorial scale [135].

Historical Evolution: The Maturation of Scientific Awareness

This convergence was not immediately. The history of this integration can be categorized into three distinct phases, reflecting the maturation of scientific needs [122] :

- **The Compartmentalization Phase (Pre-2008):** During this period, the two domains operated in isolation. BIM was the domain of architects, while GIS belonged to geographers. Researchers were only beginning to theorize the potential benefits of linking them with 3D urban management.
- **The Exploration Phase (2008–2011):** The first technical attempts emerged, though publication growth remained sluggish. Researchers struggled with format compatibility (notably **IFC vs. CityGML**) and tested manual conversions for simple use cases.
- **The Explosion Phase (Since 2012):** Interest in integration has surged dramatically. This acceleration is driven by new global imperatives: the need to develop sustainable **Smart Cities** and to strengthen infrastructure resilience in the face of climate change. It became clear to the scientific community that neither BIM nor GIS, in isolation, could address these complex, multi-scale challenges [135].

3.6.2 Systemic Synergy: The Benefits of an Integrated Approach

BIM-GIS integration is not merely a technical addition ($1 + 1 = 2$) but a **functional multiplication**. It creates an environment where the value of information is amplified tenfold through its contextualization. The scientific literature identifies three major performance levers that justify this approach for transport infrastructure [140] :

a) **Optimization of Data Acquisition (Cost and Time Efficiency):** Traditionally, urban hydraulic modelling required expensive and time-consuming topographic surveys. BIM is

a **gamechanger**: it provides an existing, native source of high-resolution geometric data. By repurposing these models for territorial analysis, the costs and delays associated with data collection are drastically reduced [131].

b) **Multi-Scale Immersive Visualization (Communication):** The BIM-GIS alliance **bridges the scale gap**. It offers fluid visual continuity, allowing decision-makers to navigate instantly from a satellite view of the watershed (GIS) down to the structural details of a specific bridge pier (BIM). This realistic 3D visualization capability serves as a powerful tool for communicating risk to **non-expert stakeholders** [19].

c) **Critical Accuracy Enhancement (Scientific Reliability):** This represents the decisive advantage for this thesis. Injecting micro-topographic BIM data (such as cross-sections and hydraulic structures) into the macro-topographic GIS context allows for the correction of **smoothing errors** inherent in traditional DEMs. This drastically improves the precision of hydraulic simulations, transforming coarse estimates into **high-fidelity diagnostics** [141].

3.6.3 Operational Applications for Flood Management

BIM-GIS integration represents a **disruptive approach** to flood management, fundamentally transforming how risks are diagnosed and addressed.

a) **Granular Assessment of Structural Impacts:** Through this coupling, it becomes possible to identify not only the extent of the inundated areas but also the specific types of damage expected for each individual asset component. By intersecting water depth data with the **material resistance classes** defined within the BIM model, structural failure can be predicted with high precision [142].

b) **High-Precision Hydraulic Simulation (GeoBIM):** Hydraulic models are no longer executed on a "naked" or empty terrain. Instead, they leverage the **exact topography** of infrastructure (such as bridges, retaining walls, and utility networks) injected directly from the BIM environment. This significantly reduces uncertainty regarding water depths and flow velocities [143].

c) **Mitigation and Resilience Planning:** The integrated platform serves as a **Decision Support System (DSS)** for designing protective measures (e.g., flood barriers or embankment elevations) and broader adaptation strategies. It enables the **virtual testing** of these measures' effectiveness prior to physical implementation [144].

3.6.4 Integration Methodology: The Three Levels of Fusion

How is this technological alliance realized in practice? Scientific literature identifies three distinct integration strategies, ranging from simple file conversion to full application-level fusion [19].

a) **Data-Level Integration:** This is the most common and mature approach. It involves the physical conversion of data from one format to another specifically, transforming a BIM file (IFC format) into a GIS format (Shapefile or CityGML) through **ETL (Extract-Transform-Load)** algorithms. While functional, this method carries the risk of losing **semantic richness** during the translation process.

b) **Process-Level Integration:** In this approach, data remains in its respective native formats. Integration is achieved through communication via **web services or APIs**. GIS acts as a client that queries the BIM database (server) to retrieve specific information (e.g., the threshold elevation of a door) without needing to import the entire complex geometry.
c) **Application-Level Integration:** This represents the **"Holy Grail"** of current research. It involves developing a unified software platform capable of **natively and simultaneously supporting** both formats (IFC and Shapefile) without prior conversion, thereby offering **seamless and bidirectional interoperability**.

3.6.5 Persistent Technical Challenges: The Interoperability Bottlenecks

Despite significant methodological progress, achieving seamless integration still faces major structural obstacles, inherent to the divergent nature of the two domains:

Semantic and Geometric Mismatch: BIM and GIS do not share the same "geometric language." BIM utilizes **solid modelling** techniques, such as **Constructive Solid Geometry (CSG)** and **Boundary Representation (B-Rep)**, defined by detailed **IFC classes** (e.g., *IfcWall*, *IfcBeam*). Conversely, GIS relies on simplified surface representations or 2D primitives (such as CityGML). Automatic conversion often results in a loss of semantic richness or geometric artifacts, rendering the model **unsuitable for computational analysis**[115] .

Conflict of Spatial Reference Systems (SRS): This is the most critical challenge for extensive **linear infrastructure assets** (e.g., highways). BIM operates within a **local Cartesian coordinate system** (X, Y, Z relative to the structure), whereas GIS functions within a **global geodetic system** (Latitude, Longitude, and Altitude on an ellipsoid). Accurate georeferencing of long BIM models requires complex mathematical transformations to account for **Earth's curvature**, a frequent source of **spatial misalignments** and coordinate discrepancies [142].

3.6.6 The Artificial Intelligence Frontier: An Accelerator, not a Replacement

Ultimately, the modern digital landscape incorporates Artificial Intelligence (AI). Current computational power has facilitated the rise of **Machine Learning (ML)** and **Deep Learning (DL)**, positioning them not as substitutes for physical modelling but as statistical accelerators.

AI as an Accelerator (Surrogate Models)

While physical hydraulic models offer high precision, they are often **computationally intensive** and slow to execute. AI(specifically **Long Short-Term Memory (LSTM)** networks(can emulate their behaviour to provide near-instantaneous, real-time forecasts, which are essential for **early warning systems** [77].

Limitations and Complementarity

Nevertheless, AI remains a **"Black Box"** approach. Its effectiveness is contingent upon the quality of historical training data, and it is inherently unable to explain the **mechanical causality** of flooding events. Consequently, AI does not replace the **deterministic modelling** (BIM-HDM) required for detailed structural diagnostics; rather, it serves as a powerful complementary tool for crisis management

3.7 Conclusion

Toward a Strategic Multi-Scale Methodology

This chapter has provided a comprehensive overview of the digital capabilities currently available to engineers. We have established that the modern professional now possesses a sophisticated arsenal: **GIS** to master spatial complexity, **Hydrodynamics** to simulate fluid flow, and **BIM** to detail the built asset.

Nevertheless, our analysis reveals a persistent paradox: while these tools are individually mature, their joint implementation remains a significant scientific challenge. The **"Scale Gap"** continues to divide territorial-scale analysis from structural-scale diagnostics.

The methodology deployed in the practical phase of this thesis does not prioritize technological performance for its own sake but rather seeks **operational efficiency**. It is founded on the core conviction that the resilience of critical infrastructure will not emerge from a single "silver bullet" tool, but from the **intelligent integration** of existing technologies.

It is this dual strategy (leveraging spatial intelligence for regional zoning and physical precision for localized diagnostics) that we will now apply to the reality of a complex and vulnerable territory: the **Mitidja Plain**, which is the focus of our next chapter.

4 The Mitidja Plain: A Strategic Territory Facing Multiple Risks

4.1 Introduction

A Stressed Landscape

The selection of a study area is a pivotal epistemological milestone in any engineering or environmental science research. A territory must not merely serve as a passive backdrop for validating a methodology; it must embody a living problem and present real-world systemic stakes.

Our research focuses on the **Mitidja Plain**, an iconic case representing contemporary Mediterranean challenges. This vast alluvial basin (historically the "breadbasket" of Algeria and the economic engine of the capital region) is currently a zone of intense friction between aggressive hydrological dynamics and rampant anthropogenic pressure. As highlighted by [145], this area is a complex system where natural hazards (flooding, erosion) and structural vulnerabilities (urbanization, road networks) constantly interact.

This chapter aims to deconstruct this territory to justify its selection as the ideal case study. Indeed, the very nature of the Mitidja necessitates the **multi-scale "funnel approach"** advocated in our work:

a) **Scale and Heterogeneity:** Its vast extent (1,450 km²) and inherent heterogeneity make high-resolution global modelling impossible. This mandates an initial **Macro-scale Zoning phase (AHP/GIS)** to identify critical sectors.

b) **Infrastructure Density:** The concentration of vital infrastructure within these risk zones subsequently requires localized **High-Fidelity Diagnostics (BIM-HDM)** to define appropriate responses, whether structural (reinforcement) or functional (crisis management).

To achieve this, we adopt a progressive analytical framework:

4.1. Presentation of the Study Area: We will analyse its physical characteristics (geometry, topography, and climate) that make it a natural receptacle for water [42].

4.2. Hydrological and Anthropogenic Challenges: We will detail the "risk production" process resulting from the conflict between a torrential hydrographic network and massive urbanization leading to extensive **soil sealing** [21].

4.3 Strategic Justification: We will conclude by demonstrating that the Mitidja constitutes the **"Perfect Laboratory"** for validating our multi-scale methodology, from regional zoning to site-specific structural diagnostics.

4.2 Presentation of the Study Area: Between Geographical Heritage and Strategic Stakes

The Mitidja Plain defines simplification as a mere administrative or topographical unit. It is a complex geographic entity, forged by millions of years of tectonic activity and centuries of anthropogenic development. Before deploying our numerical simulation tools, it is vital to grasp its physical and historical DNA.

This section portrays a paradoxical territory: a fertile sedimentary basin that has evolved into a high-density urban corridor, where the land's own geometry seems to conspire to trap water, posing a constant threat to the infrastructure traversing it.

4.2.1 Historical and Geometric Foundations: From Swamplands to Vital Basin

To comprehend the current hydrological vulnerability of the Mitidja, it is essential to return to its primordial state. As described by **the historian Julien Franc** [146], this plain was for centuries a vast, insalubrious swampland, naturally predisposed to water stagnation (notably at Lake Halloula). It was only through the implementation of colossal drainage works during the 19th and 20th centuries [146], [147], that this territory was reclaimed to become Algeria's agricultural **"breadbasket"** and later its economic heart [21]. This "memory of the soil"(that of a reclaimed floodplain) constitutes the essential backdrop for our risk analysis.

Geographically, the Mitidja is defined as a vast **subsident tectonic graben** located at the core of the Algerian Tell. It forms a strategic corridor covering approximately 1,450 km², acting as a **natural trough** oriented East-West for over 100 km, with a width varying between 5 and 20 km [145], [148].

The system is enclosed by physical boundaries that transform it into a closed **natural impluvium**:

- **To the North:** The Mediterranean Sea and the ridge of the Algiers Sahel hills, which obstruct direct drainage toward the sea.
- **To the South:** The imposing barrier of the **Blidean Atlas** (with foothills reaching 1,600 m), serving as a true "water tower" that feeds the plain through its torrential wadis.
- **At the extremities:** The Bou Mad massifs to the West and the Ain Taya dunes to the East.

Administratively, this territory is far more than a simple agricultural zone; it is the vital **hinterland** of the capital, spanning four major wilayas (Algiers, Blida, Boumerdes, and Tipaza) and concentrating a density of critical infrastructure that is unique on a national scale [42].

4.2.2 Geomorphology and Topography: The Trap of Gentle Gradients

While history explains the presence of water, topography accounts for its persistence. The geomorphology of the Mitidja functions as a true **hydraulic trap**. With an average altitude ranging from 50 to 100 meters, the basin exhibits a characteristic **depressional or "basin-like" morphology**.

The critical factor lies in the **extremely shallow gradients**: slopes are often below 0.5% in the coastal fringe and rarely exceed 3% in the eastern plain [21], [149].

Implications for Road Risk

This topographic flatness leads to a direct hydrodynamic consequence: it **negates the kinetic energy** required for efficient drainage. Instead of flowing toward the sea, runoff water stagnates, and wadis overflow through **slow lateral spreading**. This results in extensive and prolonged submersion zones that trap road infrastructure, effectively transforming highway embankments into **unintentional levees** [42].

4.2.3 Geology and Hydrogeology: A Vulnerable Reservoir

The subsurface of the Mitidja Plain represents a complex **sedimentary record**, resulting from a **detrital infill** spanning from the Pliocene to the late Quaternary [21], [150]. The stratigraphy begins with a basement of **Plaisancian marls** (Lower Pliocene), which forms the impermeable **substratum**. This is overlain by **Astian deposits** (hosting a deep aquifer), the yellow semi-permeable marls of the El-Harrach formation, and finally the **Mitidja Formation** (Soltanian-Tensiftian). Composed of sands, gravels, and pebbles, the latter houses the primary **alluvial aquifer**, a strategic resource for the capital region [145], [151].

For the road engineer, however, the characteristics of the surface soils are the decisive factor. The topsoil is dominated by fine, **silty alluvium** (the Mazafran and Halloula formations), which exhibits a dual vulnerability:

a) **Surface Impermeability:** Although fertile, these soils are prone to **surface crusting** (slaking) or rapid saturation caused by **water table rise**.

b) **Hydrological Consequence:** This saturation negates the soil's **infiltration capacity**, triggering immediate **Horton overland flow** during intense rainfall events. This effectively transforms agricultural fields into surfaces of rapid water transit [148].

4.2.4 Climatology: Mediterranean Intensity and the Breakdown of Stationarity

The Mitidja Plain is characterized by a **semi-arid Mediterranean climate**, defined by wet, cool winters and hot, dry summers [149], [152]. Average annual precipitation fluctuates between 500 and 700 mm [148], with a general mean estimated at 600 mm [145]. However, these figures mask a **brutal temporal and spatial irregularity**, where most rainfall is concentrated into short, violent episodes.

More critically, time-series analysis reveals a significant **breakdown of stationarity**. Since the mid-1970s (with a shift identified around 1973), a downward trend of 15% to 20% in annual totals has been observed [153]. Paradoxically, this global aridification is accompanied by an **intensification of extreme events** (flash floods)(a trend consistent with regional Mediterranean observations [153]. This empirically confirms the relevance of the **non-stationary approach** advocated in Chapter 1.

Simultaneously, the mean annual temperature (ranging from 18 to 25°C) shows a general upward trend, heightening evapotranspiration and **hardening the soil** prior to rainfall events [152].This soil crusting further reduces initial abstraction, directly contributing to the rapid generation of surface runoff.



Figure 4.1. Location of Mitidja plain.

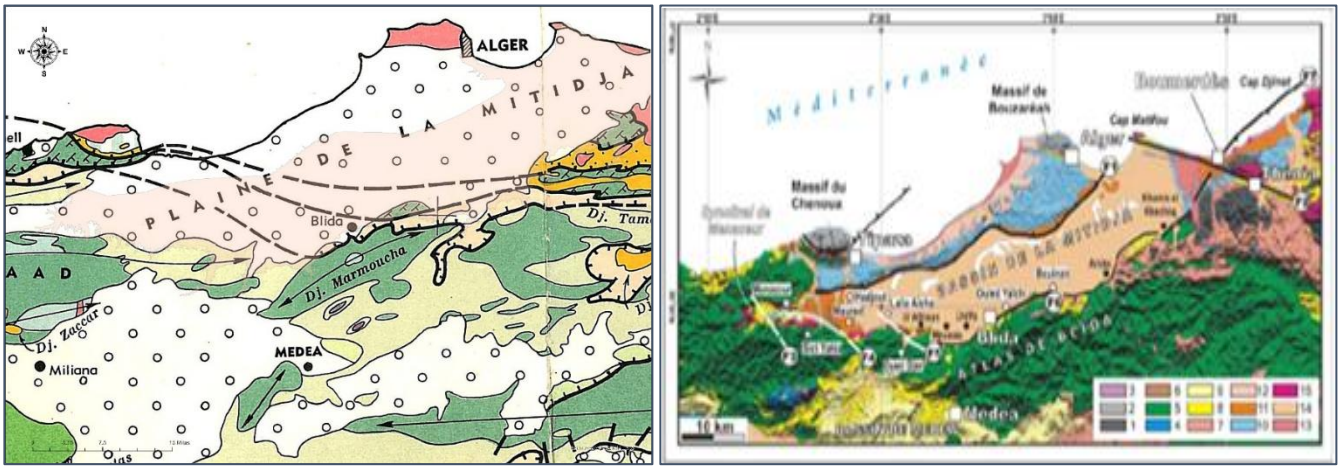


Figure 4.2. Geology Map of Mitidja plain.

4.3 Hydrological and Anthropogenic Issues: The Production of Risk

While geography predisposes the Mitidja to flooding, it is human activity that transforms this predisposition into a systemic threat. The territory is not merely a passive recipient of natural hazards; it serves as a stage for the **anthropogenic amplification of risk**. This section analyzes the stark confrontation between a **torrential hydrographic network** and massive urbanization conflict that has disrupted long-standing hydrological balances, effectively turning the plain into a **"risk factors"** for its own critical infrastructure.

4.3.1 The Hydrological System: Torrentiality and Overexploitation

The hydrology of the Mitidja Plain is characterized by a dual-natured crisis: a violent surface network and a stressed groundwater resource.

The Hydrographic Network: Wadis with Torrential Regimes

The plain is drained by a dense network of major wadis descending from the Blidean Atlas and discharging into the Mediterranean. These are categorized into the **Eastern basins** (El Harrach, Hamiz, Réghaïa) and the **Western basins** (Mazafran, Djer, Chiffa) [148], [149].

Flood Regime: These wadis exhibit a typically Mediterranean regime: severe low flows (*base flows*) in summer followed by violent **flash floods** in autumn and winter. The Mazafran Wadi, with an average discharge of 10.14 m^3/s, exemplifies this hydrological power[154].

The Sediment Threat: Wadis such as the Chiffa, which run alongside strategic corridors (e.g., the **North-South Highway**), carry considerable **sediment loads** resulting from active hillslope erosion [155]. As demonstrated by [154] for the Mazafran basin, these suspended matter loads transform floodwaters into **hyper-concentrated flows**, which are particularly destructive to bridge structures and crossings.

Hydraulic Management: An East-West Dichotomy

A clear distinction exists between the Eastern Mitidja (fed by the Hamiz dam) and the Western Mitidja (El-Moustakbal dam). These **irrigated perimeters** suffer from chronic maintenance and efficiency issues, exacerbating the overall vulnerability of the system [156].

Hydrogeology under Stress: The Quaternary Aquifer

The plain sits atop a strategic alluvial aquifer (100 to 200 m thick). However, this reservoir is currently in crisis. The **piezometric level** has dropped drastically since 1970 (by as much as 80 m), leading to negative levels (-35 m) in the Northeast. This has caused an **inversion of the hydraulic gradient**, triggering **seawater intrusion** [153]. This overexploitation destabilizes the basin's hydrological equilibrium.

4.3.2 Urban Sprawl: Soil Sealing as an Aggravating Factor

Historically dedicated to agriculture, the Mitidja has long served as the **"breadbasket of Algiers"** due to its fertile soils [145]. However, the region is currently undergoing a rapid and

profound transformation. The **urban sprawl** of the Algiers metropolitan area and its satellite towns is heavily encroaching on arable lands; indeed, a 28% loss in agricultural surface area was recorded between 1997 and 2013 [21].

The Hydraulic Consequence: This **land artificialization** radically alters the basin's hydrological response. By replacing natural soils with **impervious surfaces** (concrete and asphalt), urbanization increases **runoff coefficients** and reduces infiltration into the already overexploited aquifer. Rainwater no longer infiltrates the ground; instead, it flows instantaneously toward low-lying areas, **mechanically increasing** both pluvial and fluvial flood risks within densified zones [42].

4.3.3 Historical Disasters: A Proven and Recurring Threat

The vulnerability of the Mitidja Plain is not merely a theoretical projection; it is substantiated by a deep-seated historical record of catastrophes. Analysis of past events reveals an alarming recurrence of major disasters that have shaped the region's perception of risk [11]: **December 1957:** Widespread torrential rainfall, with 222 mm recorded at Boufarik. **March 1973 & 1974:** Major flooding of the eastern plain caused by the overflow of the Hamiz Wadi, resulting in **flood depths** of 50–60 cm in Rouiba. **November 2001 (Bab El Oued):** This remains the **seminal traumatic event** for the region. Although centered on Northern Algiers, it demonstrated the devastating violence of flash floods and mudflows in the area. **November 2007:** Significant urban flooding in Rouiba following intense rainfall of 117 mm within a 24-hour period.

These historical milestones demonstrate that the risk is tangible: it manifests in water depths sufficient to paralyze the road network and effectively isolate the capital from its economic hinterland.

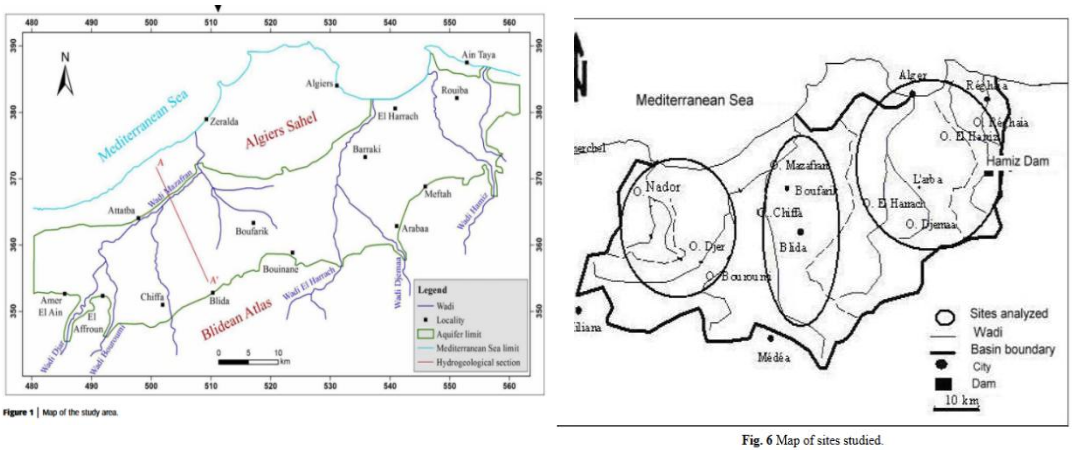


Figure 1 | Map of the study area.

Fig. 6 Map of sites studied.

Figure 4.3. Hydrology map of Mitidja plain.

4.4 Rationale for the Strategic Selection: From Territorial Complexity to Structural Precision

The strategic selection of the Mitidja Plain as a field of investigation is driven by scientific necessity rather than mere geographic convenience. This territory does not merely serve as a backdrop to validate a digital tool; it acts as the ideal **crucible** for testing the robustness of our multi-scale methodology.

Indeed, the inherent nature of the Mitidja demands a **graduated approach**. It is simultaneously too vast for comprehensive high-fidelity modelling and too complex to be addressed through simple global mapping alone. It necessitates a constant shift between **Regional Zoning**, essential for grasping watershed-wide dynamics, and **Site-Specific Diagnostics**, vital for safeguarding critical civil engineering assets.

This dual-scale requirement fundamentally justifies our methodology: **identifying risk at the kilometres scale to address it at the centimetres scale.**

4.4.1 A Territory of National Strategic Importance: The Gordian Knot

The Mitidja transcends its status as a mere agricultural plain; it represents the **logistical nerve centre** of modern Algeria. Traversed by the country's two primary **lifelines** (the East-West Highway (A1), the definitive backbone of the Maghreb, and the North-South Bypass (RN1), a critical trans-Saharan corridor) it hosts an unparalleled density of both population and industrial activity.

In this context of saturation, any infrastructure failure would not remain a localized incident; instead, it would act as the immediate trigger for a **national systemic crisis**, paralyzing freight flows and effectively isolating the Algiers metropolitan area. Consequently, flood risk management in the Mitidja is far more than a civil engineering concern; it is a vital imperative for **economic sovereignty** and **territorial continuity**.

4.4.2 Hydrological Complexity Mandating Macro-Scale Zoning

The Mitidja territory acts as a hydrological laboratory, characterized by a rare convergence of extreme phenomena. It is simultaneously threatened by **slow-onset plain flooding** in the eastern sector, violent **flash floods** descending from the Atlas foothills, and intense **urban runoff** trapped by soil sealing.

This spatial and temporal heterogeneity makes the application of high-resolution hydraulic modelling across the entire region prohibitively complex and costly. Consequently, it justifies the need for an initial **strategic screening phase**: Macro-scale Susceptibility Zoning using **AHP-GIS**. This approach allows for a comprehensive "scan" of the territory to effectively pinpoint **"hotspots"** where hazards intersect with critical assets, thereby directing in-depth diagnostic efforts toward the most vulnerable sectors.

4.4.3 The Failure of Conventional Models and the High-Fidelity Imperative (Micro-Scale)

Finally, the unique topography of the Mitidja, characterized by minute gradients (often below 0.5%), presents a significant challenge for standard modelling tools. In such a remarkably flat plain, vertical uncertainty of just a few centimetres in a satellite-derived **DEM** is sufficient to significantly distort the modelled **flood footprint**.

To address this precision challenge (specifically identified in critical reaches such as the **Oued Chiffa**) the localized deployment of a **High-Fidelity (BIM-HDM)** approach emerges as the most relevant solution. By capturing the micro-topography of the infrastructure (including drainage ditches, cross-slopes, and bridge piers), this technology provides the indispensable resolution required to diagnose the structure's actual vulnerability when confronted with the complex hazards of this territory.

4.5 Conclusion:

From the Laboratory to Experimentation

The Mitidja Plain is far more than a mere geographical study area; it represents a **full-scale laboratory** of systemic vulnerability. Within a confined space, it encapsulates the entirety of the challenges this thesis seeks to address non-stationary hydrology, unchecked urbanization, and a critical infrastructure network under severe strain.

The analysis of its physical and anthropogenic characteristics has confirmed the necessity of our **dual methodological approach**:

a) **Watershed-scale zoning** to identify precisely where the risk originates.

b) **Structure-scale diagnostics** to understand exactly how the asset withstands the hazard.

Building upon this territorial assessment, the following chapter will deploy our research's **experimental protocol**, applying our digital tools to the concrete reality of this strategic territory.

PART II:

SUSCEPTIBILITY MAPPING AT THE TERRITORIAL SCALE (MACRO-SCALE APPROACH)

5 Regional Susceptibility Mapping and Zoning

5.1 Introduction

The Zoning Dilemma in Homogeneous Landscapes

The management of natural hazards across an area as extensive as the Mitidja Plain (1,450 km²) necessitates a decisive initial stage: **strategic zoning**. Before considering infrastructure resilience or dimensioning protection works, it is imperative to identify, at the landscape scale, the priority sectors for intervention [39].

However, defining these "red zones" faces a paradoxical challenge. Unlike mountainous catchments where flood risk is naturally confined to valley floors, the Mitidja exhibits a **deceptive apparent homogeneity**: a uniformly flat topography and ubiquitous clay-heavy soils [42]. In a context where "everything seems flood-prone," how can one accurately discriminate between levels of urgency?

This zoning phase is further complicated by significant uncertainty. The absence of dense hydrological monitoring networks (**data-scarce region**) and the complexity of systemic interactions (rainfall-soil-urbanization) render any deterministic mapping hazardous [157]. At this scale, a zoning error carries heavy consequences: it leads either to a waste of resources in safe areas or, more critically, to the endangerment of populations in zones falsely deemed secure.

This chapter presents the first phase of our multi-scale methodology: **Macro-scale susceptibility analysis**. Our objective is not to produce a single, static map, but to construct a robust decision-making strategy in the face of uncertainty. To achieve this, we deploy a comparative and incremental approach structured around three validation pillars:

a. **Strategic Rationale (Section 5.2):** We first justify why the multi-criteria approach (**AHP-GIS**) emerges as the most rational method for the Algerian context, given the economic and technical limitations of global hydraulic models [67].

b. **Standard AHP Approach (Section 5.3):** We establish an initial baseline assessment based on expert judgment, integrating both physical and anthropogenic factors [91].

c. **Uncertainty Management and Sensitivity Analysis (Sections 5.4 and 5.5):** This represents the core of our contribution. Moving beyond a single map, we confront expert judgment with the rigor of **Fuzzy Logic** [107] and, crucially, deploy an unprecedented **Multi-Scenario Sensitivity Analysis**. By testing six contrasting weighting hypotheses, we aim to isolate the **"Hard Core" of vulnerability**: those areas that remain invariably at risk regardless of the underlying hydrological assumptions [76]. Finally, we validate this convergence using the statistical objectivity of **Machine Learning** [45].

The ultimate ambition of this chapter is to isolate the **"Hard Core" of vulnerability**: those territories that consistently emerge as critical across all models, and which will serve as the primary targets for our high-fidelity diagnostics.

5.2 Strategic Rationale: Justifying the Multi-Criteria Approach (AHP-GIS)

When addressing the imperative to map flood susceptibility at a regional scale (1,450 km²), researchers are confronted with a fundamental methodological dilemma: whether to opt for the apparent rigor of **physical hydraulic modelling** or the flexibility of **multi-criteria spatial analysis**.

The decision to prioritize **AHP-GIS coupling** is not a shortcut or a "simplification by default"; rather, it represents a **reasoned scientific strategy** specifically adapted to the constraints of the Algerian territory. This choice is supported by three major pillars: **data availability**, **computational efficiency**, and the **systemic nature of risk**.

5.2.1 Addressing Data Scarcity

Physical hydraulic modelling (e.g., HEC-RAS 2D) is highly **data-intensive**. It necessitates high-resolution **channel bathymetry** (cross-sections) and, more importantly, long-term, reliable **discharge time series** for **calibration and validation**.

However, the Mitidja (mirroring many watersheds in developing nations) is a characteristic **data-scarce region**. The **stream-gauging network** is often **sparse or discontinuous**. In such a context, forcing the application of a complex physical model onto incomplete or patchy data leads to the trap of **"spurious precision"**: a result that is mathematically exact but physically erroneous.

Conversely, the AHP-GIS approach leverages globally available and reliable **geospatial datasets** (satellite DEMs, Landsat/Sentinel imagery, and CHIRPS global rainfall data), providing superior **methodological robustness** in the face of **input uncertainty** [157].

5.2.2 Economic and Spatial Efficiency: The Principle of Parsimony

From an operational standpoint, modelling **high-resolution hydrodynamics** across a 1,450 km² area entails **prohibitive computational and financial costs**, which are disproportionate to the primary planning objectives.

In this context, the AHP-GIS approach offers an optimal **cost-effectiveness ratio** for the macro scale. It operates according to the **principle of parsimony**: utilizing minimum resources to achieve maximum **decision-making impact**. It enables a cost-effective "scanning" of the entire territory to identify major risk corridors. This method serves as an indispensable **strategic filter**, allowing **heavy engineering resources** to be focused exclusively where they are most needed(the critical zones(thereby avoiding the **fragmentation of resources** on safe areas [67].

5.2.3 The Multidimensional and Systemic Nature of Risk

Ultimately, reducing flood risk in the Mitidja to mere water levels would be a **conceptual fallacy**. In this region, risk is inherently **systemic and multidimensional**. It arises not only from precipitation but from the complex interplay between physical attributes (such as flat topography and impermeable clayey soils) and, crucially, **anthropogenic factors**, including rapid urbanization and the densification of the road network.

Unlike hydraulic models, which often relegate land use to a **passive roughness coefficient**, the multi-criteria AHP approach enables the explicit integration of these heterogeneous factors within a single **decision matrix**. It captures human dynamics as an **active driver of vulnerability**, providing a more **holistic understanding** of territorial susceptibility [158] .

5.3 The Standard Approach: Multi-Criteria Decision Analysis (AHP-GIS) Mapping

The integration of the **Analytic Hierarchy Process (AHP)** with **Geographic Information Systems (GIS)** is far more than just one methodology among many; it has emerged as the established global standard for assessing susceptibility to natural hazards, particularly in **data-scarce environments** [157].

This hybrid approach (originally developed and presented by the author at the **ICEAT 2025 international conference**) provides a robust analytical framework. It facilitates the synthesis of heterogeneous environmental factors, ranging from **pure morphometry** (e.g., slope) to **anthropogenic dynamics** (e.g., land use), into a unified and **actionable risk map** for decision-makers [159] .

5.3.1 Methodological Protocol: The Geospatial Processing Workflow

The adopted approach follows a rigorous and standardized protocol, structured into four sequential stages **(Fig. 5.1)**:

1. **Multi-Source Database Construction:** This involves the collection and harmonization of heterogeneous datasets, including satellite **Digital Elevation Models (DEMs)**, climatological data (CHIRPS), geological maps, and land use/land cover (LULC) imagery [67] .
2. **GIS Normalization and Feature Derivation:** Data are integrated into a unified environment (ArcGIS Pro), reprojected into the local geodetic system (**UTM Zone 31N**), and resampled to a common resolution of 30 meters. This stage includes the mathematical derivation of key morphometric factors(such as slope, curvature, and the **Topographic Wetness Index (TWI)** [89].
3. **Hierarchical Weighting (AHP):** Construction of the **pairwise comparison matrix** to determine the normalized relative weight (W_i) for each factor. This step relies on **Saaty's fundamental scale** and includes the calculation of the **Consistency Ratio (CR < 0.1)** to validate the logical consistency of the expert judgment [160].
4. **Spatial Aggregation (Weighted Overlay):** The final calculation of the **Flood Susceptibility Index (FSI)** for each pixel is performed via weighted overlay, according to the canonical equation:

$$FSI = \sum_{i=1}^{n} (W_i \times R_i)$$

(Where W_i represents the weight of criterion i and R_i is the rating of the reclassified class).

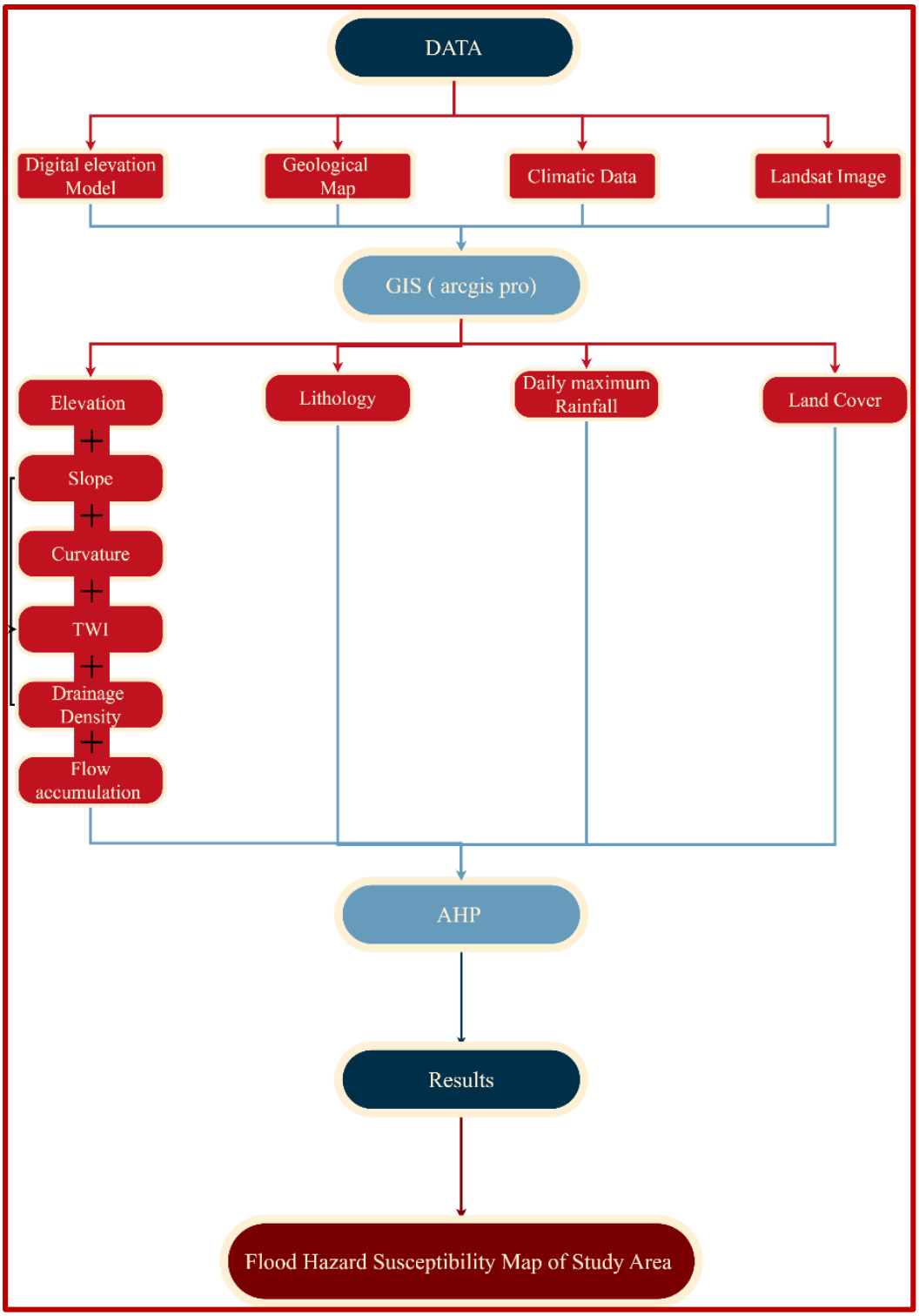


Figure 5.1. Methodology steps

5.3.2 Characterization and Analysis of Influencing Factors

The reliability of the resulting model is strictly contingent upon the selection and quality of the input data. Nine factors, categorized into three distinct groups, were selected and characterized for this study.

5.3.2.1 Morphometric Factors (Source: SRTM 30 m DEM)

- **Elevation and Slope:** The elevation map **(Fig. 5.2a)** confirms the nature of the region as a **subsiding basin** (50–100 m). The slope map **(Fig. 5.2b)** reveals critical values (below 3%) across most of the plain, identifying primary **stagnation zones**.
- **Curvature: (Fig. 5.2c)** This factor facilitates the distinction between **convex areas** (flow dispersion/divergence) and **concave areas** (flow accumulation/convergence).

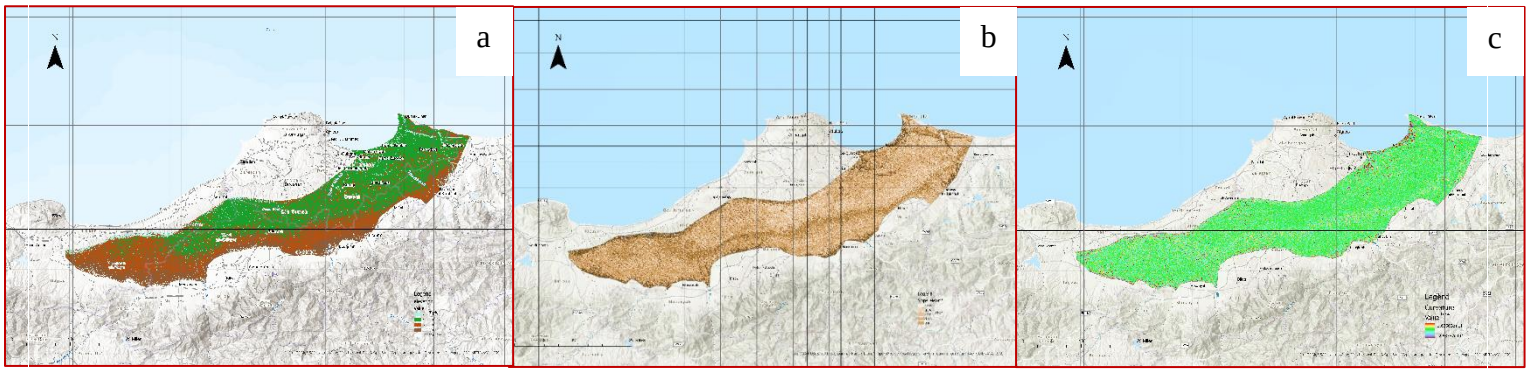


Figure 5.2. Topographical Factors: a-Elevation, b-Slope, c-Curvature

5.3.2.2 Hydrological Factors (Derived from DEM and Network Analysis)

- **Topographic Wetness Index (TWI): (Fig. 5.3a)** This physical index highlights potential soil saturation zones resulting from **flow convergence**.
- **Drainage Density: (Fig. 5.3b)** This reflects the network's capacity to collect and channel discharge. High-density areas (notably the Blida foothills) indicate a **rapid hydrological response**.
- **Flow Accumulation: (Fig. 5.3c)** This parameter quantifies the upslope contributing area for each cell. It delineates **preferential flow paths** and thalwegs where runoff concentrates heavily.

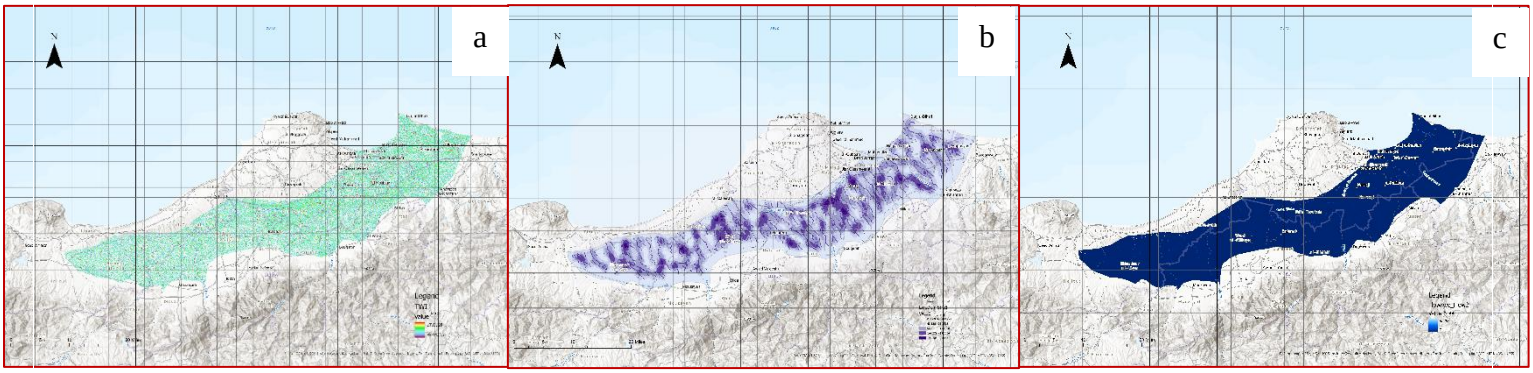


Figure 5.3. Hydrological Factors: a-TWI, b-Drainage density, c-Flow accumulation.

5.3.2.3 Geo-Environmental Factors (Heterogeneous Datasets)

- **Precipitation (Source: Digitized Isohyet Maps): (Fig. 5.4)** Although the distribution is relatively uniform across the plain, peaks are identified in the southwest (Atlas region). **Critical note:** This dataset, derived from legacy maps, carries inherent spatial uncertainty.

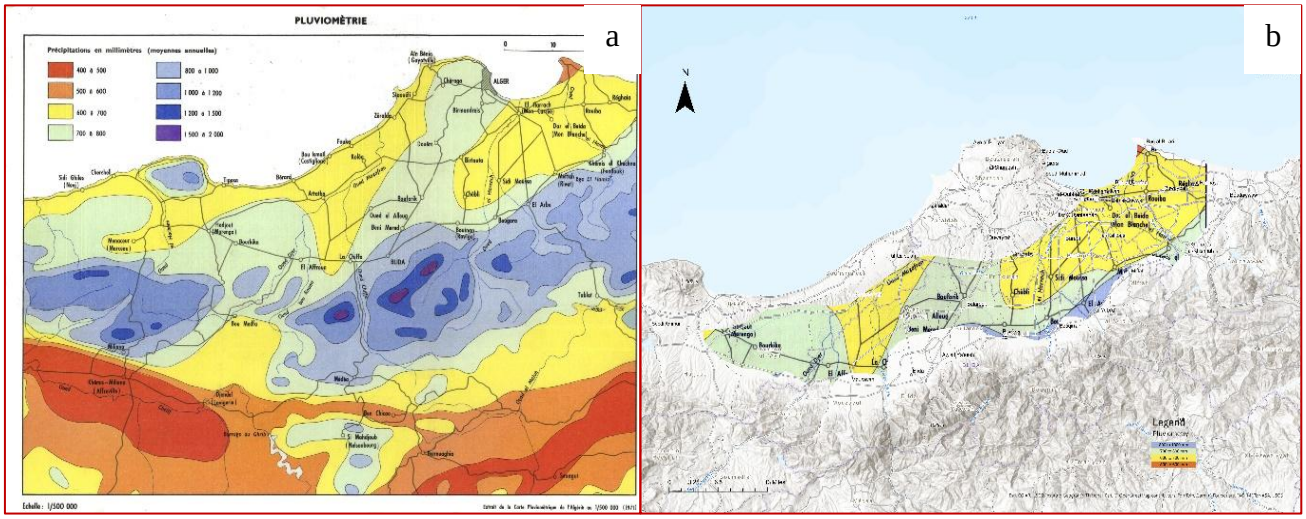


Figure 5.4. a-Pluviometry carte, b-delimitation of pluviometry carte in the Mitidja plain.

- **Lithology (Source: Geological Map): (Fig. 5.5)** The predominance of clays and alluvium confirms a low **intrinsic permeability** across the study area.

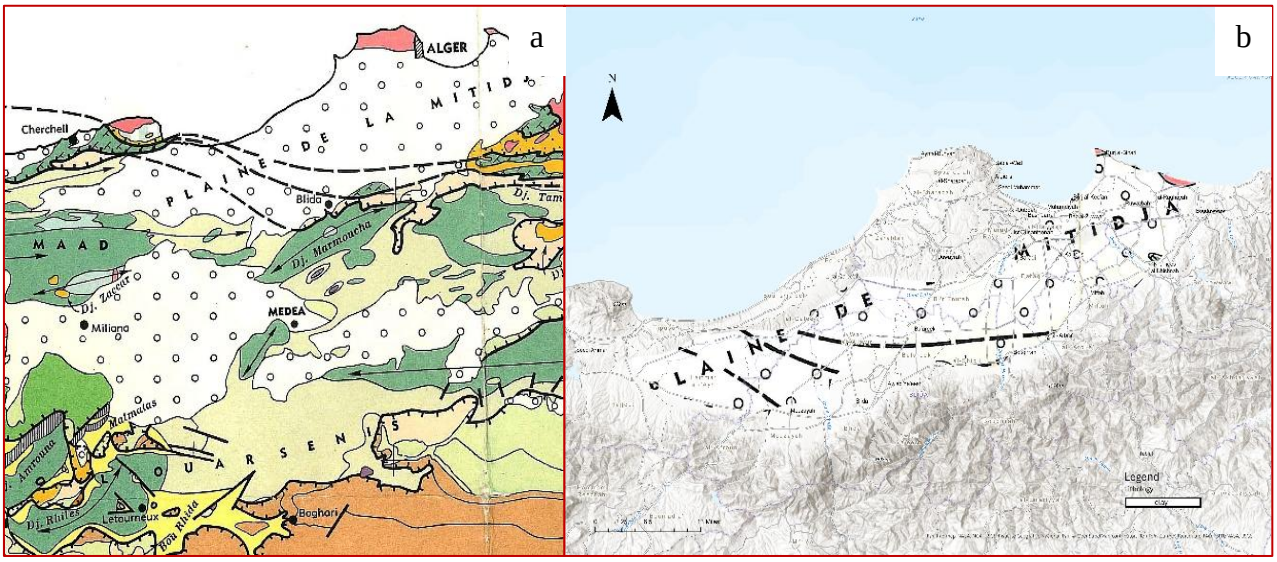


Figure 5.5. a-Geological carte, b-delimitation of geological carte in the Mitidja plain.

- **Land Use / Land Cover (LULC) (Source: Landsat Classification): (Fig. 5.6)** The LULC map highlights the extent of **built-up areas**, which constitute the primary anthropogenic factor exacerbating flood risk.

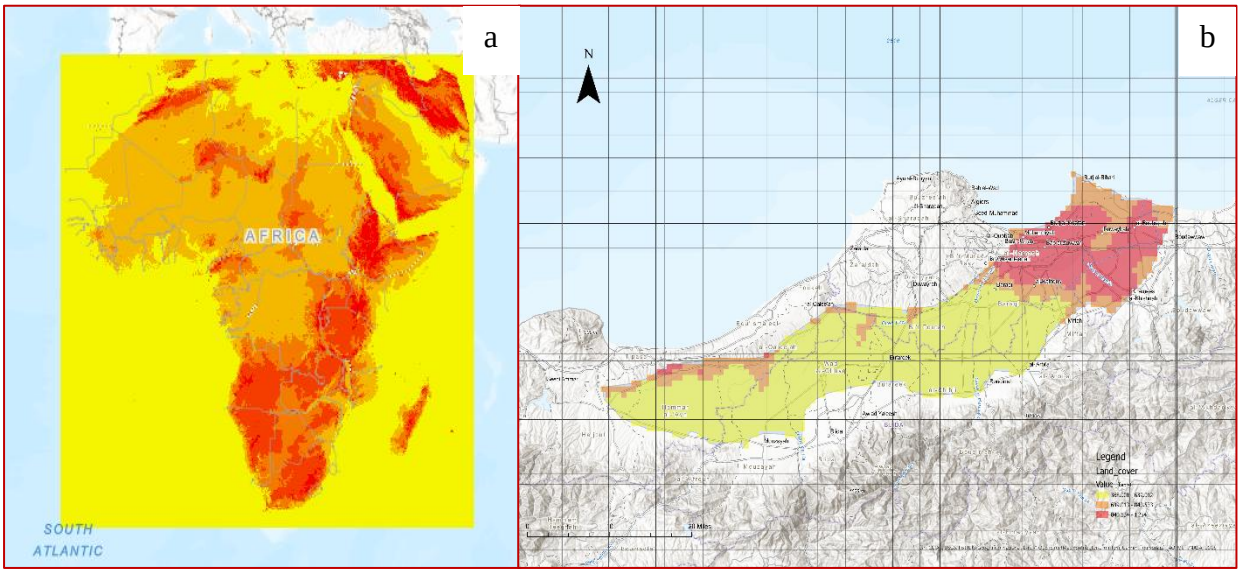


Figure 5.6. a-Land cover carte, b-delimitation of Land cover carte in the Mitidja plain.

5.3.2.4 Critical Assessment of Data Quality

The heterogeneity of the data sources represents a significant methodological limitation. While the topographical data (SRTM 30m DEM) provide an acceptable resolution for regional-scale analysis, the thematic datasets (Rainfall, Geology) derived from the **manual digitization of legacy maps** introduce spatial uncertainty. This **disparity in precision** underscores the necessity for the subsequent **sensitivity analysis** to evaluate the model's robustness against these uncertainties.

5.3.3 Identification and Weighting of Influencing Factors

For this baseline standardized approach, nine major conditioning factors were weighted based on a preliminary literature review and the distinct physical characteristics of the Mitidja Plain **(Table 5.1)**:

- **Topographical Factors (Slope, Elevation, Curvature):** The highest weight was assigned to **Slope (20%)**, as it is the critical factor governing surface runoff. **Elevation (15%)** was used to delineate low-lying areas (basin-like depressions), while **Curvature (5%)** was included to identify localized convergence zones.
- **Hydrological Factors (Drainage Density, TWI, Flow Accumulation): Drainage Density (15%)** and the **TWI (10%)** capture the capacity of the hydrographic network to concentrate flow. **Flow Accumulation (10%)** was used to simulate preferential water trajectories across the landscape.
- **Environmental Factors (Precipitation, Lithology, Land Use): Precipitation (15%)** serves as the primary driver of the hazard. **Land Use (5%)** and **Lithology (5%)** (predominantly clay-based) account for surface imperviousness and the soil's infiltration response.

This weighting scheme reflects a conventional **"Topography-Precipitation" paradigm**, consistent with established literature for regional-scale flood studies [67].

Table 5.1. Flood Susceptibility Assessment Table by Hierarchical Analysis (AHP).

Flood Causes	Unit	Class	Reclassify	Class Ranges	Ratings	Weights
Topographic wetness index (TWI)	Level	V low	1	-9.444 – 0.933	1	0.10
		Low	2	-0.933 – 1.239	2	
		Mediem	3	1.239 – 3.214	3	
		High	4	3.214 – 6.223	4	
		V high	5	6.223 – 17.023	5	
Elevation	M	V high	1	2 – 49	5	0.15
		High	2	49 – 84	4	
		Mediem	3	84 – 103	3	
		Low	4	103 – 139	2	
		V low	5	139 – 255	1	
Slope	%	V high	1	0.000001 – 6.87338	5	0.2
		High	2	6.87339 – 15.8387	4	
		Mediem	3	15.8388 – 28.0912	3	
		Low	4	28.0913 – 42.7345	2	
		V low	5	42.7345 – 76.2049	1	
Precipitation	Mm	V low	5	600 – 700	1	0.15
		Low	4	700 – 800	2	
		Mediem	3	800 – 1000	3	
Land Cover	Level	V low	1	368 – 639	1	0.05
		Low	2	639 – 840	2	
		Mediem	3	840 – 1254	3	
Drainage Density	m/km	V low	1	0.00001 – 48	1	0.15
		Low	2	48 – 96.25	2	
		Mediem	3	96.25 – 144.37	3	
		High	4	144.37 – 192.503	4	
		V high	5	192.503 – 240.6295	5	
Lithology	LEVEL	V high	5	Clay	5	0.05
Flow accumulation	Level	V low	1	0.000001 – 2561.09	1	0.10
		Low	2	2561.1 – 10610.2	2	
		Mediem	3	106103 – 25976.8	3	
		High	4	25976.8 – 52319.5	4	
		V high	5	52319.5 – 93297	5	
Curvature	Level	V low	1	-253381 – -511169	1	0.05
		Low	2	511168 – 168264	2	
		Mediem	3	168623 – 271167	3	
		High	4	271168 – 255481	4	
		V high	5	255482 –162566	5	

5.3.4 Preliminary Results and Methodological Critique

The resulting map **(Fig. 5.7)** illustrates a **near-ubiquitous** "High" to "Very High" flood susceptibility across the entire plain, extensively covering central depressions and fluvial corridors. This outcome is a direct consequence of the territory's **intrinsic homogeneity**: over vast areas, the Mitidja displays uniformly flat topography, a consistent clayey lithology, and a relatively homogeneous rainfall regime.

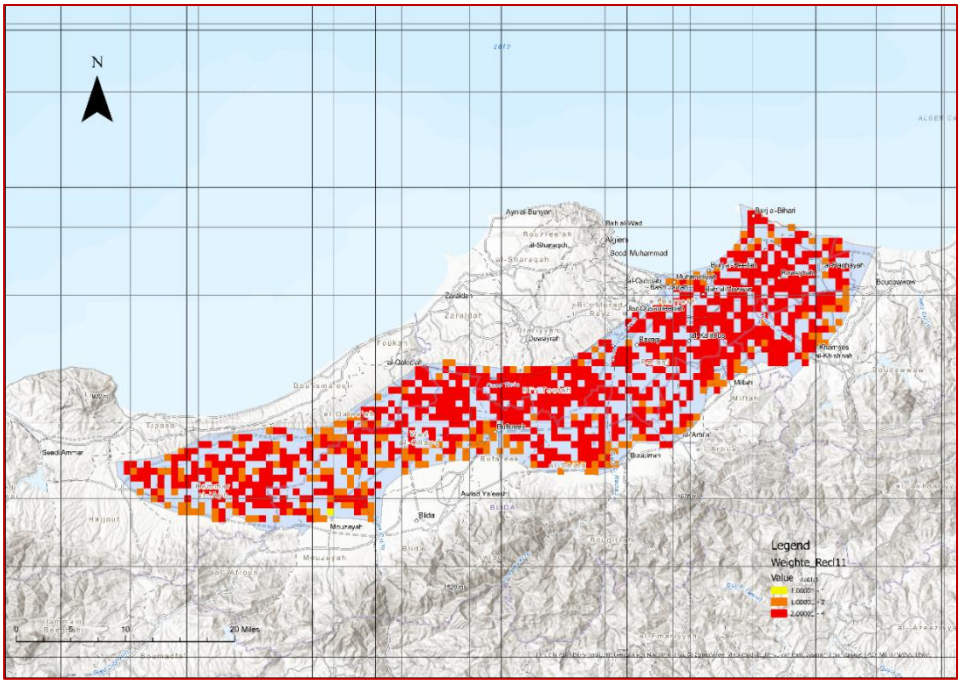


Figure 5.7. Flood Susceptibility Mapping.

However, a critical analysis highlights several major limitations that restrict the **operational utility** of this initial zoning:

1. **Lack of Spatial Discrimination:** Physical uniformity, coupled with the coarse resolution of the data, results in **diffuse zoning** (an "everything is red" effect). The method fails to isolate true priority **"hotspots."**
2. **Uncertainty in Data Sources:** The study relied on heterogeneous datasets, some of which were derived from the manual digitization of **non-georeferenced legacy maps**, thereby introducing an initial **geometric bias**.
3. **Subjectivity of Weighting:** The selection of weights rests on a single expert judgment, without any exploration of **epistemic uncertainties**.

To overcome these **methodological bottlenecks**, we have developed a second, more robust approach. This method utilizes standardized satellite datasets (**Google Earth Engine**) and a **multi-scenario sensitivity analysis** to sharpen the spatial contrast and pinpoint the **"hard core"** of the risk.

5.4 The Robust Approach: Uncertainty Management through Fuzzy-AHP and Sensitivity Analysis

While standard AHP provides a relevant initial approximation, it remains vulnerable to the subjectivity inherent in expert judgment. To overcome this critical limitation and ensure the reliability of the resulting zoning, we have developed an advanced validation methodology. This approach (submitted for publication in the ***Journal of African Earth Sciences*** under the title: "*Flood Susceptibility Mapping in the Mitidja Plain: A Multi-Scenario Sensitivity Analysis*") is based on the integration of two complementary scientific pillars:

1. **Fuzzy Logic:** This allows for the mathematical handling of the imprecision and **linguistic ambiguity** inherent in human judgment. By substituting discrete values with **fuzzy numbers**, the method absorbs and mitigates the uncertainty associated with expert elicitation [107].
2. **Multi-Scenario Sensitivity Analysis:** This explores system dynamics by intentionally varying the weighting hypotheses. This tool is essential for verifying the **spatial stability** of the risk: it determines whether a given area is classified as hazardous solely due to expert preference, or if its risk status is dictated by its physical configuration, regardless of the model's assumptions [76].

5.4.1 Methodological Protocol: Objectifying Uncertainty

Our approach aims to reduce **epistemic uncertainty** (stemming from limited knowledge) by crossing three complementary levels of analysis: a bibliographic meta-analysis, fuzzy modelling, and dynamic sensitivity analysis.

The necessary data were acquired via the Google Earth Engine (GEE) platform. This included COPERNICUS DEM Digital Elevation Models (DEMs) (30 m resolution), CHIRPS precipitation data, SoilGrids soil maps, the ESRI Land Cover 2020 map (10 m resolution), and Sentinel-2 imagery for NDVI calculation. All geospatial layers were reprojected to the WGS 84 / UTM Zone 31N coordinate system and resampled to a common 30 m resolution using GIS tools. From the DEM, several derived layers were generated, including slope, drainage density, distance to rivers, Topographic Wetness Index (TWI), and curvature. Subsequently, all layers were reclassified into five susceptibility contribution classes using the Jenks Natural Breaks classification method.

5.4.1.1 Literature-Based Benchmarking

Before applying any subjective weighting, we standardized the selection of factors through a rigorous quantitative and qualitative meta-analysis. By systematically reviewing a corpus of 20 benchmark studies on flood susceptibility worldwide **(Table 5.2 and Fig. 5.9)**(ranging from pioneering works [161] to the most recent research [162](we extracted the weights assigned by the international scientific community.

- **Results:** This analysis identified and prioritized the ten most recurring and statistically significant factors for environments similar to the Mitidja Plain (e.g., Precipitation, Slope, LULC).

- **Application:** The mean values of these bibliographic weights were used to construct our **Scenario 0 (Reference)**. This scenario represents the "state-of-the-art consensus," effectively eliminating internal bias from our own local judgment.

5.4.1.2 The Contribution of Fuzzy Logic (Fuzzy AHP)

Human judgment is rarely binary. To capture this nuance, we replaced the discrete values of Saaty's scale (1 to 9) with **Triangular Fuzzy Numbers (TFN)**. This method transforms subjective linguistic judgments (e.g., "significantly more important") into a range of probabilistic values (l, m, u), thereby absorbing the **inherent ambiguity** and vagueness associated with expert elicitation [107].

5.4.1.3 Contrasting Scenario Strategy (Sensitivity Analysis)

Given the complexity of flood mechanisms in the Mitidja, it is scientifically tenuous to declare *a priori* which factor is dominant. We therefore modelled six distinct weighting scenarios **(Fig. 5.8)** to cover the entire spectrum of possible hydrological hypotheses:

- **Scenario 0 (Bibliographic Reference):** Weighting derived from the benchmark average.
- **Scenarios 1 to 5 (Targeted Dominance):** Each scenario intentionally forces the dominance of a key factor (Precipitation, Elevation, Drainage Density, Distance to Rivers, and Land Use).

The goal is to identify zones that remain classified as "at-risk" across all scenarios. This provides the operational definition of the **"Hard Core" of vulnerability**.

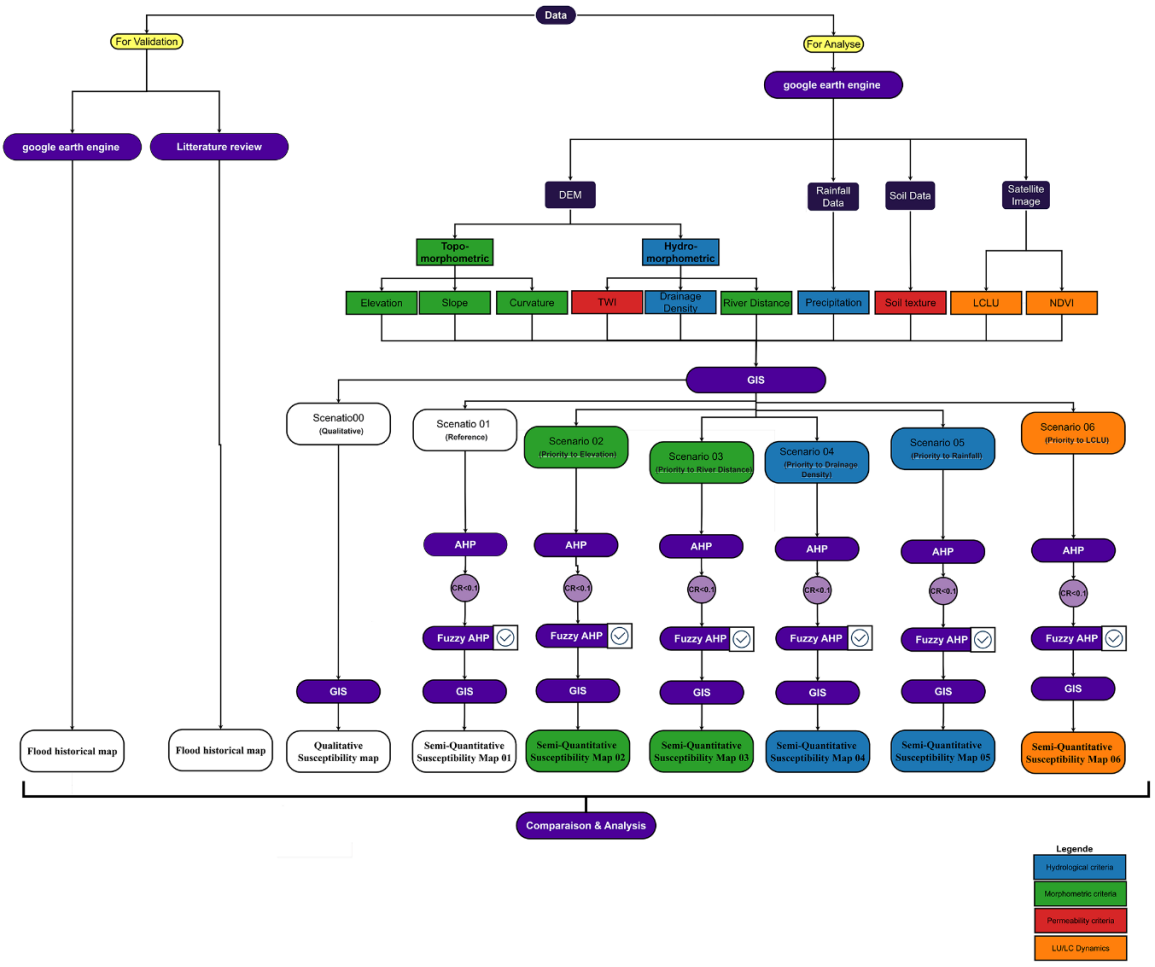


Figure 5.8. Methodology steps.

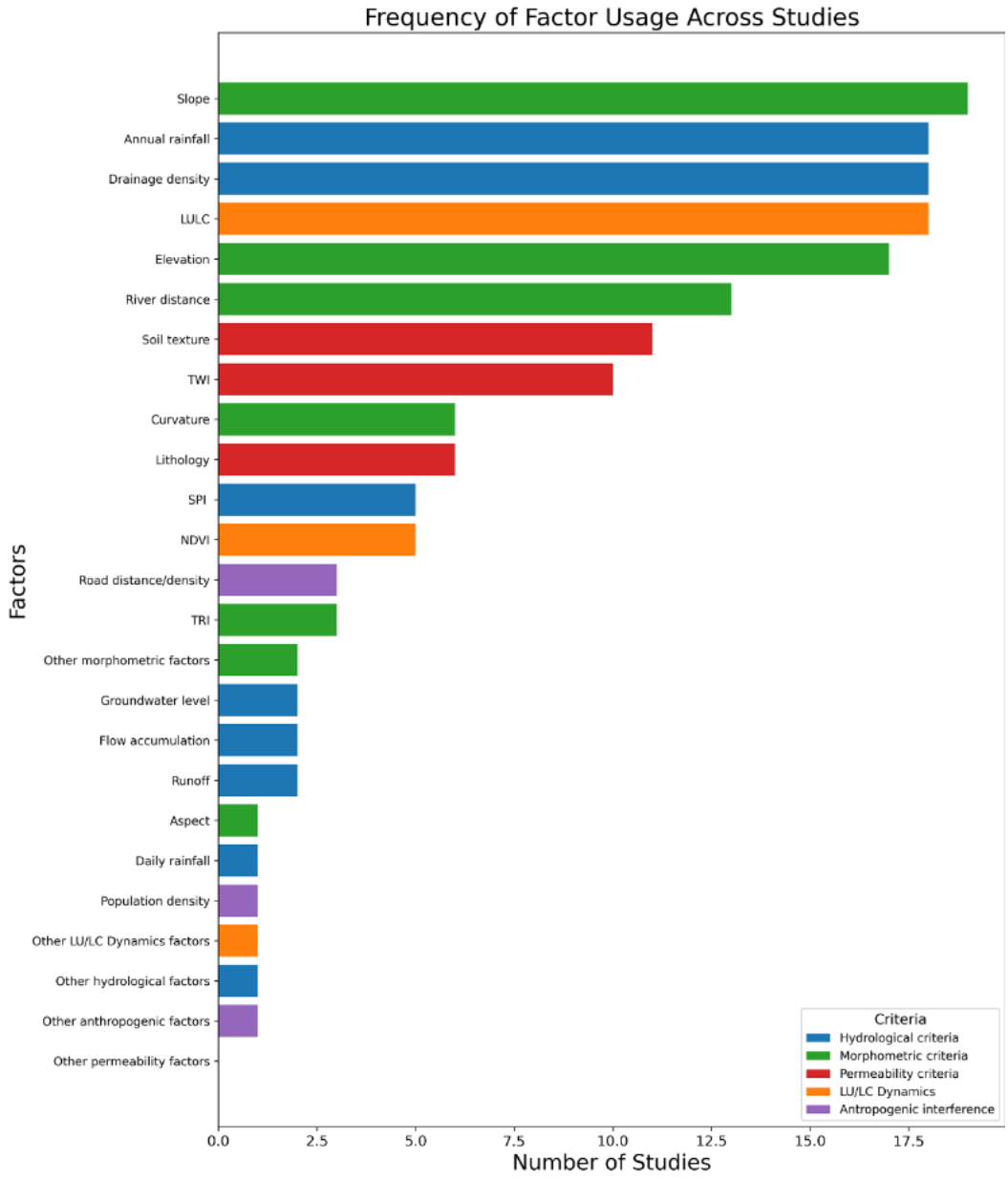


Figure 5.9. Frequency of Factor Usage Across Studies.

Table 5.2. Comparison of the Weightings of Flood Causative Factors in the Literature (1994–2025).

	Hydrological criteria								Morphometric criteria							Permeability criteria				LU/LC Dynamics			Antropogenic interference			CR	Flood Type
	AR	DR	DD	SPI	Ru	Gw	Fa	Other	El	Sl	Ast	Cu	TRI	RD	Other	TWI	Li	ST	Other	NDVI	LULC	Other	RD	PD	Other		
[161]	11.40%		6.10%						22.00%	8.70%	6.50%	5.10%		17.10%			5%	4.30%			13.70%					0.05	Pluvial flood
[163]	13%		8.20%						7.10%	18%								27.70%			26%					0.09	Compound flood
[164]	7.00%		.						38.00%	25.00%				14.00%							16.00%					0.08	Flash flood
[165]	15%		10%			3%			18%	8%							18%	5%			23%					0.07	Flash flood
[166]	5.56%	27.70%	1.53%						4.01%	5.95%								1.93%		3.26%	4.12%		10.86%	23.62%	11.39%	0.08	Flash flood

[167]	23%		5%	4%	23%				5%	7%			3%	18%		3%					9%					0.05	Pluvial flood
[168]	15%		10%			2.50%			22.50%	5%				10%			17.50%				17.50%					0.02	Pluvial flood
[169]	13.90%		6.30%		18.70%				4.90%	13.60%					11.70%						10.60%		14.10%			0.06	Pluvial flood
[170]	49.50%		8.20%							27.60%								7.10%			7.70%					0.04	Pluvial flood
[171]	49.70%									25.90%																0.09	Compound flood
[172]									5.70%	24.30%		11.20%		33%		18.10%		7.70%								0.047	Pluvial flood
[91]	12%		19%				9%		27%	18%		2%				3%	4%				6%					0.07	Flash flood

[157]	43%		16%						6%				21%				8%			6%					0.06	Pluvial flood
[173]	18%		9%						21%				11%		9%	16%	5%			9%						Flash flood
[174]	9%		9%					14%	8%				21%		13%		8%			8%		4%			0.08	Pluvial flood
[175]	5.38%		10.67%	2.09%				14.00%	8.00%		1.56%	3.92%	14.12%		2.93%				8.71%	7.14%					0.07	Flash flood
[176]	14.80%		4.45%	1%			6.43%	11.32%			5.19%	4.62%	12.48%		1.59%		2.89%		2.62%	9.39%	3.41%				0.086	Pluvial flood
[177]								33.90%	7.50%					9%	21.80%					27.80%					0.077	Flash flood
[178]	32%		55.70%	12.30%				10.30%	58.10%		8.10%		23.50%												0.08	Pluvial flood

[162]	**15.02%**		**5.90%**					**3.79%**	**15.27%**	**13.78%**				**11.80%**		**14.30%**		**6.09%**		**6.97%**	**7.05%**					**0.08**	**Pluvial flood**

5.4.2 Characterization of Influencing Factors (Robust Approach)

For this second analytical phase, the quality of the input data was substantially enhanced using the **Google Earth Engine (GEE)** platform. Ten geospatial factors, representing the topographic, hydrographic, pedological, and anthropogenic characteristics of the study area, were modelled.

5.4.2.1 Topographic and Geomorphological Factors

- **Elevation (Fig. 5.10):** The elevation map confirms the essentially flat nature of the Mitidja Plain, which functions as a **natural topographic sink**.



Figure 5.10. Elevation map of Mitidja Plain.

- **Slope (Fig. 5.11):** Extremely **gentle slopes** (< 3%) promote water stagnation and significantly hinder seaward drainage.

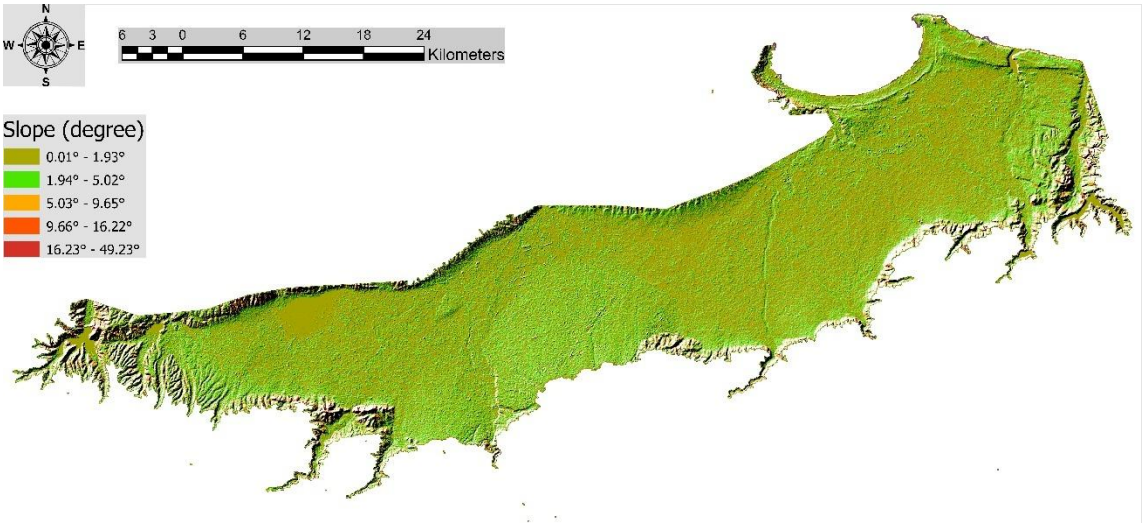


Figure 5.11. Slope map of Mitidja Plain.

- **Curvature (Fig. 5.12):** The analysis identifies numerous **concave areas (-)** that are highly prone to localized ponding and water accumulation.

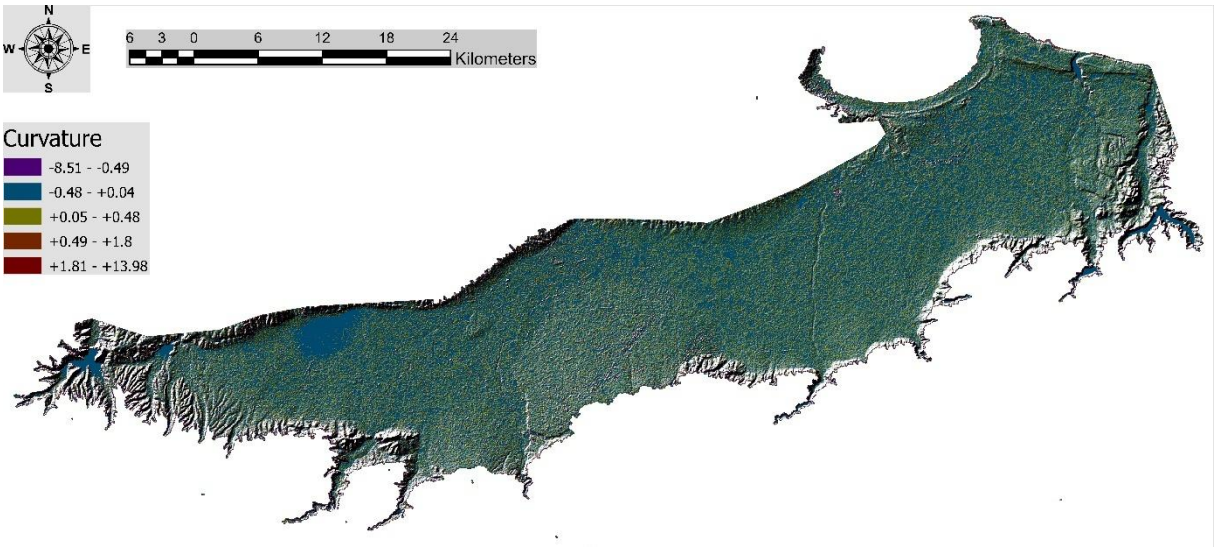


Figure5.12. Curvature map of Mitidja Plain.

5.4.2.2 Hydrographic and Climatic Factors

- **Rivers Distance (Fig. 5.13):** This map reveals that extensive areas are directly exposed to bank overflow from major wadis.

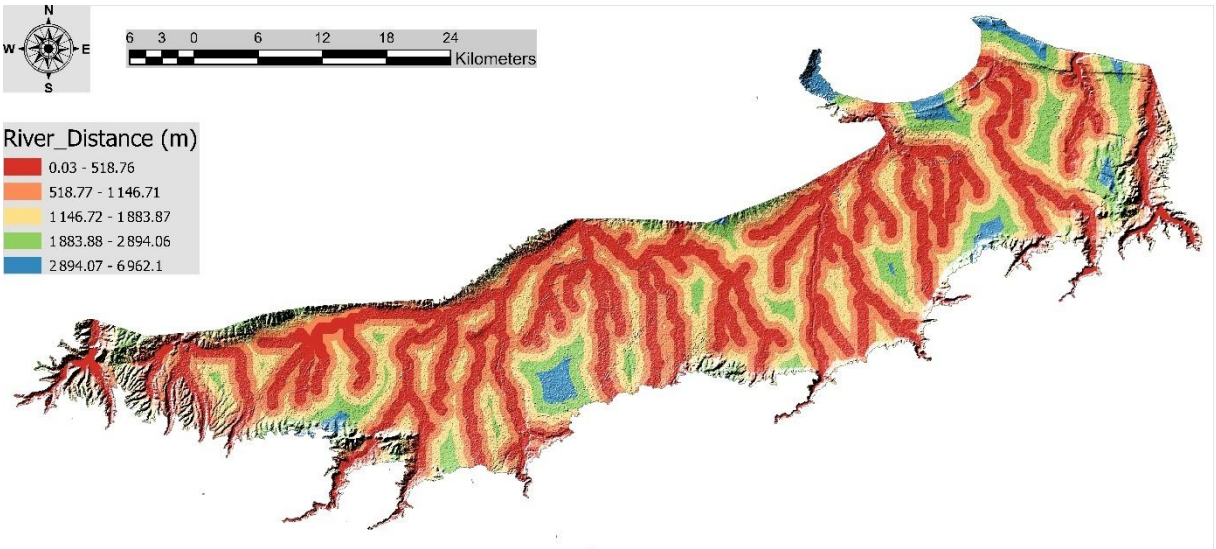


Figure 5.13. River distance map of Mitidja Plain.

- **Drainage Density (Fig. 5.14):** This factor illustrates the capacity of the stream network to concentrate rapid surface runoff.

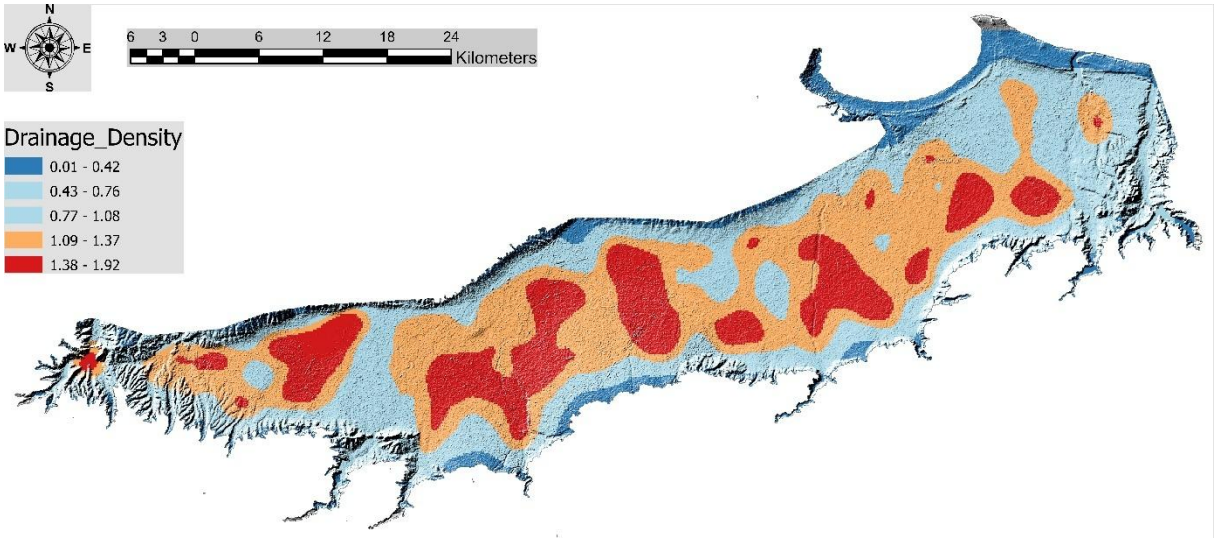


Figure 5.14. Drainage density map of Mitidja Plain.

- **Topographic Wetness Index (TWI) (Fig. 5.15):** The TWI identifies zones of potential soil saturation driven by **flow convergence**.

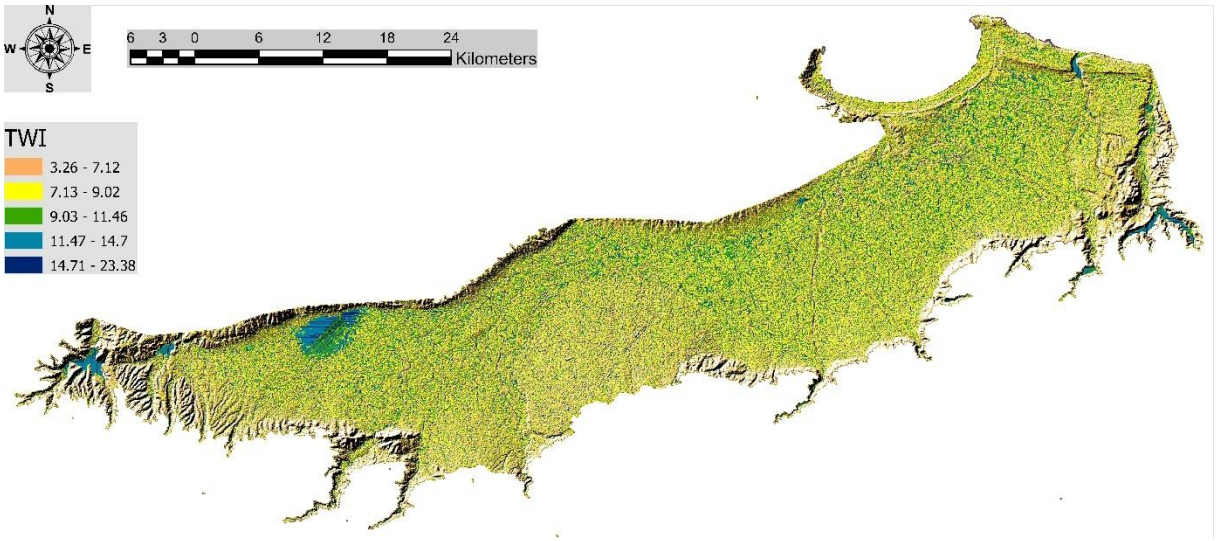


Figure 5.15. TWI map of Mitidja Plain.

- **Precipitation (Fig. 5.16):** Although generally uniform, the rainfall regime (derived from **CHIRPS data**) shows distinct peaks in the southwest (Blidean Atlas), which are capable of triggering devastating **flash floods** [42] .

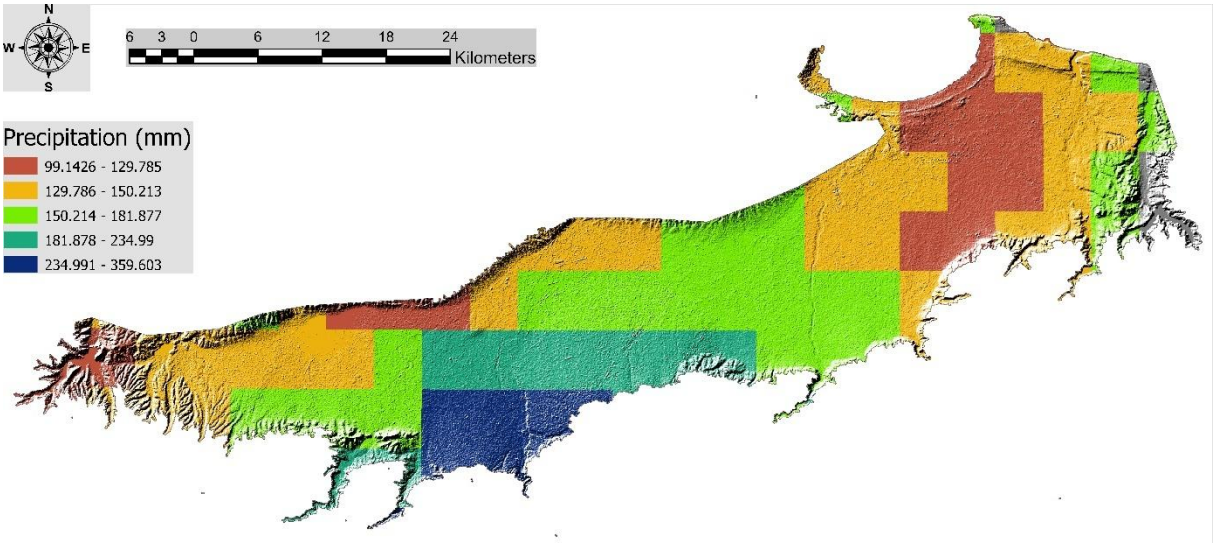


Figure 5.16. Precipitation map of Mitidja Plain.

5.4.2.3 Soil, Vegetation, and Land Use Factors

- **Soil Texture (Fig. 5.17):** The predominance of **clay-loam soils** (derived from **SoilGrids**) implies low **intrinsic permeability**, which favors rapid runoff generation[21].

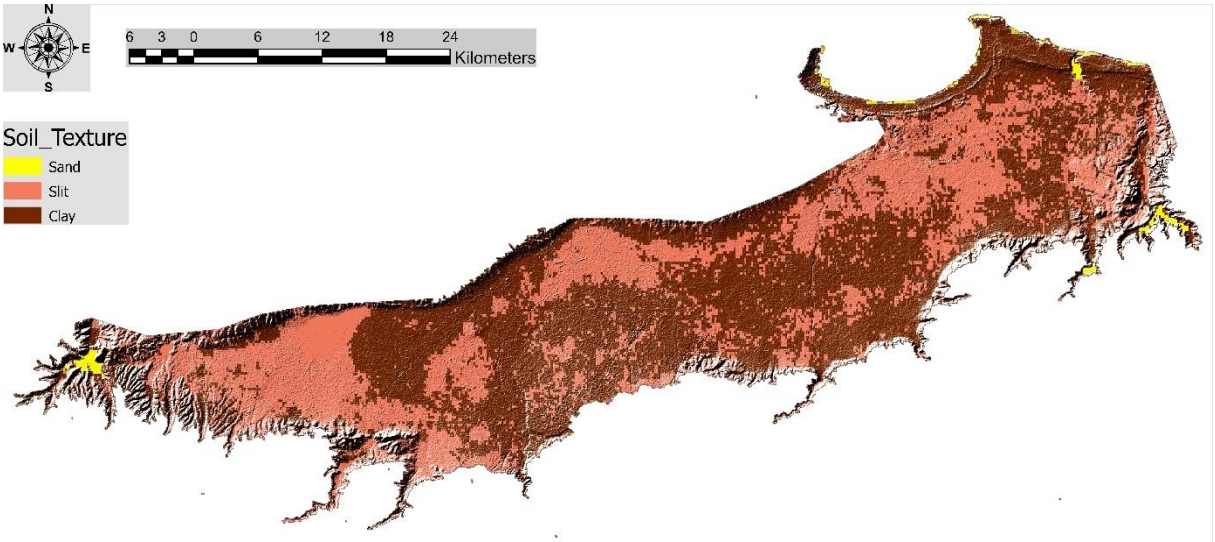


Figure 5.17. Sol texture map of Mitidja Plain.

- **NDVI (Normalized Difference Vegetation Index) (Fig. 5.18):** This index reflects the region's intense agricultural activity and vegetation cover.

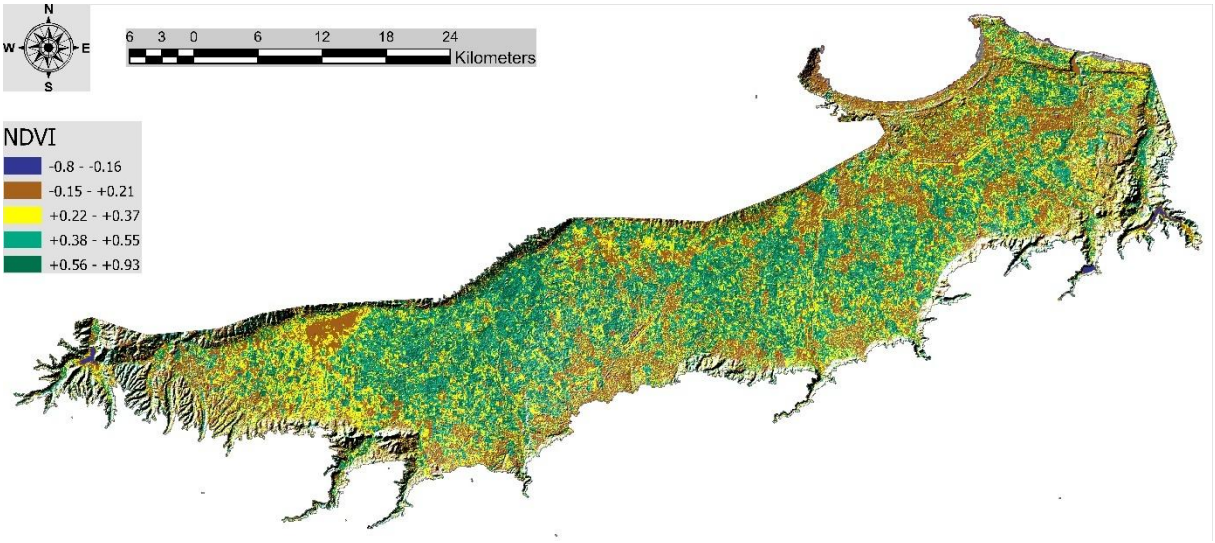


Figure 5.18. NDVI map of Mitidja Plain.

- **Land Use / Land Cover (LULC) (Fig. 5.19):** As a major anthropogenic factor, the expansion of impervious built-up areas drastically reduces infiltration and accelerates flow velocity, serving as a primary driver of escalating flood risk [42]**.**

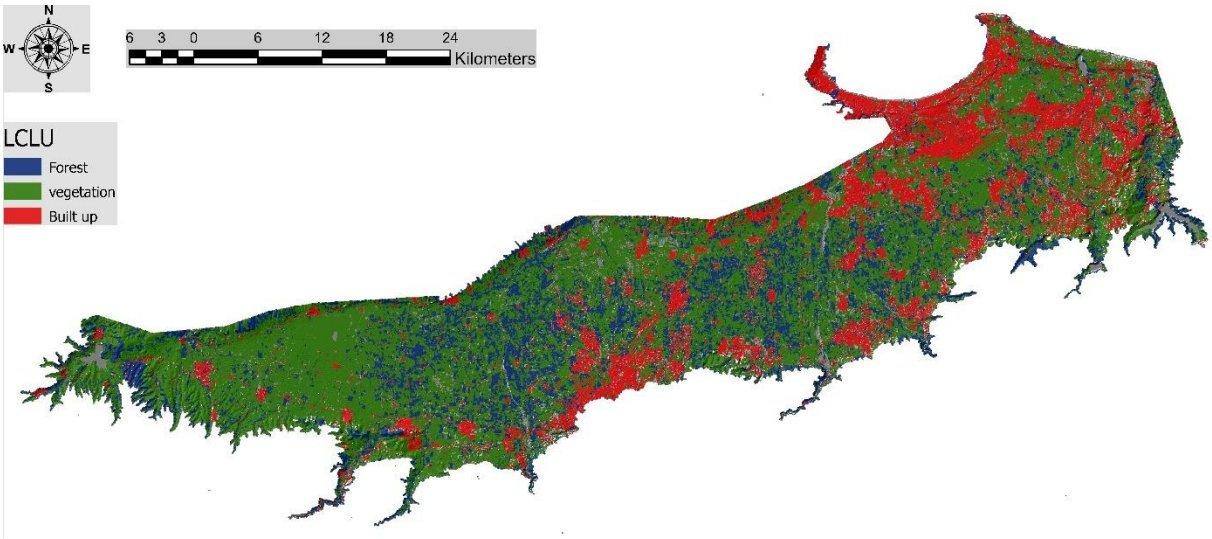


Figure 5.19. LCLU map of Mitidja Plain.

5.4.3 Detailed Analysis of Susceptibility Maps and Historical Confrontation

A comparative visual analysis of the generated maps allows us to decipher the **spatial dynamics of risk** under varying hypotheses.

5.4.3.1 The Qualitative Benchmark Map (Scenario 00 – Literature-Based)

Derived from the bibliographic average, this map **(Fig. 5.20)** exhibits **diffuse susceptibility**. While it correctly identifies the central Mitidja depression as a "default" vulnerable zone, it lacks the resolution required to discriminate between specific risk vectors. It serves primarily as the **background noise** for our broader analysis.

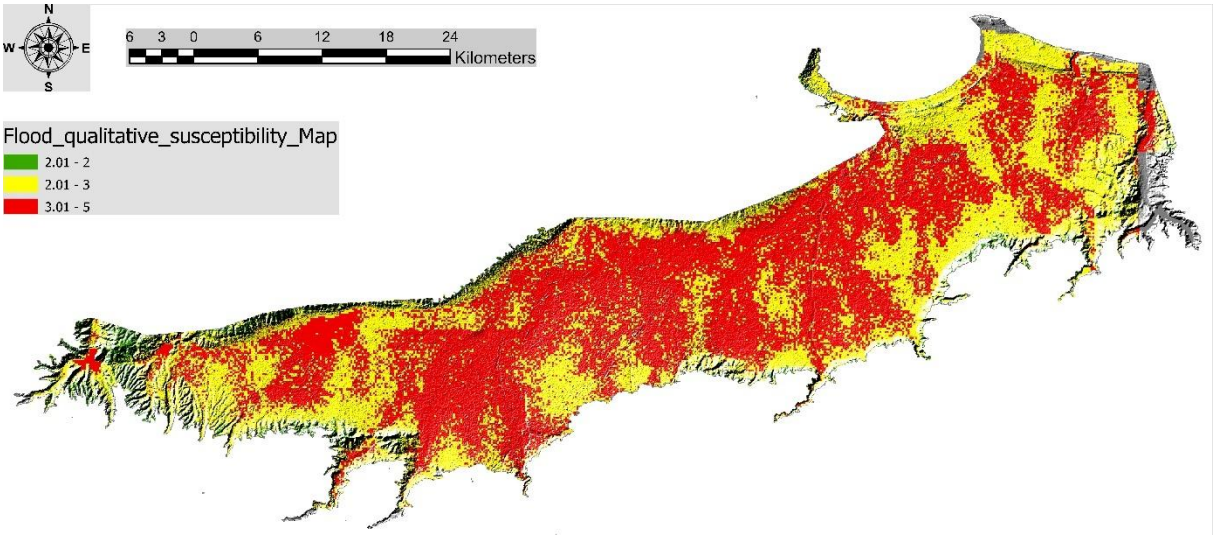


Figure 5.20. Flood qualitative susceptibility map of Mitidja Plain.

5.4.3.2 The Physical Scenarios (Scenarios 01 to 05)

- **Scenarios 01 & 02 (Reference and Elevation) [Fig. 5.21 & 5.22]:** these maps confirm the predominant role of flat topography. The high-risk (red) zones are extensive and contiguous, reflecting a generalized risk of **ponding and stagnation**.

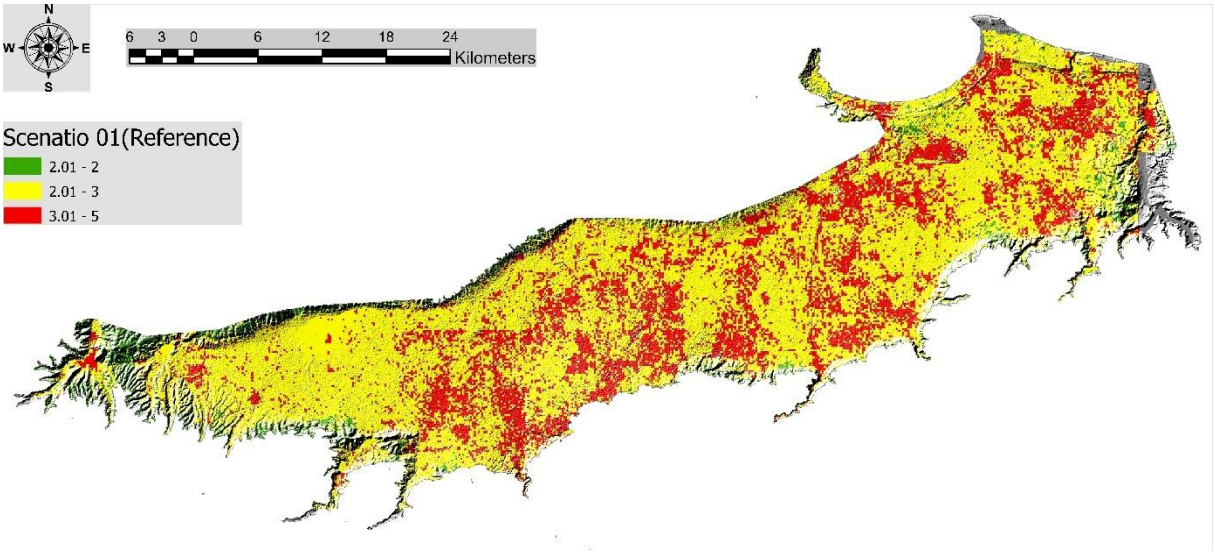


Figure 5.21. Scenario 01 map of Mitidja Plain.

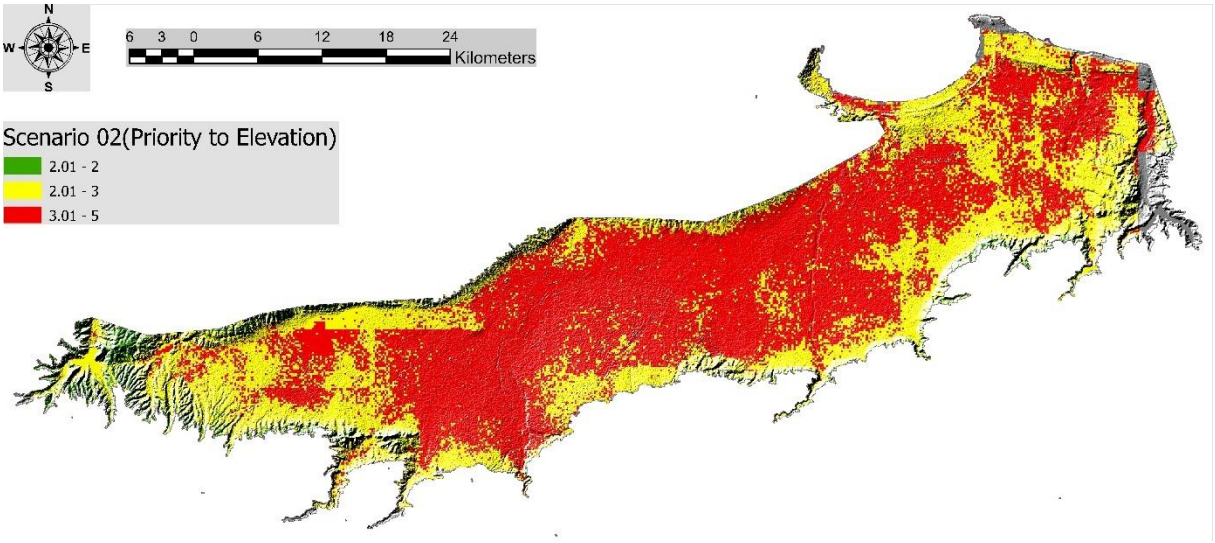


Figure 5.22. Scenario 02 map of Mitidja Plain.

- **Scenarios 03 & 04 (Hydrography) [Fig. 5.23 & 5.24]:** the map undergoes a radical spatial restructuring. Risk becomes **linear**, closely tracing the alignment of the major wadis (Chiffa, El Harrach). These scenarios effectively model the threat of **fluvial bank overflow**.

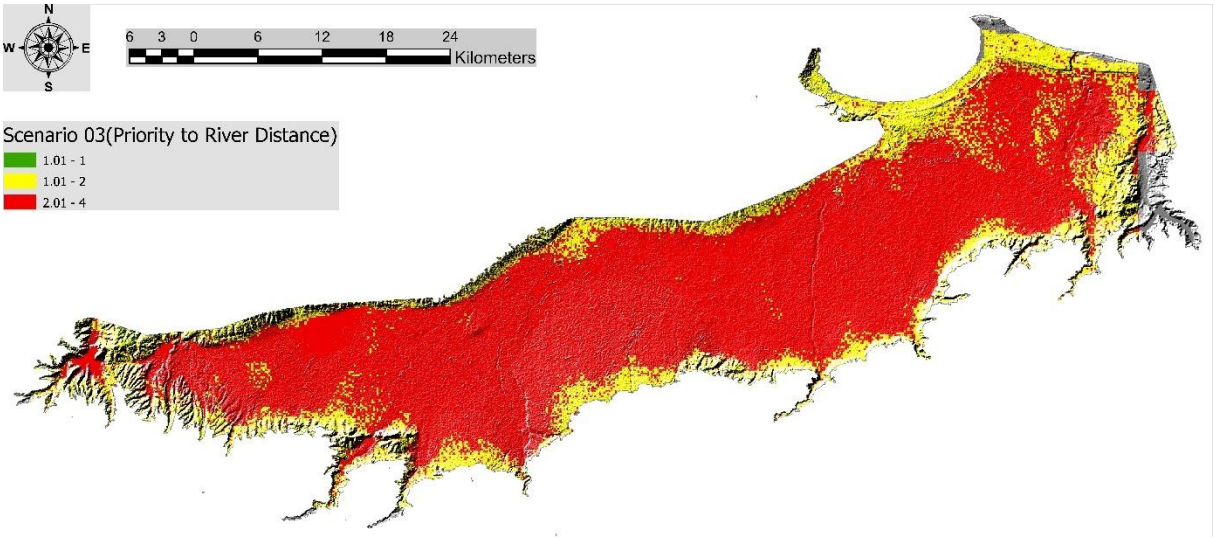


Figure 5.23. Scenario 03 map of Mitidja Plain.

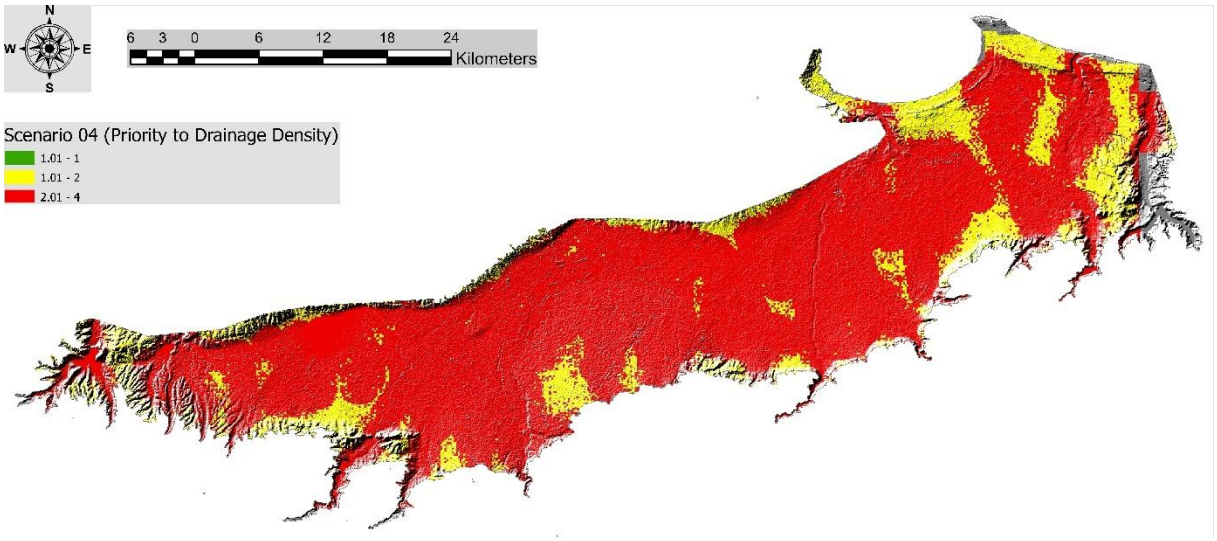


Figure 5.24. Scenario 04 map of Mitidja Plain.

- **Scenario 05 (Precipitation) [Fig. 5.25]:** the risk concentration shifts toward the Southwest (the Atlas foothills), capturing the threat of **flash floods** generated by **orographic storms**.

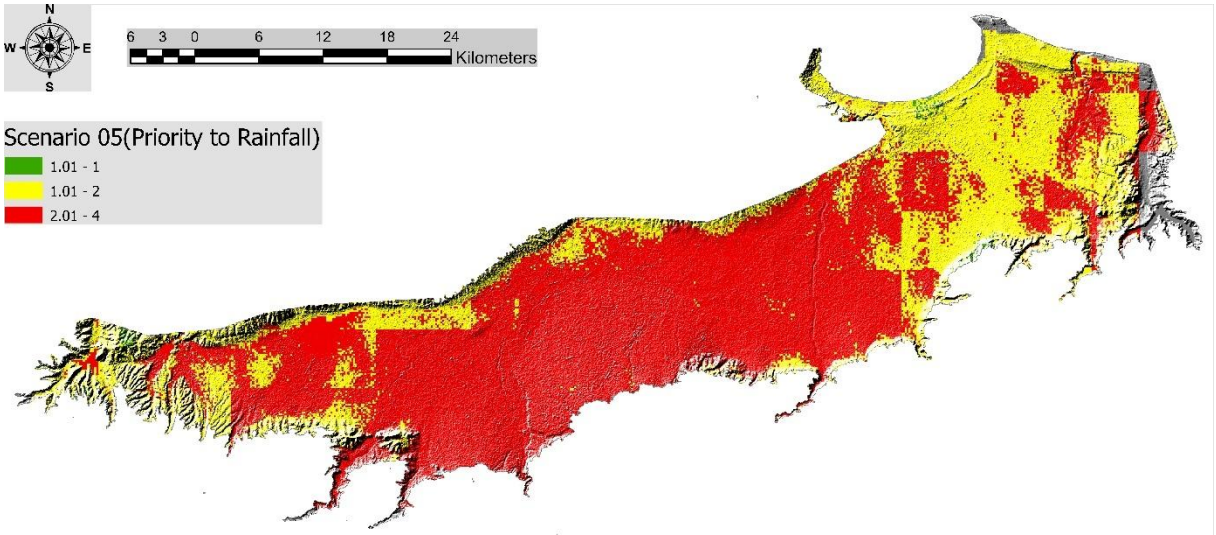


Figure 5.25. Scenario 5 map of Mitidja Plain.

5.4.3.3 The Anthropogenic Scenario (Scenario 06 – LULC)

This map **(Fig. 5.26)** reveals a new geography of risk: that of **soil sealing**. The high-risk zones mirror the **urban footprint** (Blida, Boufarik) and the primary road corridors. It illustrates the risk of **urban pluvial runoff**, which often occurs independently of the natural hydrographic network.

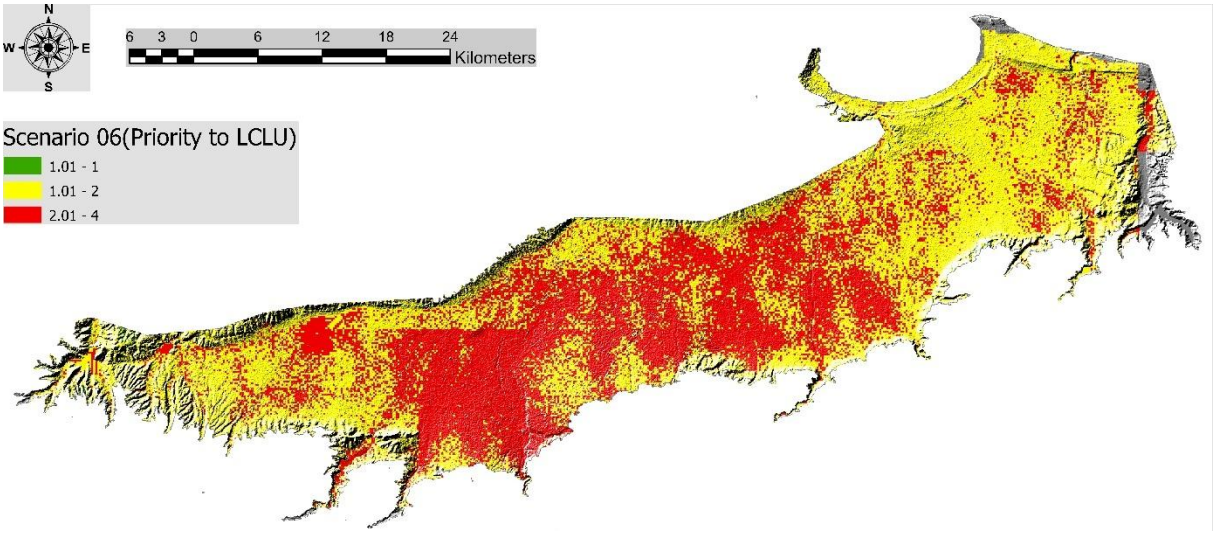


Figure 5.26. Scenario 06 map of Mitidja Plain.

5.4.3.4 Confrontation with Historical Reality (Remote Sensing)

The comparison with historical flood maps reveals a significant **shift in the hydrological regime**:

- **Legacy Historical Map (1973–2000) (Fig 5.27):** this map shows massive flooding along the northern fringe (Sahel), which acted as a **natural spillway**. This pattern aligns closely with **Scenario 04 (River-driven)**.

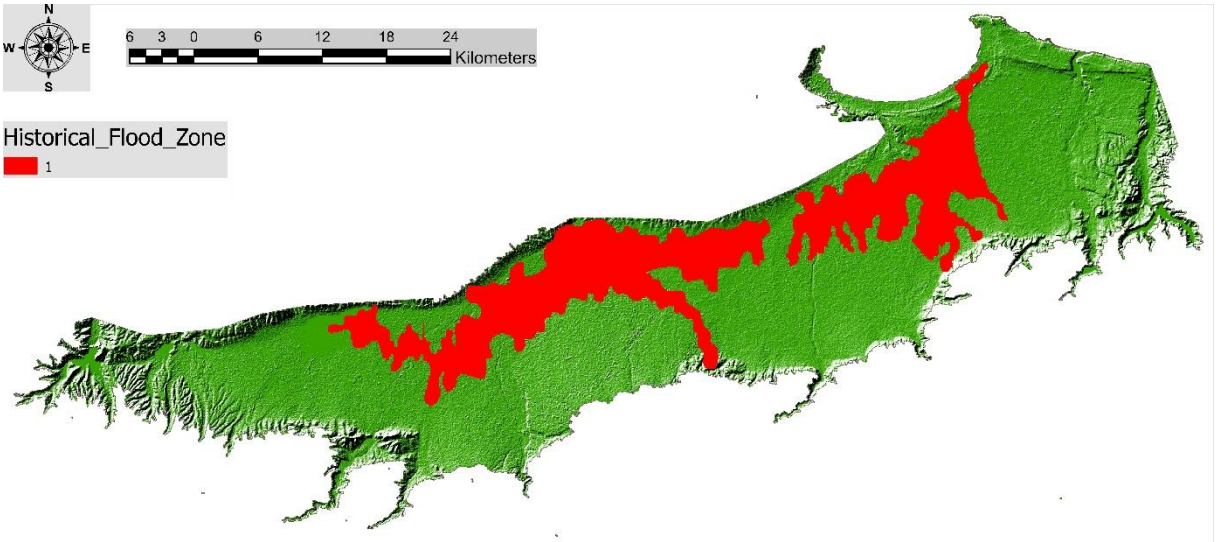


Figure 5.27. Historical zone flood [180] map of Mitidja Plain.

- **Modern Historical Map (2010–2021) (Fig.5.28):** this map displays a fragmentation of risk into a multitude of scattered, flooded "pockets." This **fragmented mosaic** corresponds more accurately to **Scenario 06 (Urban-driven)**, providing empirical evidence that urbanization has become the dominant driver of current vulnerability.

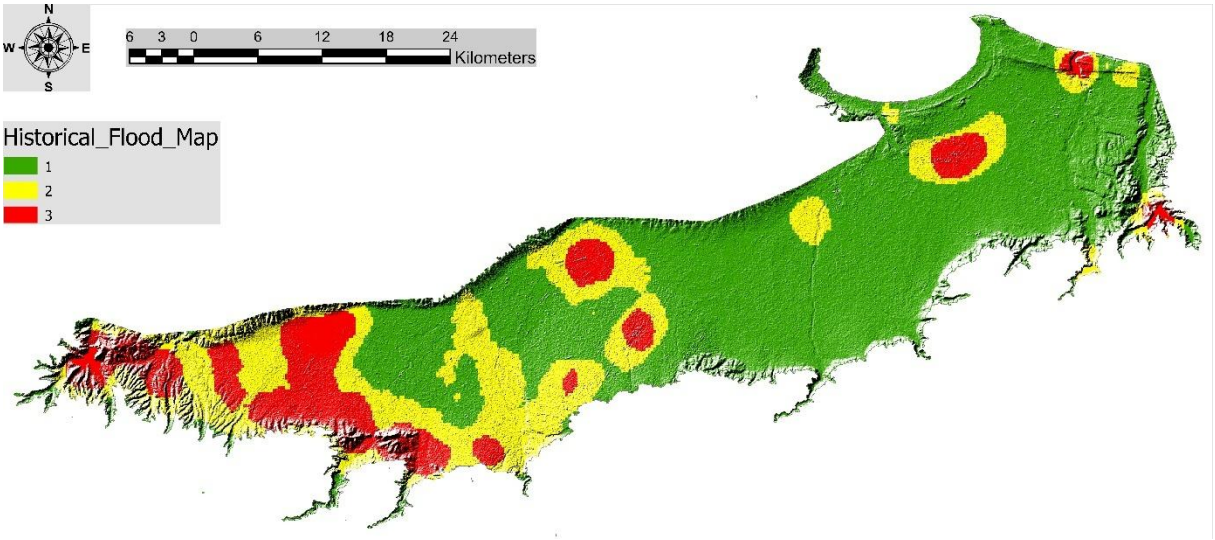


Figure 5.28. Historical flood map of Mitidja Plain.

5.4.4 Results Analysis and Historical Validation

The application of AHP and Fuzzy-AHP models across the six scenarios produced a series of contrasting susceptibility maps**,** providing a dynamic interpretation of risk.

Mathematical Consistency: Model Robustness

A comparison of the weight vectors **(Table 5.3)** reveals a very strong correlation ($R^2 > 0.95$) between standard AHP and Fuzzy-AHP across all scenarios. This convergence validates the **mathematical robustness** of our model: the introduction of "fuzzy" uncertainty does not destabilize the factor hierarchy but instead strengthens the confidence in the established weightings [173].

Spatial Variability and Identification of the "Hard Core"

Spatial analysis shows that while the extent of risk zones fluctuates depending on the chosen hypothesis, a geographic constant emerges. The **Atlas foothills** (Blida Province) and the **central river corridors** (Wadis El Harrach and Chiffa) consistently fall within the "High" to "Very High" susceptibility classes, regardless of the weight assigned to individual factors. These areas constitute the **"Hard Core"** of the Mitidja's intrinsic vulnerability.

Historical Validation through Spatial Correlation

Cross-referencing these models with the historical flood inventory (reconstructed via **remote sensing analysis of Sentinel-2 imagery** (identified **Scenario 04 (Distance-to-River Priority)** as the best-performing model in terms of spatial agreement.

Visual analysis confirms that this scenario best captures the actual extent of observed floods, demonstrating that the dominant mechanism in the Mitidja is not diffuse runoff, but rather **structured fluvial overflow** along hydrographic axes. This validates the hypothesis that proximity to the river network is the primary **risk discriminant** in this territory [179].

Table 5.3. Standard Factor Weights (%) for the Six AHP and Fuzzy AHP Scenarios, and Consistency Ratios (CR) of the Standard AHP

Factor	Scenario 00	Scenario 01		Scenario 02		Scenario 03		Scenario 04		Scenario 05		Scenario 06	
	Literature review (%)	AHP (%)	Fuzzy AHP(%)	AHP (%)	Fuzzy AHP(%)	AHP (%)	Fuzzy AHP(%)	AHP (%)	Fuzzy AHP(%)	AHP (%)	Fuzzy AHP(%)	AHP (%)	Fuzzy AHP(%)
Rainfall	17	12.41	12.19	21.00	20.91	8.20	8.26	10.39	10.58	32.39	31.50	16.19	16.60
Elevation	13	6.71	7.06	27.94	23.30	3.05	3.11	3.36	3.41	3.24	3.23	3.45	3.35
Slope	18	6.71	7.06	13.53	13.94	5.22	5.50	5.47	5.37	5.14	5.27	6.47	6.45
River Distance	16	12.41	12.19	5.62	6.51	8.46	8.55	29.59	28.54	13.87	14.31	9.94	10.37
Drainage Density	9	12.41	12.19	8.85	9.81	28.22	27.20	10.75	11.11	9.74	9.73	6.38	6.24
LULC	13	23.16	23.59	9.10	10.33	13.81	14.08	19.65	19.94	19.69	20.16	32.80	31.86
Soil Texture	2	12.41	12.19	5.62	6.51	5.92	8.06	5.81	5.77	3.24	3.23	5.77	5.95
TWI	7	6.90	7.30	3.65	4.15	3.82	20.27	10.17	10.51	8.68	8.47	14.53	14.65
Curvature	2	4.09	4.39	2.3	2.25	1.83	1.75	3.07	3.10	2.01	2.05	2.72	2.82
NDVI	3	2.78	2.83	2.37	2.29	2.61	2.60	1.74	1.67	2.01	2.05	1.75	1.69
CR<0.1	------	**0.0051**		**0.0181**		**0.0142**		**0.0025**		**0.0211**		**0.0323**	

5.5 The Data-Driven Approach: Statistical Validation via Machine Learning

To complement and cross-validate the semi-quantitative AHP approach (which is inherently influenced by expert subjectivity) we explored a purely quantitative methodology rooted in Artificial Intelligence: **Machine Learning (ML)**. This methodological shift addresses the imperative for **objective validation** in modern risk assessment [111].

The primary objective is to develop a **"data-driven"** predictive model capable of learning the complex, non-linear relationships between environmental factors and flood occurrences directly from historical observations. By doing so, the model **circumvents human bias** in the weighting process, ensuring that the resulting susceptibility map is derived purely from empirical evidence [94].

5.5.1 Methodology: Logistic Regression (LR) via Orange Data Mining

This third methodological approach, presented at the **CCRTI 2025 conference**, aims to objectify the zoning process through pure statistical modelling. The analysis was implemented using the open-source **Orange Data Mining** platform, widely recognized for its robustness and transparency in machine learning workflows.

The experimental protocol is structured around a **supervised learning workflow (Fig. 5.29)**:

Dataset Preparation:

- The ten raster layers (representing the conditioning factors) were converted into numerical data matrices. Within this framework, each pixel in the study area is treated as an **"instance"** characterized by its specific attributes (e.g., Slope, Elevation, NDVI).
- The **target variable** comprises the historical flood inventory derived from remote sensing analysis (see Section 5.4.3.4). This transforms the assessment into a **binary classification task** (Class 0: Non-Flooded / Class 1: Flooded).

Model Training:

- **Logistic Regression (LR)** was selected as the core algorithm. Unlike "black-box" models (such as Deep Learning), LR offers high **interpretability**, allowing for the clear explanation of causal relationships.
- The model automatically "learns" the statistical correlations between the predictors (X) and the actual occurrence of floods (Y), calculating objective weighting coefficients without human intervention.

Cross-Validation:

- To ensure the reliability of the results and prevent **overfitting**, a **k-fold cross-validation** technique was employed. This process evaluates the model's predictive performance on unseen data subsets, ensuring its ability to generalize across the entire study area.

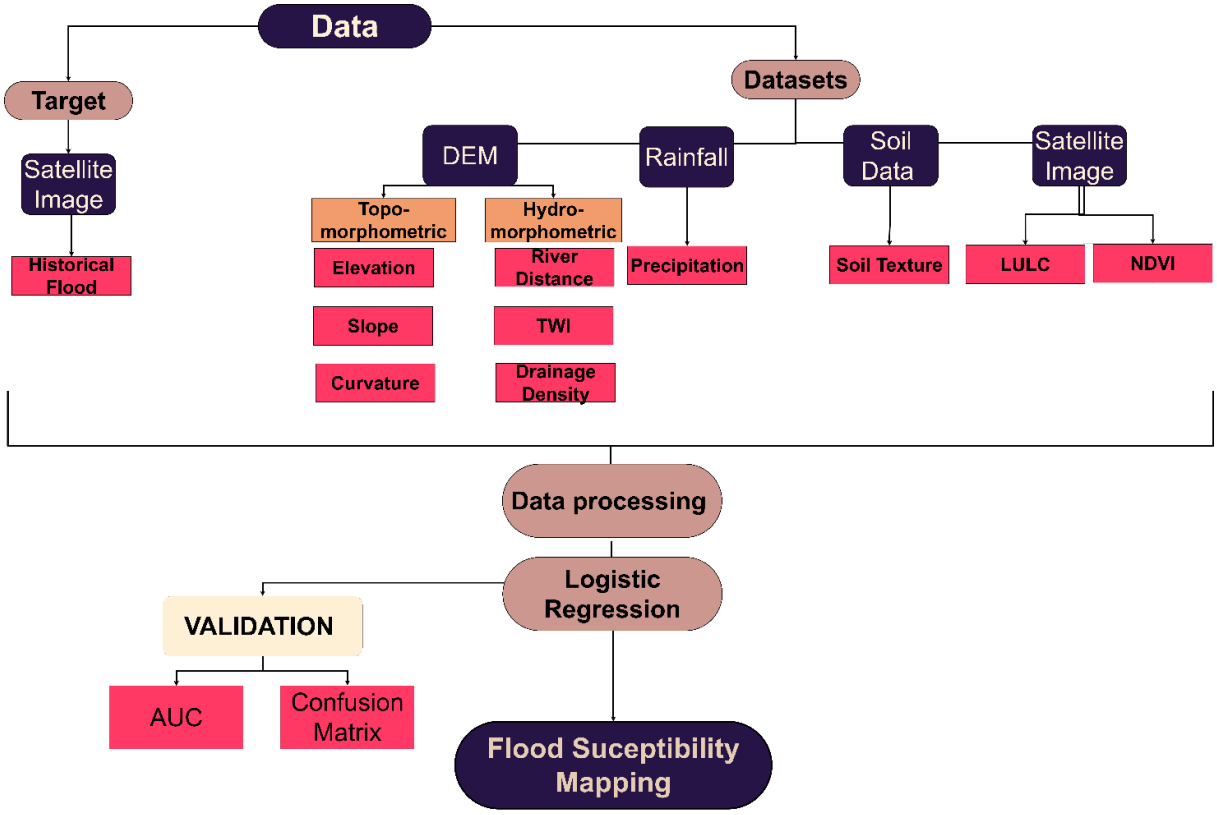


Figure 5.29. Methodology steps.

5.5.2 Results: Statistical Convergence and "Hard Core" Validation

The Logistic Regression model achieved a satisfactory predictive performance, yielding an **Area Under the Curve (AUC)** of 0.743. This score confirms the algorithm's capability to effectively discriminate between flood-prone and safe areas based solely on the physical characteristics of the terrain.

The ML (Machine Learning) Map (Fig. 5.30): The spatialization of predicted probabilities produces a susceptibility map that **strikingly corroborates** the results of the AHP approach. The areas identified as critical by the algorithm (specifically **incised valleys**, confluences, and the low-lying zones of the Sahel) overlap almost perfectly with the **"Hard Core"** identified through our multi-scenario analysis. This convergence between two independent methodologies (one expert-led and the other data-driven) significantly **bolsters confidence** in the final zoning.

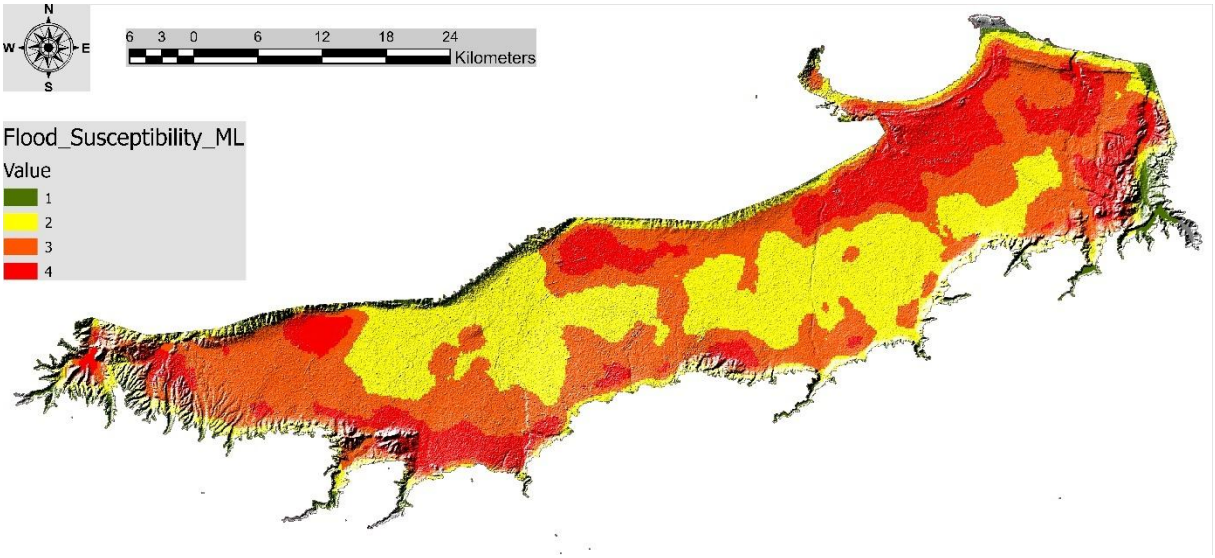


Figure 5.30. Flood susceptibility ML map of Mitidja Plain.

Objective Factor Quantification: Analysis of the regression coefficients allowed for the quantification of the actual weight of each factor. It statistically confirms the predominant role of **Slope** and **Drainage Density** as major **driving factors**, providing *a posteriori* validation for the expert hypotheses established in our AHP scenarios (specifically Scenario 03).

5.6 Conclusion

Convergence of Evidence and the Shift in Scale

At the conclusion of this regional analysis, we have reached a decisive milestone: the transformation of territorial intuition into **cartographic certainty**.

The remarkable convergence between our two independent approaches (the **deductive, expert-driven method** (Multi-Scenario AHP) and the **inductive, data-driven method** (Machine Learning)) validates the existence of a **"Hard Core"** of structural vulnerability within the Mitidja Plain. We have statistically demonstrated that flood risk is not a random occurrence in this region but is fundamentally dictated by the geomorphology of the watershed itself.

However, this mapping success must not overshadow a critical physical reality: zoning is a **planning tool, not an engineering design tool**. While it identifies "Hotspots," it remains silent on the complex fluid mechanics at play. For an engineer tasked with protecting a strategic viaduct, simply knowing that the Oued Chiffa area is "highly susceptible" is insufficient. The critical question remains: is the threat a static inundation or a **hyper-concentrated sediment flow**?

To meet this demand for physical precision, a **fundamental scale shift** is imperative. We must now move beyond the top-down satellite perspective to engage with the reality of the field. The following chapter will delve into the heart of the critical **Chiffa catchment** to unravel, through **morpho-dynamic modelling**, the complex and destructive nature of the hazards (such as sediment transport and debris flows) that directly threaten the infrastructure.

6 Susceptibility Mapping of Debris Flow Hazards

6.1 General Introduction

Beyond Clear Water

The regional analysis conducted in the previous chapter identified major susceptibility zones across the Mitidja Plain. Among these **hotspots**, the Oued Chiffa catchment stands out due to its exceptional criticality. Situated at the sharp interface between the Blidean Atlas and the plain, this natural corridor serves as the essential route for **National Road 1 (RN1)**, a vital artery for the national economy.

However, in this mountainous context, the nature of the hazard undergoes a radical transformation. We are no longer dealing with a simple rise in water levels typical of plain flooding, which can be modelled through classical hydraulics. Here, the dynamics are both **torrential and sedimentary**. Water is no longer merely a clear fluid; it becomes a vector for **sediment transport**, carrying tons of silt, boulders, and debris. To accurately diagnose infrastructure vulnerability in this sector, it is imperative to undergo a **paradigm shift**: moving beyond pure hydraulics toward **morpho-dynamics**.

This chapter aims to deconstruct this physical complexity through three stages, structured as follows:

Section 6.2: Presentation of the Study Area. We define the geographical context and the physical constraints (geology, climate) that establish this basin as a **strategic bottleneck**.

Section 6.3: Sediment Dynamics (The IC-RUSLE Approach). We evaluate the **functional connectivity** of the catchment to understand the origin of the sediment threat, moving beyond the limitations of traditional topographic indices.

Section 6.4: Debris Flow Hazards. We characterize the specific susceptibility to debris flows true **"geotechnical projectiles"** that pose a direct threat of impact to the RN1.

6.2 Presentation of the Study Area: The Strategic Choke Point of the Chiffa

The Oued Chiffa catchment is more than a mere hydrological subunit of the Mitidja Plain; it serves as a critical strategic and hydraulic **choke point**. Situated at the **abrupt interface** between the Atlas highlands and the alluvial plain, this territory represents the **archetypal mountain risk**.

In this region, the topography does not merely channel water; it accelerates and concentrates it, converting diffuse runoff into a **high-energy destructive flow**. It is within this **narrowly constrained corridor** (where fragile geology converges with aggressive climatology) that the **National Road 1 (RN1)** winds, acting as a vital **lifeline** positioned on the front lines of hazard exposure.

6.2.1 A Constrained Geographical Corridor

The Oued Chiffa catchment, located approximately 50 km southwest of Algiers, constitutes a complex hydrological system spanning 585.02 km² [91]. Its morphology is characterized by a **sharp structural duality** that makes it a natural focal point for hazards **(Fig.6.1):**

- **Upstream (Southeast Sector):** The vast Ouzera-Médéa plateau exhibits a Southeast-Northwest orientation. It's moderate to gentle slopes act as an extensive **contributing area**, accumulating surface runoff across large catchment surfaces.
- **Downstream (North Sector):** The basin pivots toward a South-North orientation and narrows abruptly to form the **Chiffa Gorges**. This deep incision through the Blidean Atlas functions as a **hydraulic bottleneck**. Characterized by steep gradients (>45%) and an **incised valley** profile, this morphology accelerates flows via the **Venturi effect** and promotes the development of substantial **flood stages** [91], [180].

6.2.2 The Infrastructure Stake: RN1 in the Eye of the Storm

The strategic significance of this catchment transcends its physical geography; it lies in the critical infrastructure it hosts. The Chiffa Gorges represent the historic and sole mandatory corridor for one of the nation's most vital transport axes: **National Road 1 (RN1)**, a veritable economic backbone linking Algiers to the High Plateaus and the Deep South.

In this sector, however, the road exists in **direct spatial conflict** with the river. Constrained by a hostile topography, the infrastructure is forced to flank the **main channel** of the wadi, sharing the constricted valley floor. Consequently, it traverses numerous **engineering structures** (bridges, viaducts, and tunnels) that are positioned on the front lines of exposure to both fluvial **overbanking** and **slope instabilities** [91]. The vulnerability of this corridor represents far more than a localized hazard; it is a **systemic socio-economic risk**. Any disruption of this link would isolate the hinterland from the coast, effectively paralyzing national trade and logistics.

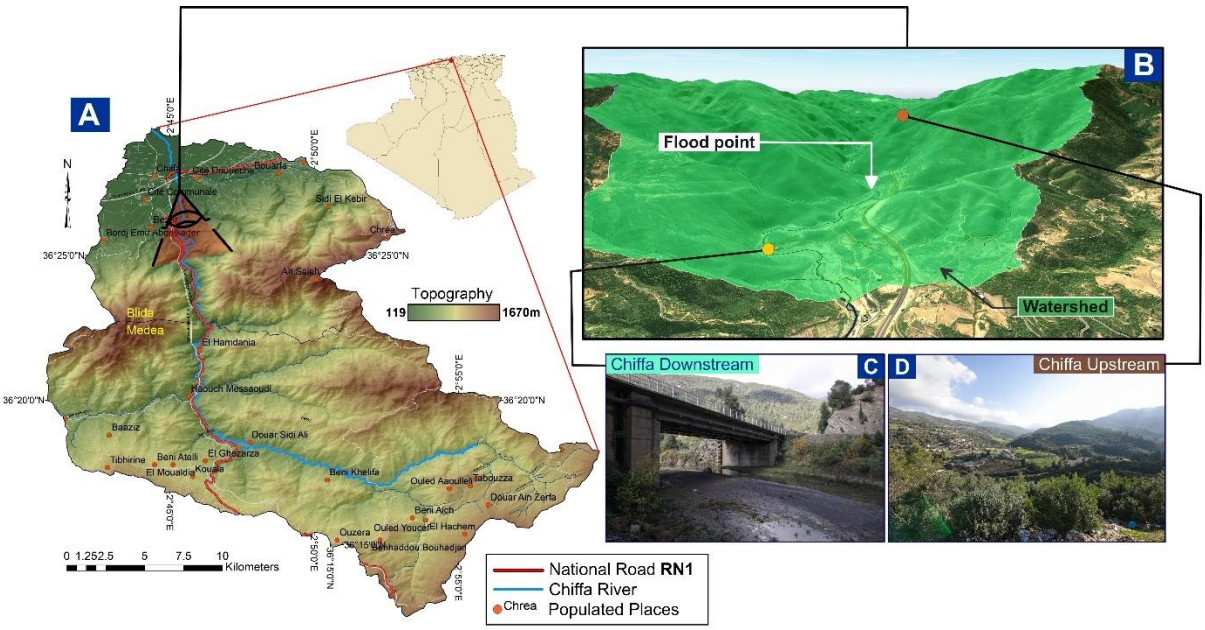


Figure 6.1. A. Extent of the Chiffa watershed. B. Three-dimensional model of the watershed. C. Photograph upstream of the watershed. D. Photograph at the watershed outlet.

6.2.3 An Aggravating Hydro-Geological Context

The hazard potential of the catchment is structurally amplified by the convergence of unfavourable geological and climatic factors **(Table 6.1):**

a) **Impermeable and Fragile Geology:** The basin is dominated by geological formations belonging to the **Maghrebide units** [181]. Upstream, the sequence consists of **marly-sandstone alternations** from the Miocene, while downstream, it is composed of **Lower Cretaceous schists**. Both formations exhibit very low overall permeability. This lithology promotes a high **runoff coefficient**, leading to the near-instantaneous conversion of precipitation into **surface runoff (Fig. 6.2b).**

b) **Torrential Hydrology:** Formed by the confluence of the Ouzera and Mouzaia wadis, the Oued Chiffa displays a violent flow regime. Flood discharges are characterized by extreme variability and sharp peaks (ranging from 98 to 313 m^3/s). These events mobilize **significant sediment loads** due to active hillslope erosion [91] **(Fig. 6.2a&c)**.

c) **Non-Stationary Climatology:** The Mediterranean semi-continental climate imposes intense precipitation (800 to 1,500 mm/year upstream), concentrated during the cold season. Furthermore, the impact of climate change is already evident: a temperature increase of **+1.7°C** (notably higher than the global average of 0.7°C) exacerbates **soil aridity** and the intensity of **convective storms**. This shift renders historical statistical time-series potentially obsolete for future forecasting and design **(Fig. 6.3)**.

Table 6.1. Main Physical and Environmental Characteristics of the Chiffa Catchment.

Domain	Key Characteristics	References
Geomorphology	**Total Area:** 585.02 km²	[91]
	Elevation: 143 m (downstream) to 1,670 m (upstream)	
	Slopes: Steep gradients (> 45%) in the central zone (Blida Massif); Moderate on the Médéa plateau (South**).**	
Geology	**Dominant formations:** Marly-sandstone alternations (Miocene) upstream; Marly-limestone (Upper Cretaceous) in the centre; Schists (Lower Cretaceous) downstream**.**	[181], [182]
	Key property: Generalized low permeability, promoting surface runoff.	
Hydrology	**Network:** Dense and dendritic.	[91]
	Regime: Torrential with high seasonal variability.	
	Flood discharges: Observed peaks ranging from 98.75 to 313 m³/s (November–May period).	
Climatology	**Type:** Semi-continental Mediterranean (Cold/wet winters, hot/dry summers).	[91], [183]
	Precipitation: 800–1,500 mm/year (Upstream), 500–800 mm/year (Downstream).	
	Climate Change: Temperature increase of +1.7°C (1970–2017).	

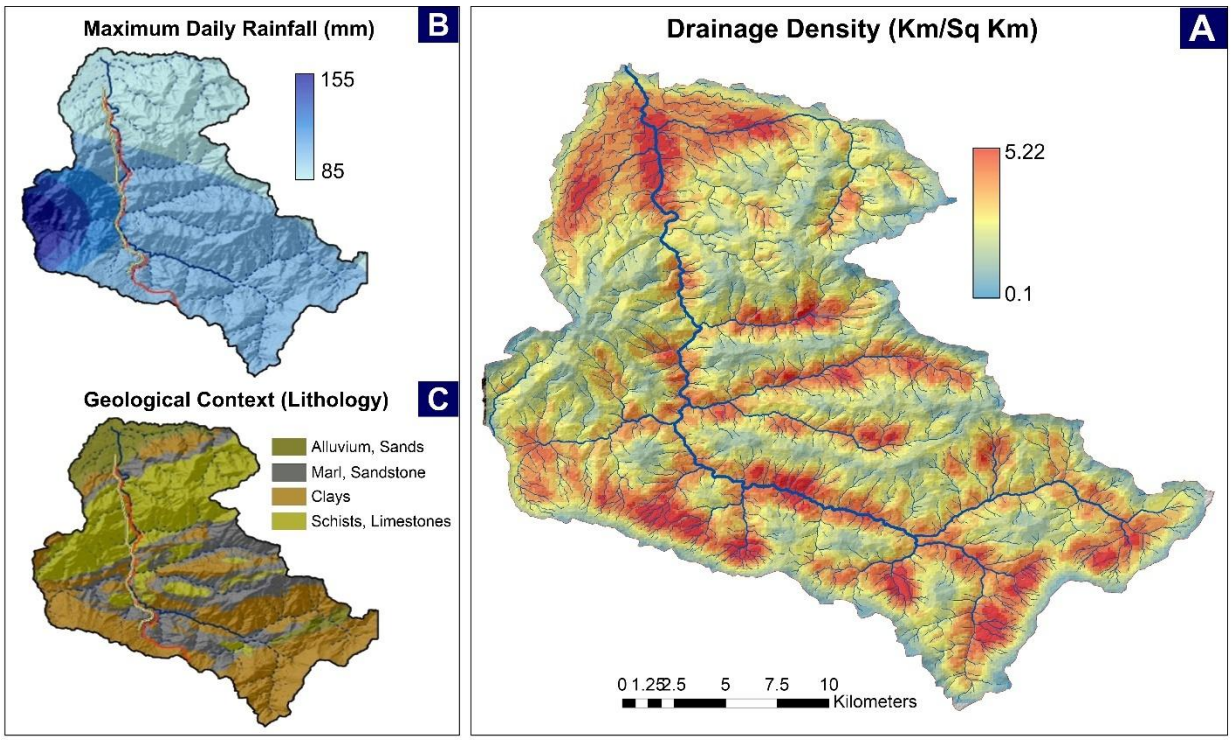


Figure 6.2. Descriptive maps of the study area [91] . A. Hydrological context. B. Climatic context. C. Geological context.

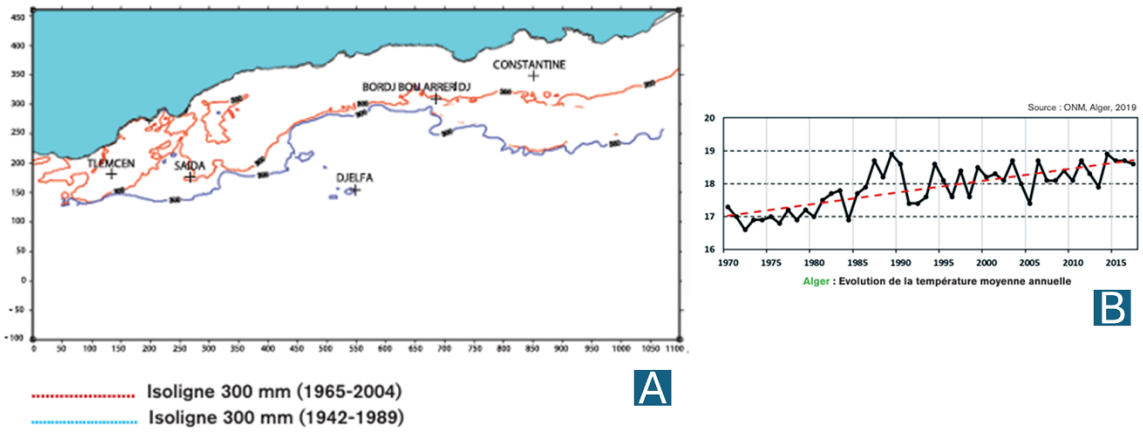


Figure 6.3. Consequence of climate change (from[185]). A. Evolution of the position of the 300 mm isohyets between the periods 1942-1989 and 1965-2004. B. Evolution of average annual temperature.

6.3 Sediment Dynamics: From Erosion Potential to Functional Connectivity (IC-RUSLE)

While previous studies [91] have established the high **erosion susceptibility** of the Chiffa catchment, a pivotal question remains for infrastructure management: does this mobilized sediment actually reach the road network?

The core challenge lies not only in identifying where soil erosion occurs (**the Source**) but in understanding the mechanisms by which it is transported to the hydrographic network (**the Transfer**). This process, known as **Sediment Connectivity**, is what transforms upstream agricultural soil loss into a tangible risk of **siltation** and the **clogging** of downstream engineering structures.

To develop effective mitigation strategies, it is therefore crucial to move beyond the mere mapping of potential erosion and instead analyse the **effective transfer pathways** toward the outlet.

6.3.1 Problem Statement: Structural versus Functional Connectivity

The **Index of Connectivity (IC)** [184], [185] . is established as the standard tool for assessing sediment transfer. It quantifies the landscape's structural capacity to convey sediment based primarily on topographical parameters such as slope and roughness effectively representing the **"plumbing"** of the catchment.

However, as highlighted by recent reviews [186], this purely structural approach has a major limitation: it neglects **actual sediment availability**. A hillslope may be steeply inclined and thus high in structural connectivity yet remain entirely stable due to forest cover. Conversely, an agricultural plateau with a gentle gradient may serve as a massive source of **active erosion**.

Consequently, distinguishing between **structural connectivity** (potential) and **functional connectivity** (actual) is essential for a realistic and reliable risk assessment [187].

6.3.2 Methodology: The IC-RUSLE Coupling Approach

To address this gap, we propose an innovative approach: integrating **potential soil erosion**, modelled through the **Revised Universal Soil Loss Equation (RUSLE)**, directly as a weighting factor in the connectivity calculation.

6.3.2.1 Modelling Potential Soil Erosion (RUSLE)

The spatial distribution of annual soil loss (A) was modeled using the revised equation:

$$A = R \times K \times LS \times C \times P$$

Each factor was spatialized within a GIS environment using high-resolution global datasets: **CHIRPS** for rainfall erosivity (R), **SoilGrids** for soil erodibility (K), and **Sentinel-2** imagery for the vegetation cover factor (C).

6.3.2.2 Calculation of the Functional Index (IC_{RUSLE})

Two distinct indices were compared using the **SedInConnect** software [188] **(Fig. 6.4)** :

- **Structural IC (IC_{struc}):** Utilizes **topographic roughness** as the weighting factor (W).
- **Functional IC (IC_{RUSLE}):** Utilizes the inverse of the normalized RUSLE potential erosion as the weighting factor:

$$W_{RUSLE} = 1 - RUSLE_{normalized}$$

Physical Hypothesis: Areas characterized by high erosion rates offer low **impedance** to sediment transport, thereby facilitating downstream delivery [85].

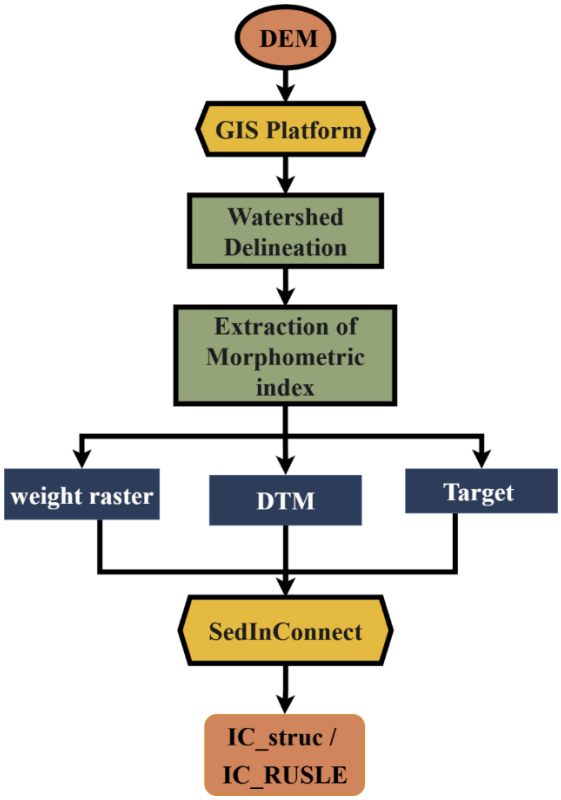


Figure 6.4. Methodology steps.

6.3.3 Characterization of Input Factors: Topography and Erosion Potential

Before analysing connectivity, it is essential to characterize the spatial distribution of the primary factors governing it.

6.3.3.1 Topography and Surface Roughness (Structural Impedance)

The **DEM (Fig. 6.5)** highlights the sharp morphological contrast of the catchment. The **topographic roughness** map **(Fig. 6.6)**, derived from this DEM, shows that areas of high roughness (values > 2.2) are concentrated within the central gorges and along the **dissected hillslopes**. In the structural model, these zones act as **impedance barriers** to sediment transfer. Conversely, the Ouzera plateaus appear smooth, theoretically suggesting low structural friction.

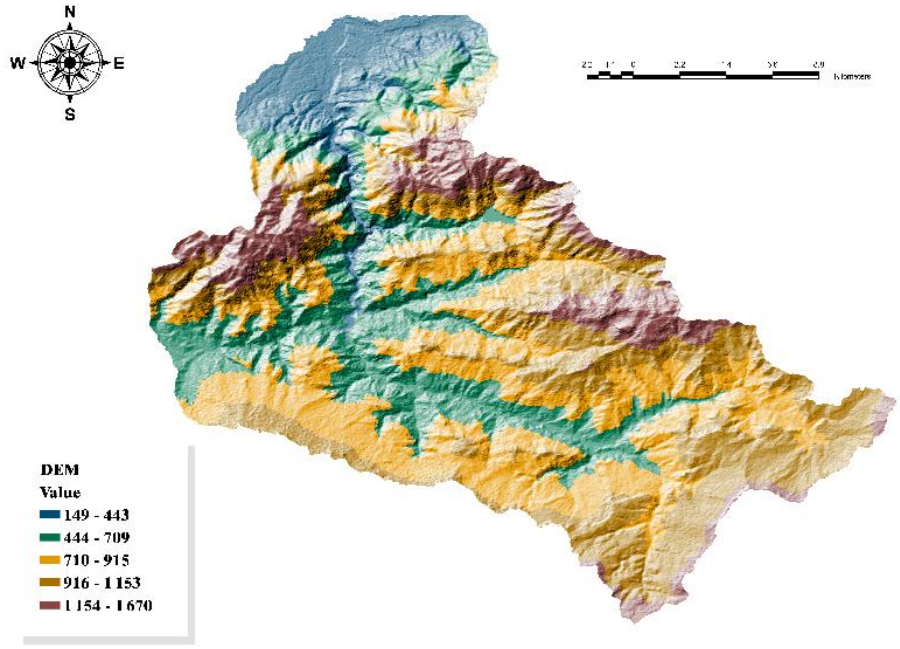


Figure 6.5. DEM map of Chiffa watershed.

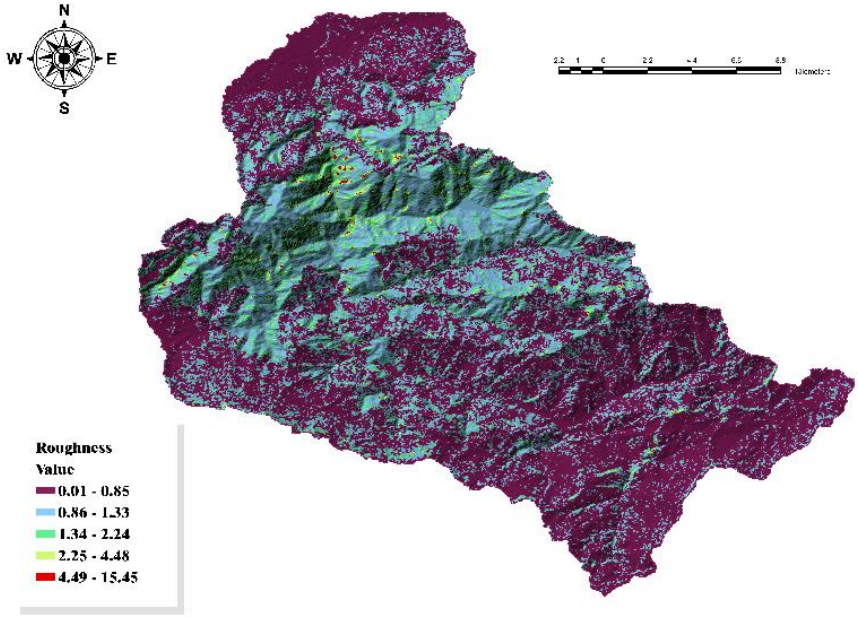


Figure 6.6. Roughness map of Chiffa watershed.

6.3.3.2 RUSLE Erosion Potential (Functional Impedance)

The annual soil loss map **(Fig. 6.7)** provides a contrasting interpretation. Potential erosion is highly heterogeneous, ranging from 0 to 700 t/ha/year.

- **Erosion Hotspots:** These are primarily concentrated on the western and southwestern slopes. These areas correspond to agricultural lands situated on moderate gradients with highly **erodible soils**.

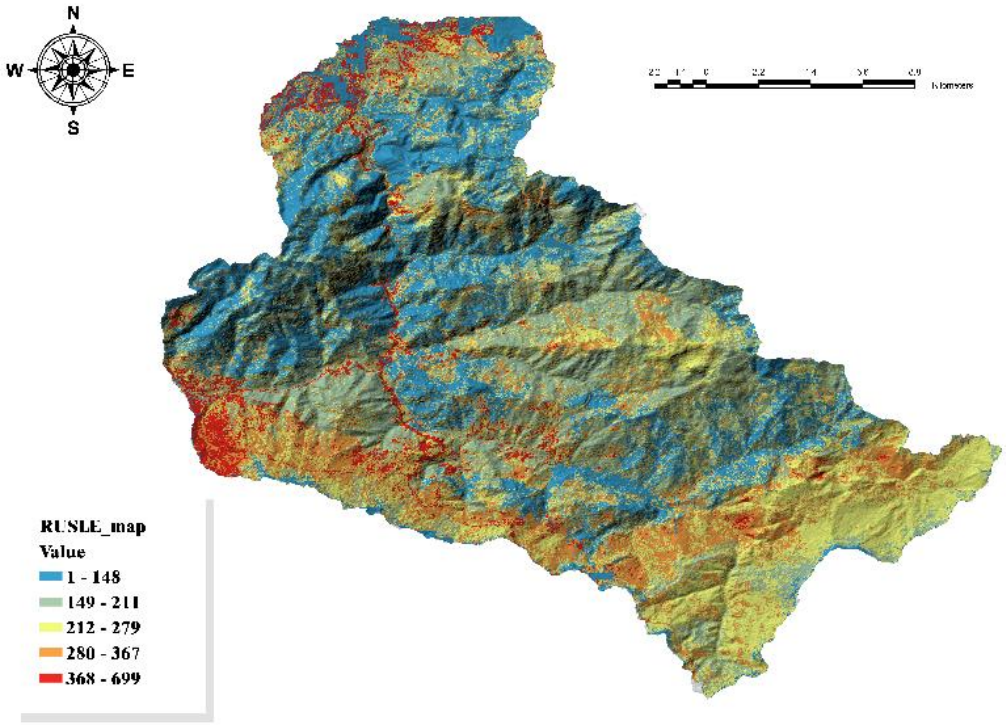


Figure 6.7. Rusle map of Chiffa watershed.

- **Weighting Inversion for Connectivity (Fig. 6.8):** In our functional model, these high-erosion zones are transformed into areas of **low impedance** ($W \approx 0$). The underlying physical hypothesis is that detached soil particles effectively **"lubricate"** the transfer process. This transforms these agricultural zones into **"sediment highways,"** contradicting the conclusions suggested by simple surface roughness analysis.

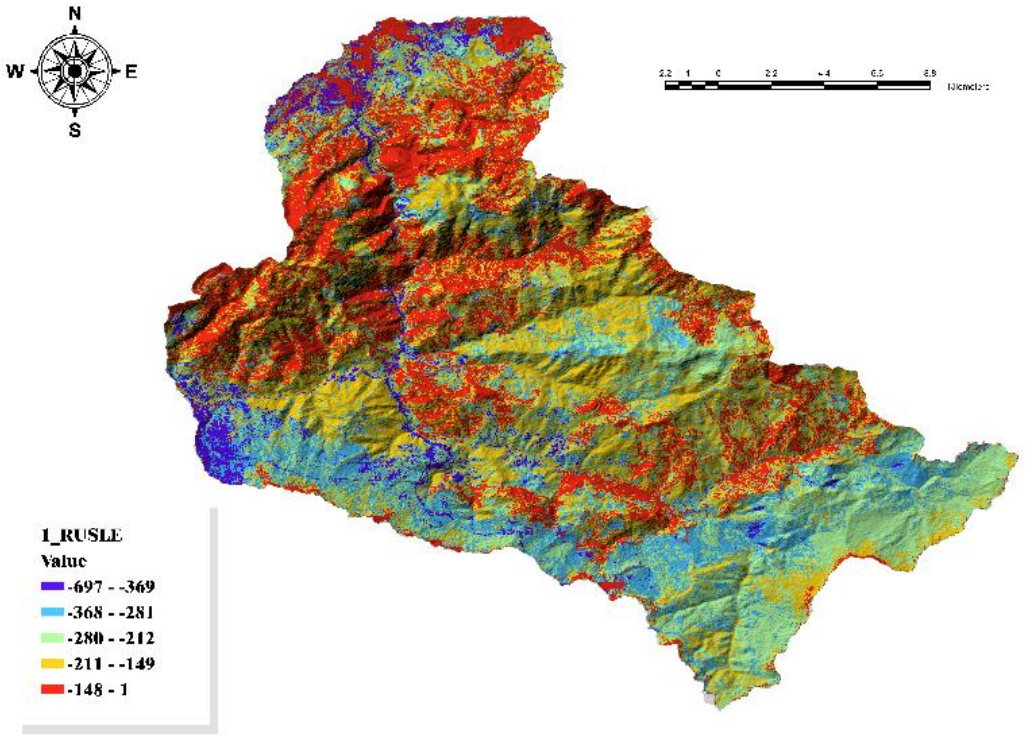


Figure 6.8. Rusle inverse map of Chiffa watershed.

6.3.4 Results and Discussion: Pinpointing Agricultural "Hotspots"

A comparative analysis of the connectivity maps reveals a radical spatial reorganization of sediment risk, validating the scientific relevance of the functional approach.

- **The Structural Model (IC_{struc}) (Fig. 6.9):** This model identifies steep central gorges almost exclusively as connected zones. While it delineates the topographical "highways" for sediment transit, it remains **blind** to the actual areas of sediment production.

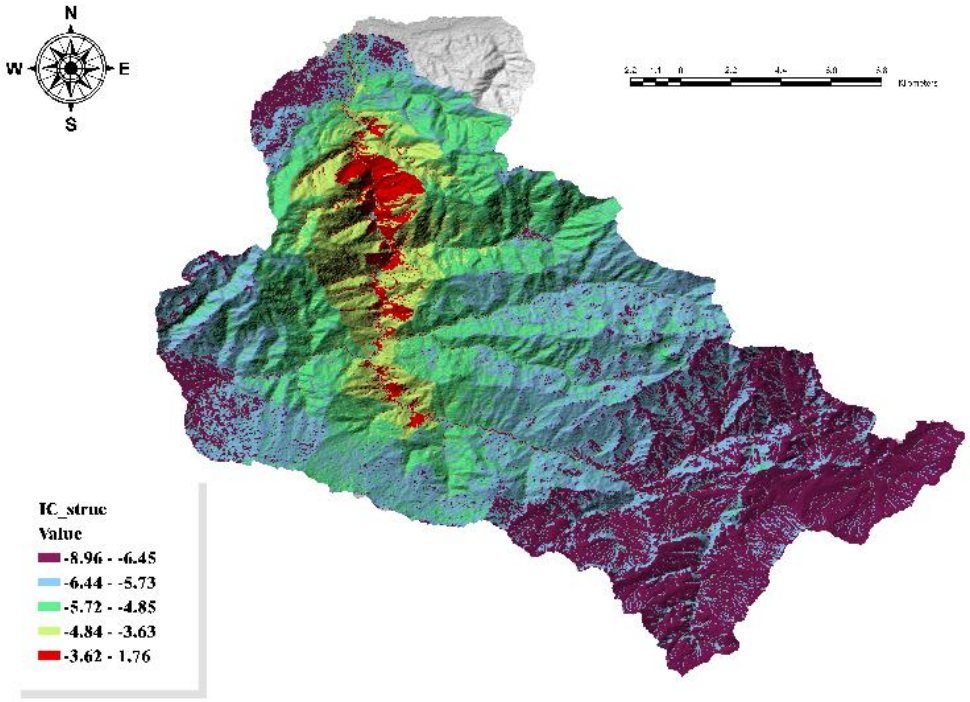


Figure 6.9. Ic structure of Chiffa watershed.

- **The Functional Model (IC_{RUSLE}) (Fig. 6.10):** This provides a much more nuanced and alarming spatial pattern:
    - **Confirmation:** The gorges remain highly connected, confirming their role as the primary **transit vectors**.
    - **Revelation:** Vast stretches of agricultural plateaus in the south and west, despite their moderate gradients, emerge as **major sediment sources** that are functionally connected to the hydrographic network.
    - **Discrimination:** Stable forested areas, even those on steep terrain, are correctly identified as **disconnected**, highlighting the stabilizing effect of vegetation cover.

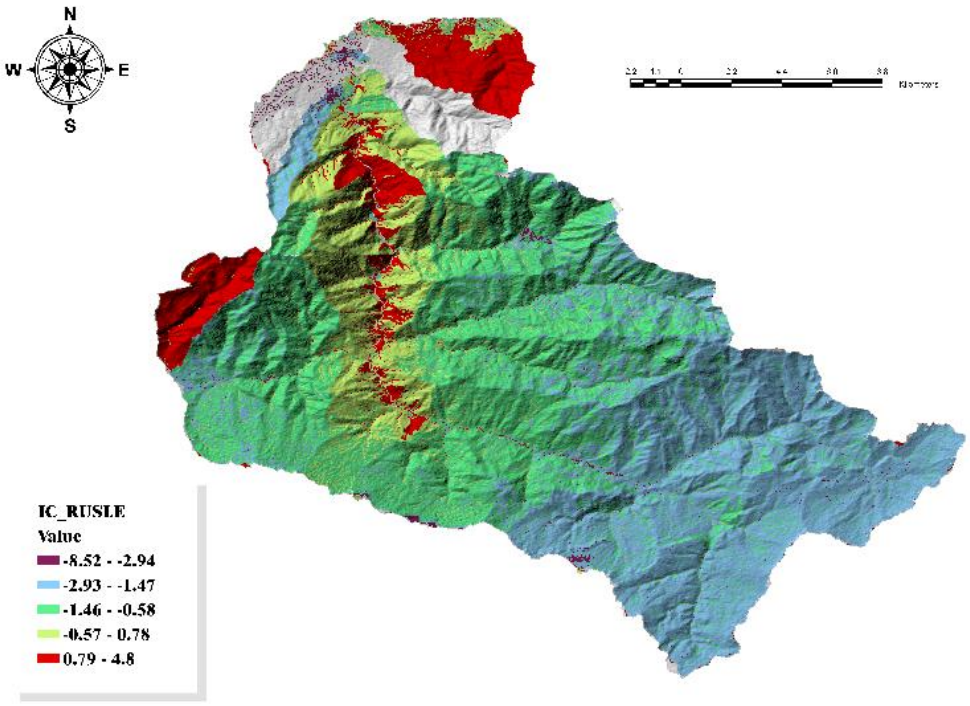


Figure 6.10. Ic RUSLE of Chiffa watershed.

Major Implication for Infrastructure

These results demonstrate that the downstream **RN1 highway** is not merely threatened by runoff from adjacent hillslopes; it serves as the ultimate **sink** for an expansive upstream agricultural erosive system. Consequently, **hydraulic structures** (such as culverts and box culverts) must be dimensioned to manage **hyper-concentrated sediment-laden flows** rather than just clear water. Failure to account for this sediment load risks rapid **clogging and siltation**, which would compromise the road's drainage capacity during extreme events.

6.4 Debris Flow Hazard: The Ballistic Threat to Infrastructure

While soil erosion (as analysed in the previous section) threatens infrastructure through the slow-onset processes of **siltation** and **hydraulic clogging** (bedload transport), **Debris Flows** pose a fundamentally different type of threat: immediate mechanical destruction.

In the steepest reaches of the Chiffa catchment, sediment concentration can exceed the critical threshold ($C_v > 47\%$). At this point, the water-sediment mixture undergoes a radical **rheological shift**, transforming into a viscous, **non-Newtonian fluid**. It is no longer a simple liquid flow but a dense, cohesive mass acting as a devastating **geotechnical projectile**, capable of severing or obliterating engineering structures through sheer **impact force** [70].

6.4.1 Morphometric Methodology and Simulation

In the absence of detailed in-situ rheological data for the soil materials, a robust **GIS-based morphometric approach** was adopted [189]. The workflow, summarized in **(Fig. 6.11)**, is structured around two critical stages: **source area identification** and **runout simulation**.

6.4.1.1 Identification of Initiation Zones

Source areas (initiation zones) were identified by coupling three distinct spatial indicators:

a) The **Stream Power Index (SPI)**, calculated according to the formulation by [190].

b) The **critical initiation slope threshold**, defined by the empirical power-law relation from [191] :

   a. $S > 0.32A^{-0.2}$

c) The **Index of Connectivity (IC)**, used to verify the effective downstream delivery of mobilized materials.

6.4.1.2 Runout Simulation

To evaluate the potential impact on infrastructure, the spatial extent of the flows was modelled using two complementary approaches:

- **1D Estimation (Vandre's Method):** An analytical calculation of the **runout distance** along the longitudinal profile of the channel.
- **2D Simulation (Modified Single Flow - MSF):** The MSF algorithm was employed to model the spatial spreading of the flow over the DEM. This simulation is pivotal for predicting whether the debris flow possesses sufficient energy to reach and **overtop** the roadway [192].

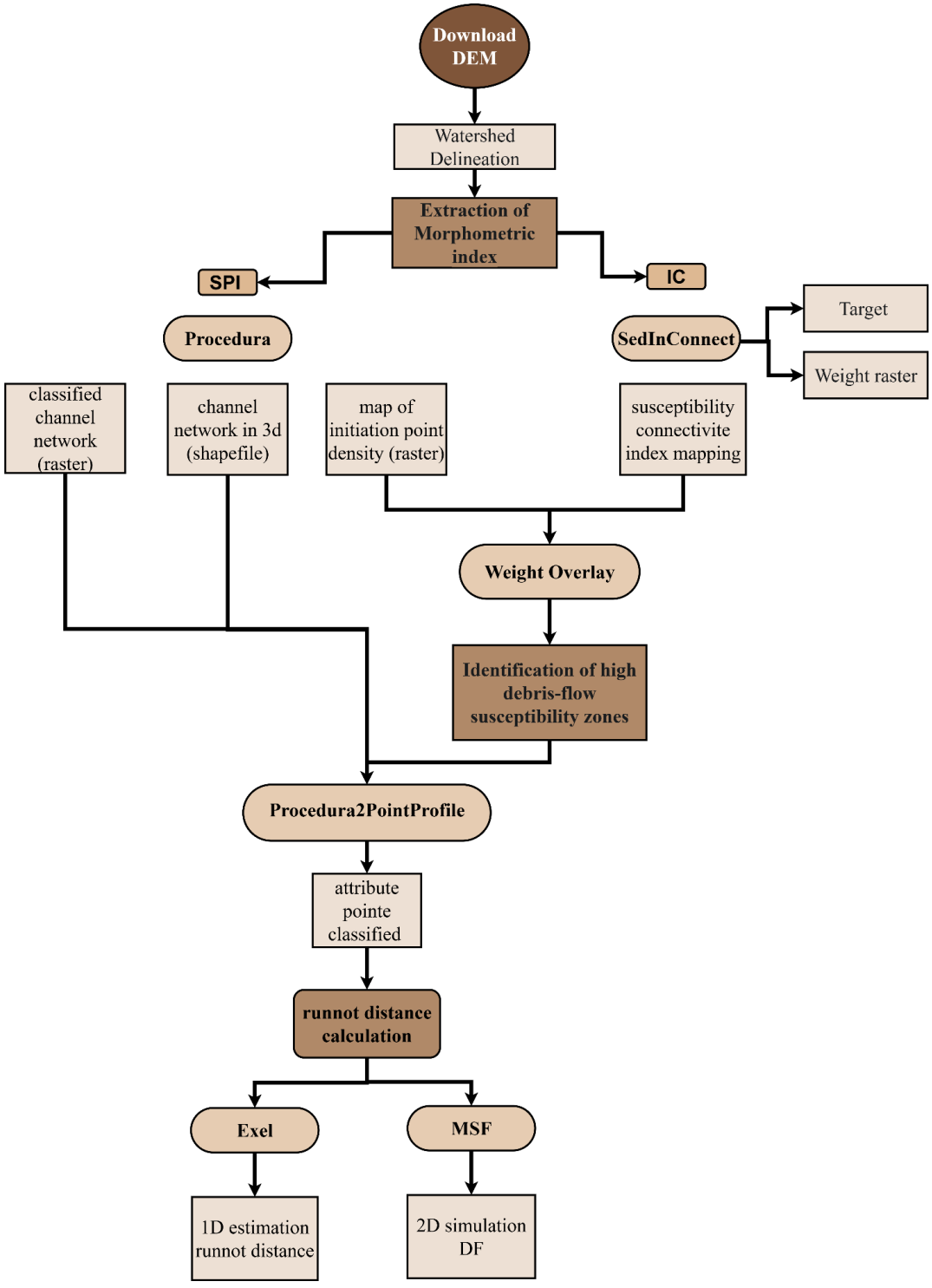


Figure 6.11. Methodology steps.

6.4.2 Results: From Morphometric Characterization to the Threat on RN1

The morphometric analysis of the Chiffa catchment yielded a series of thematic maps that deconstruct the mechanics of debris flow hazards within the study area.

6.4.2.1 Initial Morphometric Characterization

- **Hypsometry (Fig. 6.12):** The terrain is characterized by extremely **rugged relief**, with a total **elevation drop** of over 1,500 m between the mountain crests (1,670 m) and the outlet.

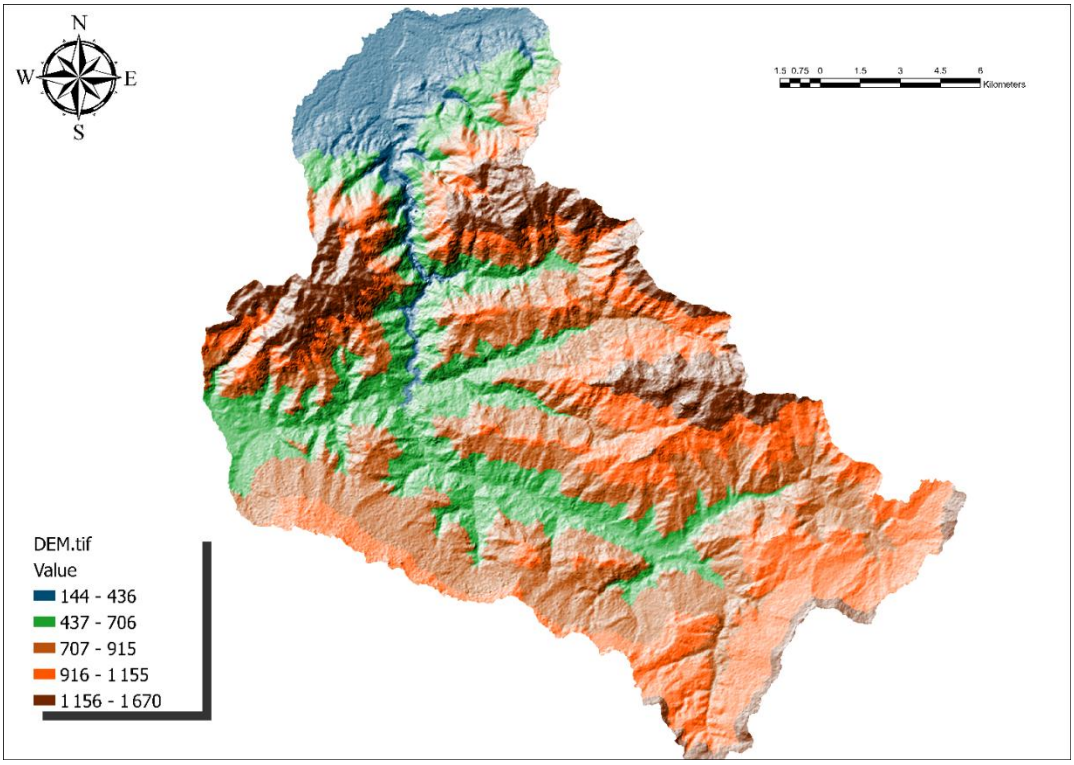


Figure 6.12. DEM map of Chiffa watershed.

- **Surface Roughness (Fig. 6.13):** The roughness index highlights areas of high local instability (represented by high values in red/yellow), primarily concentrated in the northwestern sector of the basin. These zones of **"topographic disarray"** are primary candidates for sediment mobilization and initiation.

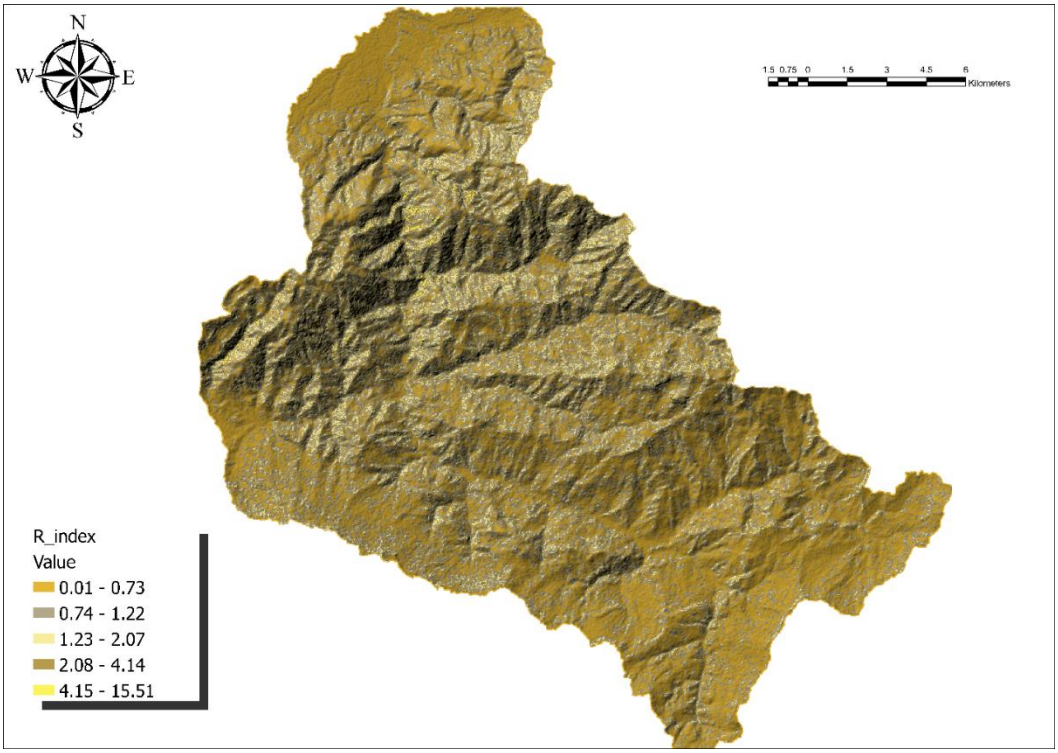


Figure 6.13. Surface roughness index map of Chiffa watershed.

6.4.2.2 Hazard Zonation

- **Extraction and Classification of the Hydrographic Network:**
  - Initially, the application of the **Stream Power Index (SPI)** threshold (SPI > 5) on the DEM enabled the extraction of the raw active drainage network geometry **(Fig. 6.14)**, revealing a dense **dendritic structure** typical of mountainous catchments.
  - Subsequently, a **morphometric reach classification (Fig. 6.15)** was performed to segment the network according to flow dynamics. It clearly distinguishes **initiation zones** (shown in red, steep slopes > 15°), **propagation reaches** (blue), and **deposition zones** (green/yellow), accurately locating the segments where debris flows form and where they eventually decelerate.

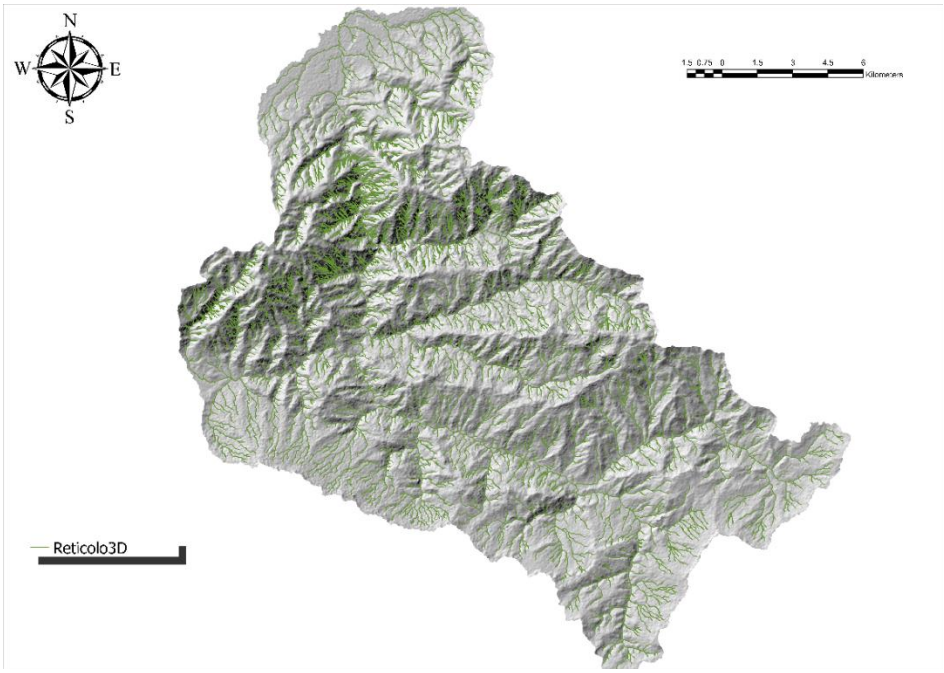


Figure 6.14. Channel network of the Oued Chiffa watershed.

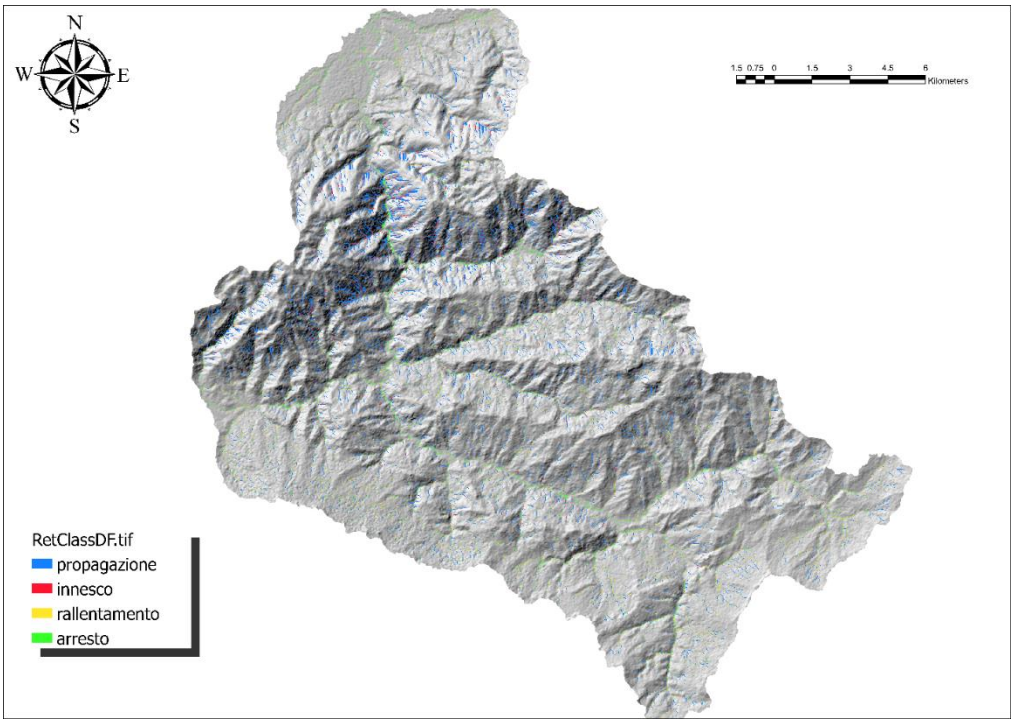


Figure 6.15. Classification of the channel network reaches based on potential debris flow processes (initiation, propagation, deceleration, and stopping).

- **Initiation Point Density (Fig. 6.16):** By applying the Zimmermann threshold, a **Heatmap** of initiation probability was generated. It reveals critical **hotspots** concentrated in the northwestern headwaters, directly **overlooking** the road infrastructure.

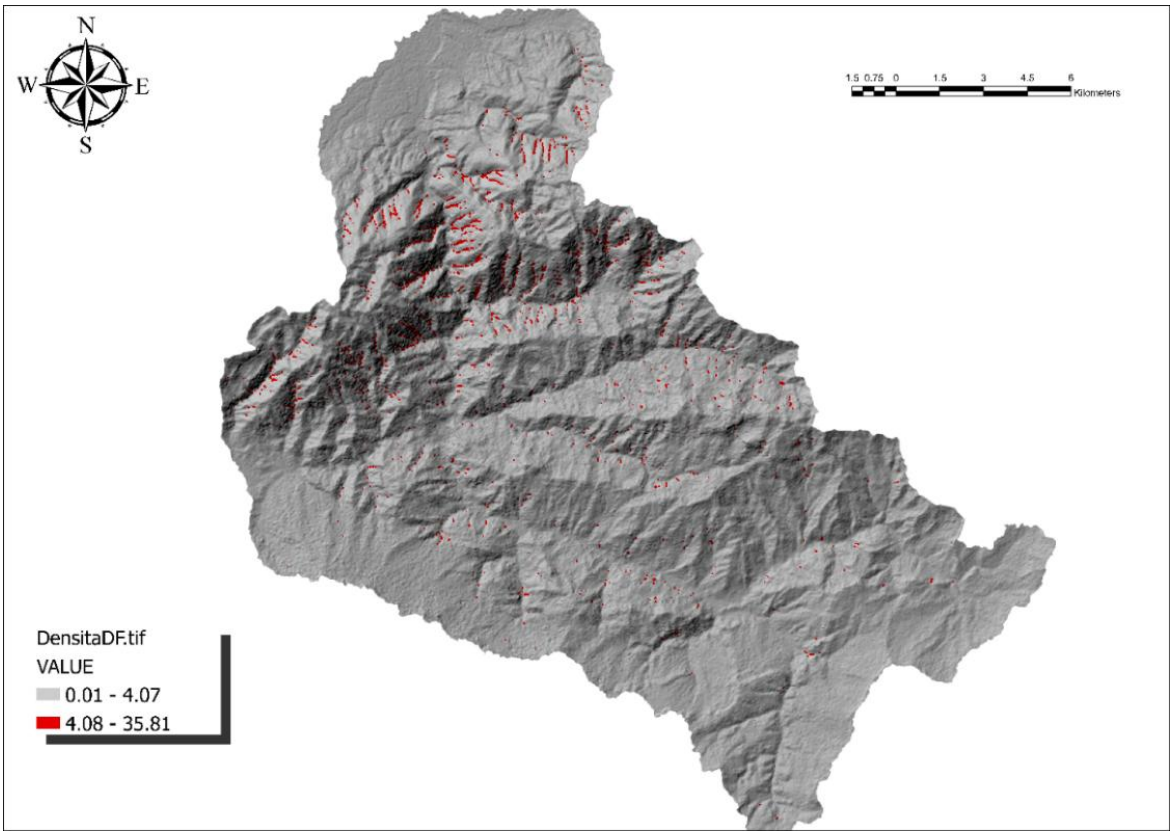


Figure 6.16. Density map of potential debris flow initiation points.

6.4.2.3 Composite Susceptibility and Connectivity Map

The final susceptibility map **(Fig. 6.17)** results from the **weighted overlay** (50/50 ratio) of initiation density and the **Index of Connectivity (IC) (Fig. 6.18)**.

- **Results:** The "Very High" susceptibility zones are not spatially random. They correspond to hillslopes that are simultaneously unstable (high source density) and highly connected (high IC) to the main channel.

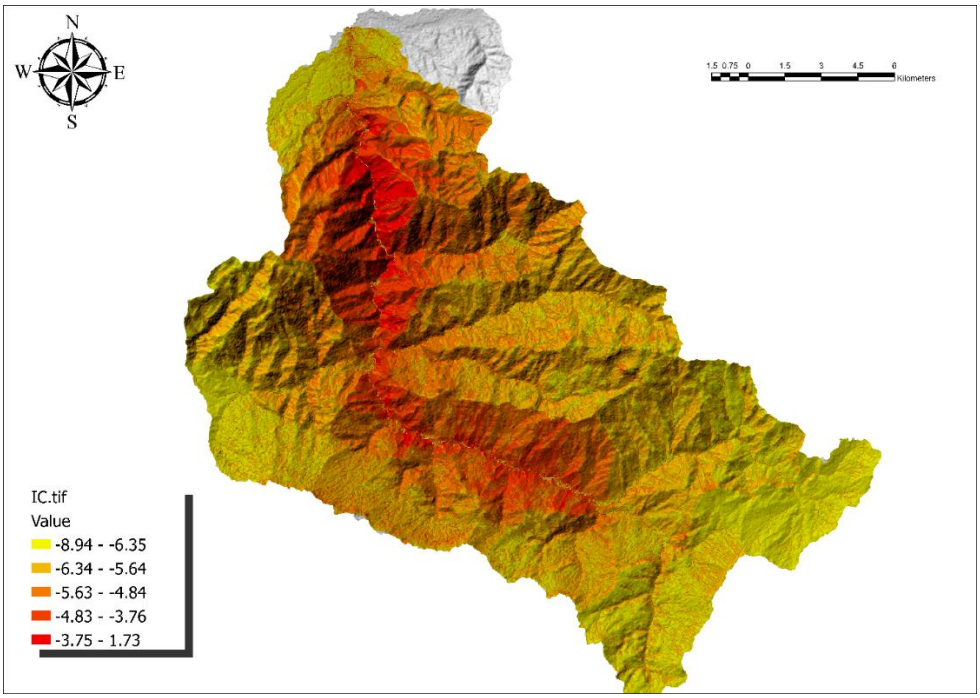


Figure 6.17. Sediment Connectivity Index (IC) map.

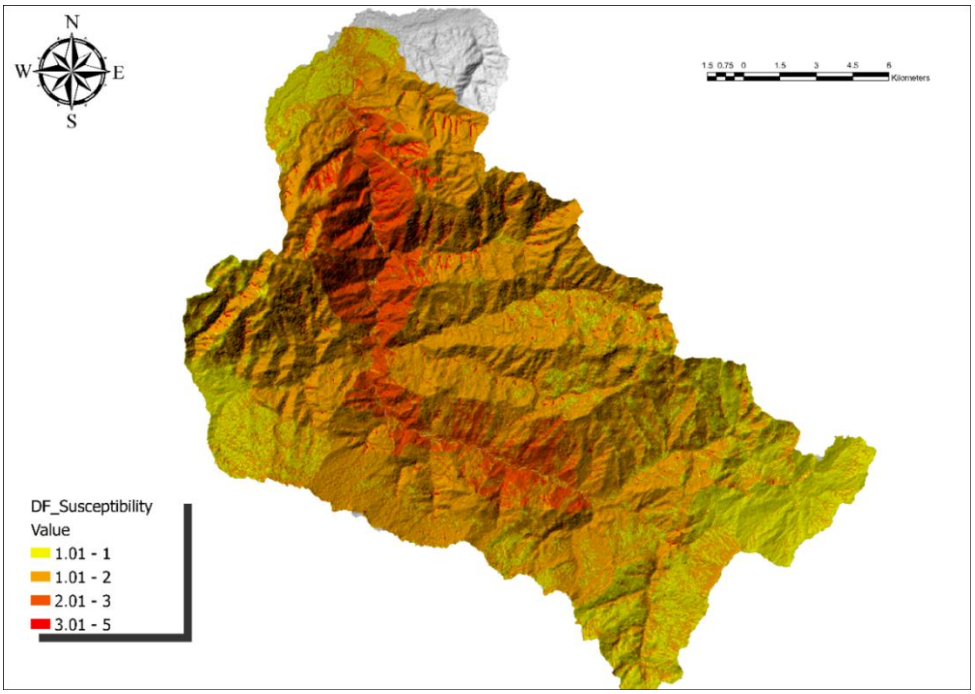


Figure 6.18. Final debris flow susceptibility map, obtained by combining the initiation density and connectivity indices.

6.4.2.4 Estimation of Impact Simulation on the RN1

The 2D **runout simulation (MSF)** translates this susceptibility into an estimation of **impact scenario (Fig. 6.19)**.

- The model predicts that debris flows generated on lateral slopes possess sufficient **kinetic energy** to reach the valley floor.
- **Critical Insight:** The simulation demonstrates that the flow (yellow) **encroaches upon** the RN1 and spreads across the pavement structure. The **peak impact zones** (red) are located precisely at **confluence points**, validating the risk of total drainage obstruction and the potential destruction of engineering structures through **ballistic impact**.

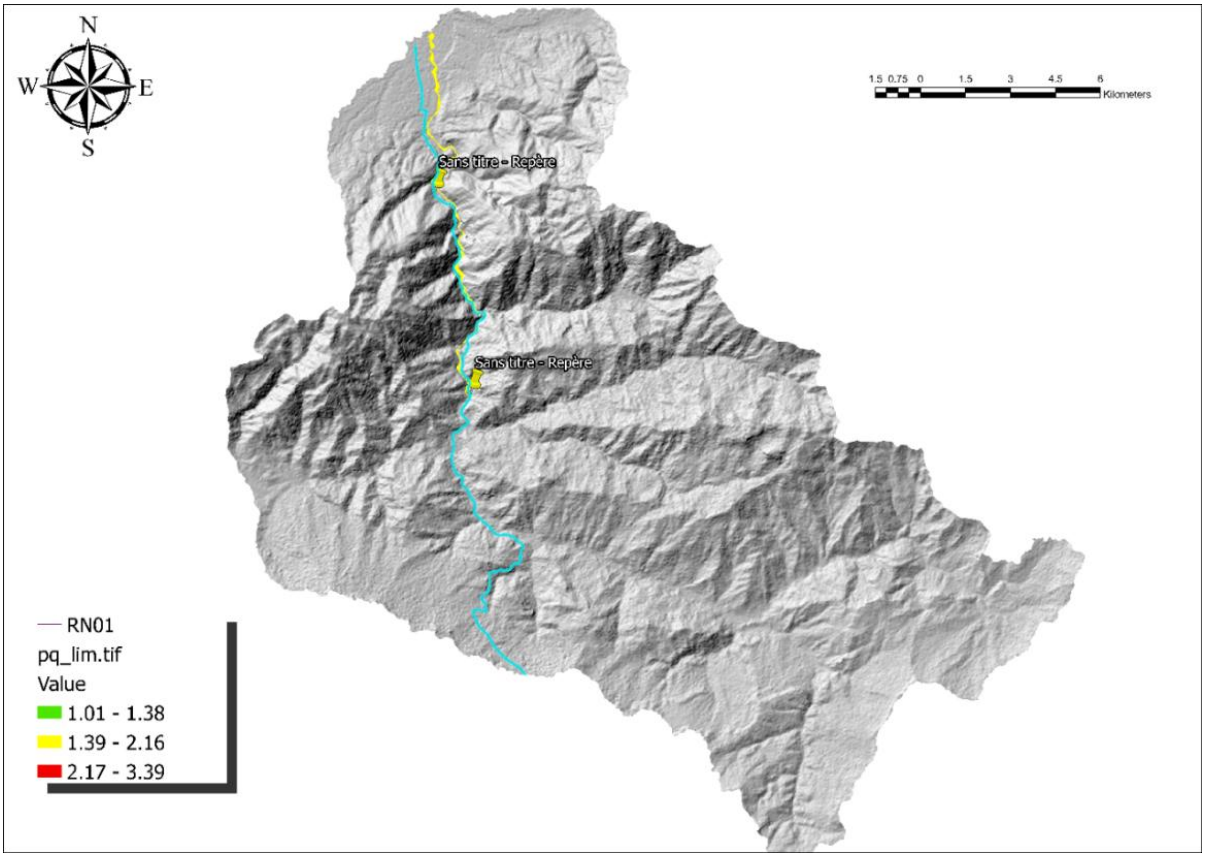


Figure 6.19. .Final debris flow susceptibility map, obtained by combining the initiation density and connectivity indices.

6.4.3 Synthesis: The Critical Exposure Profile of the RN1

The combined analysis of the susceptibility map **(Fig 6.18)** and the propagation simulation **(Fig 6.19)** highlight a critical situation for the road infrastructure.

- **Spatial Clustering of the Threat:** Critical initiation zones are heavily concentrated in the northwestern sector of the catchment, directly **overlooking** the entrance to the Chiffa Gorges.
- **Impact Simulation (2D Runout):** Propagation scenarios demonstrate that flows generated on these lateral slopes possess sufficient **kinetic energy** to reach the valley floor.
- **Infrastructure Impact:** The model predicts that debris flows do not merely intersect the RN1; they spread across the pavement, forming **alluvial fans** (debris cones) that result in the total obstruction of the roadway.
- **Field Validation:** The modelled high-risk zones correlate perfectly with historical records of road closures and in-situ observations of slope instability.

Technical Conclusion: This analysis demonstrates that along this specific segment, the road is exposed to a hazard behaving as a **"geotechnical projectile."** This justifies the implementation of heavy-duty protection measures (such as **rockfall protection galleries** and **sediment deposition basins**) requirements that cannot be identified or addressed through conventional hydraulic dimensioning alone.

6.5 Conclusion

From Physical Understanding to the High-Fidelity Imperative

The investigation conducted in this chapter on the Chiffa catchment represents a decisive milestone in our comprehension of the hazard: the transition from **clear-water hydrology** to the **morpho dynamics of complex environments**.

We have demonstrated that in mountainous regions, neglecting sediment transport is equivalent to overlooking the primary source of danger. Through the innovative **IC-RUSLE coupling**, we have established that the infrastructure does not merely withstand runoff from adjacent slopes but serves as the ultimate recipient for the **sediment load** of the entire basin. More critically, morphometric simulations have revealed the **ballistic threat** posed by debris flows, which directly target the National Road 1 (RN1).

The core takeaway of this chapter is both rheological and physical. **Volumetric sediment concentration (C_v)** is not a mere academic parameter; it fundamentally alters the nature of the flow physics. When a flood crosses the critical threshold to become a **non-Newtonian fluid**, classical hydraulic equations are no longer valid. In this regime, water no longer simply flows; it strikes. Consequently, the selection of mitigation measures (such as **deposition basins**, **reinforced gabions**, or **rockfall protection galleries**) depends exclusively on the accuracy of this initial diagnosis. Any misclassification of the hazard inevitably leads to a **fatal under-design** of the engineering structure.

At this stage, the danger has been localized and its underlying physics understood. However, morphometric indicators (SPI, IC) have reached their operational limit: while they predict *where* a debris flow will strike the road, they cannot quantify the **impact pressure** on a bridge pier or the exact **inundation depth** on the pavement structure.

To transform this hazard knowledge into **resilience engineering**, we must now shift both our scale and our analytical tools. It is time to move beyond the topographical approximations of regional DEMs to embrace the **actual geometric complexity** of the infrastructure. This is the objective of the next chapter, which introduces **High-Fidelity (BIM-HDM) coupling** the only technology capable of resolving the complex interaction between a destructive fluid and a civil engineering asset.

PART III:

VULNERABILITY ASSESSMENT AT THE INFRASTRUCTURE SCALE (MICRO-SCALE APPROACH)

7 Analysis of Flood-Infrastructure Interaction through BIM-HDM Integration

7.1 Introduction

From Territory to Asset: The Paradigm Shift

The analyses conducted in the preceding chapters (ranging from the regional zoning of the Mitidja Plain to the morpho-dynamic characterization of the Chiffa catchment) have enabled the localization and qualification of the threat. We now know where the risk is concentrated. However, for the manager of a strategic network such as the RN1, this information remains insufficient. Identifying that a road traverses a flood-prone area is an urban planning observation; determining whether that road will remain passable during a **100-year flood** or face structural failure is a matter of **precision engineering**, necessitating a radical shift in scale [6].

The answer to this critical question hinges on a single physical parameter: the **actual water depth on the pavement structure**. Yet, conventional tools(such as GIS and satellite-derived DEMs(suffer from an inherent "structural blindness" at the asset scale, creating a **"Scale Gap"** that degrades risk assessment into a potentially dangerous approximation [19] .

This chapter introduces the core of our methodological contribution: the transition to **High-Fidelity (Hi-Fi) modelling**. We propose an innovative framework, **BIM-HDM**, which merges the territorial intelligence of GIS (Macro) with the geometric fidelity of BIM (Micro) to create a **hybrid simulation environment**. The objective is to define and validate a new operational indicator(the **Flooded Road Height (FRH)**(capable of translating complex hydraulic outputs into a binary criterion of **Functional Vulnerability** (passable/impassable), while establishing the foundation for future structural integrity analyses [84].

To demonstrate the superiority of this approach, the chapter is structured around three key stages:

Section 7.2: The Failure of the Conventional Approach (C-HDM). We analyse the limitations of classical models using the critical Chiffa road segment as a case study, highlighting the diagnostic errors induced by low topographic resolution.

Section 7.3: The BIM-HDM Methodological Framework. We detail the technical architecture of our solution, explaining how the integration of a digital **"As-built"** model into the hydraulic engine enables the reconstruction of a **high-precision composite terrain**.

Section 7.4: Validation and Comparative Results. We confront the models with historical records to validate the **FRH indicator**, proving that geometric precision is the decisive lever for a reliable diagnosis.

7.2 Problem Statement: Limitations of the Conventional Approach (C-HDM)

Assessing the functional vulnerability of a road (specifically its capacity to remain serviceable during a flood event) is contingent upon a critical parameter: the **water depth across the pavement structure**. However, conventional methodologies based on GIS-Hydrodynamic (**C-HDM**) coupling encounter a fundamental limitation rooted in **spatial resolution**.

7.2.1 The Topographic Blindness of DEMs

Conventional hydraulic models (e.g., HEC-RAS) typically rely on satellite-derived **Digital Elevation Models (DEMs)**, such as SRTM or ALOS PALSAR. However, their spatial resolution(typically ranging from 12.5 m to 30 m(is inadequate for engineering-grade analysis [109]. At this coarse scale, road infrastructure is essentially **"dissolved"** into the surrounding landscape; the road's geometry is **averaged out** against the natural terrain. Consequently, its precise elevation, **cross-sectional profile**, and the presence of critical features such as retaining walls are entirely omitted. This oversimplification leads to substantial errors in estimating **Fluid-Structure Interaction** [12].

7.2.2 Application to the Chiffa Case Study: Proof through Failure

In an initial study presented at the **ICCE 2024 international conference**, this standard methodology **(Fig. 7.1)** was applied to the critical segment of the RN1 within the **Chiffa Gorges** to evaluate its operational reliability.

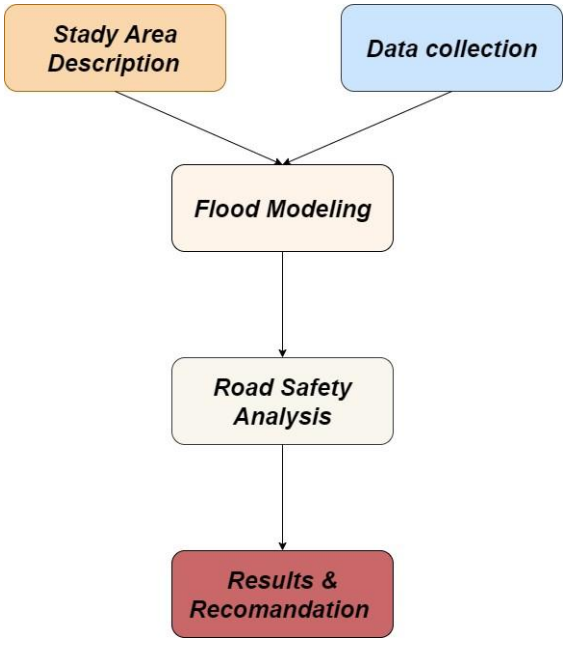


Figure 7.1. Methodology steps.

7.2.2.1 Simulation Protocol and Mesh

The simulation was conducted using **HEC-RAS 6.5**, employing a **coupled 1D/2D hydrodynamic model**. The terrain geometry was based on an **ALOS PALSAR DEM** with a spatial resolution of 12.5 meters. As illustrated in **(Fig 7.2)**, the model defines **cross-sections** along the thalweg to calculate the **water surface profile**.

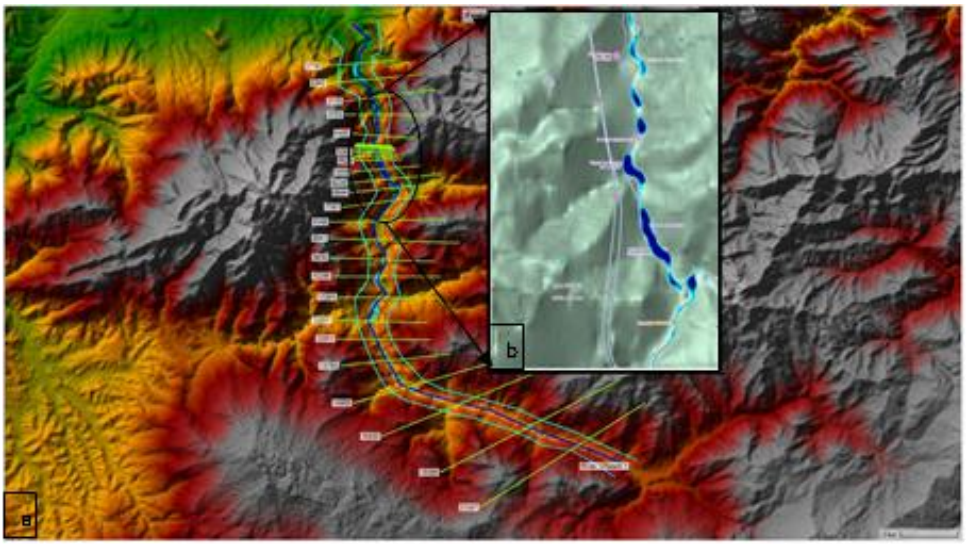


Figure 7.2. Identification of areas with high flood hazard.

7.2.2.2 Hydraulic Results Analysis

The hazard map **(Fig. 7.2)** correctly identifies a major danger zone (**"High Flood Hazard"**) at the entrance of the gorges. However, a granular analysis of the cross-sections **(Fig. 7.3)** reveals a significant **physical inconsistency**. Within the cross-sectional view, the model positions the road (RN1) at the same elevation as (or even below) the calculated water line. This occurs because the coarse resolution of the DEM has **"smoothed out"** the protective road embankment.

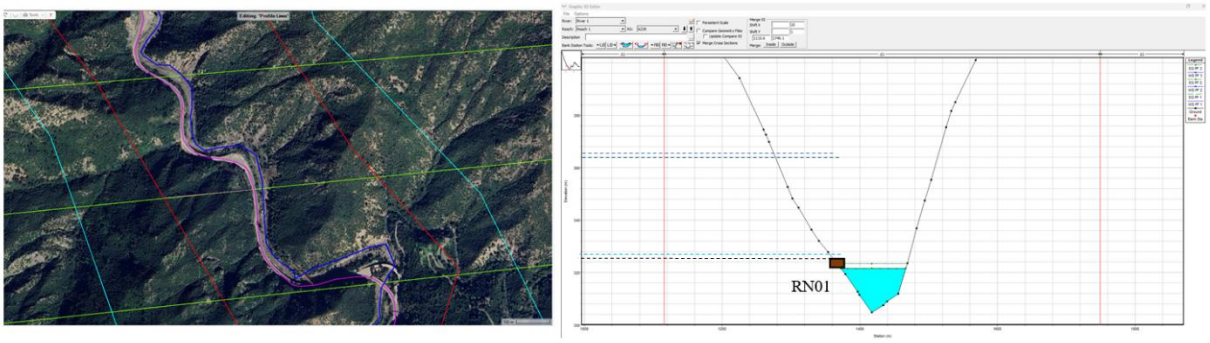


Figure 7.3. Identifying Road flood levels of the river station n° 6239.

7.2.2.3 Error Quantification

The numerical outputs **(Table 7.1)** confirm this **computational aberration**. The model predicts catastrophic **Flooded Road Heights (FRH)**:

- At station 4917: 2.94 m of water on the roadway.
- At station 4853: 1.94 m.
- At station 6239: 1.46 m.

Table 7.1. Comparison of Flood Levels and Road Elevations.

River station	Distance between Road and Bank line (m)	Z Road (m)	Z flood (m)	Flooded road height (m)
4853	36.1	307	308.94	1.94
4873	40.9	307	308.94	1.94
4896	44	308	308.94	0.94
4917	52.3	306	308.94	2.94
5146	372.3	307	308.94	1.94
5859	186.7	320	321.46	1.46
6239	286.6	320	321.46	1.46
6644	475.6	320	321.46	1.46

7.2.2.4 Assessment of the C-HDM Approach: A Strategic Screening Tool

Although the water depths are significantly overestimated, this modelling phase successfully fulfils its **pre-diagnostic mandate**. It enabled the precise identification and localization of the specific kilometres-scale segments susceptible to flooding **(Fig. 6.16)**, serving as an effective **rapid screening tool** [193].

This approach is therefore valid for **qualitative vulnerability assessment** (identifying *where* to intervene). It constitutes the essential **strategic filter** required to target specific areas that now demand high-resolution quantitative analysis (determining *how* to intervene). This imperative transition from qualitative assessment to high-precision quantification justifies the next methodological step: the integration of **BIM data** [76].

7.3 High-Fidelity Methodology: The BIM-HDM Framework

To overcome the spatial resolution **bottleneck**, we developed an innovative methodological framework(**BIM-HDM**(whose theoretical foundations and results have been published in the flagship journal ***Reliability Engineering and System Safety*** [194].

This approach is rooted in a fundamental **paradigm shift**: rather than oversimplifying reality to fit the constraints of a conventional model, we enrich the model to accurately capture the **"As-Built"** reality of the infrastructure.

7.3.1 The Tripartite Architecture of the Integrated Framework

The framework extends beyond the simple utilization of a specific tool, orchestrating the fusion of three core technologies within a **unified simulation environment (Fig. 7.4)**:

1. **Territorial Intelligence (GIS – Macro Scale):** This component provides the necessary **boundary conditions** (watershed dynamics) and the regional topographic context.
2. **Structural Fidelity (BIM – Micro Scale):** This layer contributes the **exact geometry** of the engineering structure, including detailed elements such as piers, decks, and precise cross-sectional profiles.
3. **Fluid Physics (HDM):** The **Hydrodynamic Modelling** engine solves the **Saint-Venant equations** across this **high-resolution hybrid mesh**, enabling the precise simulation of water behaviour.

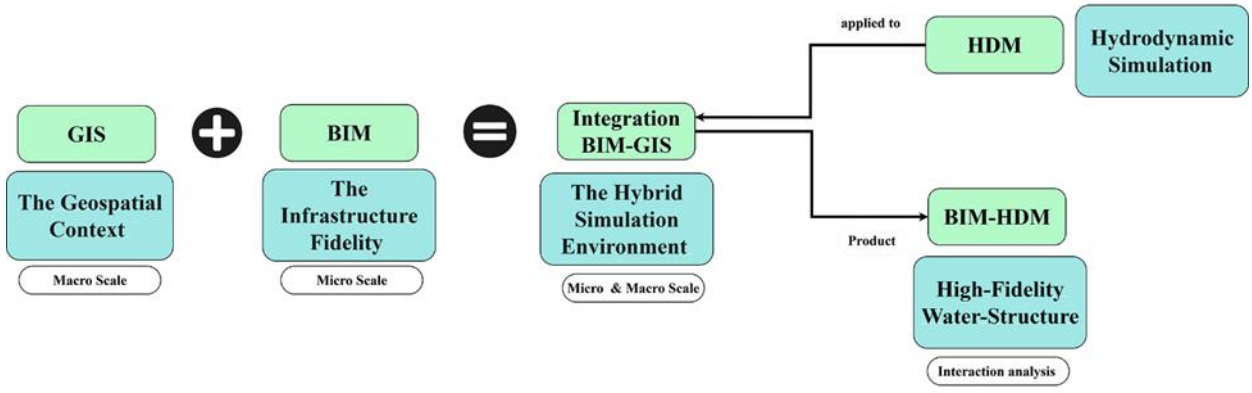


Figure 7.4. Framework BIM-HDM.

7.3.2 Experimental Validation: The Chiffa Wadi Case Study

To validate the robustness of the proposed framework, it was deployed on the previously identified **"hotspot"**: the RN1 highway segment at **KP 65.862**, a site characterized by **recurring flood events**.

7.3.2.1 Implementation of the Simulation Workflow

The construction of the hybrid model followed a rigorous workflow **(Fig.7.5)**, structured as follows:

- **Geometric Data Fusion:** The regional DEM was enhanced through the integration of high-fidelity BIM models for both the road and the bridge. These assets were modelled using their **actual cross-sectional profiles**, incorporating critical details such as **superelevation's (cross-slopes)**, drainage ditches, and **concrete safety barriers**.
- **Hydraulic Parameterization:** A **steady-state simulation** was performed, utilizing a **100-year peak discharge** ($Q_{100} = 90m^3/s$) as the primary hydraulic input.

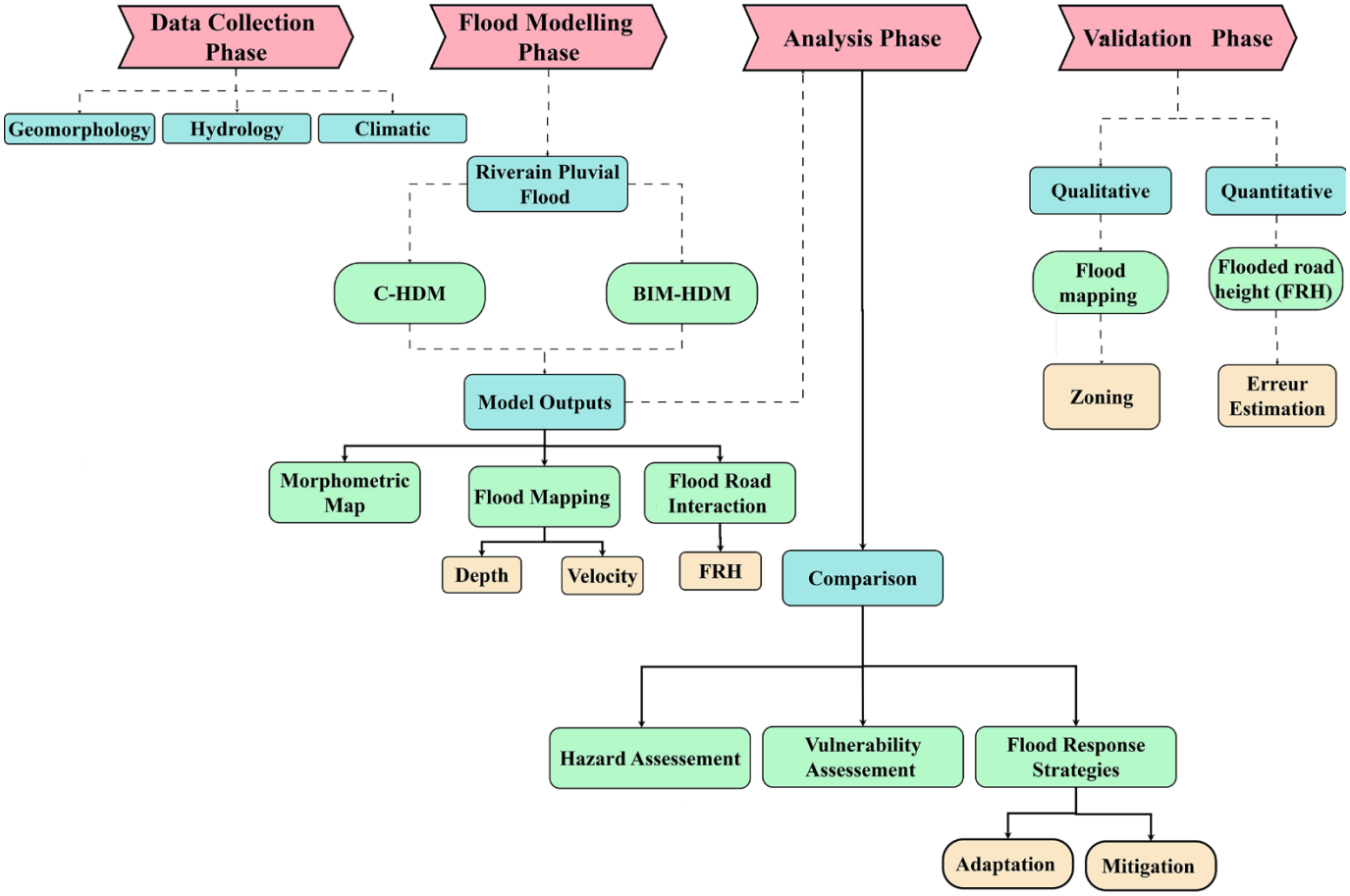


Figure 7.5. Methodological Workflow for the Comparative Study.

7.3.2.2 In-Depth Analysis of Simulation Results

The BIM-HDM simulation does not merely provide discrete point heights; it generates a comprehensive spatial characterization of the **Fluid-Structure Interaction (FSI)**.

Flood Extent: The Value of 3D Visualization

A comparison of the extent maps **(Fig. 7.6)** reveals a similar overall **flood footprint** for both models. However, the primary distinction lies in the visualization quality of the **water-infrastructure interface**. The integration of the 3D asset model allows for a direct and realistic interpretation of the submersion [19]. This facilitates the identification of impacted zones relative to the road alignment, whereas the conventional model only provides an **abstract planimetric view** [138].

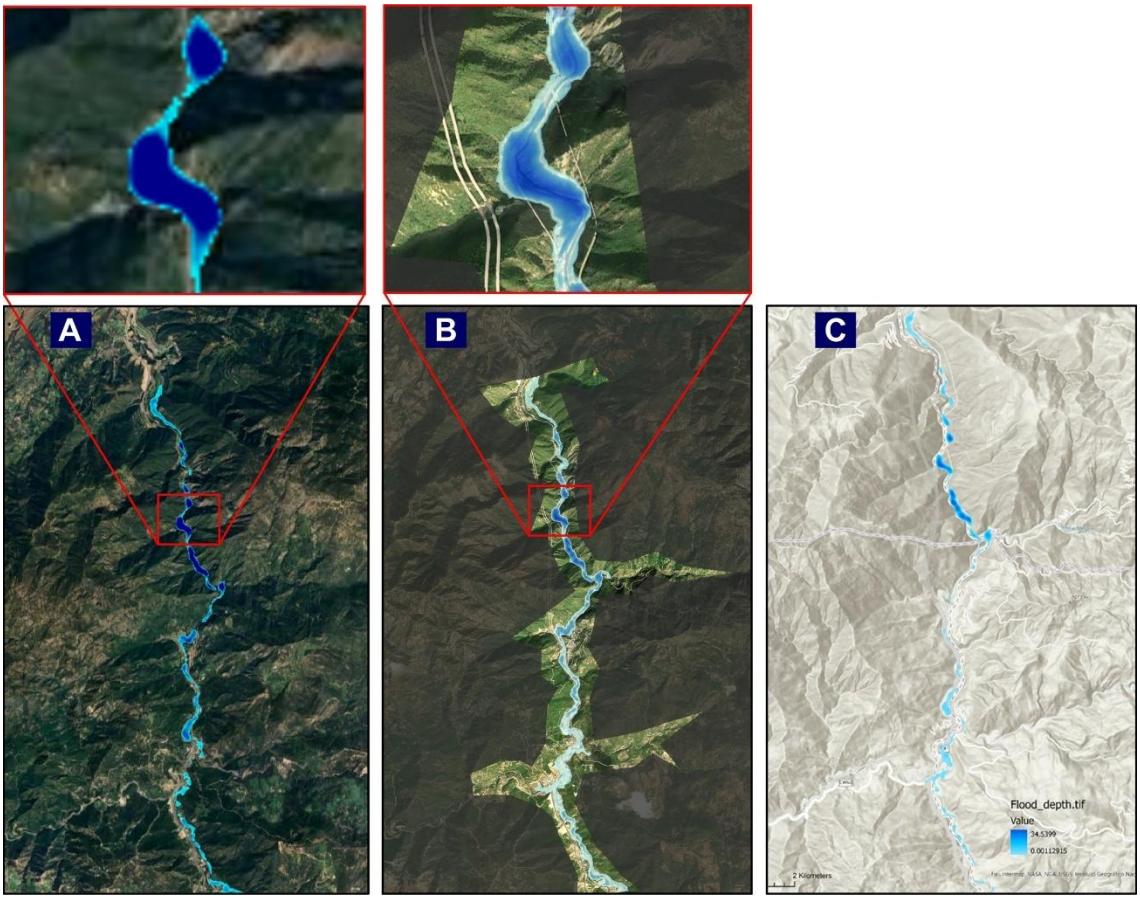


Figure 7.6. Flood Depth in the study area. A. InfraWorks results. B. HEC-RAS result in RasMapper. C. HEC-RAS results in ArcGIS PRO.

Velocity Hazard Mapping: Hydraulic Convergence

The comparison of velocity maps **(Fig. 7.7)** confirms a strong similarity in hydraulic results at the segment scale. Both models identify the same **flow corridors** and acceleration zones within the valley's **bottlenecks**.

This observation is significant: it validates that the integration of BIM geometry does not disrupt the global physics of the flow. This kinetic energy mapping serves as the essential input data for the subsequent evaluation of **mechanical stressors**(such as hydrodynamic thrust and scouring(on roadside structures [15].

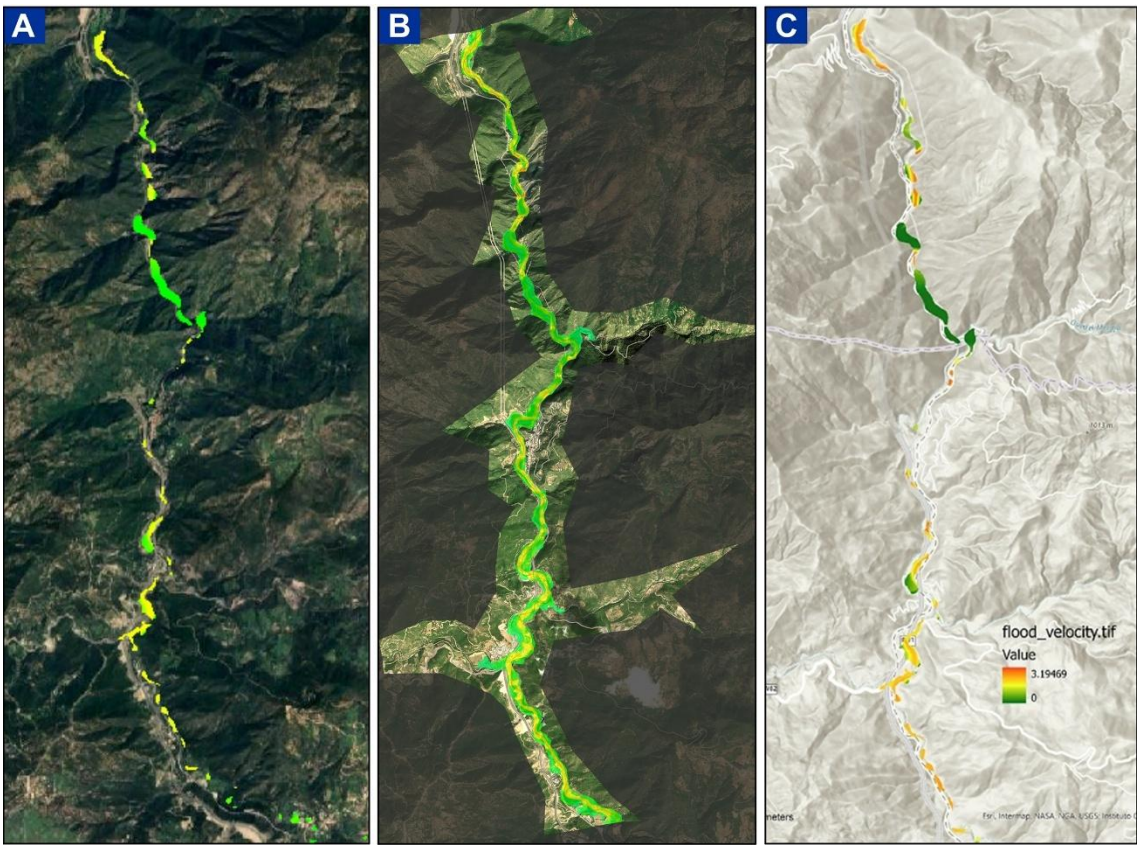


Figure 7.7. Flood velocity in the study area. A. InfraWorks results. B. HEC-RAS result in RasMapper. C. HEC-RAS results in ArcGIS PRO.

The FRH Indicator: From Hydraulics to Functionality

The critical divergence between the two approaches emerges during the extraction of the **Flooded Road Height (FRH)** longitudinal profile.

- **C-HDM Interpretation (Fig.7.8):** The model projects the water surface onto the terrain DEM. Because the road is "absent" from the DEM, the resulting height reflects that of the flooded valley floor ($H \approx 2m$).

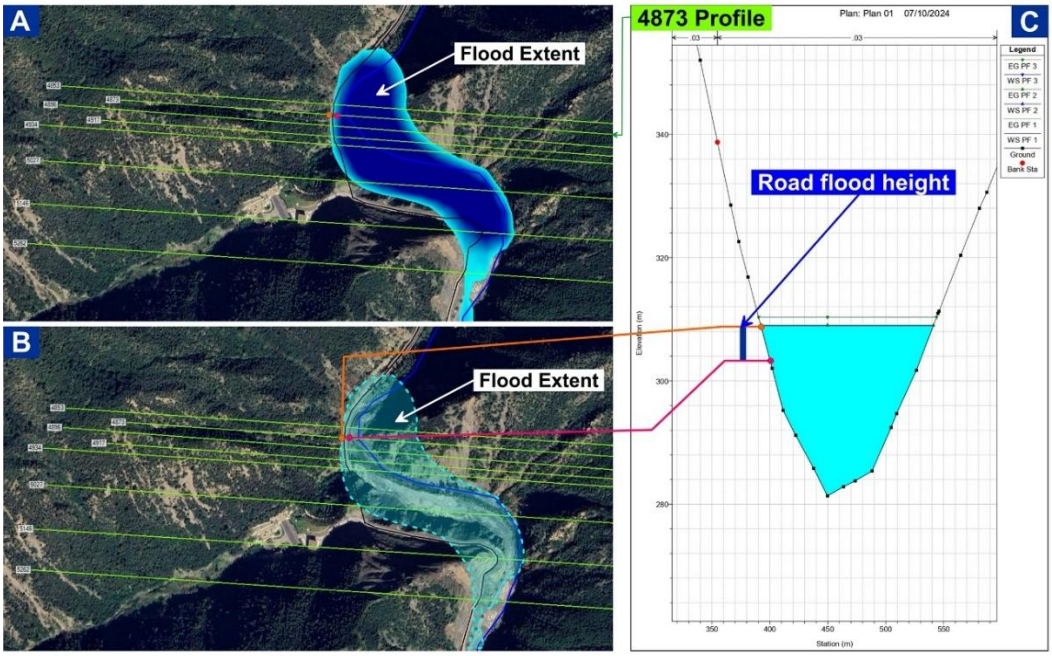


Figure 7.8. Process for identifying road-flood interaction using C-HDM. A. First step. B. Second step. C. third step.

- **BIM-HDM Interpretation (Fig. 7.9):** The model projects the water surface onto the 3D road geometry. This allows for the measurement of the **residual water depth** specifically above the asphalt surface ($H \approx 0.55m$).

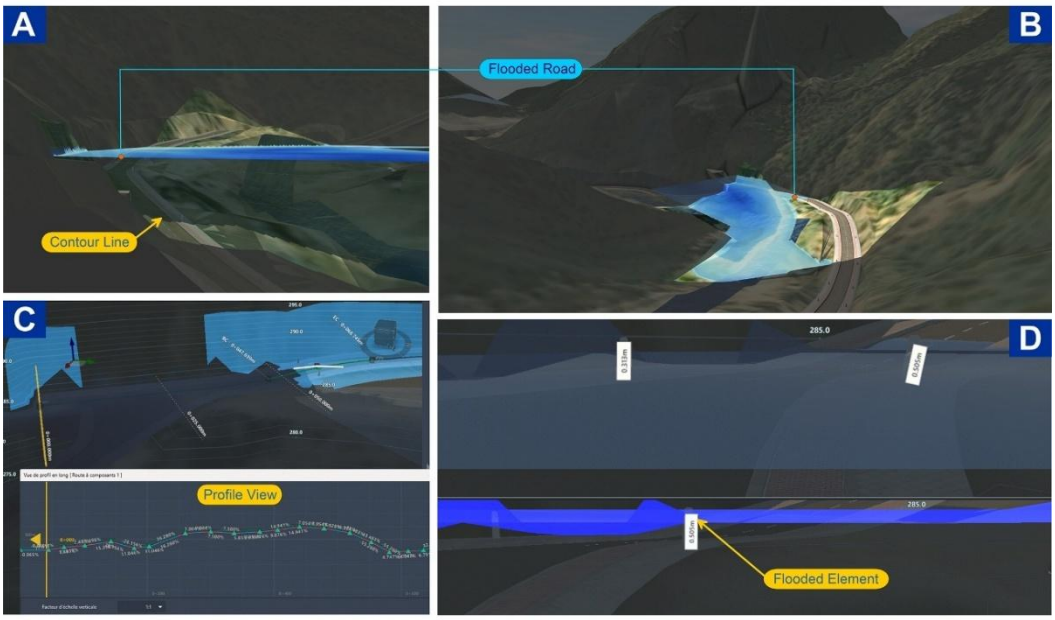


Figure 7.9. Process for identifying road-flood interaction using BIM-HDM.A. Reading the elevation from contour lines.B.3D visualization. C. Profile view of the road. D. Measurement of a partially flooded element.

Table 7.2 synthesizes the values obtained by these two methods for the most critical cross-sections of the segment.

Table 7.2. Comparison of Flood Levels and Road Elevations.

PK road	Parameters obtained with the C-HDM software					Parameters obtained with the BIM-HDM software		
	River sections under HECRAS	Distance between Road and Bank line (m)	Z Road (m)	Z flood (m)	Flooded road height (m)	Z Road (m)	Z flood (m)	Flooded road height (m)
65,882	4873	40.9	307	308.94	1.94	288.68	289	0.311
65,862	4896	44	308	308.94	0.94	288.42	289	0.571
65,840	4917	52.3	306	308.94	2.94	286.00	289	3

7.3.2.3 Quantitative Validation and Error Analysis

The cross-validation of these readings with observed reality **(Fig. 7.10)** allows for the quantification of the **accuracy gain** provided by the integrated approach **(Table 7.3 and Fig. 7.11).**

- **Ground Truth (Photogrammetric Analysis):** The water depth measured against the safety guardrail on-site was **0.55 m**.
- **C-HDM Error:** With a predicted depth of 0.94 m, the relative error reaches **+71%**. This represents a massive overestimation caused by the **omission of the road embankment** in the coarse DEM.
- **BIM-HDM Error:** With a prediction of 0.571 m, the residual error drops significantly to **+3.8%**.

Table 7.3. Validation of Simulated Flood Depths against Photo-Estimated Observations at PK 65.862.

Model	Observed Depth (m) (Photo-estimated)	Simulated FRH (m)	Absolute ERROR	Relative ERROR
C-HDM	0.49-0.61≈0.55	0.94	+0.39	+71%
BIM-HDM	0.49-0.61≈0.55	0.571	+0.02	+3.8%



Figure 7.10. Methodology for estimating observed water depth for model validation. (A) On-site measurement of the safety guardrail height (80 cm) used as a reference object. (B, C, D) Archival imagery from historical flood events (Feb 2017, Apr 2018, Dec 2018) used

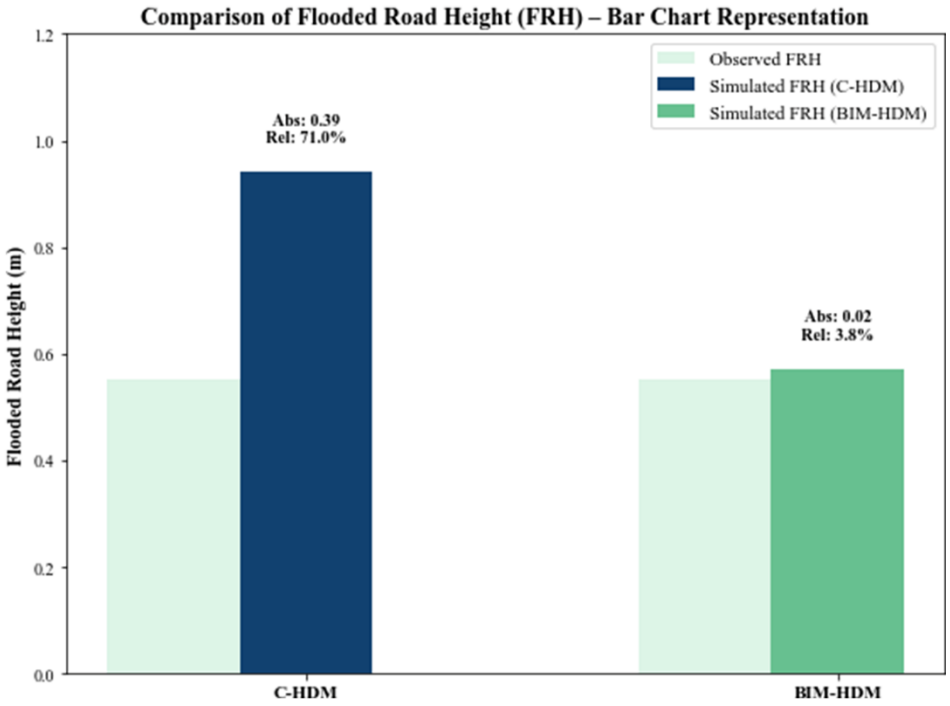


Figure 7.11. Comparison of Flooded Road Height (FRH) – Bar Chart Representation.

This dramatic reduction in error validates the thesis's central hypothesis: for an operational vulnerability diagnosis, the **geometric precision of the asset (BIM)** is more decisive than the complexity of the hydraulic engine alone.

7.3.2.4 Visual Confrontation and Functional Validation

Beyond numerical performance, **(Fig 7.12)** provides compelling **visual evidence** of the **Fluid-Structure Interaction (FSI)**.

- **Model Fidelity (Fig 7.12, A):** The high-fidelity rendering in InfraWorks demonstrates that the simulated water surface profile accurately follows the road's **cross-slopes** and the specific structural obstacles modelled in BIM.
- **Hazard Reality (Fig 7.12,B):** Archival photographs confirm this spatial extent. Notably, in Figure 60B (right), a light commercial vehicle is seen navigating a **water sheet** whose depth corresponds precisely to the critical **FRH** predicted by our model.

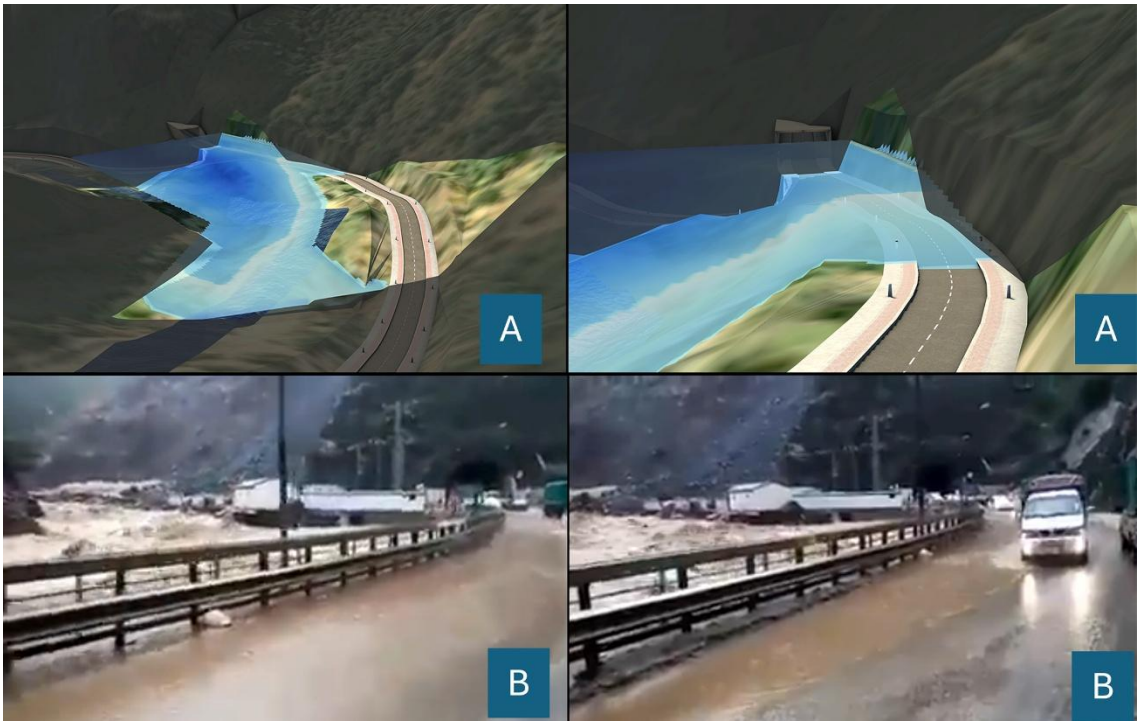


Figure 7.12. Flooded area. A. Flood simulation by GIS-BIM-HDM approach (InfraWorks software). B. Picture of a flood that occurred on 05/02/2017.

This significant reduction in computational error, corroborated by the visual evidence in **(Fig 7.12)**, confirms that high-fidelity geometric data is the **pivotal factor** for a reliable vulnerability assessment. We now possess a validated **FRH indicator**, capable of confidently informing the resilience strategies presented in the final chapter.

7.4 Discussion and Perspectives: Toward High-Fidelity Engineering

This chapter successfully validated our core hypothesis: the integration of BIM fundamentally redefines the nature of vulnerability diagnostics. By reducing the margin of error from 71% to a mere 3.8%, we have transformed a **crippling uncertainty** into an instrument of **surgical operational precision**.

Nevertheless, the FRH (Flooded Road Height) indicator is only the **first stepping stone**. The computational power of the hybrid simulation environment we have developed unlocks immense prospects for addressing the **full spectrum of vulnerability dimensions** initially identified in Chapter 1.

7.4.1 Generalizing the Model across the Vulnerability Triad

The established hybrid environment provides a robust foundation for addressing the three dimensions of vulnerability through high-fidelity analysis:

- **Functional Vulnerability (Validated):** The **FRH** indicator enables the precise prediction of **service loss** (road closure conditions). This data directly informs traffic flow and accessibility models, allowing for more reliable contingency planning [49].
- **Physical Vulnerability (Potential Application):** By coupling localized velocity vectors (V_s) extracted from the hydrodynamic model with the **mechanical properties** stored within the BIM model (such as concrete grade and **reinforcement detailing**), it is now possible to calculate precise failure indicators. This includes assessing the risk of **overturning moments** and predicting **scouring depth** with unprecedented accuracy [15]**.**
- **Complex Hazards (Debris Flow Modelling):** The same workflow can be adapted to simulate **non-Newtonian fluids**. By incorporating the specific viscosity and density of debris flows (as analysed in Chapter 6), the model can transition from calculating simple inundation depths to quantifying **ballistic impact forces** against embankments and structural components [70].

7.4.2 Toward the Resilience Digital Twin

This research lays the essential groundwork for a **Resilience Digital Twin**, capable of simulating the comprehensive interaction between diverse hazard types and the real-world complexity of infrastructure assets. It effectively evolves the static BIM model into a **dynamic stress-testing laboratory**, providing a proactive environment for evaluating system performance under extreme conditions [132].

7.5 Conclusion

From Diagnostic Precision to Strategic Action

By establishing the superiority of high-fidelity diagnostics, this chapter has effectively resolved the final methodological **bottleneck** of our research. We now possess a computational tool capable of determining with certainty whether a road segment will remain **passable** or not during a major flood event.

This level of precision is a **gamechanger** for response strategies: we are no longer relegated to merely enduring the hazard or reacting to it with uncertainty. Armed with this reliable diagnosis, we can now design targeted and effective mitigation and resilience measures.

This is the core focus of the final chapter, which will explore how to translate this granular risk knowledge into concrete resilience actions ranging from localized **structural protection** to large-scale **sustainable territorial planning**.

PART IV:

RISK TREATMENT AND RESILIENCE STRATEGIES

8 Risk Treatment Strategies: Mitigation, Resilience, and Crisis Management

8.1 Introduction

The Imperative for a Hybrid Response

The high-fidelity diagnosis established in the previous chapter has served as a **diagnostic revelation**: our road infrastructures (the vital lifelines of our economy) exhibit critical failure points where intrinsic vulnerability intersects with **climatic unpredictability**. Faced with this stark reality, the conventional 20th-century paradigm, cantered on the **"all-concrete"** philosophy and the absolute mastery of hazards (**Flood Control**), has reached a dual threshold: a financial one, given the staggering scale of maintenance requirements, and an ecological one, driven by the imperative to reduce carbon footprints and align with the **Sustainable Development Goals (SDGs)** [27].

This chapter proposes moving beyond this binary vision to construct a **hybrid resilience strategy**. Within this framework, resilience is redefined as a "**Collective Adaptive Capacity**" [28]. It introduces a holistic perspective where a measure's effectiveness is no longer evaluated solely by its physical robustness, but by its contribution to the functional stability of the overall system. The objective is no longer merely to struggle against water, but to learn to manage its presence to guarantee **service continuity**[58].

This adaptive capacity rests on three fundamental pillars (**Knowledge** (modelling), **Anticipation** (forecasting), and **Reaction** (intervention)) and is structured around three complementary action levers:

Section 8.2: Civil Engineering Interventions (Structural Lever). Guided by the precision of our **FRH indicator**, these solutions navigate the trade-off between **Mitigation** (reducing exposure through avoidance) and **Adaptation** (reinforcing structures to coexist with the hazard). They aim to physically secure the critical nodes identified through **BIM-HDM interoperability**.

Section 8.3: Crisis Management and Organizational Resilience (Non-Structural Lever). When **residual risk** becomes unavoidable [60], safety relies on network intelligence. This section addresses the deployment of an **Early Warning System (EWS)**, whose implementation is optimized for the high-risk zones identified by our diagnostics. This system utilizes the FRH indicator as a physical decision threshold to protect users in real-time, offering an **agile alternative** to heavy structural works [29].

Section 8.4: Source Control Management (Nature-Based Solutions). Through the application of the **"Sponge City"** concept to the city of Rouiba, we demonstrate a sustainable resilience approach. This lever proves that hazards can be reduced by restoring the natural hydrological cycle, thereby minimizing the carbon footprint while protecting downstream infrastructure [195].

By pragmatically acknowledging the existence of a manageable residual risk, this hybrid strategy transforms infrastructure from a state of passive vulnerability into one of **active resilience**.

8.2 Civil Engineering Interventions: Balancing Resistance and Hydraulic Transparency

Civil engineering interventions, often categorized as **"Hard Mitigation,"** constitute the direct physical response to securing the pivotal nodes identified through our diagnostics. Guided by the precision of the **FRH (Flooded Road Height)** indicator, these measures aim to recalibrate the balance of the "Hazard-Infrastructure" interaction. Technical decision-making is structured around two distinct philosophies: **Mitigation through avoidance** and **Adaptation through robustness**.

8.2.1 Structural Mitigation: Strategies for Avoidance and Control

Mitigation aims to reduce infrastructure exposure by physically limiting its interaction with floodwaters. Within our BIM-HDM framework, this trade-off is activated when the FRH exceeds critical safety thresholds.

- **Vertical Alignment Raising:** This measure involves elevating the road's **grade line** above the Peak Water Level (PWL). While it ensures service continuity, implementing this on existing structures (such as at KP 65.862) is complex. It requires massive **earthwork volumes**, resulting in high financial overhead and a substantial carbon footprint [96].
- **Hydraulic Transparency (Cross-Drainage Structures):** Mitigation also involves reducing the "dam effect" caused by road embankments. Replacing undersized circular culverts with large-section **box culverts** increases discharge capacity, thereby reducing upstream hazard levels and downstream scouring phenomena [69].

8.2.2 Structural Adaptation: Coexisting with the Hazard (Robustness)

Adaptation is rooted in the philosophy of **"living with the hazard."** Unlike avoidance-based mitigation, this approach accepts the interaction between water and infrastructure but reinforces the system to ensure that the asset maintains its structural and functional integrity during and after the event [58].This strategy is particularly relevant for legacy assets, as illustrated by the diagnostic analysis of KP 65.862 **(Fig 8.1)**.

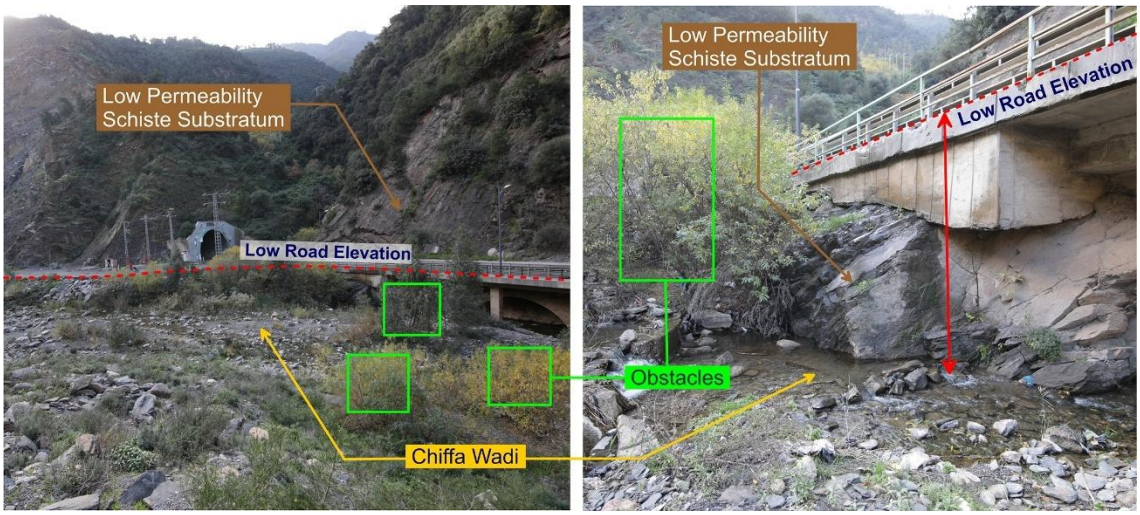


Figure 8.1. Specific characteristics of the PK 65,862 km area. A.Low road elevation. B.Low permeability schist substratum.

- **Riverbed Recalibration (Spatial Adaptation):** Site examination reveals critical road elevation and the presence of natural obstructions within the Chiffa Wadi bed **(Fig 8.1A andB)**. These geometric constraints make massive pavement raising prohibitively expensive. The adaptive solution therefore focuses on the "container": **widening the concave bank** and dredging identified obstacles. This intervention, validated through hydraulic modelling, increases the flow section and mechanically lowers the FRH without modifying the existing road structure [69].
- **Armouring and Stabilization (Adaptation through Robustness):** The presence of a low-permeability **schistose substratum (Fig 8.1B)** complicates infiltration management and increases the risk of slope instability due to saturation. Given the simulated critical velocities ($V_s > 3m/s$), reinforcement using riprap, gabion walls, or a combination of anchors and **shotcrete** becomes necessary to "armour" the road. The objective is to reduce the intrinsic vulnerability of the **pavement structure** to guarantee immediate **recovery** following the flood event [16].
- **Management of Sediment and Debris Flows:** In this deeply incised topography, resilience depends not only on water management but also on sediment control. The construction of **upstream deposition basins** and **debris traps** allows the watercourse to be "filtered," capturing boulders and woody debris before they can impact crossing structures [70].

8.2.3 BIM-HDM Interoperability as a Decision-Support Engine

The originality of the resilience approach developed in this thesis lies in the use of **BIM interoperability** as a primary decision-support engine [194]. Unlike traditional static design methods, the BIM-HDM workflow enables the simulation and validation of the geotechnical and hydraulic feasibility of solutions prior to any physical intervention. **Figure 8.2** concretely illustrates this process of transforming field data into an optimized technical solution.

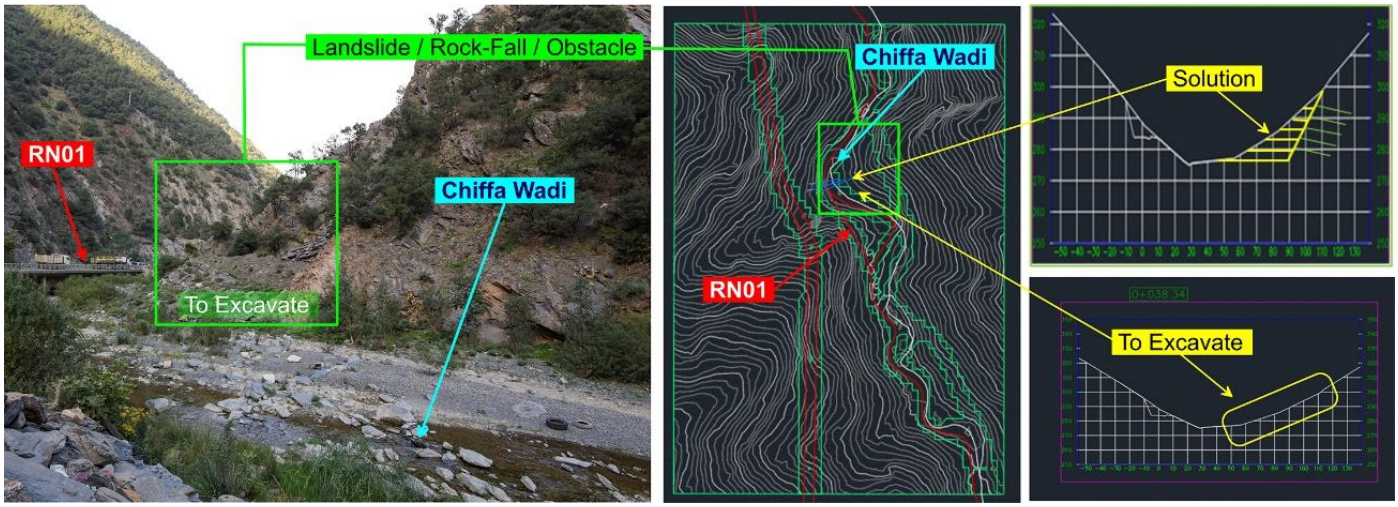


Figure 8.2. Examples of BIM interoperability: A. Pictures illustrate the sinuosity of the terrain. B. Infraworks to Civil 3D. C. Civil 3D to geotechnical software.

- **From Field Reality to Conceptual Model (Fig 8.2A):** The process begins with a high-resolution site characterization. Field photography identifies critical zones subject to wadi sinuosity and instability risks (landslides, rockfalls). This visual reconnaissance is essential for contextualizing the hydraulic obstacles that exacerbate the FRH indicator.
- **Geometric Design and Sinuosity Analysis (Fig 8.2 B):** Through the interoperable link between **InfraWorks** and **Civil 3D**, the complex topography of the Chiffa Wadi is digitized. This workflow allows for the analysis of the alignment's sinuosity and the precise identification of conflict zones between the watercourse and the RN1. At this stage, recalibration solutions are drafted; the model allows for the testing of various bank excavation scenarios to maximize hydraulic capacity while minimizing earthwork volumes and the project's carbon footprint [110].
- **Geotechnical Optimization and Excavation Calculation (Fig 8.2 C):** The final phase involves exporting Civil 3D cross-sections to geotechnical analysis software. As shown in the "To Excavate" detail in **Figure 8.2**, BIM enables the definition of volumes to be removed with **centimetres precision** to lower the water surface profile. This step ensures that the proposed riverbed recalibration does not destabilize adjacent slopes and remains compatible with the mechanical strength of the substratum [69].

This **precision engineering** transforms risk management. By using the integrated workflow as a decision-making baseline, engineers no longer need to "over-design" structures out of uncertainty; instead, they tailor the structural response to the physical reality of the site. Interoperability thus becomes the guarantor of an **economically viable and technically robust resilience**, enabling real-time arbitration between intervention costs and safety gains regarding the FRH indicator [194].

8.3 Organizational Resilience: Early Warning Systems (EWS) Optimized by FRH

When an extreme hazard surpasses the structural design capacity of an asset (**residual risk**), safety no longer relies on concrete reinforcements but on the intelligence of crisis management. **Organizational resilience** involves adapting network operations in real-time to minimize user exposure [196]. As demonstrated in our research published in ***Reliability Engineering & System Safety*** [194], the integration of BIM, GIS, and hydrodynamic modelling enables the design of an EWS that is no longer generic, but **spatially and physically optimized**

8.3.1 From Model to Operational Digital Twin: The BIM-HDM Advantage

Our methodological framework extends beyond static diagnostics; it serves as the foundation for a **dynamic alert system**. By evolving the simulation model into a connected **Digital Twin**, we transition from reactive management to **proactive anticipation** [110].

The originality of this approach lies in utilizing the **Flooded Road Height (FRH)** indicator as the system's primary **decision-making engine**. The data workflow (illustrated in **Fig 8.3**) links models derived from Autodesk Revit, Dynamo, and InfraWorks to field-based **IoT sensors**. This architecture optimizes the placement of monitoring instrumentation exclusively within the high-risk zones identified by our diagnostics, thereby reducing infrastructure costs while maximizing network reliability.

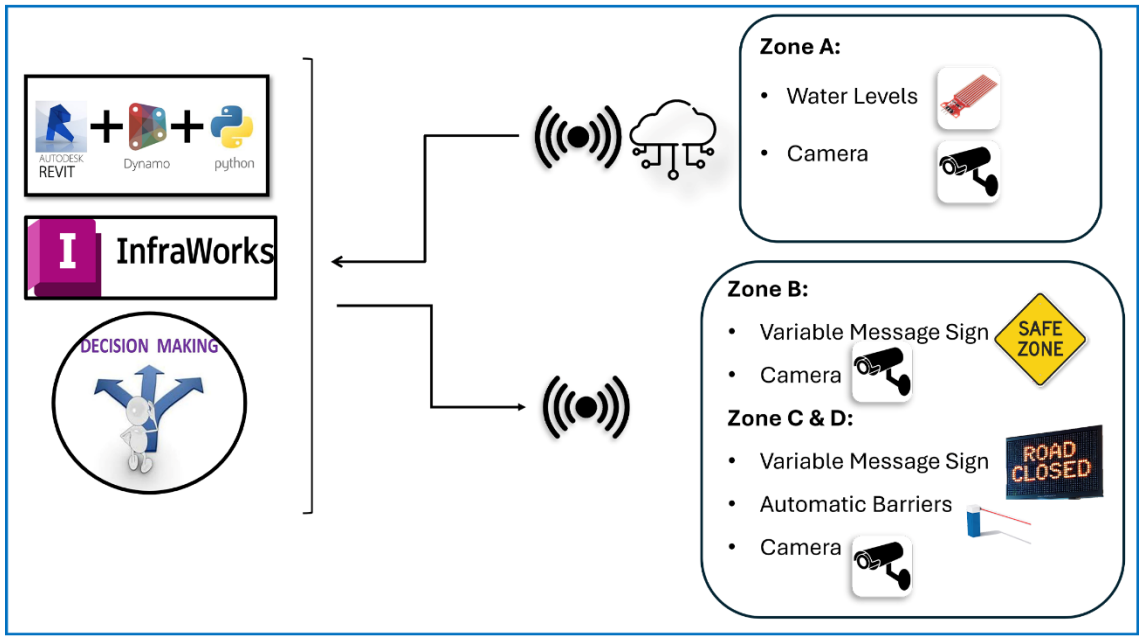


Figure 8.3. Alert system flowchart.

8.3.2 Zoning Protocol and Crisis Management for the RN1

Based on our functional vulnerability analysis and the geometric precision provided by BIM, we propose an **automated zoning protocol** for the critical Chiffa Wadi segment **(Fig 8.4)**:

a) **Zone A (Detection and Monitoring - A1, A2):** Strategically located at the hydraulic upstream. It is equipped with **limn meters** (water-level sensors) and connected cameras. This zone serves as the system's **"optic nerve,"** detecting rising water levels before they impact the pavement.

b) **Zones C and D (Closure and Diversion - C1, C2, D1, D2):** These are the strategic **cutoff points** located at interchanges and junctions upstream of the risk area. As soon as the Digital Twin predicts an **FRH > 30 cm** (the critical buoyancy threshold), the system triggers real-time automated barriers and **Variable Message Signs (VMS)** to divert traffic, specifically toward the A1 highway.

c) **Zone B (Refuge and Safety - B1, B2):** Identification of elevated refuge areas located between the detection and cutoff points. These zones allow users already traveling within the segment to seek shelter in flood-free areas, following model-validated secure routes [197].

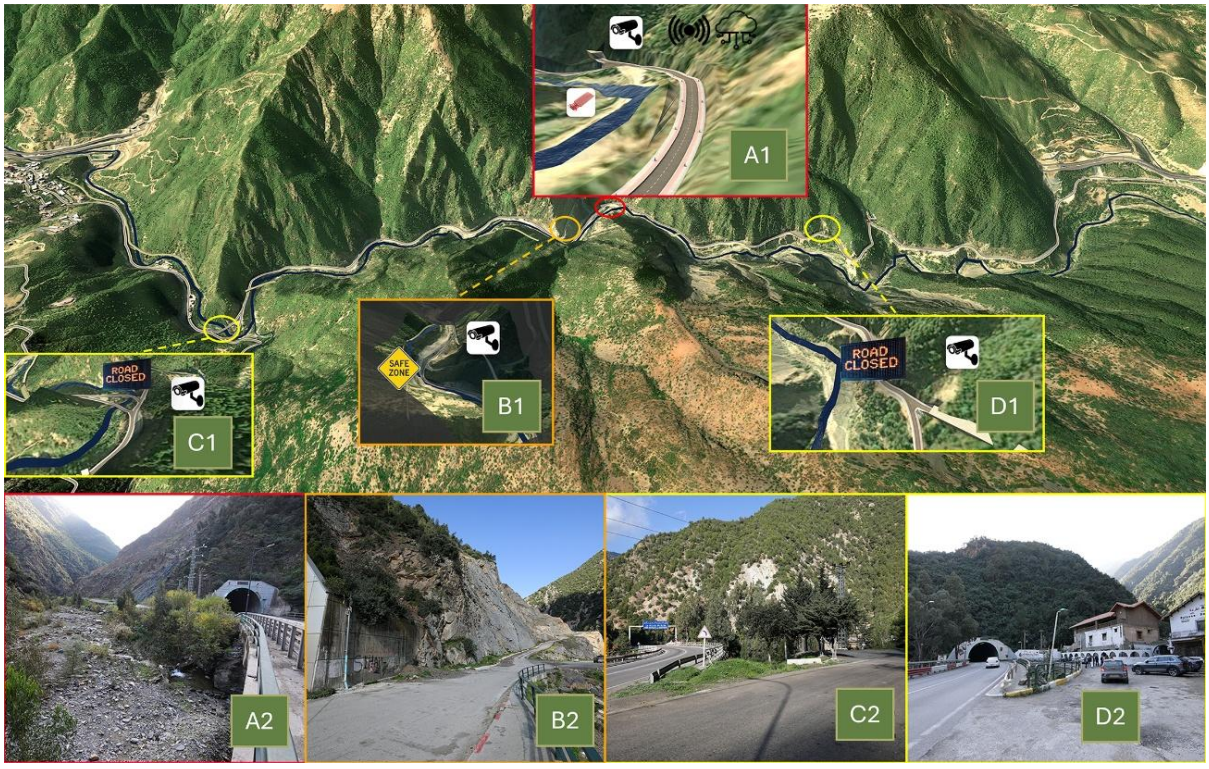


Figure 8.4. Zone description. A. High flood risk Zone. B. Safety Zone. C. The first diversion.

8.3.3 Synthesis: Efficiency through Physical Precision

The interoperability between Revit, InfraWorks, and Python/Dynamo scripts (Figure 63) enables the **automation of the decision-making process**. This approach fundamentally transforms road management: rather than merely enduring the flood, accidents are prevented by relying on the **actual physics of the asset** [198].

In conclusion, optimizing an EWS through the **BIM-FRH coupling** offers an **"agile" resilience** solution. It enables the management of extreme events (e.g., millennial floods) without the need for massive structural reconstruction, while ensuring a **"zero-casualty" objective** through the precise mastery of organizational response times.

8.4 Sustainable Strategy: A Proof-of-Concept Study of the "Sponge City" (Rouiba Case Study)

While civil engineering interventions address flood symptoms at the infrastructure level, a comprehensive sustainability strategy mandates targeting the very **genesis of the risk**. The traditional "Grey Infrastructure" approach (dikes, concrete channels) relies on the rapid evacuation of water. However, the intensification of extreme rainfall events frequently overwhelms these networks, exacerbating urban flooding and paralyzing road connectivity [14].

In response, the **"Sponge City"** concept proposes a paradigm shift: transforming the urban fabric to absorb, store, and infiltrate water at its source. This study aims to demonstrate, through numerical modelling, that the integration of **Nature-Based Solutions (NBS)** constitutes an effective, resilient, and low-carbon mitigation alternative.

8.4.1 Methodology: Urban Hydrological Modelling (SWMM)

To validate this approach within the Algerian context, a modelling study was conducted for the city of **Rouiba** (East Mitidja), a dense and highly vulnerable urban area.

The experimental protocol **(Fig. 8.5)**, presented at the **CCRTI 2025 conference**, is based on an **EPA SWMM** hydrological simulation of two distinct scenarios for a **10-year design storm** (50 mm over 10 hours):

- **Grey Scenario (Baseline):** Conventional drainage network (high imperviousness, concrete conduits).
- **Green Scenario (Sponge City):** Integration of **Low Impact Development (LID)** techniques: green roofs, rain gardens, and infiltration trenches [59].

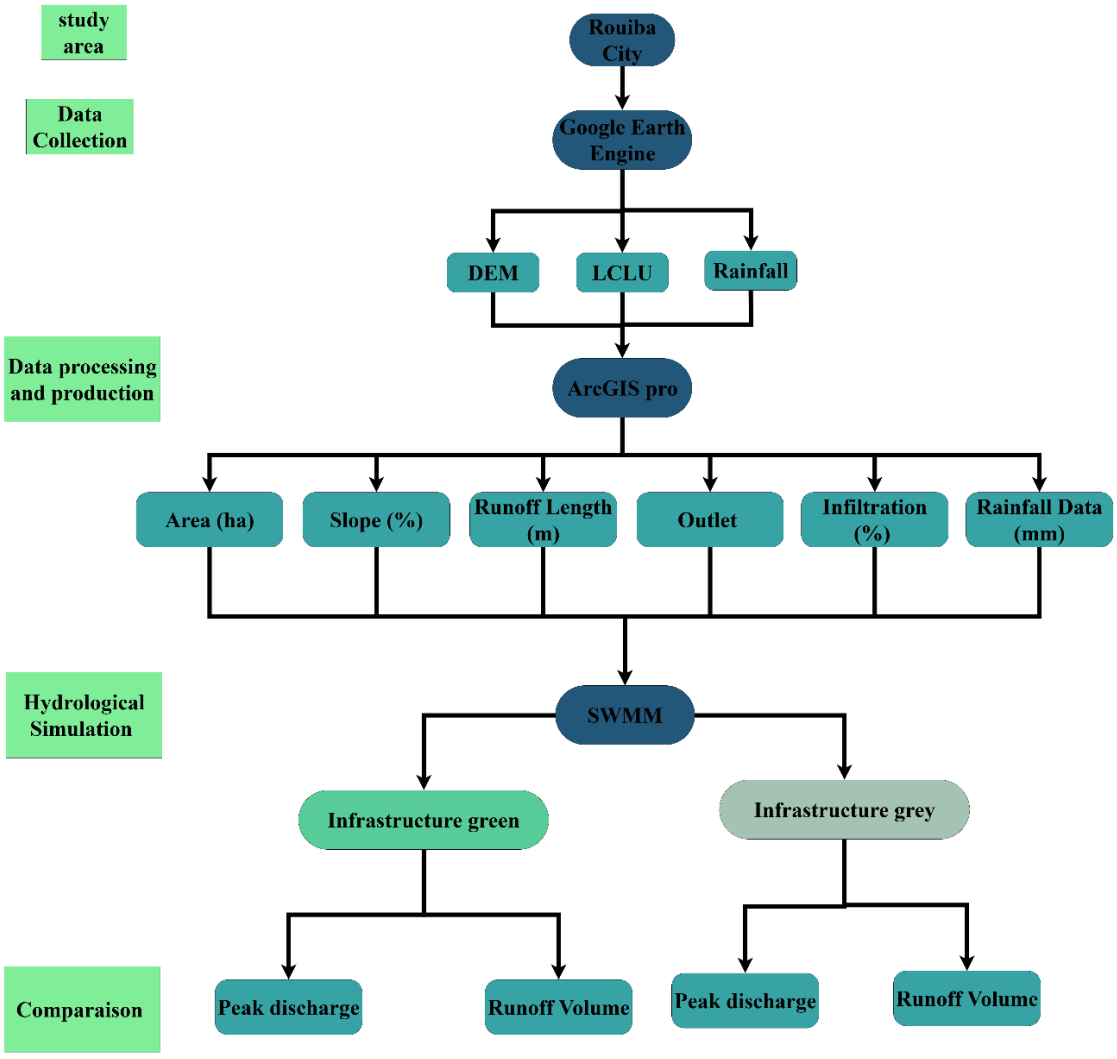


Figure 8.5. Methodology steps.

8.4.2 Geospatial Characterization: Urban Vulnerability Diagnosis

Prior to the modelling phase, a multi-criteria spatial analysis was performed to decipher Rouiba's complex hydrological dynamics and identify opportunity zones for green infrastructure.

8.4.2.1 Morphology and Flow Dynamics

The Elevation **DEM (Fig. 8.6)** and Slope **(Fig. 8.7)** maps reveal the site's general morphology and potential runoff velocity gradients. The addition of a **Curvature map (Fig. 8.8)** refines this diagnosis: it identifies **concave areas** where water naturally tends to converge and accumulate, as well as **convex areas** where it accelerates. This data is fundamental for positioning rain gardens and **bioretention cells** where the terrain already favours flow concentration.

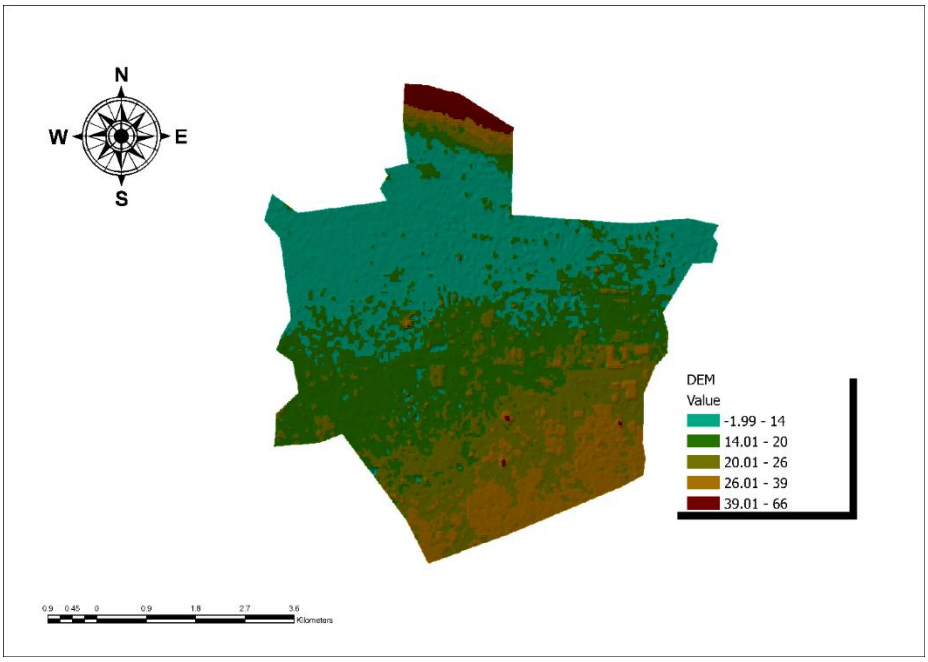


Figure 8.6. Dem of Rouiba city

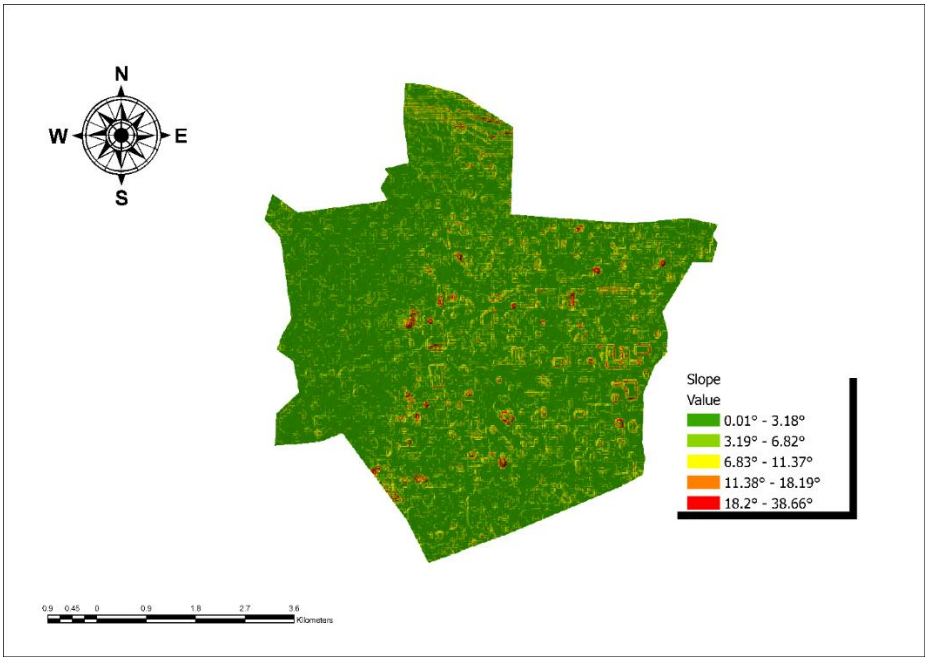


Figure 8.7. Slope of Rouiba city.

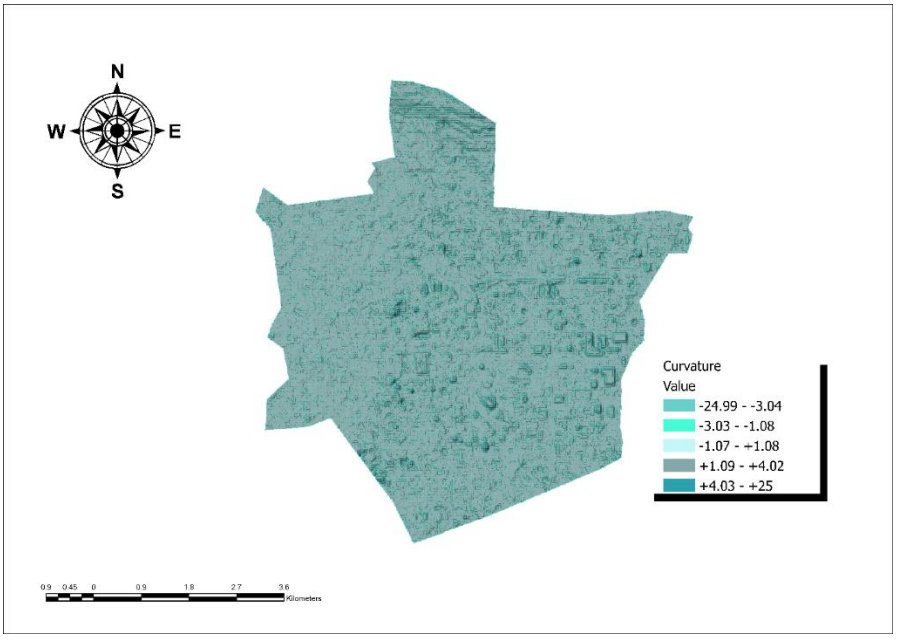


Figure 8.8. Curvature of Rouiba city.

8.4.2.2 Flow Accumulation and Urban Thalwegs

The flow accumulation **(Fig 8.9)** map is particularly instructive. By simulating water pathways across the topography, it identifies natural drainage axes, or **"urban thalwegs."** These concentration vectors are the critical points where the existing sewage network is most strained and where LID implementation will have the most significant impact on **peak flow reduction**.

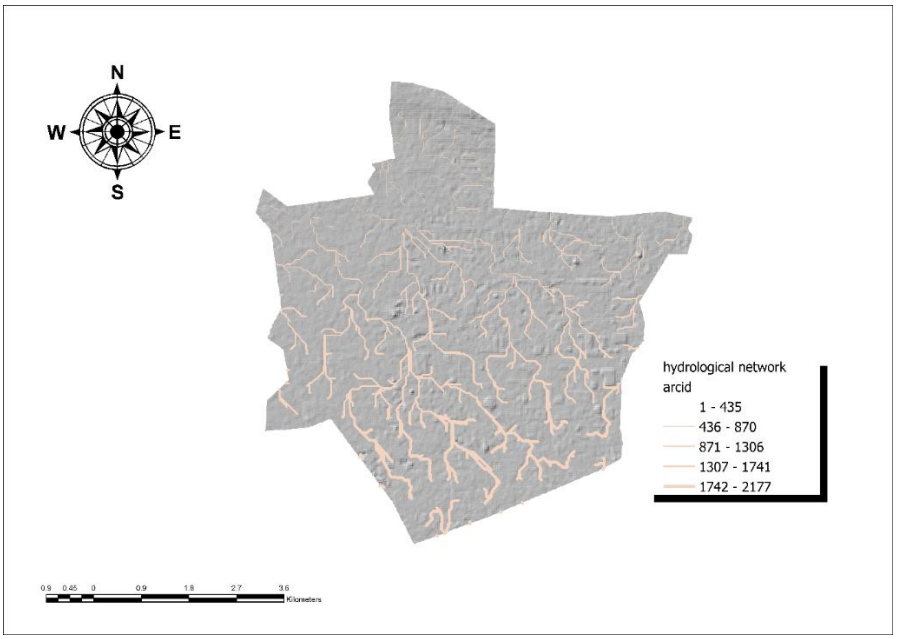


Figure 8.9. Flow accumulation of Rouiba city.

8.4.2.3 Imperviousness and Infiltration

The infiltration map **(Fig 8.10)**, derived from land-use data, highlights the fragmentation of the urban fabric. The extensive purple zones (**infiltration coefficient** ≈ 0) correspond to dense built-up areas and road networks. These **"sealed surfaces"** generate critical runoff. The contrast between high accumulation zones and zero-infiltration zones underscores the imperative need for **de-paving** (impervious surface reduction) to restore the natural water cycle.

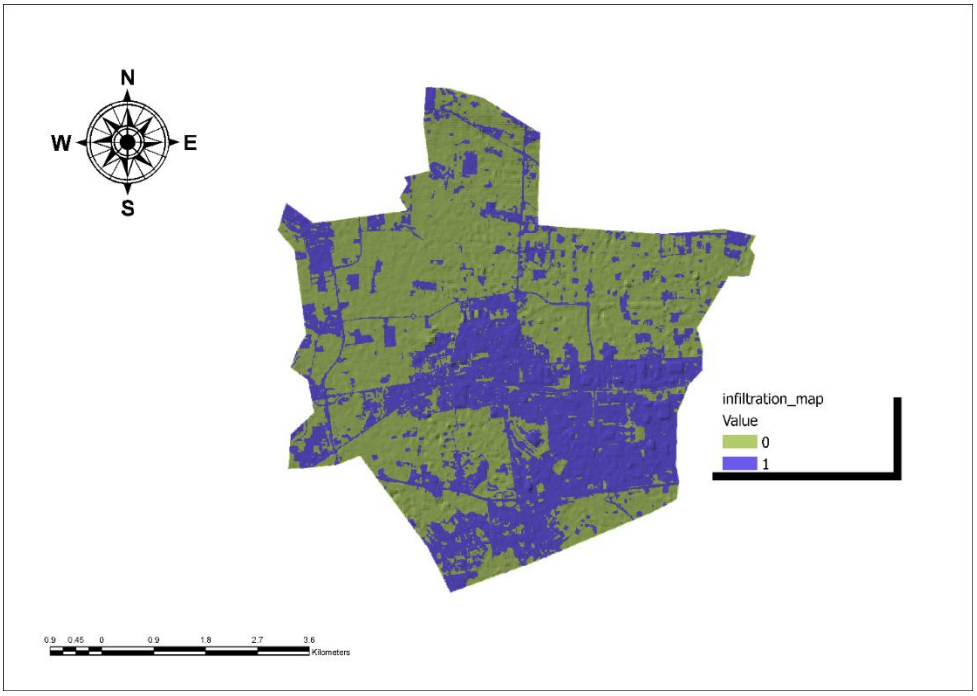


Figure 8.10. Infiltration of Rouiba city.

8.4.2.4 Selection of Target Sub-catchments

Based on this cross-diagnostic (steep slopes + concave curvature + high accumulation + zero infiltration), two sub-catchments (**S1 and S2**) **(Fig 8.11)** were isolated. They represent the **"worst-case" hydrological scenario**, serving as priority zones for this demonstrative study.

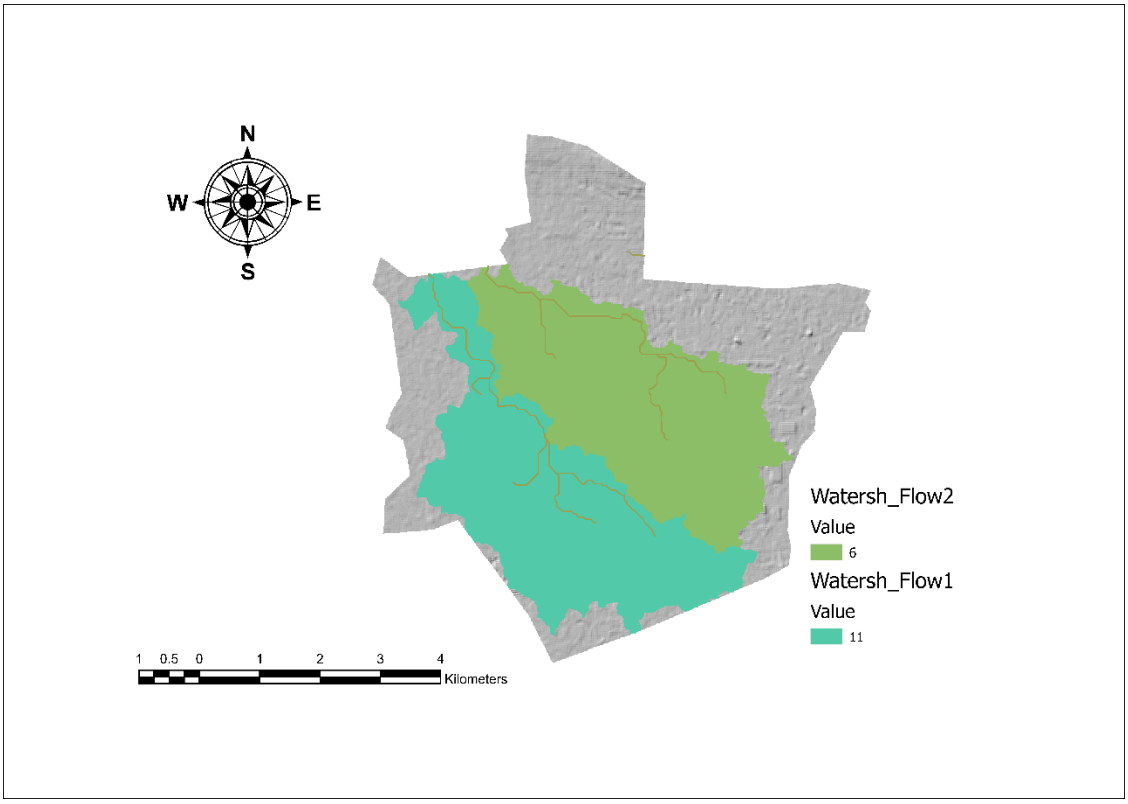


Figure 8.11. Selected sub-catchments.

8.4.3 Results: A Radical Transformation of Hydrological Response

The simulation results, synthesized in **Table 8.1** and the comparative charts **(Fig 8.12, 8.13, 8.14)**, demonstrate the **remarkable effectiveness** of nature-based solutions.

Table 8.1. Comparative analysis of hydrological indicators (Conventional "Grey" Scenario vs. "Green" Strategy).

Sub-catchment	Development Scenario	Total Precip. (mm)	Runoff (mm)	Volume Reduction	Infiltration (mm)	Peak Flow (m^3/s)	Peak Reduction	Runoff Coeff. (C_r)
S1	**Grey** (Conventional)	50.0	44.2		6.1	0.083		0.884
	Green (Sponge City)	50.0	20.3	**- 54 %**	29.7	~ 0.000	**- 100 %**	0.406
S2	**Grey** (Conventional)	50.3	45.5		4.8	0.070		0.908
	Green (Sponge City)	50.3	25.9	**- 43 %**	23.9	~ 0.000	**- 100 %**	0.518

- **Runoff Volume Reduction (Fig 8.12):** The integration of green infrastructure reduces the discharged water volume by **54%** for catchment S1 and **43%** for S2. Water is trapped at the source instead of overwhelming the streets.

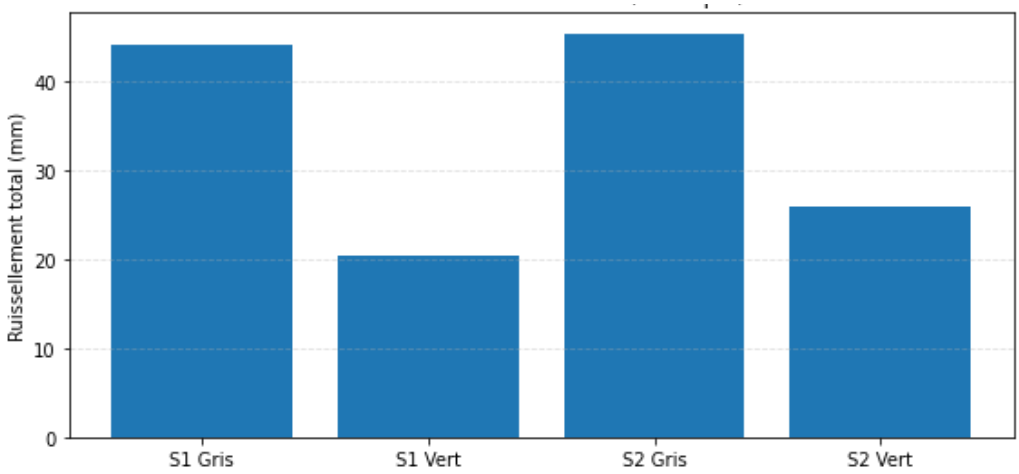


Figure 8.12. Runoff graph - Grey vs Green

- **Peak Flow Attenuation (Fig 8.13):** This is the most critical result for safety. While the Grey scenario generates a sharp peak discharge ($0.083 m^3/s$ for S1), the green scenario achieves a **100% reduction in direct runoff peak flow**.

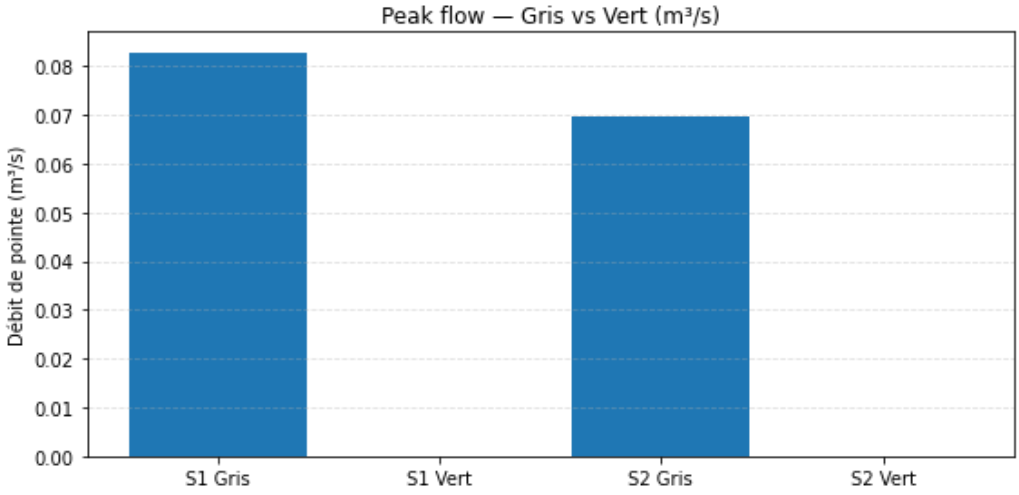


Figure 8.13. Peak Flow- Grey vs Green.

- **Hydrograph Analysis (Fig 8.14):** The temporal comparison of discharges is striking. The "Grey" hydrograph shows a violent, immediate, and **"flashy"** peak, typical of sudden urban flooding. In contrast, the "Green" hydrograph is **flat** ($Q \approx 0$). The water is entirely stored and infiltrated, transforming a **reactive system** into an **absorbent** one

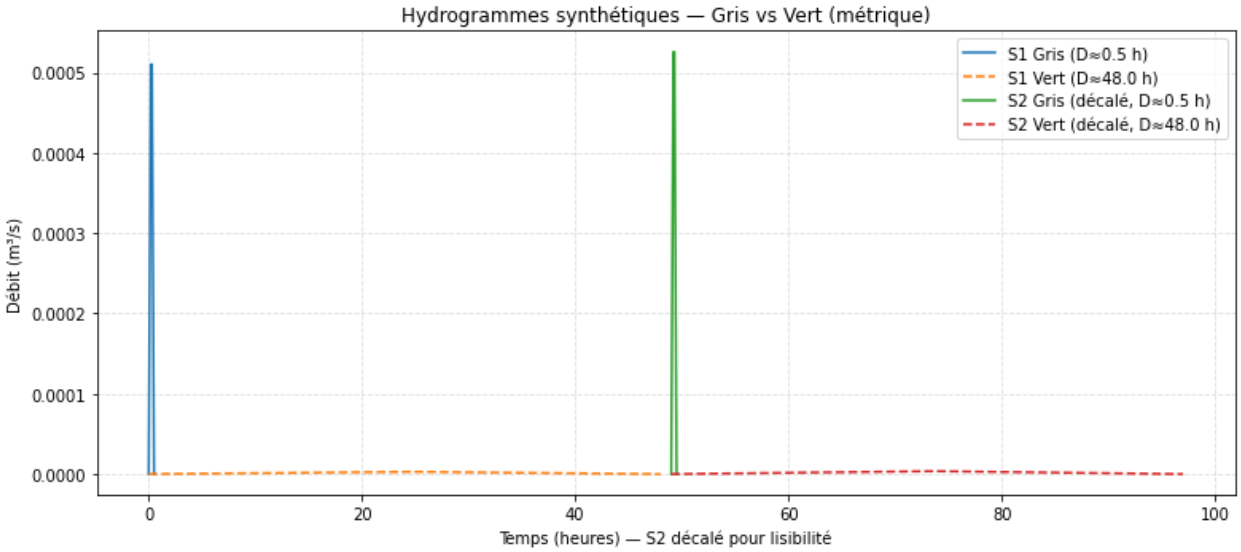


Figure 8.14. Synthetic Hydrographs - Grey vs Green

8.4.4 Discussion: Proof of Concept for the Mitidja

The attainment of a **"flat hydrograph"** constitutes tangible proof of this strategy's success. By substituting a **"flashy" hydrological response** (characterized by rapid and reactive water rise) with an **"absorbent" (resilient) response**, green infrastructure provides effective upstream protection for the road network. This approach prevents the formation of the critical **water sheets** that typically paralyze traffic. The study validates the technical feasibility and the significant hydrological value of integrating NBS into the urban planning of the Mitidja, offering a viable alternative to relieve chronically undersized drainage networks.

Beyond hydraulic performance, this demonstration establishes the Sponge City as a **source-control mitigation solution**. By managing runoff before it reaches pivotal nodes, it secures the road network without requiring heavy civil engineering works, such as bridge reconstruction or expensive pavement elevation.

Furthermore, this approach aligns with **decarbonization and sustainability goals**, focusing on three key pillars:

a) **Reduction of the "Grey Footprint":** Decreasing the reliance on concrete and heavy infrastructure (pipes, collectors) for water management.

b) **Carbon Sequestration:** Urban revegetation acts as a **carbon sink** while mitigating the **Urban Heat Island (UHI)** effect.

c) **Adaptive Flexibility:** It provides a resilient and modular response to the increasing uncertainty of climate scenarios [195].

The Rouiba case study confirms the strategic importance of integrating nature-based solutions into Algerian territorial planning. By transitioning from reactive management to an **absorbent city model**, it becomes possible to sustainably relieve drainage systems while

ensuring the **operational availability** of the road network, even under extreme weather conditions.

8.5 Synthesis of Strategic Levers: Navigating between Minimization and Coexistence

The multiplicity of terms (prevention, protection, adaptation, and mitigation) reflects the inherent complexity of risk management. To clarify our resilience strategy, these measures are categorized based on their primary objective within the **Hazard-Infrastructure interaction**.

8.5.1 Mitigation Logic (Attenuation and Minimization)

Mitigation encompasses actions aimed at reducing the overall magnitude of the risk. It is structured around two distinct levers:

- **Prevention (Source-Level Control):** Exemplified by the **Sponge City** approach. The goal is to "prevent" flooding upstream by mitigating **runoff generation**. This represents a sustainable, low-carbon mitigation strategy.
- **Protection (Exposure-Level Control):** Exemplified by **road elevation** or **levee construction**. The goal is to safeguard the infrastructure by physically preventing any contact with floodwaters. This is a physical and often **rigid** form of mitigation.

8.5.2 Adaptation Logic (Coexistence and Resilience)

Adaptation accepts the inevitable presence of the hazard and adjusts the system to ensure it is not compromised by the event.

- **Environmental Adaptation:** Exemplified by **riverbed recalibration**. Rather than attempting to suppress the flood, the terrain is modified to allow the water to flow without inducing **mechanical stress** on the road network.
- **Structural Adaptation:** Exemplified by **embankment hardening** and enhanced drainage systems. In this scenario, submersion is accepted, but the asset is engineered to be robust enough to **withstand the shock** and maintain its integrity.
- **Organizational Adaptation:** Exemplified by **Early Warning Systems (EWS)**. This involves adjusting road operations (e.g., proactive closures) to guarantee human safety when physical structural capacities are exceeded (**residual risk**).

8.6 Conclusion

Resilience as the Mastery of Time

This chapter concludes our demonstration by proposing a comprehensive spectrum of hybrid solutions. However, it is fundamental to recognize that neither prevention (reducing the hazard at its source) nor protection (isolating the asset) is sufficient to define resilience. These measures primarily ensure **robustness** of the static capacity of a system to withstand a predicted shock.

True **Resilience** is dynamic and resides in the mastery of **Recovery Time**. It does not consist of preventing floods at all costs (an often-futile quest in the face of increasing climatic extremes) but rather in ensuring that system dysfunction is as brief and as manageable as possible.

By adopting a vision of "**Collective Adaptive Capacity**," our strategy integrates three inseparable timeframes:

- **a) The Long-Term Perspective (Systemic Prevention):** Addressing the watershed scale through **Sponge City** concepts to mitigate future hydraulic pressure and restore natural hydrological cycles.
- **b) The Event-Duration Phase (Structural Protection):** Ensuring, through transparent drainage and reinforced embankments, that the infrastructure sustains no irreversible damage that would necessitate months of reconstruction.
- **c) The Crisis-Phase (Organizational Response):** Leveraging **FRH-optimized early warning systems** to save lives, manage the emergency in real-time, and facilitate the immediate reopening of routes as soon as floodwaters recede.

It is this ability to **compress downtime** that transforms a vulnerable road network into a truly resilient system. By articulating the digital intelligence of **BIM-HDM** with the sustainability of nature-based solutions, we transition from an **engineering of resistance** toward an **engineering of survival and continuity**.

PART V:

FUTURE PROSPECTS AND RECOMMENDATIONS

9 Perspectives and Future Outlook

9.1 Introduction

Initiating a New Paradigm

Scientific perfection is an asymptote: an ever-receding horizon that researchers pursue without ever claiming to reach. Consequently, this research does not pretend to be a definitive answer to the systemic complexity of hydrological risks; rather, it serves as a necessary initiation into a new frontier of road engineering. Faced with the collapse of the stationarity paradigm [23] , the static and deterministic models inherited from the previous century are reaching their operational limits. This thesis has laid the groundwork for an **epistemological transition**: shifting from an **engineering of certainty** (based on absolute control) toward a **dynamic mastery of uncertainty** (based on resilience).

While our BIM-HDM framework has successfully bridged the **"scale gap"** to quantify functional vulnerability (specifically network operational availability) with unprecedented precision, it simultaneously unlocks a vast field of further investigation. We have proven that diagnostic error can be significantly reduced; however, achieving comprehensive resilience now mandates moving beyond geometry to embrace physical, temporal, and computational complexity. This chapter explores priority research perspectives, structured around four evolutionary axes toward what we define as **Resilience Engineering 4.0**:

Section 9.2: From Clear Water to Complex Media Physics (Rheological Evolution). Our current diagnostics focus on Newtonian fluids. The immediate perspective is to integrate **non-Newtonian constitutive laws** to model the mechanical impact of **debris flows**, effectively transforming the FRH from a simple depth measure into a **ballistic pressure indicator** [70].

Section 9.3: From Static Diagnostics to Cognitive Digital Twins (Temporal Evolution). The transition from "snapshot" simulations to real-time management represents the next technological leap. This involves coupling BIM with **IoT data streams**, enabling the infrastructure to autonomously anticipate and react to imminent threats.

Section 9.4: AI as a "Surrogate Model" for Real-Time Analysis (Computational Evolution). To mitigate the high computational overhead of high-fidelity numerical simulations, **Artificial Intelligence (Deep Learning)** offers a disruptive path forward. These **surrogate models** (or metamodels) could deliver BIM-HDM-level precision at near-instantaneous speeds a *sine qua non* for widespread, large-scale early warning systems.

Section 9.5: Toward Multi-Hazard and Structural Resilience (Systemic Evolution). This thesis intentionally focused on functional vulnerability. The goal is to extend this framework to **physical vulnerability** (**Structural Health Monitoring**) and transform the BIM model into a **holistic health record** capable of managing compound stressors (floods, earthquakes, landslides), thereby ensuring the longevity of the national road asset portfolio.

By pragmatically acknowledging the limitations of this work, we pave the way for an engineering approach that no longer merely endures a crisis but master's it through **data intelligence**.

9.2 From Clear Water to Complex Media Physics: The Rheological Evolution

One of the primary findings from the territorial diagnosis conducted in Chapter 5 was the identification of a **hybrid morpho-dynamic hazard** within the Chiffa catchment. The modelling of debris flows is subject to a constant trade-off between physical precision and operational feasibility.

9.2.1 Rationale for the Approach Inherited from Chapter 6

Given the intrinsic complexity of mathematical and physical models(which demand in-situ rheological data often unavailable (**Data Scarcity**) and entail prohibitive computational costs at large scales(Chapter 6 prioritized a **GIS-based morphometric approach**[13], [189]. This method facilitated an efficient "scanning" of the catchment to identify initiation zones and propagation corridors with an optimal **cost-effectiveness ratio**.

9.2.2 The Research Gap: From Form (GIS) to Force (Numerical Simulation)

However, this index-based approach possesses a structural limitation: it remains **"blind"** to the internal physical processes of the flow. While GIS identifies *where* a debris flow is likely to occur, it fails to quantify the **dynamic interaction** with the engineering structure.

- **The Technological Leap:** The research outlook now focuses on transitioning from GIS-based models (simplified and regional) toward integrated **numerical and physical simulation models** within the BIM-HDM framework.
- **Transcending Saint-Venant:** Current submersion models (Chapter 6) rely on the Newtonian fluid assumption (clear water). Yet, for debris flows where volumetric sediment concentration exceeds the critical threshold ($C_v > 47\%$), classical hydraulic laws are invalidated.

9.2.3 Future Perspective: Impact Engineering for Infrastructure

The next stage involves injecting **non-Newtonian constitutive laws** (e.g., Bingham, Herschel-Bulkley) directly into the BIM-coupled simulation engine. The objective is to leverage the capabilities of advanced numerical simulation models to:

a) **Quantify physical impact:** Shifting from a simple depth measurement (FRH) to a **ballistic impact pressure** measurement (expressed in **kPa**) exerted on bridge piers or retaining walls.

b) **Simulate sedimentation and obstruction:** Predicting deposition volumes at culverts to anticipate **clogging**, a major shortcoming of current GIS-centric models.

c) **Support structural design trade-offs:** Utilizing the **semantic richness** of BIM (mechanical material properties) to test the structural survival of assets when subjected to the thrust of hyper-concentrated sediment flows.

In conclusion, moving toward **Resilience Engineering 4.0** requires transforming our framework from a functional diagnostic tool into a true **dynamic geotechnical laboratory**. This evolution will finally bridge the divide between territorial planning (GIS) and high-precision engineering design (BIM), providing a robust response to the most destructive hazards in high-relief areas [70]**.**

9.3 From Static Diagnostics to Cognitive Digital Twins: The Temporal Evolution

The approach developed in this thesis provides a **high-fidelity diagnostic snapshot**: it enables the precise simulation of infrastructure behaviour under specific hydraulic stresses at a given moment in time (T). However, resilience(as defined by "**Collective Adaptive Capacity**" [28](is not a static property but a dynamic process of uncertainty management. Faced with flash floods whose kinetics are increasingly unpredictable, the transition from simulation to real-time operational management represents the next critical technological leap.

9.3.1 From BIM to the Digital Twin

The first disruptive perspective involves evolving our BIM-HDM model from a design tool into a dynamic **Digital Twin**. Unlike a static digital representation, a digital twin is a **cyber-physical system** maintained in constant synchronization with field reality.

- **The IoT "Nervous System":** Instrumenting the Chiffa Gorges and the Mitidja Plain with a network of intelligent sensors (**Internet of Things - IoT**)(including radar stage sensors, connected rain gauges, and **embankment saturation sensors**) would provide the framework with continuous data streams.
- **Semantic Data Integration:** The challenge lies in semantically linking these field data to the BIM object structure, effectively transforming every road component into a **live data point**.

9.3.2 From Proactive Response to "Cognitive" Infrastructure

The goal of this evolution is to endow infrastructure with its own intelligence, capable of processing information to anticipate a crisis before it physically manifests on the roadway.

- **The Critical Anticipation Window ($T + 30$ min):** By coupling short-term meteorological models (**Nowcasting**) with our FRH indicator, the system would no longer merely diagnose the current state but predict the road's condition over a 30-minute horizon. This specific window represents the **optimal trade-off for operational resilience**. According to [199], a 30-minute **lead time** provides the necessary notice to automate safety procedures while minimizing the uncertainty inherent in the violent kinetics of flash floods, where response times in Mediterranean catchments are often under one hour [200].
- **Autonomous Decision-Making:** This perspective paves the way for the **cognitive management** of the network. As soon as the Digital Twin predicts a future violation of the critical FRH threshold, it can autonomously direct the safety protocols for the segment: triggering automated barriers, instantaneously updating **Variable Message Signs (VMS)**, and sending direct notifications to **connected vehicles** traveling on the RN1. In this way, the infrastructure transitions from "enduring" the hazard to "directing" avoidance.

9.3.3 Radical Reduction of Recovery Time

This mastery of time is the most powerful lever for resilience. By anticipating submersion by 30 minutes, the risk of trapped vehicles is nullified, and emergency response deployment is optimized. In the post-flood phase, the Digital Twin would facilitate an immediate **Structural Health Monitoring (SHM)** diagnosis by comparing the load data recorded during the event with the mechanical properties stored in the BIM. This would drastically reduce the time required to safely reopen this strategic corridor.

In conclusion, the transition toward a **Cognitive Digital Twin** marks the advent of **Resilience Engineering 4.0**. It transforms passive road infrastructure into an intelligent territorial actor, capable of learning from its environment and dynamically adjusting its functional response to **climatic non-stationarity** [110].

9.4 AI as a "Surrogate Model" for Real-Time Analysis: Computational Evolution

High-fidelity diagnostics through the BIM-HDM framework, while surgically precise, inevitably encounter a **"computational wall."** Numerically solving Saint-Venant or Navier-Stokes equations on complex topographic meshes derived from BIM requires massive computational resources and processing times that are incompatible with the urgency of real-time alerts. To transform our diagnostic model into an operational emergency tool, the evolution toward **Artificial Intelligence (AI)** acting as a **Surrogate Model** (or Metamodel) represents a major technological breakthrough.

9.4.1 AI as an Accelerator: Shifting from Offline Simulation to Real-Time Inference

The research outlook focuses on leveraging **Deep Learning** algorithms (specifically **Long Short-Term Memory (LSTM)** recurrent networks or **Graph Neural Networks (GNNs)**) to "learn" the site's hydraulic behaviour.

- **Training Strategy:** By using thousands of pre-calculated BIM-HDM simulations (conducted in **offline mode**) as a training dataset, the AI constructs a statistical mapping of the system's responses.
- **Instantaneous Inference:** Once trained, the surrogate model becomes capable of predicting the **FRH indicator** within milliseconds (**online mode**), whereas the physical model would have required several hours of computation.

9.4.2 The Nature of AI: A Predictive "Black Box"

In the interest of scientific rigor, it is imperative to clarify that AI cannot replace fundamental physics.

- **Correlation vs. Causality:** AI acts as a **"black box"**; it identifies statistical correlations between inputs (discharge, rainfall) and outputs (FRH) without "understanding" the governing laws of mass or energy conservation. By nature, it cannot replicate the inherent rigor of differential equations.
- **BIM-HDM as the "Teacher":** In our vision, AI does not substitute for the physical model; instead, it serves as its rapid **proxy**. The BIM-HDM framework remains the guarantor of physical truth, used to generate **ground truth** training data and to periodically validate AI predictions to prevent any **statistical drift** [77].

9.4.3 Toward "Physics-Informed Machine Learning" (PINN)

The ultimate horizon of this research axis is the integration of physics directly into the AI architecture via **Physics-Informed Neural Networks (PINNs)**.

- **The Objective:** To constrain the AI's learning process with fluid mechanics equations, thereby mitigating the "black box" effect.

- **The Contribution:** This hybridization would yield a surrogate model that is simultaneously ultra-fast (AI) and **physically consistent** (HDM). Such an advancement would provide RN1 managers with a tool capable of simulating submersion scenarios **"on-the-fly,"** enabling instantaneous decision-making during the most volatile climatic crises [95].

9.5 Toward Multi-Hazard and Structural Resilience: The Systemic Evolution

While this thesis has specifically focused on **functional vulnerability** (defined by the infrastructure's capacity to maintain operational service during a hazard) the validation of the **FRH indicator** represents only the first tier of resilience: the prediction of network disruption. However, achieving comprehensive resilience necessitates a transition from analysing **unavailability** to analysing **structural integrity**. The systemic evolution of our framework must now embrace two critical dimensions: structural health and hazard interaction.

9.5.1 From Unavailability to Failure: Structural Vulnerability

The immediate research outlook involves converting the hydraulic outputs of the BIM-HDM framework into **mechanical loading inputs** for structural engineering. BIM must no longer be perceived merely as a geometric envelope, but as a comprehensive **resistance database**.

- **Fluid-Structure Interaction (FSI):** By injecting velocity vectors (V_s) and water depths (H_s) from the simulation into **Finite Element Analysis (FEA)** models, it becomes possible to calculate the actual mechanical stresses exerted on assets.
- **Bridge Scour and Structural Stability:** A major challenge for the RN1 corridor concerns **bridge scour**. The integrated framework would enable the prediction of erosion depth at pier foundations as a function of localized flow turbulence.
- **Pavement Structure Degradation:** Beyond surface submersion, the prolonged soaking of base layers alters their **bearing capacity** (resulting in a drop in the **CBR index**). Integrating geotechnical properties into the BIM environment would allow for the simulation of **punching shear** or irreversible **rutting** risks during the passage of emergency convoys, thereby ensuring the post-flood durability of the road.

9.5.2 The Road as a Multi-Hazard System

In a geographical context such as the Blidean Atlas, flooding rarely occurs in isolation. Infrastructure is subjected to coupled aggressions that demand a **multi-hazard approach**.

- **Cascading Effects:** Intense precipitation that saturates soils often triggers simultaneous landslides or rockfalls alongside wadi flooding. An embankment weakened by an erosive flood (hydraulic hazard) will exhibit heightened vulnerability when confronted with a seismic event (telluric hazard).
- **The Total Vulnerability Matrix:** The long-term vision is to utilize BIM as a **"Digital Health Record,"** capable of centralizing the infrastructure's **fragility curves** across diverse hazards (flood, earthquake, landslide). This integrated model would enable an assessment of the overall resilience of the road corridor when faced with **compounded crisis scenarios**.

9.5.3 The Final Horizon: Resilient Asset Management

The culmination of this systemic evolution lies in the full integration of resilience into **Infrastructure Asset Management**.

- **Optimized Retrofitting:** Rather than uniform network reinforcement, managers (e.g., DTP, Ministries) could leverage this framework to target **retrofitting interventions** on specific components whose physical failure would lead to a total collapse of national connectivity.
- **Sovereignty and Longevity:** This vision transforms infrastructure into a system capable of enduring climatic lifecycles while minimizing not only repair costs but also the environmental impact associated with massive reconstruction projects.

In conclusion, the transition from functional vulnerability to **structural and multi-hazard resilience** marks the maturity of **Resilience Engineering 4.0**. The goal is to ensure that, even under the combined assault of natural elements, the vital lifeline of the **RN1** maintains its physical integrity, thereby securing the safety and socio-economic development of the territories it sustains.

9.6 Conclusion

Resilience as a Horizon

In conclusion, the perspectives outlined in this chapter reflect a fundamental reality: the completion of this research does not represent a conclusion, but rather an anchor point for a broader technological and societal ambition. We have established the foundations of what we define as **Resilience Engineering 4.0**.

We have demonstrated that the convergence of **BIM's semantic knowledge** and **HDM's simulation power** enable a drastic reduction in diagnostic error, transforming uncertainty into **actionable data**. However, the future of our critical infrastructure now depends on our ability to integrate these tools into a **dynamic lifecycle**:

a) By embracing the physics of complex media to anticipate the **brutal force of debris flows**.

b) By evolving static models into **cognitive Digital Twins** synchronized via **IoT**.

c) By leveraging **Artificial Intelligence** as a **computational accelerator** for real-time early warning systems.

d) And finally, by adopting a **systemic, multi-hazard vision** to safeguard the physical integrity of the structure itself.

The stakes transcend the purely technical sphere. It is a matter of transforming infrastructure so that it is no longer a passive victim of **climatic non-stationarity**, but rather a resilient system capable of learning from its environment, anticipating shocks, and recovering with **agility**. This definitive transition from **"management by fear"** to the **"mastery of time"** represents the only path toward ensuring the sustainability and **sovereignty** of our transport networks in the face of the global challenges of the decades to come.

10 Recommendations for Integrated Risk Management on the Mitidja Road Network

10.1 Introduction

Bridging the Gap between Scientific Knowledge and Public Action

The ultimate value of doctoral research in civil engineering lies in its capacity to translate a complex scientific diagnosis into an operational lever for action. The investigations conducted throughout this work converge toward an undeniable conclusion: the safety of the road network against hydrological extremes can no longer rely on isolated or reactive solutions. This chapter translates our technological advancements into a prioritized and adaptive strategic roadmap, aiming to guarantee service continuity within the context of the global climate crisis.

The imperative to provide recommendations stems from a granular understanding of the **"risk production process"** (the *fabrique du risque*) within the Mitidja region. Our research has revealed that flooding here is the product of a fatal convergence between a **topographic trap** (stagnation due to slopes < 0.5%), **hydrological forcing** (rapid saturation of clayey soils), and **anthropogenic exacerbation** (massive urban runoff). To break this cycle, resilience must become a **"Collective Adaptive Capacity"** [28], applied with equal rigor to legacy assets currently in service(which are often geometrically constrained(as well as to the design of future projects.

This chapter is structured around four fundamental decision-making pillars:

Section 10.2: Methodological Synthesis (The Integrated Risk Equation). We propose the theoretical framework that must henceforth govern project evaluation. By positioning resilience as a divisor of vulnerability, we offer an optimal methodology for developing nations, prioritizing data efficiency and resource optimization.

Section 10.3: Decision-Making Synthesis (The Multi-Scale Diagnosis as a Compass). This section demonstrates how **BIM-HDM coupling** resolves the **"scale gap."** We define the **FRH indicator** as the new benchmark for prioritizing investments and transitioning from reactive maintenance to predictive asset management.

Section 10.4: Prioritized Action Plan (From Emergency to Sustainability). We detail a strategy across three horizons (Short, Medium, and Long-term). This plan distinguishes between the "coexistence" actions required for legacy structures (Early Warning Systems, Retrofitting) and systemic prevention actions for future land-use planning (Sponge City).

Section 10.5: Future Vision (The Geospatial Digital Twin). We conclude by advocating for a transition toward **Engineering 4.0**, where a national management platform would enable real-time simulation of the resilience of the country's vital lifelines.

By articulating these levers, we transition from "failure management" toward the **mastery of recovery time**, the only viable path to ensure economic sovereignty and citizen safety in the face of **climatic non-stationarity**.

10.2 Methodological Synthesis: The Integrated Risk Equation (Conceptual Model)

The primary recommendation of this research is paradigmatic: we advocate for the replacement of binary assessment methods (flood-prone vs. non-flood-prone) with an integrated, multidimensional approach. As suggested by [201], risk management must pivot away from hazard control toward vulnerability reduction. In light of the collapse of the climatic stationarity paradigm [23], the evaluation of road projects must henceforth incorporate the dynamics of recovery and service restoration.

10.2.1 Formalizing the Resilience Framework

Drawing upon established dynamic vulnerability frameworks [50], [202], we propose formalizing **Risk (**R**)** not as a static inevitability, but as a systemic equilibrium. The innovative conceptual model submitted for infrastructure management is as follows:

$$R(Zone,t) = E(Zone) \times \sum_{Process} \left[\frac{H_{Non-Stat}(H_s,V_s) \times \sum V_i}{A_{Collective}(t)}\right] + R_{Residual}$$

10.2.2 Resilience (A) as a Divisor: A Paradigm Shift

The core originality of this recommendation lies in positioning **Resilience (**A**)** in the denominator.

- **The Damping Effect:** Mathematically, resilience acts as a "damage reducer." The higher the **Collective Adaptive Capacity** [28] (through EWS, network redundancy, and crisis management(the more the final risk is minimized, even in the presence of a severe hazard.
- **Moving Beyond "Concrete-only" Solutions:** This approach corroborates the vision of [58] : it is often more efficient to invest in **organizational intelligence** (increasing A) than in rigid protection infrastructures whose failure would be catastrophic [3].

10.2.3 An Optimal Methodology for Data-Scarce Contexts

In developing nations where **Data Scarcity** represents a major bottleneck [157], this model offers superior strategic efficiency:

a) **Resource Optimization:** Instead of uniformly raising kilometres of embankments, this model enables the targeting of investments toward the **critical nodes** identified through high-fidelity diagnostics [194] .

b) **Data Efficiency through BIM:** By utilizing the BIM-HDM coupling as the primary source of geometric information, we mitigate the lack of precise global topographic surveys. We transition from an **engineering of over-design** toward an **engineering of precision** [39].

c) **Management of Residual Risk (R_{Res}):** By explicitly integrating this term, we align with the philosophy of [203]. The objective is no longer to promise absolute protection but to guarantee **functional durability**, an approach that is economically more viable for territories like the Mitidja Plain.

10.2.4 Operational Application across the Infrastructure Lifecycle

This equation constitutes the recommended **decision matrix** for each phase of the asset lifecycle [27] :

- **Design Phase:** To arbitrate between different alignment variants by minimizing the $H \times V$ product.
- **In-Service Phase:** To calibrate the alert thresholds of the Early Warning System (EWS) and maximize the resilience denominator (A) [29].

Methodological Conclusion: By adopting this theoretical framework, road engineering transitions from an era of passive resistance into one of **active resilience**. This model transforms flood management from a pure civil engineering problem into a challenge of **technological governance**.

10.3 Decision-Making Synthesis: The Multi-Scale Diagnosis as a Strategic Compass

The complexity of flood risk in territories like the Mitidja Plain mandates the use of a **"decision-making compass"** capable of navigating between broad territorial oversight and structural physical reality. This section outlines how the resolution of the **"Scale Gap"** through our BIM-HDM framework fundamentally transforms strategic decision-making.

10.3.1 Resolving the Scale Gap: An Operational Breakthrough

The state-of-the-art review conducted in Chapter 1 highlighted a critical deficiency: the compartmentalization between macro-territorial analysis (GIS) and microscopic asset engineering [6], [39].

- **Precision Diagnostics:** Where conventional models (**C-HDM**) based on coarse satellite DEMs fail to perceive infrastructure geometry (evidenced by a 71% error rate at KP 65.862), the BIM-HDM coupling re-integrates **"As-Built"** geometry into the fluid physics.
- **The GeoBIM Advantage:** This integration, as advocated by [135], enables the transition from indicative zoning to the actual measurement of physical interactions. This precision is the *sine qua non* for ending the practice of **"blind investment"** in oversized or poorly positioned protection structures.

10.3.2 The FRH Indicator: The New Benchmark for Assessment

We define the **Flooded Road Height (FRH)** indicator as the universal benchmark for managing road connectivity.

- **A Serviceability Criterion:** Unlike discharge (Q), which remains an abstract value for network operators, the FRH translates the hazard into a physical **Serviceability Limit State (SLS)** [101].
- **Prioritization of Interventions:** By mapping the FRH across a network, managers (e.g., DTP, Ministries) can now classify assets according to their criticality:

    a) **FRH < 15 cm:** Vigilance Zone (traffic maintained).

    b) **15 cm < FRH < 30 cm:** Alert Zone (risk of loss of traction).

    c) **FRH > 30 cm:** Functional Rupture Point (mandatory closure).

This approach facilitates the identification of **"Resilience Critical Nodes"** for funding priority, ensuring that every currency unit invested serves to minimize the overall network downtime [204] .

10.3.3 Toward Predictive and Proactive Asset Management

The culmination of this decision-making synthesis is the transition from **"reactive maintenance"** to **"predictive management"** of the infrastructure lifecycle [108].Historically, engineers repair what has failed (reactive logic). Through BIM-HDM, they can now:

- **Simulate Pre-Crisis Scenarios:** Identify segments that will fail during a future millennial flood, even if they have not experienced submersion in the past.
- **Optimize Retrofitting:** Select the most effective adaptation measure (e.g., embankment hardening or riverbed recalibration) regarding the FRH indicator before any physical work begins [194].
- **Structural Longevity:** Anticipate invisible damages(such as **pavement structure saturation**(that conventional models ignore, thereby preserving the nation's infrastructure capital in the face of climatic non-stationarity [15].

Section Conclusion: High-fidelity diagnostics are no longer an academic option but a governance imperative. By utilizing the FRH as a compass, decision-makers possess a scientific tool to steer the sovereignty of their transport networks, transforming a hydrological threat into a mastered and resilient risk.

10.4 Prioritized Action Plan: From Emergency Management to Long-term Sustainability

The resilience of a strategic road network (such as that of the Mitidja Plain) cannot result from isolated interventions; rather, it requires a sequenced strategy. We propose an action plan structured around three temporal horizons, distinguishing between the management of legacy assets (**coexistence logic**) and the planning of future projects (**systemic prevention logic**).

10.4.1 Short-Term Horizon: Crisis Control and User Safety

The immediate objective is not to modify the infrastructure but to adapt its operational management to eliminate life-safety risks at the identified hotspots (e.g., KP 65.862).

- **Deployment of Early Warning Systems (EWS):** Based on our Digital Twin architecture [194], instrument zones with critical FRH levels using **IoT sensors** (connected limnimeters).
- **Dynamic Traffic Management:** Automate diversion protocols via **Variable Message Signs (VMS)** once the 30 cm threshold is exceeded. As highlighted by [29], this **organizational resilience** guarantees a "zero-casualty" objective without requiring heavy engineering, by intelligently managing **lead times**.

10.4.2 Medium-Term Horizon: Structural Retrofitting and Managed Coexistence

The focus here is to enhance the physical robustness of existing structures to minimize **Recovery Time** following a shock [58].

- **Surgical Retrofitting:** Leverage BIM-HDM precision to target embankment reinforcements (anchors, shotcrete) exclusively where simulated velocities (V_s) threaten stability [16].
- **Enhancing Hydraulic Transparency:** Initiate a program for resizing discharge structures. Replacing obsolete culverts with large-scale **box culverts** eliminates the "dam effect" and reduces upstream hazard intensity [69].
- **Riverbed Recalibration:** Scale up the environmental adaptation approach (concave bank widening) validated for the Chiffa Wadi. This measure mechanically lowers the water surface profile without necessitating costly and carbon-intensive pavement reconstruction [96].

10.4.3 Long-Term Horizon: Systemic Prevention and Green Resilience

Sustainable resilience mandates addressing the very **genesis of the hazard** to relieve the downstream network. This marks the transition from **"grey" to "green" infrastructure**.

- **Scaling the "Sponge City" Concept:** Our study in Rouiba proved that source-level management via **Low Impact Development (LID)** techniques (e.g., rain gardens, bioswales) can eliminate 100% of the peak flow for a 10-year storm. We advocate for the integration of **Nature-Based Solutions (NBS)** into all new urban development plans within the Mitidja catchment [20].
- **Binding Urban Planning:** Utilize the susceptibility maps produced by our Macro/GIS approach to restrict urbanization within natural drainage corridors. By restoring the

hydrological cycle, the hydraulic loading on road assets is reduced, providing **passive and low-carbon protection** for the network [14], [195].

Summary: This prioritized plan demonstrates that resilience is a trajectory. By combining **digital responsiveness** (Alerts), **engineering precision** (BIM), and **environmental wisdom** (Sponge City), we offer the Mitidja region a comprehensive adaptation model capable of reconciling the protection of legacy assets with the sustainability of future developments.

10.5 Future Vision: The Geospatial Digital Twin and Resilience Engineering 4.0

The goal of the recommendations formulated in this research lies in a necessary transition toward what we define as **Resilience Engineering 4.0**. This technological shift represents a move beyond modelling solely for design purposes toward **digitization for operational governance**. The ultimate perspective advocated here is the transition from site-specific diagnostics to a national management platform based on the **Geospatial Digital Twin**.

10.5.1 Cyber-Physical Fusion: BIM, GIS, and IoT

The Geospatial Digital Twin represents the definitive integration of the technological triad explored in this thesis. Unlike static digital models, it constitutes a living **cyber-physical system**:

- **Data Intelligence:** By merging the structural fidelity of BIM with the territorial intelligence of GIS, the digital twin creates a high-fidelity replica of the road network.
- **Real-Time Synchronization:** Integrating **IoT data streams** (water level sensors, connected rain gauges, AI-powered cameras) allows the model to reflect the infrastructure's status at any given moment. As highlighted by [110], this connectivity transforms infrastructure from a passive asset into a **"cognitive" system** capable of diagnosing its own vulnerabilities and impending failures.

10.5.2 A National Platform for the Country's Vital Arteries

We recommend the establishment of a centralized resilience platform for Algeria's strategic corridors (e.g., RN1, East-West Highway, Trans-Saharan Highway). Such a tool would empower the Ministry of Public Works and Civil Protection to:

a) **Execute Climate Stress-Tests:** Virtually test network resilience against scenarios of millennial floods or complex debris flows, identifying failure points before they occur.
b) **Steer Crisis Management in Real-Time:** Visualize the **FRH indicator** across the entire national territory on a single dashboard, automating alerts and optimizing the deployment of emergency services [205].
c) **Guarantee Economic Sovereignty:** By protecting the **"critical nodes"** of national connectivity, the platform ensures the continuity of logistical flows, minimizing the massive economic losses associated with traffic disruptions on major axes [194].

10.5.3 Lifecycle Optimization and Sustainability

Beyond emergency response, the Digital Twin becomes the pivotal tool for **Infrastructure Asset Management**. It enables the optimization of preventive maintenance cycles and the prioritization of structural retrofitting investments based on the **real-world criticality** calculated by the model. This precision engineering not only reduces public expenditure but also limits the **carbon footprint** associated with the massive reconstruction projects that typically follow disasters.

Conclusion: The transition to Engineering 4.0 is no longer a technological option but a **governance imperative** in the face of climate uncertainty. By equipping Algeria with a Geospatial Digital Twin, we move from the passive management of vulnerability to the **proactive mastery of resilience**, transforming the data from this thesis into a permanent **technological shield** for the country's territories.

10.6 Conclusion

Ultimately, this chapter has effectively translated scientific diagnostics into an operational framework for risk management. By harmonizing technological innovation (specifically **BIM-HDM coupling**) with conceptual rigor through the **integrated risk equation**, we have demonstrated that the safety of the Mitidja's road network is no longer solely contingent upon material resistance, but rather on the agility of the system.

The primary breakthrough introduced herein lies in the transition from an engineering paradigm of **"absolute protection"**(which is often illusory in the face of climatic non-stationarity) toward a paradigm of **"active resilience."** The **FRH indicator** emerges as the cornerstone of this transition, providing managers with a precise **decision-making compass** for the prioritization of infrastructure investments. Whether implemented through emergency responses such as early warning systems, structural retrofitting, or the integration of **Sponge City** concepts, the proposed strategy offers a realistic and scalable roadmap. By paving the way for a **Geospatial Digital Twin**, this work provides more than just a technical solution; it initiates a fundamental paradigm shift: that of **"cognitive infrastructure"** capable of dynamic adaptation to ensure, always, both economic sovereignty and citizen safety.

11 GENERAL CONCLUSION

This thesis has addressed a major structural challenge for territories exposed to hydrological hazards: the precise, multi-scale assessment of road infrastructure vulnerability. Confronted with the limitations of conventional approaches (which are systematically siloed between large-scale territorial analysis and site-specific asset engineering) we have demonstrated that the synergetic alliance of **GIS and BIM technologies** successfully overcomes the **"Scale Gap"** to provide high-fidelity diagnostics.

Using the Mitidja Plain as a primary laboratory, this research has established a robust integrated methodology, transforming often fragmentary geospatial data into a tool for the **surgical management of resilience**. The results confirm the core hypothesis of our research: the articulation of the macroscopic vision of GIS with the microscopic precision of BIM is the *sine qua non* for proactive risk management.

11.1 Synthesis of Major Contributions

The culmination of this research trajectory has materialized through three disruptive scientific contributions:

a) **The Objectification of Territorial Susceptibility:** Beyond a conventional application of the AHP-GIS method, this work neutralized the subjectivity inherent in expert judgment through multi-scenario sensitivity analysis and cross-validation with **Machine Learning**. This approach enabled the isolation of the **"Hard Core"** of high-risk zones within the Mitidja, offering unprecedented reliability to territorial diagnostics.

b) **Resolving the Scale Conflict via the BIM-HDM Framework:** This represents the flagship contribution of this thesis. By substituting coarse DEMs with the **"As-Built"** digital model of the structure, we proved that geometric precision takes precedence over hydraulic complexity. The validation on the Chiffa case study is unequivocal: our framework reduced the water depth prediction error from **71% to a mere 3.8%**, establishing the **FRH (Flooded Road Height) indicator** as a reliable benchmark for civil security.

c) **Quantifying Green Resilience (Sponge City):** By translating the qualitative "Sponge City" concept into quantifiable benefits using **EPA SWMM**, we demonstrated that a source-control mitigation strategy enables the **total elimination (100%)** of the runoff peak for a 10-year design storm. This result validates a low-carbon resilience trajectory, safeguarding the road network without systematic reliance on heavy civil engineering.

11.2 Theoretical Synthesis: The Integrated Risk Model

The scope of this thesis transcends the technical framework to propose a new formalization of risk for critical infrastructure. Our collective findings converge toward the following synthetic equation:

$$R(Zone,t) = E(Zone) \times \sum_{Process} \left[\frac{H_{Non-Stat}(H_s, V_s) \times \sum V_i}{A_{Collective}(t)}\right] + R_{Residual}$$

This model establishes **Resilience (A)** as the priority lever for action: while hazard and exposure are often unavoidable, the **collective adaptive capacity** enables the drastic reduction of final risk by mastering **recovery time**.

11.3 Limitations and Perspectives

Any modelling endeavour involves limitations that warrant highlighting:

- **Data and Uncertainties:** Precision remains contingent upon the resolution of input data and the representativeness of historical records.
- **Physical Simplifications:** Our models rely on Newtonian fluid assumptions, which should be extended to the complex rheology's of **debris flows**.
- **Generalization:** While the framework is transferable, the quantitative parameters remain specific to the morpho-climatic context of the Mitidja Plain.

In summary, this doctoral work has laid the groundwork for **Resilience Engineering 4.0**. By transitioning from the reactive management of failure to the **predictive mastery of service continuity**, we provide infrastructure managers with a roadmap to transform vulnerable assets into systems capable of coexisting with the climatic extremes of tomorrow.

References

[1] A. Díez-Herrero and J. Garrote, “Flood risk analysis and assessment, applications and uncertainties: a bibliometric review,” *Water*, vol. 12, no. 7, p. 2050, Jul. 2020, doi: 10.3390/w12072050.

[2] F. Dottori *et al.*, “Increased human and economic losses from river flooding with anthropogenic warming,” *Nat. Clim. Change*, vol. 8, no. 9, pp. 781–786, Sep. 2018, doi: 10.1038/s41558-018-0257-z.

[3] S. Jonkman, “Global Perspectives on Loss of Human Life Caused by Floods,” *Nat. Hazards*, vol. 34, pp. 151–175, 2005, doi: 10.1007/S11069-004-8891-3.

[4] E. E. Koks *et al.*, “A global multi-hazard risk analysis of road and railway infrastructure assets,” *Nat. Commun.*, vol. 10, no. 1, p. 2677, Jun. 2019, doi: 10.1038/s41467-019-10442-3.

[5] S. Setunge, “Vulnerability of Road Bridge Infrastructure”.

[6] A. Rebally, C. Valeo, J. He, and S. Saidi, “Flood Impact Assessments on Transportation Networks: A Review of Methods and Associated Temporal and Spatial Scales,” *Front. Sustain. Cities*, vol. 3, p. 732181, Sep. 2021, doi: 10.3389/frsc.2021.732181.

[7] S. Petricola, M. Reinmuth, S. Lautenbach, C. Hatfield, and A. Zipf, “Assessing road criticality and loss of healthcare accessibility during floods: the case of Cyclone Idai, Mozambique 2019,” *Int. J. Health Geogr.*, vol. 21, no. 1, p. 14, Oct. 2022, doi: 10.1186/s12942-022-00315-2.

[8] H. Boutaghane *et al.*, “Flood Analysis and Mitigation Strategies in Algeria,” in *Wadi Flash Floods: Challenges and Advanced Approaches for Disaster Risk Reduction*, T. Sumi, S. A. Kantoush, and M. Saber, Eds., Singapore: Springer, 2022, pp. 95–118. doi: 10.1007/978-981-16-2904-4_3.

[9] O. Chabou, Y. Lazri, S. Mannucci, A. Ciardiello, F. Rosso, and M. Ferrero, “Advancing Flood Resilience in North African Coastal Cities: A Contextual Analysis of Jijel, Algeria,” 2025, *SSRN*. doi: 10.2139/ssrn.5119555.

[10] B. Remini, “Flash Floods in Algeria,” *LARHYSS Journal*, 2023.

[11] Y. Djellouli and E. A. Saci, “Catastrophe « Naturelle »: Les Inondations Devastatrices Du 9 Et 10 Novembre 2001 À Bab El Oued (alger, Algérie)”.

[12] B. Abdulla, A. Kiaghadi, H. Rifai, and B. Birgisson, “Characterization of vulnerability of road networks to fluvial flooding using SIS network diffusion model,” *J. Infrastruct. Preserv. Resil.*, vol. 1, p. null, 2020, doi: 10.1186/s43065-020-00004-z.

[13] K. Hutter, B. Svendsen, and D. Rickenmann, “Debris flow modeling: A review,” 1996.

[14] A. Kadaverugu, K. V. Gorthi, and N. R. Chintala, “Impacts of urban floods on road connectivity - a review and systematic bibliometric analysis,” *Curr. World Environ.*, vol. 16, no. 2, pp. 575–593, Aug. 2021, doi: 10.12944/CWE.16.2.22.

[15] A. K. Kazantzi, K. Bakalis, and S.-A. Mitoulis, “Flood fragility assessment of bridges—Unified framework,” *Reliab. Eng. Syst. Saf.*, vol. 262, p. 111196, Oct. 2025, doi: 10.1016/j.ress.2025.111196.

[16] R. Wang and H. Tang, “OPEN Stability analysis of roadbed under flood scouring,” *Sci. Rep.*.

[17] S. A. Mitoulis, S. A. Argyroudis, and R. Lamb, “Risk and resilience of bridgeworks exposed to hydraulic hazards,” presented at the IABSE Congress, New York, New York

2019: The Evolving Metropolis, New York, New York, USA, 2019, pp. 436–441. doi: 10.2749/newyork.2019.0436.
[18] B. Hankin, I. Craigen, W. Rogers, J. Morphet, A. Bailey, and M. Whitehead, “Flood Risk to the Strategic Road Network in England,” *E3S Web Conf.*, vol. 7, p. 10001, 2016, doi: 10.1051/e3sconf/20160710001.
[19] S. Amirebrahimi, A. Rajabifard, P. Mendis, and T. Ngo, “A BIM-GIS integration method in support of the assessment and 3D visualisation of flood damage to a building,” *J. Spat. Sci.*, vol. 61, no. 2, pp. 317–350, Jul. 2016, doi: 10.1080/14498596.2016.1189365.
[20] D. Yin *et al.*, “Sponge city practice in China: A review of construction, assessment, operational and maintenance,” *J. Clean. Prod.*, vol. 280, p. 124963, Jan. 2021, doi: 10.1016/j.jclepro.2020.124963.
[21] A. Tahraoui, R. Kheddam, and A. Belhadj Aissa, “Sustainable agricultural lands management by analyzing and predicting urban growth—a case study of Mitidja Plain, Algeria,” *J. Appl. Remote Sens.*, vol. 17, no. 01, Feb. 2023, doi: 10.1117/1.JRS.17.014511.
[22] K. Smith and R. Ward, *Floods: physical processes and human impacts*. Chichester: John Wiley & Sons, 1998.
[23] P. C. D. Milly *et al.*, “Stationarity Is Dead: Whither Water Management?,” *Science*, vol. 319, no. 5863, pp. 573–574, Feb. 2008, doi: 10.1126/science.1151915.
[24] R. Brázdil, Z. W. Kundzewicz, and G. Benito, “Historical hydrology for studying flood risk in Europe,” *Hydrol. Sci. J.*, vol. 51, no. 5, pp. 739–764, Oct. 2006, doi: 10.1623/hysj.51.5.739.
[25] A. N. Angelakis *et al.*, “Evolution of Floods: From Ancient Times to the Present Times (ca 7600 BC to the Present) and the Future,” *Land*, vol. 12, no. 6, p. 1211, Jun. 2023, doi: 10.3390/land12061211.
[26] D. Rincón, U. T. Khan, and C. Armenakis, “Flood Risk Mapping Using GIS and Multi-Criteria Analysis: A Greater Toronto Area Case Study,” *Geosciences*, vol. 8, no. 8, p. 275, Jul. 2018, doi: 10.3390/geosciences8080275.
[27] L. Wang *et al.*, “A review of the flood management: from flood control to flood resilience,” *Heliyon*, vol. 8, no. 11, p. e11763, Nov. 2022, doi: 10.1016/j.heliyon.2022.e11763.
[28] J. Caprario and A. R. Finotti, “Socio-technological tool for mapping susceptibility to urban flooding,” *J. Hydrol.*, vol. 574, pp. 1152–1163, Jul. 2019, doi: 10.1016/j.jhydrol.2019.05.005.
[29] H. Yu and S. An, “Emergency Management and Planning Framework of Transportation Evacuation for Urban Flood Calamity,” *Appl. Mech. Mater.*, vol. 353–356, pp. 2345–2348, 2013, doi: 10.4028/www.scientific.net/AMM.353-356.2345.
[30] A. Morawski, “Flood vulnerability of the critical infrastructure in Poland,” *Secur. Def. Q.*, Aug. 2022, doi: 10.35467/sdq/150456.
[31] J. C. Gill and B. D. Malamud, “Reviewing and visualizing the interactions of natural hazards: Interactions of Natural Hazards,” *Rev. Geophys.*, vol. 52, no. 4, pp. 680–722, Dec. 2014, doi: 10.1002/2013RG000445.
[32] V. Kumar, K. Sharma, T. Caloiero, D. Mehta, and K. Singh, “Comprehensive overview of flood modeling approaches: a review of recent advances,” *Hydrology*, vol. 10, no. 7, p. 141, Jun. 2023, doi: 10.3390/hydrology10070141.

[33] D. Alexander, “The Study of Natural Disasters, 1977–97: Some Reflections on a Changing Field of Knowledge,” *Disasters*, vol. 21, no. 4, pp. 284–304, 1997, doi: 10.1111/1467-7717.00064.
[34] A. Maranzoni, M. D’Oria, and C. Rizzo, “Quantitative flood hazard assessment methods: a review,” *J. Flood Risk Manag.*, vol. 16, no. 1, p. e12855, Mar. 2023, doi: 10.1111/jfr3.12855.
[35] G. Rossi, “Historical development of flood analysis methods,” in *Coping with Floods*, G. Rossi, N. Harmancioğlu, and V. Yevjevich, Eds., Dordrecht: Springer Netherlands, 1994, pp. 11–34. doi: 10.1007/978-94-011-1098-3_2.
[36] G. N. Crockford, “The Bibliography and History of Risk Management : Some Preliminary Observations,” *Geneva Pap. Risk Insur.*, vol. 7, no. 23, pp. 169–179, 1982.
[37] C. Ancey, *Risques hydrologique et Aménagement de territoire*.
[38] V. W. Griffis and J. R. Stedinger, “Evolution of Flood Frequency Analysis with *Bulletin 17*,” *J. Hydrol. Eng.*, vol. 12, no. 3, pp. 283–297, May 2007, doi: 10.1061/(ASCE)1084-0699(2007)12:3(283).
[39] R. Mudashiru, N. Sabtu, I. Abustan, and W. Balogun, “Flood hazard mapping methods: A review,” *J. Hydrol.*, vol. 603, p. 126846, 2021, doi: 10.1016/J.JHYDROL.2021.126846.
[40] L. Cafiero, P. Mazzoglio, A. Viglione, and F. Laio, “Flood frequency elasticity to extreme precipitation: a practical approach for Climate Change projection of flood probabilities.” Accessed: Jun. 19, 2024. [Online]. Available: https://meetingorganizer.copernicus.org/EGU24/EGU24-4543.html
[41] O. D. Aribisala, S.-G. Yum, M. D. Adhikari, and M.-S. Song, “Flood Damage Assessment: A Review of Microscale Methodologies for Residential Buildings,” *Sustainability*, vol. 14, no. 21, p. 13817, Oct. 2022, doi: 10.3390/su142113817.
[42] M. A. Keraghel and F. Gaouaou, “Assessing flood dynamics in Algiers, Algeria: influence of land cover change and precipitation regimes,” *Theor. Appl. Climatol.*, vol. 156, no. 1, p. 15, Dec. 2024, doi: 10.1007/s00704-024-05226-9.
[43] L. J. Slater *et al.*, “Nonstationary weather and water extremes: a review of methods for their detection, attribution, and management,” *Hydrol. Earth Syst. Sci.*, vol. 25, no. 7, pp. 3897–3935, Jul. 2021, doi: 10.5194/hess-25-3897-2021.
[44] M. Saber *et al.*, “Enhancing flood risk assessment through integration of ensemble learning approaches and physical-based hydrological modeling,” *Geomat. Nat. Hazards Risk*, vol. null, p. null, 2023, doi: 10.1080/19475705.2023.2203798.
[45] W. Zhang, B. Hu, Y. Liu, X. Zhang, and Z. Li, “Urban Flood Risk Assessment through the Integration of Natural and Human Resilience Based on Machine Learning Models,” *Remote Sens.*, vol. 15, no. 14, Art. no. 14, Jan. 2023, doi: 10.3390/rs15143678.
[46] S. W. ASTITE, “Analyse Et Evaluation De La Vulnerabilite Aux Inondations. Cas Du Grand Alger.,” FACULTE DES SCIENCES DE LA TERRE, DE LA GEOGRAPHIE ET DE L’AMENAGEMENT DU TERRITOIRE (FSTGAT)., UNIVERSITE DES SCIENCES ET DE LA TECHNOLOGIE HOUARI BOUMEDIENE, Alger, 2018.
[47] C. P. Capoccioni, D. Cœur, D. Chenier, B. Chazelle, C. Saint-Marc, and M. Lang, “Impacts Des Inondations Historiques Sur Un Reseau De Transport: Exemple Des Installations Et Des Circulations Ferroviaires En France,” p. 8, 2013.
[48] Pascale BOIZARD and Frédéric RICARD, “Rapport_Coupure de l’autoroute A10 et autres infrastructures,” france, final, 2016.

[49] P. Kiparisov, V. Lagutov, and G. Pflug, “Quantification of Loss of Access to Critical Services during Floods in Greater Jakarta: Integrating Social, Geospatial, and Network Perspectives,” *Remote Sens.*, vol. 15, no. 21, p. 5250, Nov. 2023, doi: 10.3390/rs15215250.
[50] J. Birkmann, Ed., *Measuring vulnerability to natural hazards: towards disaster resilient societies*, 2. ed. Tokyo: United Nations Univ. Press, 2013.
[51] N. Lee Siew Len, N. Bolong, R. Roslee, F. Tongkul, A. K. Mirasa, and J. Lynn Ayog, “Flood vulnerability of critical infrastructures – review,” *Malays. J. Geosci.*, vol. 2, no. 1, pp. 34–37, Jan. 2018, doi: 10.26480/mjg.01.2018.34.37.
[52] N. S. Romali, M. @ S. A. K. Sulaiman, Z. Yusop, and Z. Ismail, “Flood Damage Assessment: A Review of Flood Stage–Damage Function Curve,” in *ISFRAM 2014*, S. H. Abu Bakar, W. Tahir, M. Ab. Wahid, S. R. Mohd Nasir, and R. Hassan, Eds., Singapore: Springer Singapore, 2015, pp. 147–159. doi: 10.1007/978-981-287-365-1_13.
[53] Y. D. Tomety, “Exposition et vulnérabilité face aux risques d’inondation au burkina faso : cas de la ville de dori,” Université Liége, 2017.
[54] S. Dong, X. Gao, A. Mostafavi, J. Gao, and U. Gangwal, “Characterizing resilience of flood-disrupted dynamic transportation network through the lens of link reliability and stability,” *Reliab. Eng. Syst. Saf.*, vol. 232, p. 109071, Apr. 2023, doi: 10.1016/j.ress.2022.109071.
[55] T. Tredgold, *Elementary Principles of Carpentry: A Treatise on the Pressure and Equilibrium of Timber Framing, the Resistance of Timber, and the Construction of Floors, Roofs, Centres, Bridges, &c. with Practical Rules and Examples. To which is Added an Essay on the Nature and Properties of Timber, Including the Methods of Seasoning, and the Causes and Prevention of Decay, with Descriptions of the Kinds of Wood Used in Building. Also Numerous Tables of the Scantlings of Timber for Different Purposes, the Specific Gravities of Materials, &c. Illustrated by Twenty-two Engravings, and Several Wood Cuts*. J. Taylorat the Architectural Library, 1828.
[56] C. S. Holling, “Resilience and Stability of Ecological Systems,” *Annu. Rev. Ecol. Syst.*, vol. 4, pp. 1–23, 1973.
[57] L. C. Carro, R. C. Delgado, and P. A. González, “A review of the concept of resilience in the field of disasters and its evolution,” *Rev. Esp. Comun. En Salud*, pp. 8–18, Mar. 2019, doi: 10.20318/recs.2019.4590.
[58] M. Santamaria-Ariza, M. Liu, H. S. Sousa, J. C. Matos, and M. H. Faber, “Probabilistic resilience model for management of road infrastructure systems subject to flood events,” 2023.
[59] L. Zhu, “Rainwater runoff regulation effect in sponge reconstruction area based on rainstorm flood management model,” *Desalination Water Treat.*, vol. 319, p. 100507, Jul. 2024, doi: 10.1016/j.dwt.2024.100507.
[60] E. Arango, M. Santamaria, M. Nogal, H. S. Sousa, and J. C. Matos, “Flood risk assessment for road infrastructures using Bayesian networks: case study of Santarem - Portugal,” *Acta Polytech. CTU Proc.*, vol. 36, pp. 33–46, Aug. 2022, doi: 10.14311/APP.2022.36.0033.
[61] N. Gendreau, M. Longhini, and P. M. Combe, “19.Gestion du risque d’inondation et méthode Inondabilité: une perspective socio-économique,” no. 14, 1998.

[62] F. Renard and D. Soto, “Une représentation du risque à l’intersection de l’aléa et de la vulnérabilité: cartographies des inondations lyonnaises,” *Geogr. Helvetica*, vol. 70, no. 4, pp. 333–348, Nov. 2015, doi: 10.5194/gh-70-333-2015.
[63] S. Charaud, “Cartographie pour la directive inondation,” Gestion des Crises Routières, 2015.
[64] A. C. Miller and T. M. Ravens, “Assessing Coastal Road Flood Risk in Arctic Alaska, a Case Study from Hooper Bay,” *J. Mar. Sci. Eng.*, vol. 10, no. 3, p. 406, Mar. 2022, doi: 10.3390/jmse10030406.
[65] C. Gonzalez-Duenas and J. E. Padgett, “A performance-based coastal engineering framework,” *Coast. Eng. Proc.*, no. 36v, p. 16, Dec. 2020, doi: 10.9753/icce.v36v.management.16.
[66] A. Chissende, M. S. Mehmood, A. Huo, P. Lou, and Z. Wang, “Riverine flood susceptibility assessment using drainage basin morphometry in the Bahe River,” *Int. J. Disaster Risk Reduct.*, vol. 117, p. 105181, Feb. 2025, doi: 10.1016/j.ijdrr.2025.105181.
[67] M. Msabi and M. Makonyo, “Flood susceptibility mapping using GIS and multi-criteria decision analysis: A case of Dodoma region, central Tanzania,” *Remote Sens. Appl. Soc. Environ.*, vol. 21, p. 100445, 2021, doi: 10.1016/j.rsase.2020.100445.
[68] S. Mukherjee *et al.*, “Comparison of on-site versus NOAA’s extreme precipitation intensity-duration-frequency estimates for six forest headwater catchments across the continental United States,” *Stoch. Environ. Res. Risk Assess.*, vol. 37, no. 10, pp. 4051–4070, Oct. 2023, doi: 10.1007/s00477-023-02495-0.
[69] C. Achraf, L. Nour-Eddine, I. Mounsif, and M. Leila, “Contribution of hydraulic modeling and hydrology to flood prevention and design of engineering structures: Case study of a bridge over the Oued Ourika – Morocco,” *E3S Web Conf.*, vol. 489, p. 04007, 2024, doi: 10.1051/e3sconf/202448904007.
[70] M. G. Winter, “The John Mitchell Lecture 2023: road asset, socio-economic and fatality risk from debris flow,” *Q. J. Eng. Geol. Hydrogeol.*, vol. 57, no. 2, pp. qjegh2023-167, May 2024, doi: 10.1144/qjegh2023-167.
[71] D. De Wrachien, S. Mambretti, and A. Sole, “Mathematical models in flood management: overview and challenges,” in *Proceedings of the 2nd International Conference on Flood Recovery, Innovation and Response (FRIAR 2010)*, Milan, Italy: WIT Press, May 2010, pp. 61–72. doi: 10.2495/FRIAR100061.
[72] Y. Zhang, Y. Wei, R. Yao, P. Sun, N. Zhen, and X. Xia, “Data Uncertainty of Flood Susceptibility Using Non-Flood Samples,” *Remote Sens.*, vol. 17, no. 3, p. 375, Jan. 2025, doi: 10.3390/rs17030375.
[73] M. J. Lighthill and G. B. Whitham, “On kinematic waves I. Flood movement in long rivers,” *Proc. R. Soc. Lond. Ser. Math. Phys. Sci.*, vol. 229, no. 1178, pp. 281–316, 1955.
[74] A. Afra *et al.*, “Application of the Rainfall–Runoff–Inundation Model for Flood Risk Assessment in the Mekerra Basin, Algeria,” *GeoHazards*, vol. 6, no. 1, p. 2, Jan. 2025, doi: 10.3390/geohazards6010002.
[75] S. Mukherjee *et al.*, “A watershed-scale multi-approach assessment of design flood discharge estimates used in hydrologic risk analyses for forest road stream crossings and culverts,” *J. Hydrol.*, vol. 632, p. 130698, Mar. 2024, doi: 10.1016/j.jhydrol.2024.130698.
[76] L. Dasallas, H. An, and S. Lee, “Providing solutions for data scarcity in urban flood modeling through sensitivity analysis and DEM modifications,” *J. Hydroinformatics*, vol. 26, no. 2, pp. 459–479, Feb. 2024, doi: 10.2166/hydro.2024.173.

[77] M. Batalini de Macedo *et al.*, “Performance analysis of physically-based (HEC-RAS, CADDIES) and AI-based (LSTM) flood models for two case studies,” in *Proceedings of IAHS*, Copernicus GmbH, Apr. 2024, pp. 41–46. doi: 10.5194/piahs-386-41-2024.
[78] Y. Shen and C. Jiang, “A comprehensive review of watershed flood simulation model,” *Nat. Hazards*, vol. 118, no. 2, pp. 875–902, Sep. 2023, doi: 10.1007/s11069-023-06047-1.
[79] H. S. Wheater, “Progress in and Prospects for Fluvial Flood Modelling,” *Philos. Trans. Math. Phys. Eng. Sci.*, vol. 360, no. 1796, pp. 1409–1431, 2002.
[80] A. N. R. Orozco, N. Bertrand, L. Pheulpin, A. Migaud, and M. Abily, “Comparison Between HEC-RAS and TELEMAC-2D Hydrodynamic Models of the Loire River, Integrating Levee Breaches,” in *Advances in Hydroinformatics—SimHydro 2023 Volume 1*, P. Gourbesville and G. Caignaert, Eds., in Springer Water. , Singapore: Springer Nature Singapore, 2024, pp. 41–55. doi: 10.1007/978-981-97-4072-7_3.
[81] F. E. Hicks and T. Peacock, “Suitability of HEC-RAS for flood forecasting,” *Can. Water Resour. J.*, vol. 30, no. 2, pp. 159–174, Jan. 2005, doi: 10.4296/cwrj3002159.
[82] A. Azouagh, R. E. Bardai, I. Hilal, and J. S. el Messari, “Integration of GIS and HEC-RAS in floods modeling of martil river (northern morocco),” *Eur. Sci. J. ESJ*, vol. 14, no. 12, pp. 130–130, Apr. 2018, doi: 10.19044/esj.2018.v14n12p130.
[83] T. C. Pierson and J. E. Costa, “A rheologic classification of subaerial sediment-water flows,” in *Debris Flows/Avalanches: Process, Recognition, and Mitigation*, vol. 7, J. E. Costa and G. F. Wieczorek, Eds., Geological Society of America, 1987, p. 0. doi: 10.1130/REG7-p1.
[84] M. Zhang, M. Xu, Z. Wang, and C. Lai, “Assessment of the vulnerability of road networks to urban waterlogging based on a coupled hydrodynamic model,” *J. Hydrol.*, vol. 603, p. 127105, Dec. 2021, doi: 10.1016/j.jhydrol.2021.127105.
[85] Y. Liu, H. Zhang, H. Chen, and C. Chen, “Flood impact on urban roads and commuting: A case study of Wuhan, China,” *Front. Environ. Sci.*, vol. 10, p. 1056854, Nov. 2022, doi: 10.3389/fenvs.2022.1056854.
[86] Wangninan Ange Osée FATOMON, “Mém_Evaluation des dommages associées aux inondations sur les routes et ouvrages D’assainissement,” INGENIEUR DE CONCEPTION, ECOLE POLYTECHNIQUE D’ABOMEY CALAVI, Benin, 2015.
[87] M. Saber *et al.*, “Examining LightGBM and CatBoost models for wadi flash flood susceptibility prediction,” *Geocarto Int.*, vol. 37, pp. 7462–7487, 2021, doi: 10.1080/10106049.2021.1974959.
[88] C. Sánchez-García and L. Schulte, “Historical floods in the southeastern Iberian Peninsula since the 16th century: Trends and regional analysis of extreme flood events,” *Glob. Planet. Change*, vol. 231, p. 104317, Dec. 2023, doi: 10.1016/j.gloplacha.2023.104317.
[89] R. Albano and J. Adamowski, “Use of digital elevation models for flood susceptibility assessment via a hydrogeomorphic approach: A case study of the Basento River in Italy,” *Nat. Hazards*, Feb. 2025, doi: 10.1007/s11069-025-07144-z.
[90] X. Kong *et al.*, “Post-event flood mapping for road networks using taxi GPS data,” *J. Flood Risk Manag.*, vol. 15, no. 2, p. e12799, Jun. 2022, doi: 10.1111/jfr3.12799.
[91] A. Goumrasa, M. Guendouz, M. S. Guettouche, and A. Belaroui, “Flood hazard susceptibility assessment in Chiffa wadi watershed and along the first section of Algeria North–South highway using GIS and AHP method,” *Appl. Geomat.*, vol. 13, no. 4, pp. 565–585, Dec. 2021, doi: 10.1007/s12518-021-00381-4.

[92] M. Meddi, S. Toumi, and A. A. Assani, “Application of the L-moments approach to the analysis of regional flood frequency in Northern Algeria,” 2017.
[93] K. D. Nastiti, Y. Kim, K. Jung, and H. An, “The Application of Rainfall-Runoff-inundation (RRI) Model for Inundation Case in Upper Citarum Watershed, West Java-Indonesia,” *Procedia Eng.*, vol. 125, pp. 166–172, 2015, doi: 10.1016/j.proeng.2015.11.024.
[94] R. Costache and D. T. Bui, “Spatial prediction of flood potential using new ensembles of bivariate statistics and artificial intelligence: A case study at the Putna river catchment of Romania.,” *Sci. Total Environ.*, vol. 691, pp. 1098–1118, 2019, doi: 10.1016/J.SCITOTENV.2019.07.197.
[95] J. T. Bersabe and B.-W. Jun, “The Machine Learning-Based Mapping of Urban Pluvial Flood Susceptibility in Seoul Integrating Flood Conditioning Factors and Drainage-Related Data,” *ISPRS Int. J. Geo-Inf.*, vol. 14, no. 2, p. 57, Feb. 2025, doi: 10.3390/ijgi14020057.
[96] U. C. Sahoo, S. R. Dash, and C. S. Sahu, “Climate-resilient road design in coastal areas subjected to cyclones and associated floods,” *Infrastruct. Asset Manag.*, vol. 8, no. 4, pp. 209–218, Dec. 2021, doi: 10.1680/jinam.21.00010.
[97] S. A. Argyroudis, S. A. Mitoulis, M. G. Winter, and A. M. Kaynia, “Fragility of transport assets exposed to multiple hazards: State-of-the-art review toward infrastructural resilience,” *Reliab. Eng. Syst. Saf.*, vol. 191, p. 106567, Nov. 2019, doi: 10.1016/j.ress.2019.106567.
[98] N. Goldbeck, P. Angeloudis, and W. Y. Ochieng, “Resilience assessment for interdependent urban infrastructure systems using dynamic network flow models,” *Reliab. Eng. Syst. Saf.*, vol. 188, pp. 62–79, Aug. 2019, doi: 10.1016/j.ress.2019.03.007.
[99] Y. Zhang, “Economic Impact of Bridge Damage in a Flood Event”.
[100] A. N. Ghani, A. A. Hamid, and N. Kasnon, “STUDY ON THE USE OF OBSTRUCTING OBJECTS TO DIFFUSE FLOOD WATER VELOCITY DURING ROAD CROSSING,” *Int. J. Geomate*, vol. 8, pp. 1245–1249, 2015, doi: 10.21660/2015.16.4142.
[101] S. Shabou *et al.*, “MobRISK: a model for assessing the exposure of road users to flash flood events,” *Nat. Hazards Earth Syst. Sci.*, vol. 17, no. 9, pp. 1631–1651, Sep. 2017, doi: 10.5194/nhess-17-1631-2017.
[102] R. C. B. Bucar and Y. M. Hayeri, “Quantitative flood risk evaluation to improve drivers’ route choice decisions during disruptive precipitation,” *Reliab. Eng. Syst. Saf.*, vol. 219, p. 108202, Mar. 2022, doi: 10.1016/j.ress.2021.108202.
[103] M. Borowska-Stefańska, M. Kowalski, S. Wiśniewski, and M. A. Dulebenets, “The impact of self-evacuation from flood hazard areas on the equilibrium of the road transport,” *Saf. Sci.*, vol. 157, p. 105934, Jan. 2023, doi: 10.1016/j.ssci.2022.105934.
[104] X. Lu, F. K. Shun Chan, W.-Q. Chen, H. K. Chan, and X. Gu, “An overview of flood-induced transport disruptions on urban streets and roads in Chinese megacities: lessons and future agendas,” *J. Environ. Manage.*, vol. 321, p. 115991, Nov. 2022, doi: 10.1016/j.jenvman.2022.115991.
[105] L. G. Brunner, R. A. M. Peer, C. Zorn, R. Paulik, and T. M. Logan, “Understanding cascading risks through real-world interdependent urban infrastructure,” *Reliab. Eng. Syst. Saf.*, vol. 241, p. 109653, Jan. 2024, doi: 10.1016/j.ress.2023.109653.
[106] F. J. Shahdani, M. Santamaria-Ariza, H. S. Sousa, M. Coelho, and J. C. Matos, “Assessing Flood Indirect Impacts on Road Transport Networks Applying Mesoscopic Traffic

Modelling: The Case Study of Santarém, Portugal," *Appl. Sci.*, vol. 12, no. 6, p. 3076, Mar. 2022, doi: 10.3390/app12063076.
[107] Y. Duan *et al.*, "Flood vulnerability assessment using the triangular fuzzy number-based analytic hierarchy process and support vector machine model for the Belt and Road region," *Nat. Hazards*, vol. 110, no. 1, pp. 269–294, Jan. 2022, doi: 10.1007/s11069-021-04946-9.
[108] F. Biondini *et al.*, "Bridge vulnerability and hazard assessment for risk-based infrastructure management," in *Bridge Safety, Maintenance, Management, Life-Cycle, Resilience and Sustainability*, 1st ed., London: CRC Press, 2022, pp. 1864–1873. doi: 10.1201/9781003322641-231.
[109] Chanjin Jeong, Dong-Hyun Kim, Hyung-Ju Yoo, and Seung-Oh Lee, "Selection of Elevation Models for Flood Inundation Map Generation in Small Urban Stream: Case Study of Anyang Stream," *Adv. Technol. Innov.*, vol. 9, no. 1, pp. 28–41, Dec. 2023, doi: 10.46604/aiti.2023.12000.
[110] F. Yuan *et al.*, "Smart flood resilience: harnessing community-scale big data for predictive flood risk monitoring, rapid impact assessment, and situational awareness," *Environ. Res. Infrastruct. Sustain.*, vol. 2, no. 2, p. 025006, Jun. 2022, doi: 10.1088/2634-4505/ac7251.
[111] H. Yang, T. Zou, and B. Liu, "Assessment of urban flood susceptibility based on a novel integrated machine learning method," *Environ. Monit. Assess.*, vol. 197, no. 1, p. 25, Dec. 2024, doi: 10.1007/s10661-024-13496-z.
[112] M. Bakillah and S. Liang, "Open geospatial data, software and standards," *Open Geospatial Data Softw. Stand.*, vol. 1, no. 1, pp. 1, s40965-016-0004–1, Dec. 2016, doi: 10.1186/s40965-016-0004-1.
[113] T. Gilbert, S. Barr, P. James, J. Morley, and Q. Ji, "Software Systems Approach to Multi-Scale GIS-BIM Utility Infrastructure Network Integration and Resource Flow Simulation," *ISPRS Int. J. Geo-Inf.*, vol. 7, no. 8, p. 310, Aug. 2018, doi: 10.3390/ijgi7080310.
[114] A. Iqbal, L. Soni, A. W. Qazi, and H. Nazir, "Utilizing Remote Sensing for Sponge City Development: Enhancing Flood Management and Urban Resilience in Karachi," *Remote Sens.*, vol. 17, no. 11, p. 1818, Jan. 2025, doi: 10.3390/rs17111818.
[115] S. Amirebrahimi, A. Rajabifard, P. Mendis, and T. Ngo, "A Data Model for Integrating GIS and BIM for Assessment and 3D Visualisation of Flood Damage to Building".
[116] M. Schrenk and Verein CORP - Competence Center of Urban and Regional Planning, Eds., *Expanding cities – diminishing space: are "smart cities" the solution or part of the problem of continuous urbanisation around the globe?* Wien: Selbstverlag des Vereins CORP - Competence Center of Urban and Regional Planning, 2018.
[117] İ. B. Peker, S. Gülbaz, V. Demir, O. Orhan, and N. Beden, "Integration of HEC-RAS and HEC-HMS with GIS in Flood Modeling and Flood Hazard Mapping," *Sustainability*, vol. 16, no. 3, Art. no. 3, Jan. 2024, doi: 10.3390/su16031226.
[118] Maguire, D.J, "Overview and definition of Gis," in *Geographical information systems: principles and applications*, Maguire, D. J. Goodchild, M. F.Rhind, D. W., vol. 1, 2 vols., Harlow, Essex: Longman Scientific & Technical, 1991, pp. 9–20.
[119] V. Hingmire and N. Thomas, "GIS & BIM in Construction – A Timeline Study and the Way Forward".

[120] K. J. Sowmiya Narayanan and A. Manimaran, “Recent developments in geographic information systems across different application domains: a review,” *Knowl. Inf. Syst.*, vol. 66, no. 3, pp. 1523–1547, Mar. 2024, doi: 10.1007/s10115-023-01969-5.
[121] J. Carneiro, R. J. F. Rossetti, D. C. Silva, and E. C. Oliveira, “BIM, GIS, IoT, and AR/VR integration for smart maintenance and management of road networks: a review,” in *2018 IEEE International Smart Cities Conference (ISC2)*, Kansas City, MO, USA: IEEE, Sep. 2018, pp. 1–7. doi: 10.1109/ISC2.2018.8656978.
[122] H. Wang, Y. Pan, and X. Luo, “Integration of BIM and GIS in sustainable built environment: A review and bibliometric analysis,” *Autom. Constr.*, vol. 103, pp. 41–52, Jul. 2019, doi: 10.1016/j.autcon.2019.03.005.
[123] S. Amirebrahimi, A. Rajabifard, P. Mendis, and T. Ngo, “A framework for a microscale flood damage assessment and visualization for a building using BIM–GIS integration,” *Int. J. Digit. Earth*, vol. 9, no. 4, pp. 363–386, Apr. 2016, doi: 10.1080/17538947.2015.1034201.
[124] N. Muhamad *et al.*, “Geo-smart city flood mitigation and monitoring using geospatial technology,” in *Advances in Geoinformatics Technologies*, R. N. Yadava and M. U. Ujang, Eds., Cham: Springer Nature Switzerland, 2024, pp. 393–405. doi: 10.1007/978-3-031-50848-6_20.
[125] S. Sulong, “Flood damage assessment: a review of multivariate flood damage models,” *Int. J. GEOMATE*, vol. 22, no. 93, May 2022, doi: 10.21660/2022.93.gxi439.
[126] K. C. H. Van Ginkel, F. Dottori, L. Alfieri, L. Feyen, and E. E. Koks, “Direct flood risk assessment of the European road network: an object-based approach,” Apr. 16, 2020. doi: 10.5194/nhess-2020-104.
[127] D. Wagenaar, S. Lüdtke, K. Schröter, L. M. Bouwer, and H. Kreibich, “Regional and Temporal Transferability of Multivariable Flood Damage Models,” *Water Resour. Res.*, vol. 54, no. 5, pp. 3688–3703, 2018, doi: 10.1029/2017WR022233.
[128] L. Barazzetti, M. Previtali, and M. Scaioni, “Roads Detection and Parametrization in Integrated BIM-GIS Using LiDAR,” *Infrastructures*, vol. 5, no. 7, p. 55, Jul. 2020, doi: 10.3390/infrastructures5070055.
[129] K. Arroyo Ohori, F. Biljecki, A. Diakité, T. Krijnen, H. Ledoux, and J. Stoter, “Towards an Integration of Gis and Bim Data: What Are the Geometricand Topological Issues?,” *ISPRS Ann. Photogramm. Remote Sens. Spat. Inf. Sci.*, vol. IV-4/W5, pp. 1–8, Oct. 2017, doi: 10.5194/isprs-annals-IV-4-W5-1-2017.
[130] O. O. Akinade, “Bim-Based Software for Construction Waste Analytics Using Artificial Intelligence Hybrid Models”.
[131] M. F. Bin Mohd Idris and M. Tahir, “Barriers to building information modeling (BIM) implementation in pakistan during the post-flood era: an interpretive structural modelling (ISM) approach,” *J. Infrastruct. Policy Manag.*, vol. 6, no. 1, pp. 53–68, Oct. 2023, doi: 10.35166/jipm.6.1.53-68.
[132] S. Shirowzhan, W. Tan, and S. M. E. Sepasgozar, “Digital Twin and CyberGIS for Improving Connectivity and Measuring the Impact of Infrastructure Construction Planning in Smart Cities,” *ISPRS Int. J. Geo-Inf.*, vol. 9, no. 4, p. 240, Apr. 2020, doi: 10.3390/ijgi9040240.
[133] H. Y. Chong, R. Lopez, J. Wang, X. Wang, and Z. Zhao, “Comparative Analysis on the Adoption and Use of BIM in Road Infrastructure Projects,” *J. Manag. Eng.*, vol. 32, no. 6, p. 05016021, Nov. 2016, doi: 10.1061/(ASCE)ME.1943-5479.0000460.

[134] M. Q. Huang, J. Ninić, and Q. B. Zhang, “BIM, machine learning and computer vision techniques in underground construction: Current status and future perspectives,” *Tunn. Undergr. Space Technol.*, vol. 108, p. 103677, Feb. 2021, doi: 10.1016/j.tust.2020.103677.
[135] D. E. Andrianesi and E. Dimopoulou, “An Integrated Bim-Gis Platform for Representing and Visualizing 3d Cadastral Data,” *ISPRS Ann. Photogramm. Remote Sens. Spat. Inf. Sci.*, vol. VI-4/W1-2020, pp. 3–11, Sep. 2020, doi: 10.5194/isprs-annals-VI-4-W1-2020-3-2020.
[136] A. Borrmann, M. König, C. Koch, and J. Beetz, “Building information modeling: why? What? How?,” in *Building Information Modeling: Technology Foundations and Industry Practice*, A. Borrmann, M. König, C. Koch, and J. Beetz, Eds., Cham: Springer International Publishing, 2018, pp. 1–24. doi: 10.1007/978-3-319-92862-3_1.
[137] S. Kaewunruen, J. Sresakoolchai, and Z. Zhou, “Sustainability-based lifecycle management for bridge infrastructure using 6D BIM,” *Sustainability*, vol. 12, no. 6, p. 2436, Mar. 2020, doi: 10.3390/su12062436.
[138] F. Banfi, M. Previtali, and R. Brumana, “Towards the development of a cloud-based BIM platform and VR apps for complex heritage sites subject to the risk of flood and water level changes,” *IOP Conf. Ser. Mater. Sci. Eng.*, vol. 949, no. 1, p. 012105, Nov. 2020, doi: 10.1088/1757-899X/949/1/012105.
[139] W. Bonenberg and X. Wei, “Green BIM in sustainable infrastructure,” *Procedia Manuf.*, vol. 3, pp. 1654–1659, 2015, doi: 10.1016/j.promfg.2015.07.483.
[140] F. D’Amico, A. Calvi, E. Schiattarella, M. D. Prete, and V. Veraldi, “BIM and GIS data integration: a novel approach of technical/environmental decision-making process in transport infrastructure design,” *Transp. Res. Procedia*, vol. 45, pp. 803–810, 2020, doi: 10.1016/j.trpro.2020.02.090.
[141] S. Khanmohammadi, M. Arashpour, and Y. Bai, “Applications of building information modeling (BIM) in disaster resilience: present status and future trends,” presented at the 37th International Symposium on Automation and Robotics in Construction, Kitakyushu, Japan, Oct. 2020. doi: 10.22260/ISARC2020/0191.
[142] S. A. F. Syed Abdul Rahman, K. N. Abdul Maulud, and W. S. Wan Mohd Jaafar, “BIM-GIS in catalyzing 3D environmental simulation,” in *Advances in Geoinformatics Technologies*, R. N. Yadava and M. U. Ujang, Eds., Cham: Springer Nature Switzerland, 2024, pp. 183–200. doi: 10.1007/978-3-031-50848-6_10.
[143] K. K. Mwiya B., “Flood simulation with GeoBIM,” in *Smart and Resilient Infrastructure For Emerging Economies: Perspectives on Building Better*, CRC Press, 2023.
[144] A. Benedetto and A. Chiavari, “Flood risk: a new approach for roads vulnerability assessment,” vol. 6, no. 6, 2010.
[145] M. R. Khouli and L. Djabri, “Impact of Use of Agricultural Inputs on the Quality of Groundwater Case of Mitidja Plain (algeria)”.
[146] A. Reussner, “Franc (Julien). — La colonisation de la Mitidja,” 1931, Accessed: Jan. 09, 2026. [Online]. Available: https://www.persee.fr/doc/outre_0399-1377_1931_num_19_79_1044_t1_0076_0000_2
[147] H. Marchand, “Station néolithique du lac Halloula (Algérie),” 1933, doi: 10.3406/bspf.1933.12143.
[148] A. Boufekane, H. Meddi, and M. Meddi, “Delineation of groundwater recharge zones in the Mitidja plain, north Algeria, using multi-criteria analysis,” *J. Hydroinformatics*, vol. 22, no. 6, pp. 1468–1484, Nov. 2020, doi: 10.2166/hydro.2020.082.

[149] G. Cheikhlounis, D. Belhai, J.-L. Chatelain, M. Hellel, D. Machane, and B. Samet, "Évaluation Du Phénomène D'inondation Dans La Plaine Orientale De La Mitidja (oued El Hamiz Et Oued Réghaïa) Alger – Algérie.".
[150] S. Kourat, B. Touaïbia, and A. Yahiaoui, "Curve Flow-duration-Frequency. The flood modelling regime of the Wadi Mazafran catchment in the north of Algeria," *J. Water Land Dev.*, pp. 121–130, Sep. 2022, doi: 10.24425/jwld.2022.141563.
[151] F. Kastali, M. Meddi, A. Boufekane, and A. Longobardi, "Integrated modeling of surface water and groundwater interactions in the Eastern Mitidja Plain, North Algeria: investigating the impact of human activities and climate change," *J. Water Clim. Change*, vol. 15, no. 11, pp. 5570–5586, Nov. 2024, doi: 10.2166/wcc.2024.413.
[152] A. M. Negm, A. Bouderbala, H. Chenchouni, and D. Barceló, Eds., *Water Resources in Algeria - Part I: Assessment of Surface and Groundwater Resources*, vol. 97. in The Handbook of Environmental Chemistry, vol. 97. Cham: Springer International Publishing, 2020. doi: 10.1007/978-3-030-57895-4.
[153] N. Makhlouf, D. Maizi, and A. Boufekane, "Impact of climatic variability on groundwater resources in the Eastern Mitidja plain, Algeria," *Acque Sotter. - Ital. J. Groundw.*, vol. 12, no. 1, pp. 9–23, Mar. 2023, doi: 10.7343/as-2023-641.
[154] A. E. F. Bouras, N. M. Nacer, R. Buscail, and N. Zoubida, "Supplies of suspended matter by surface water of the Mazafran drainage basin (western Algiers, Algeria)," *Arab. J. Geosci.*, vol. 13, no. 18, p. 900, Sep. 2020, doi: 10.1007/s12517-020-05862-1.
[155] A. Goumrasa, M. Guendouz, M. S. Guettouche, D. Akziz, and H. Bouguerra, "Spatial assessment of water erosion hazard in Chiffa wadi watershed and along the first section of the Algerian North-South highway using remote sensing data, RUSLE, and GIS techniques," *Arab. J. Geosci.*, vol. 14, no. 20, p. 2152, Oct. 2021, doi: 10.1007/s12517-021-08377-5.
[156] K. Laoubi and M. Yamao, "Management of irrigation schemes in Algeria: an assessment of water policy impact and perspectives on development," presented at the WATER RESOURCES MANAGEMENT 2009, Malta, Aug. 2009, pp. 503–514. doi: 10.2495/WRM090451.
[157] P. Ramkar and S. M. Yadav, "Flood risk index in data-scarce river basins using the AHP and GIS approach," *Nat. Hazards*, vol. 109, no. 1, pp. 1119–1140, Oct. 2021, doi: 10.1007/s11069-021-04871-x.
[158] R. K. Shah and R. K. Shah, "GIS-based flood susceptibility analysis using multi-parametric approach of analytical hierarchy process in Majuli Island, Assam, India," *Sustain. Water Resour. Manag.*, vol. 9, no. 5, p. 139, Oct. 2023, doi: 10.1007/s40899-023-00924-0.
[159] D. Tadesse, V. S. Karuturi, and D. Nedaw, "GIS-Based Flood Hazard Mapping in Itang District of the Gambella Region, Ethiopia," 2021, doi: 10.21203/rs.3.rs-430787/v1.
[160] T. L. Saaty, "An Exposition on the AHP in Reply to the Paper 'Remarks on the Analytic Hierarchy Process,'" *Manag. Sci.*, vol. 36, no. 3, pp. 259–268, 1990.
[161] A. Abdullah, K. Iki, and M. Morozumi, "An integrated approach of AHP and GIS applications to analyse and develop recreational zoning: a study to determine suitability and priority zones in the ASO national park," *J. Archit. Plan. Trans. AIJ*, vol. 59, no. 463, pp. 213–222, 1994, doi: 10.3130/aija.59.213_2.

[162] R. Sharker *et al.*, “GIS-based AHP approach to flood susceptibility assessment in Tangail district, Bangladesh,” *J. Earth Syst. Sci.*, vol. 134, no. 1, p. 26, Jan. 2025, doi: 10.1007/s12040-024-02480-3.
[163] Y. Ouma and R. Tateishi, “Urban Flood Vulnerability and Risk Mapping Using Integrated Multi-Parametric AHP and GIS: Methodological Overview and Case Study Assessment,” *Water*, vol. 6, no. 6, pp. 1515–1545, May 2014, doi: 10.3390/w6061515.
[164] A. Ghosh and S. K. Kar, “Application of analytical hierarchy process (AHP) for flood risk assessment: a case study in Malda district of West Bengal, India,” *Nat. Hazards*, vol. 94, no. 1, pp. 349–368, Oct. 2018, doi: 10.1007/s11069-018-3392-y.
[165] S. Hammami *et al.*, “Application of the GIS based multi-criteria decision analysis and analytical hierarchy process (AHP) in the flood susceptibility mapping (Tunisia),” *Arab. J. Geosci.*, vol. 12, no. 21, p. 653, Oct. 2019, doi: 10.1007/s12517-019-4754-9.
[166] 文朝菊, “Risk Assessment of Mountain Flood Disaster in Banqiao Small Watershed of Luoping County Based on AHP and ArcGIS,” *Adv. Geosci.*, vol. 09, no. 06, pp. 489–506, 2019, doi: 10.12677/AG.2019.96054.
[167] A. Tella and A.-L. Balogun, “Ensemble fuzzy MCDM for spatial assessment of flood susceptibility in Ibadan, Nigeria,” *Nat. Hazards*, vol. 104, no. 3, pp. 2277–2306, Dec. 2020, doi: 10.1007/s11069-020-04272-6.
[168] D. Souissi, L. Zouhri, S. Hammami, M. H. Msaddek, A. Zghibi, and M. Dlala, “GIS-based MCDM – AHP modeling for flood susceptibility mapping of arid areas, southeastern Tunisia,” *Geocarto Int.*, vol. 35, no. 9, pp. 991–1017, Jul. 2020, doi: 10.1080/10106049.2019.1566405.
[169] S. Kittipongvises, A. Phetrak, P. Rattanapun, K. Brundiers, J. L. Buizer, and R. Melnick, “AHP-GIS analysis for flood hazard assessment of the communities nearby the world heritage site on Ayutthaya Island, Thailand,” *Int. J. Disaster Risk Reduct.*, vol. 48, p. 101612, Sep. 2020, doi: 10.1016/j.ijdrr.2020.101612.
[170] B. D. Nguyen, D. T. Minh, A. Ahmad, and Q. L. Nguyen, “The Role Of Relative Slope Length In Flood Hazard Mapping Using Ahp And Gis (Case Study: Lam River Basin, Vietnam),” *Geogr. Environ. Sustain.*, vol. 13, no. 2, pp. 115–123, Jun. 2020, doi: 10.24057/2071-9388-2020-48.
[171] K. C. Swain, C. Singha, and L. Nayak, “Flood Susceptibility Mapping through the GIS-AHP Technique Using the Cloud,” *ISPRS Int. J. Geo-Inf.*, vol. 9, no. 12, p. 720, Dec. 2020, doi: 10.3390/ijgi9120720.
[172] M. A. Mujib *et al.*, “Assessment of Flood Hazard Mapping Based on Analytical Hierarchy Process (AHP) and GIS: Application in Kencong District, Jember Regency, Indonesia,” *Geosfera Indones.*, vol. 6, no. 3, p. 353, Dec. 2021, doi: 10.19184/geosi.v6i3.21668.
[173] D. Souissi *et al.*, “Flood hazard mapping and assessment using fuzzy analytic hierarchy process and GIS techniques in Takelsa, Northeast Tunisia,” *Arab. J. Geosci.*, vol. 15, p. null, 2022, doi: 10.1007/s12517-022-10541-4.
[174] Md. N. Hossain and U. H. Mumu, “Flood susceptibility modelling of the Teesta River Basin through the AHP-MCDA process using GIS and remote sensing,” *Nat. Hazards*, vol. 120, no. 13, pp. 12137–12161, Oct. 2024, doi: 10.1007/s11069-024-06677-z.
[175] V. Shivhare, A. Kumar, R. Kumar, S. Shashtri, J. Mallick, and C. K. Singh, “Flood susceptibility and flood frequency modeling for lower Kosi Basin, India using AHP and Sentinel-1 SAR data in geospatial environment,” *Nat. Hazards*, vol. 120, no. 13, pp. 11579–11610, Oct. 2024, doi: 10.1007/s11069-024-06614-0.

[176] T. Agaj, “Integrating AHP and MCDA for flood risk assessment in Kosovo: a catchment-based perspective,” *Nat. Hazards*, Mar. 2025, doi: 10.1007/s11069-025-07212-4.
[177] A. Nath, B. Koley, T. Choudhury, and A. Biswas, “Prioritizing flood drivers: an AHP-based study of physical factors in Digha’s coastal belt, East Coast, India,” *Spat. Inf. Res.*, vol. 33, no. 2, p. 12, Apr. 2025, doi: 10.1007/s41324-025-00615-2.
[178] N. Essahlaoui *et al.*, “Using GIS and Analytical Hierarchy Process (AHP) for flood hazard assessment based on morphological and hydrological criteria, case of the Meknes region, Morocco,” *E3S Web Conf.*, vol. 607, p. 04009, 2025, doi: 10.1051/e3sconf/202560704009.
[179] H. Ha *et al.*, “Flash flood susceptibility prediction mapping for a road network using hybrid machine learning models,” *Nat. Hazards*, vol. 109, no. 1, pp. 1247–1270, Oct. 2021, doi: 10.1007/s11069-021-04877-5.
[180] A. Bernard and É. Ficheur, “Les régions naturelles de l’Algérie,” *Ann. Géographie*, vol. 11, no. 57, pp. 221–246, 1902, doi: 10.3406/geo.1902.18171.
[181] J. Aubouin and M. Durand-Delga, “Aire méditerranéenne,” in *Encyclopaedia Universalis*, vol. 10, Paris: Encyclopaedia Universalis, 1971, pp. 743-745.
[182] O. Kireche, “Evolution géodynamique de la marge tellienne des maghrebides d’après l’étude du domaine parautochtone schistose,” Toulouse, 1993. Accessed: Feb. 11, 2025. [Online]. Available: https://www.ccdz.cerist.dz/admin/notice.php?id=134961
[183] “Plan National Climat,” Ministère de l’Environnement et de la Qualité de la Vie, Algérie, Alger, Feb. 2020. [Online]. Available: https://www.me.gov.dz/telechargement/plan-national-climat/
[184] L. Borselli, P. Cassi, and D. Torri, “Prolegomena to sediment and flow connectivity in the landscape: A GIS and field numerical assessment,” *CATENA*, vol. 75, no. 3, pp. 268–277, Nov. 2008, doi: 10.1016/j.catena.2008.07.006.
[185] M. Cavalli, S. Trevisani, F. Comiti, and L. Marchi, “Geomorphometric assessment of spatial sediment connectivity in small Alpine catchments,” *Geomorphology*, vol. 188, pp. 31–41, Apr. 2013, doi: 10.1016/j.geomorph.2012.05.007.
[186] T. Heckmann *et al.*, “Indices of sediment connectivity: opportunities, challenges and limitations,” *Earth-Sci. Rev.*, vol. 187, pp. 77–108, Dec. 2018, doi: 10.1016/j.earscirev.2018.08.004.
[187] L. Xiao, B. Yu, R. Li, P. Wu, and F. Cai, “Defining watershed-scale sediment delivery ratio using functional connectivity: Exploring the relationship between monthly-scale sediment delivery ratio and soil erosion — A case study from a karst watershed,” *CATENA*, vol. 246, p. 108443, Nov. 2024, doi: 10.1016/j.catena.2024.108443.
[188] S. Crema and M. Cavalli, “SedInConnect: a stand-alone, free and open source tool for the assessment of sediment connectivity,” *Comput. Geosci.*, vol. 111, pp. 39–45, Feb. 2018, doi: 10.1016/j.cageo.2017.10.009.
[189] M. Cavalli, S. Crema, S. Trevisani, and L. Marchi, “GIS tools for preliminary debris-flow assessment at regional scale,” *J. Mt. Sci.*, vol. 14, no. 12, pp. 2498–2510, Dec. 2017, doi: 10.1007/s11629-017-4573-y.
[190] L. Marchi and G. Dalla Fontana, “GIS morphometric indicators for the analysis of sediment dynamics in mountain basins,” *Environ. Geol.*, vol. 48, no. 2, pp. 218–228, Jul. 2005, doi: 10.1007/s00254-005-1292-4.
[191] M. Zimmermann, *Murganggefahr und Klimaänderung - ein GIS-basierter Ansatz*. vdf Hochschulverlag AG, 1997.

[192] G. Rosatti and L. Begnudelli, “Two-dimensional simulation of debris flows over mobile bed: Enhancing the TRENT2D model by using a well-balanced Generalized Roe-type solver,” *Comput. Fluids*, vol. 71, pp. 179–195, Jan. 2013, doi: 10.1016/j.compfluid.2012.10.006.
[193] A. P. Pratiwi, F. I. W. Rohmat, E. O. Nugroho, M. Farid, and M. S. B. Kusuma, “Flood hazard comparison based on geomorphic flood index and hydraulic HEC-RAS (Case study in Ciliwung Watershed, Jakarta),” *IOP Conf. Ser. Earth Environ. Sci.*, vol. 1314, no. 1, p. 012084, Mar. 2024, doi: 10.1088/1755-1315/1314/1/012084.
[194] R. Allalou, R. Hebib, M. Bersi, and A. Lefkir, “BIM-GIS integrated hydrodynamic modeling for road flood risk assessment: A case study in Algeria’s Chiffa Wadi,” *Reliab. Eng. Syst. Saf.*, vol. 267, p. 111906, Mar. 2026, doi: 10.1016/j.ress.2025.111906.
[195] Z. Zheng, X. Zhang, W. Qiao, and R. Zhao, “Emergency Response to Urban Flooding: An Assessment of Mitigation Performance and Cost-Effectiveness in Sponge City Construction,” *Water Resour. Manag.*, vol. 39, no. 5, pp. 1993–2007, Mar. 2025, doi: 10.1007/s11269-025-04139-0.
[196] R. J. Moore, V. A. Bell, and D. A. Jones, “Forecasting for flood warning,” *Comptes Rendus Geosci.*, vol. 337, no. 1–2, pp. 203–217, Jan. 2005, doi: 10.1016/j.crte.2004.10.017.
[197] T. Baykal, S. Terzi, and E. D. Taylan, “Examination of safe routes for emergency responders and people during urban flood: a case study of Isparta, Türkiye,” *Nat. Hazards*, vol. 119, no. 3, pp. 1379–1397, Dec. 2023, doi: 10.1007/s11069-023-06171-y.
[198] F. Jing, L. Yang, Y. Peng, Y. Wang, X. Zhang, and D. Zhang, “Enhancing the effectiveness of flood road gauges with color coding,” *Nat. Hazards*, vol. 88, pp. 55–70, 2017, doi: 10.1007/s11069-017-2856-9.
[199] P.-A. Versini, P.-A. Versini, É. Gaumé, E. Gaume, H. Andrieu, and H. Andrieu, “Application of a distributed hydrological model to the design of a road inundation warning system for flash flood prone areas,” *Nat. Hazards Earth Syst. Sci.*, 2010, doi: 10.5194/nhess-10-805-2010.
[200] M. Borga, E. N. Anagnostou, G. Blöschl, and J.-D. Creutin, “Flash flood forecasting, warning and risk management: the HYDRATE project,” *Environ. Sci. Policy*, vol. 14, no. 7, pp. 834–844, Nov. 2011, doi: 10.1016/j.envsci.2011.05.017.
[201] P. O’Hare and I. White, “Beyond ‘just’ flood risk management: the potential for—and limits to—alleviating flood disadvantage,” *Reg. Environ. Change*, vol. 18, pp. 1–12, Feb. 2018, doi: 10.1007/s10113-017-1216-3.
[202] B. Smit and J. Wandel, “Adaptation, adaptive capacity and vulnerability,” *Glob. Environ. Change*, vol. 16, no. 3, pp. 282–292, Aug. 2006, doi: 10.1016/j.gloenvcha.2006.03.008.
[203] A. Coulombe, “Évaluation De Mesures D’adaptation Aux Inondations Avec Pcswmm Et Promethee Pour Un Très Petit Bassin Versant,” ÉCOLE DE TECHNOLOGIE SUPÉRIEURE UNIVERSITÉ DU QUÉBEC, Québec, Canada, 2021.
[204] S. Tachaudomdach, A. Upayokin, N. Kronprasert, and K. Arunotayanun, “Quantifying Road-Network Robustness toward Flood-Resilient Transportation Systems,” *Sustainability*, vol. 13, no. 6, p. 3172, Mar. 2021, doi: 10.3390/su13063172.
[205] E. Zio, “Critical Infrastructures Vulnerability and Risk Analysis,” *Eur. J. Secur. Res.*, vol. 1, no. 2, pp. 97–114, Oct. 2016, doi: 10.1007/s41125-016-0004-2.